January 1972

URS 7030-7

SHOCK TUNNEL TESTS OF WALL PANELS

TECHNICAL REPORT

Volume I

Test Information

and

Analysis

Contract No. DAHC20-71-C-0223

OCD Work Unit 1123G

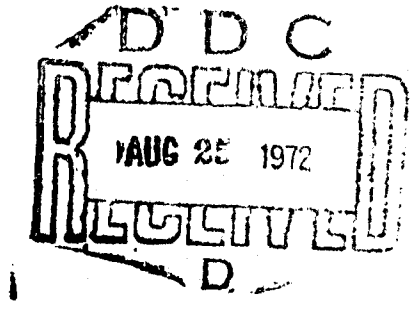

A URS Systems Affiliate

urs research company • 155 bovet road • san mateo, california 94402

UNCLASSIFIED

Security Classification

DOCUMENT CONTROL DATA - R & D

(Security classification of title, body of abstract and indexing annotation must be entered when the overall report is classified)

1 ORIGINATING ACTIVITY (Corporate author) URS Research Company 155 Bovet Road San Mateo, California 94402	2a. REPORT SECURITY CLASSIFICATION UNCLASSIFIED 2b. GROUP

3. REPORT TITLE

SHOCK TUNNEL TESTS OF WALL PANELS

4 DESCRIPTIVE NOTES (Type of report and inclusive dates)

Final Report

5 AUTHOR(S) (First name, middle initial, last name)

B. Gabrielsen
C. Wilton

6. REPORT DATE	7a. TOTAL NO. OF PAGES	7b. NO. OF REFS
June 1972	192 181	8

8a. CONTRACT OR GRANT NO.	9a. ORIGINATOR'S REPORT NUMBER(S)
DAHC20-71-C-0223	7030-7
b. PROJECT NO.	
c. Work Unit 1123E	9b. OTHER REPORT NO(S) (Any other numbers that may be assigned this report)
d.	

10. DISTRIBUTION STATEMENT

Approved for Public Release; Distribution Unlimited.

11. SUPPLEMENTARY NOTES	12. SPONSORING MILITARY ACTIVITY
	Defense Civil Preparedness Agency Washington, D.C. 20310

13. ABSTRACT

Test information and analytical results for a variety of wall geometries subjected to blast loads, and for short statically loaded beams are presented in Volume 1. Volumes 2 and 3 contain digitized gage data taken from tests with nonfailing solid walls, walls with doors, and walls with windows. (Volumes 2 and 3 are available for review at DCPA Headquarters.) The reported results contained in Volume 1 are as follows.

Non-preloaded solid walls tested stronger than predicted. Preloading with the equivalent of one or two stories added only 10 to 20 percent to wall strength. Walls with doorways and with windows behaved as predicted, with concrete block walls being very weak comparatively. Interior walls of hollow clay tile and concrete block failed at very low overpressures.

DD FORM 1 NOV 68 1473 REPLACES DD FORM 1473, 1 JAN 64, WHICH IS OBSOLETE FOR ARMY USE.

UNCLASSIFIED

Security Classification

14. KEY WORDS	LINK A		LINK B		LINK C	
	ROLE	WT	ROLE	WT	ROLE	WT
Structural loading						
Structural response						
Wall panels						
Dynamic loading						
Static loading						
Shock tunnel						
Shelters						
Brittle failure						
Fatigue failure						

January 1972

URS 7030-7

SHOCK TUNNEL TESTS OF WALL PANELS

TECHNICAL REPORT

Volume I

Test Information

and

Analysis

Contract No. DAHC20-71-C-0223

OCD Work Unit 1123G

By

C. Wilton and B. Gabrielsen

Engineering Research Division

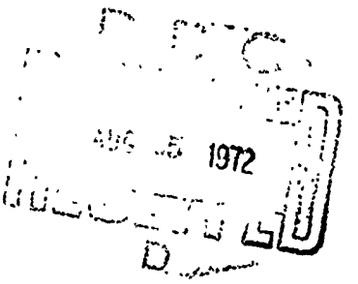

Prepared for

DEFENSE CIVIL PREPAREDNESS AGENCY

Washington, D. C. 20310

urs research company • 155 bovet road • san mateo, california 94402

ACKNOWLEDGEMENTS

The authors are pleased to acknowledge the very substantial contributions of Messrs Joseph Boyes and Paul Kennedy who were largely responsible for the field test program; Mr. Phillip Morris who prepared the data reduction computer programs; Ms. Salliann Spenny who aided immeasurably in data reduction and with report editing and production. Overall editing was provided by Mrs. Patty Reitman, and the overall program was under the general direction of Mr. Kenneth Kaplan.

Especial acknowledgements are due Mr. Norward A. Meador, the Technical Monitor, and Mr. George Sisson, Chief of Shelter Research.

January 1972 URS 7030-7

SHOCK TUNNEL TESTS OF WALL PANELS

TECHNICAL REPORT SUMMARY

Volume I

Test Information and Analysis

Contract No. DAHC20-71-C-0223

OCD Work Unit 1123G

By

C. Wilton and B. Gabrielsen

Engineering Research Division

Prepared for

DEFENSE CIVIL PREPAREDNESS AGENCY

Washington, D. C. 20310

urs research company • 155 bovet road • san mateo, california 94402

Summary Report

SHOCK TUNNEL TESTS OF WALL PANELS

OBJECTIVES AND SCOPE OF THE REPORT

The overall objective of the program under which the work described in this report was carried out is to determine the failure mechanisms under blast loadings of full-scale exterior and interior wall panels. Work to the date of this report has been concentrated on panels of "brittle" materials (nonreinforced brick, concrete block, and clay tile) and on evaluating the importance of wall geometries (i.e., whether doors or windows are present or absent); of wall mountings (whether the wall is supported as a beam or a plate); of wall preload (whether the wall is loaded vertically by upper stories in a building); and of material properties.

This report contains test information, test data, and analytical work on a variety of test geometries. The majority of data were taken during so-called loading studies, tests in which the walls exposed to the blast were designed not to fail and were instrumented with pressure gages. Digitized gage records from these tests are presented in Volumes 2 and 3* of this report, with Volume 2 containing data on solid walls and exterior walls with doors, and Volume 3, data on exterior walls with windows.

Volume 1 of this report contains information on four different test geometries, as well as information on the static test program which is concerned with determining properties of the materials used in the tests. The four geometries reported on are:

- Exterior solid walls, both with and without preload.
- Exterior walls with a doorway.

---

* Only a limited number of Volumes 2 and 3 were prepared. They are available for study in the Shelter Research Division at the Defense Civil Preparedness Agency.

- Exterior walls with a window (two window sizes were studied).
- Interior walls in a room with a window.

The first three geometries did not include a second wall behind the exterior wall (as in a room) and thus are, in effect, "infinite rooms." (Data taken in finite room geometries will be presented in later reports.) For exterior walls with doors and windows the "net loading" results from loading study tests are presented graphically. (Net loading results are from pairs of gages on the front – upstream – and the back – downstream – sides of each wall. Overpressures from these gages have been differenced electronically to produce a trace which shows the net overpressure in the direction of shock wave motion at the location on the wall of each gage pair.)

For exterior solid walls and interior walls behind walls with windows, the graphical presentation of loading study results is of "average loadings" (overpressures from three or more gages located at about mid-height and at different horizontal positions on the walls).

For all test geometries a graph of displacement vs time of the center of failing walls is given. A summary of the results presented in each section of the report follows.

GENERAL RESULTS

Solid Walls

Analytical predictions for non-preloaded, 12-in. thick walls, mounted as beams (i.e., supported at the top and bottom only) indicated that the expected rupture modulus with static loading was about 117 psi, from which the expected loading pressure to cause failure would be about 1.42 psi. With a dynamic overload of about 3:1, the expected rupture modulus was about 164 psi, corresponding to a loading pressure to cause failure of about 2 psi.

A 12-in. wall subjected to shock waves from one strand of Primacord (loading pressure of about 1.6 psi) did not fail, and did not show any signs of

cracking. The same wall subjected to a shock wave from two strands of Primacord (loading pressure of about 4 psi) did fail as expected, but analysis of crack gage data suggested that failure occurred at a stress far greater than the expected value.

In order to study preloaded walls, a preloading mechanism was designed and built which (through designed plastic failure of the lever system providing the preload) maintained the value of preload during shock wave loading close to what it was prior to that loading. Analytical work indicated that preloads equivalent to one or two extra stories above the test wall would increase failure (cracking) resistance by only 10 to 20 percent, and tests in the Tunnel appeared to bear this out.

Walls with Doorway

Loading study tests indicated that the net loadings at various points away from the doorway would have to differ with time. Such loadings were derived from the tests, and their generalized representations were fed into the SAMIS finite-element computer code in order to obtain contours of wall deflection vs time. The program suggested that failure should first occur furthest from the door; tests in the Shock Tunnel appeared to bear this out.

Walls with Window

Loading study results indicated that — contrary with experience of walls with doorways — there was no need to use different net-loading-with-time information for different locations around the window. Common to all locations appeared to be a sharp spike then a very rapid decrease to a loading value near the incident overpressure. All test walls behaved generally as predicted. Failures (cracks) appeared first at the window corners and progressed generally horizontally away from the corners. The brick walls were far stronger than the concrete block walls. Failure (cracking) occurred with a rupture modulus σ_r of about 140 psi with the former and only about 27 psi with the latter.

Room with a Window – Interior Wall

Few analytical predictions were made except to note that with σ_r of about 18 psi for clay tile and about 27 psi for concrete block, low loadings would be required for failure. This was amply borne out in that two concrete block walls cracked when subjected to shock waves from a single 10-ft long strand of Primacord (loading pressure < 1 psi). The clay tile walls were first subjected to shock waves from 2-ft long strands of Primacord (loading pressure < 0.5 psi) and did not crack. All walls failed with one 60-ft length strand of Primacord (the normal minimum) whose loading pressures ≃ 1.5 psi.

Static Test Program

The static test program was reviewed. Tabulated results indicated that static rupture modulii, with beams that are short (~ 2 ft) compared with a wall, varied from 68 psi to 326 psi, with most values clustering from 140-240 psi. Similar tests were made with clay tile and concrete block beams, all of which proved to be weak in flexure.

ABSTRACT

This Abstract deals with the test information and analytical results for a variety of wall geometries subjected to blast loads, and for short statically loaded beams, presented in Volume 1. Volumes 2 and 3 contain digitized gage data taken from tests with nonfailing walls with and without doors and windows. (Volumes 2 and 3 are available for review at DCPA headquarters.)

Analytical studies for 12-in. thick solid walls mounted as beams indicated a lower rupture modulus at failure than seemed to be observed in the Shock Tunnel. Analysis of the effect of vertically preloading a test wall indicated that failure (cracking) resistance would increase only 10 to 20 percent for preloads equivalent to one or two stories. Tests in the Shock Tunnel with a specially designed preloading mechanism appeared to bear the predictions out.

The SAMIS finite element computer program predicted failure of walls with a doorway to start furthest from the door. Loading inputs to the program were derived from Shock Tunnel tests and differed with time at various points on the wall.

Similar SAMIS studies of walls with a window indicated that cracking should occur first at the corners of the windows. Tests with brick and concrete block walls bear this out though σ_r for the brick walls was about 140 psi but only about 27 psi for the concrete block walls.

Interior walls behind windows made of clay tile and concrete blocks failed at very low stress levels ($\sigma_r \simeq$ 180 psi for the former, $\simeq$ 27 psi for the latter).

The static test program with short beams show most values of rupture modulus for brick beams to cluster from 140-240 psi. Clay tile and concrete block beams are considerably weaker.

CONTENTS

CONTENTS (cont.)

ILLUSTRATIONS

ILLUSTRATIONS (cont.)

ILLUSTRATIONS (cont.)

ILLUSTRATIONS (cont.)

ILLUSTRATIONS (cont.)

ILLUSTRATIONS (cont.)

ILLUSTRATIONS (cont.)

TABLES

NOTATION

$d/dt = \dot{x}$	Differential with respect to time (L/T)
E	Energy (FL)
E	Modulus of elasticity (F/L^2)
F	Force (F)
$F_j[f(t)]$	Force, time variant (F)
$\bar{F}$	Fracture force (F)
g	Gravity (F/T^2)
H	Centerline shear at fracture
I	Area moment of inertia (L^4)
k	Stiffness (F/L)
L	Length (L)
ℓ	Length (L)
m	Mass ($F \cdot T^2/L$)
M	Bending moment (FL)
m,n	Integers
p_i	Incident pressu e (F/L^2)
p_r	Reflected pressure (F/L^2)
P_v	Vertical load (F)
R	Resistance (F)
t	Time, variable (T)
T	Period (T)
V	Shear (F)
V	Velocity (L/T)
W	Weight (F)
x,y,z	Coordinate axes (L)
$\bar{x}$	Mean value
$1/\alpha$	Measure of dispersion
δ	Virtual displacement (L)
η	Coordinate axis (L)
θ	Angle (rad)

NOTATION (cont.)

μ	Modal value
ρ	Mass density ($F \cdot T^2/L^4$)
σ	Standard deviation
σ_c	Compressive stress (F/L^2)
σ_r	Rupture modulus (F/L^2)
σ_t	Tensile stress (F/L^2)
τ	Time, variable (T)
ω	Natural frequency (rad/T)
Ω	Frequency (rad/T)

Section 1
INTRODUCTION

This report is one of a series describing the progress of a long-range shock tunnel research program to determine the loading, structural response, and debris characteristics of wall panels. The report presents the data from tests with nonfailing walls (loading studies) and with wall panels composed of brittle materials, conducted during the time period from November 1, 1970 to October 30, 1971. In addition, some further analysis of data are presented from selected tests conducted prior to November 1970.

This program is sponsored by the Defense Civil Preparedness Agency (DCPA) under Contract No. DAHC20-71-C-0223. The primary objective of the program is to provide information, obtained both analytically and experimentally, on the strength of a wide range of structural wall panels of interest to DCPA. This information is being used by URS and other investigators to improve building damage and personnel casualty estimates.

The method of approach has been to conduct closely coordinated analytical and experimental efforts. First, preliminary analytical work was performed to identify, within the scope of the survey data available, those classes of wall panels which are of primary concern to the DCPA shelter research program. This was further refined to determine, within those classes, the panel types whose general structural response characteristics were expected to be similar. The resulting wall panel types are being studied through a comprehensive research program which includes: loading study tests in which nonfailing walls are subject to blast loading, and are conducted primarily to obtain loading information on various structural wall geometries; wall panel response tests in which full size structural wall panels are subjected to blast loadings; and an analytical program which encompasses the design of the experimental tests (both loading and response), the analysis of data from these tests, and the development of techniques for predicting wall panel failure. As these prediction techniques are developed, the need for conducting experiments on various types of panels within one class will decrease.

In this report, results of 81 tests, all part of the wall panel test program are given. Four additional tests were conducted for DCPA and the General American Transportation Company to investigate the blast resistance of stored DCPA shelter equipment. The results from these tests were presented in Ref. 2. Finally, 25 experimental tests were designed to investigate blast fire interaction. Their results were presented in two separate reports, Refs. 3 and 4.

Section 2

GENERAL DISCUSSION OF THE EXPERIMENTAL TEST PROGRAM

The data from a total of 81 shock tunnel tests are presented in the report. Thirty-four of these tests were conducted using full-scale structural wall panels of nonreinforced brick, concrete block, or hollow clay tile. The remaining 47 were loading study tests conducted using nonfailing instrumented walls. The purpose of these loading study tests was to determine the characteristics of the air blast pulse (e.g., maximum overpressure, duration, and pulse shape) as a function of the quantity of the explosive used, and to obtain the time history of the loadings on the various structural wall geometries tested in the full-scale response tests. This information is used to aid in the design of the full-scale response tests and in the interpretation of data from these tests.

To discuss the results of these tests it is convenient to organize them with regard to test geometry. The various test geometries investigated were as follows:

1. Single solid wall completely blocking the shock tunnel.
2. Single wall with a doorway.
3. Single wall with a window.
4. A room with a window in the front wall (toward the blast) and a solid back wall.

The kinds and number of tests covered in this report are tabulated in Tables 2-1 and 2-2. In both tables, reference is made to "strands of Primacord" which is a measure of the strength of the shock wave incident on a wall. The general relationship between shock wave overpressure and strands of Primacord is given in Fig 2-1.

The tests conducted with each of these test geometries will be discussed in Sections 3 through 6. Certain elements including the instrumentation and

Table 2-1

LOADING STUDY TESTS, NO. CONDUCTED

TYPE OF TESTS	NO. OF 60-FT LONG STRANDS OF PRIMACORD				
	1	2	3	4	5
Solid Wall	1	3	3	1	3
Wall with Doorway	3	-	3	-	3
Wall with Window					
62-in. x 64-in. window	3	-	3	-	4
38-in. x 62-in. window	3	-	3	-	3
Room with Window	2	2	2	2	-

Table 2-2

RESPONDING WALL TESTS

TYPE OF TEST	WALL NO.	PRIMACORD LENGTH	NO. STRANDS	NO. TESTS	DESCRIPTION OF TESTS
SOLID WALLS					
12-in. brick beam, no preload	52	60	1	3	No signs of damage.
	52	60	2	1	Wall failed.
8-in. brick beam, preload	64	60	1	2	16,500 lbs preload. Wall cracked on first test; failed on second.
	65	60	1	1	16,500 lbs preload. Wall failed.
	66	60	1	1	23,500 lbs preload. Wall cracked.
	67	60	3	1	23,500 lbs preload. Wall failed.
WALLS WITH DOORWAY					
8-in. brick beam (33-1/2-in. wide)	45	12	1	1	Test for natural period.
	45	60	2	1	Wall failed.
	48	10	1	1	Test for natural period.
	48	60	1	3	No visible damage.
	48	60	2	1	Wall failed.
WALLS WITH WINDOW					
8-in. Brick beam (62-in. x 38-1/2-in. window)	56	60	2	1	Wall failed.
	57	60	1	3	Cracks on first test increased in size.
	57	60	2	1	Wall failed.
8-in. concrete block beam (62-in. x 39-in. window)	60	10	1	1	Test for natural period, wall cracked.
	60	60	1	1	Wall failed.
	61	10	1	1	Test for natural period, wall cracked.
	61	60	1	2	Cracks enlarged on first test; failed on second.
ROOM WITH WINDOW (Interior Walls)					
8-in. concrete block beam	58	10	1	1	Test for natural period, wall cracked.
	58	60	1	1	Wall failed.
	59	2	1	1	Test for natural period.
	59	60	1	1	Wall failed.
6-in. hollow clay tile beam	62	2	1	1	Test for natural period.
	62	60	1	1	Wall failed.
	63	2	1	1	Test for natural period.
	63	60	1	1	Wall failed.

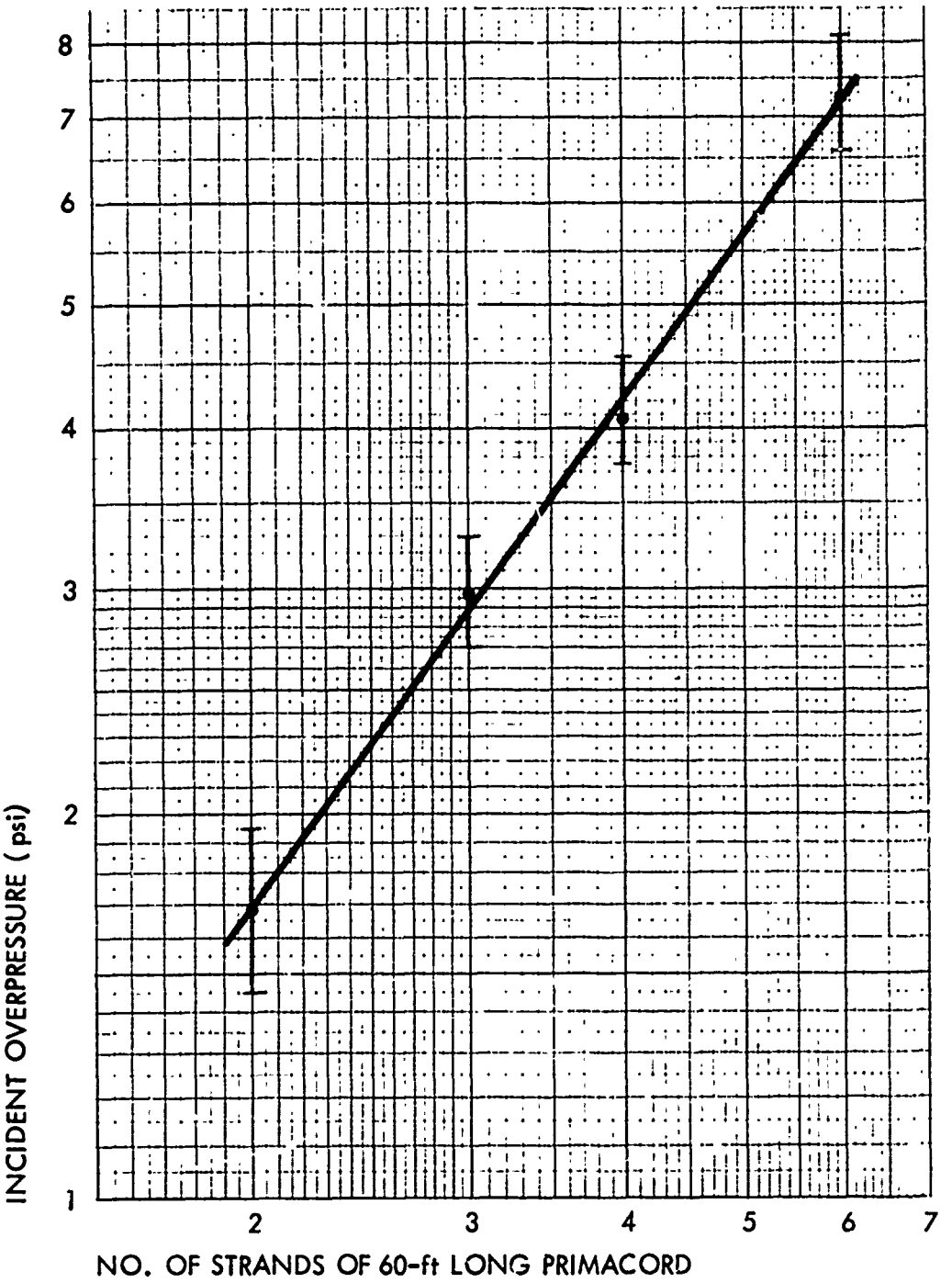

Fig. 2-1. Incident Overpressure as a Function of the Number of 60-ft Long Strands of Primacord Detonated Simultaneously in the Compression Chamber. Bars indicate one standard deviation from the mean.

data analysis techniques are common to all test geometries and are included in this general discussion.

In addition to the shock tunnel tests, static loading tests of the materials being used were also carried out. These along with some crack gage tests, are discussed in Section 7.

Test data for the loading studies are available in three appendices constituting Volumes 2 and 3 of this report. Volume 2 contains Appendix A, the test data for the solid wall loading study, and Appendix B, the test data for the loading study on exterior walls with doors. Volume 3 contains Appendix C, the test data for the loading study on exterior walls with windows.

Only a limited number of Volumes 2 and 3 were prepared. They are available for review at the Shelter Research Division of the Defense Civil Preparedness Agency.

INSTRUMENTATION

The instrumentation used during a typical loading study test includes pressure gages located on the wall of the shock tunnel and on the nonfailing wall or walls, and load cells located on the support structure, which monitor the total load imparted to this support structure. Occasionally, this instrumentation is supplemented with time-of-arrival gages, strain gages and motion picture cameras.

The same basic instrumentation is used for the structural wall panel tests. The pressure gages are located on the shock tunnel wall, and the load cells monitor the transmitted load on the wall panel support structure. Also used are time-of-arrival gages, strain gages, displacement/velocity gages, crack gages, high-speed movie cameras, and pre-shot and post-shot still photography.

The various elements of the instrumentation system are as follows:

- Pressure gages - Susquehanna Instrument Co., Model ST-2 and Kistler Instrument Co. Model 606-L. These are used with Kistler Model 504A charge amplifiers.

- Load cells - Lockheed Electronics Co. Model LCPC-50 (50,000 lb capacity) and Model LCPC-200 (200,000 lb capacity). These are used with Bell & Howell Model 1-165 high gain amplifiers.

- Time-of-arrival gages - Two types have been used: a URS-fabricated foil-leaf switch, and, more recently, an inexpensive microphone fastened to the front face of the wall.

- Strain gages - BLH Electronics, Inc., SR4 type.

- Displacement/velocity gages - Two types have been used. On tests where the primary interest was small displacements (< a quarter of an in.) a G.L. Collins Corp. linear displacement transducer was used. On the more recent tests where measurements of large displacements (> 4 in.) were desired, a G L. Collins velocity gage, Model LMV 05710, was used. The velocity gage is bonded to the center of the upstream face of each wall.

- Crack gages - Various types have been used throughout the test program, including strips of conducting epoxy, conducting paint, and, in the majority of the tests, a thin strip of aluminum foil (approximately one-eighth of an in. wide) embedded in a rigid epoxy. Recently, a development/calibration study has been conducted on these crack gages; the results of this investigation is presented in Section 7.

- Recording system - The data from the various sources is recorded on either a Bell & Howell VR3300 14 channel tape recorder or on Tektronix Dual-Beam Oscilloscopes, Model 502 and 502A, equipped with Polaroid cameras. To obtain hard copy traces for data reduction and analysis, the tape recorded data are speed scaled, i.e., data which is recorded at 60 in. per second is played back at 3.75 in. per second and is displayed on light-sensitive paper using a Honeywell Model 1508A Visicorder.

DATA REDUCTION PROCEDURE

The hard copy records are first placed in the URS Data Reader and the pressure-time, load-time, etc., records are digitized. Subsequent data reduction and processing is accomplished by a series of computer codes written for a time-sharing XDS 940 computer which is available through a national subscription service, Tymshare Inc. Each pressure-time record is stored as a data file and identified by the test number and gage location. A number of data files, which represent replications of a test condition, are processed simultaneously. The output of these programs is in the form of a table of average pressure at millisecond intervals, and a computer plot of average pressure vs time.

The tabulated pressure-time information includes a listing of the tables of the data files which were processed in addition to the descriptive information contained in the table heading. A table of impulse-time information is also printed, in which the impulse was determined by integrating the pressure-time data at 1 msec intervals. Tests where pressure measurements were made on both sides of a wall with a pair of gages were processed to output net pressure and impulse information. The tabular output for these gage pairs also included a listing of front, back, and net pressure and impulse for each test and gage pair location, in addition to the averages of these quantities for all the replications of a test condition.

A standard deviation is determined from the pressure-time information, using the following formula:

$$\sigma^2 = \frac{\sum_{i=1}^{n} \sum_{t=0}^{m} \left(P_t - P_{avg}\right)^2}{n(m) - 1}$$

where σ = standard deviation

n = number of gage records

m = maximum duration (msec)

P_t = pressure at time t of a record

P_{avg} = average pressure of n records at time t

Thus the standard deviation, expressed in psi, is determined from deviations from the mean over the entire duration of the record. This provides some measure of the reproducibility of the tests. It also means that 95 percent of the data used in establishing the average pressure vs time plot falls within a band 2σ above and below the average pressure-time curve.*

* Standard deviation was determined from net pressure for paired gages, thus, if one gage of a pair on a test did not function, its readings were not used in determining σ, but were used in determining average net pressure for tab and plot output.

All output was carefully checked against the original gage record data files to eliminate errors. In addition, the value of standard deviation was used as a further check on the accuracy of gage records, and aided in pinpointing gage malfunctions.

Velocity gage records from failing wall tests were also processed by computer. The output is in the form of a table of velocity and displacement for each millisecond of the record, and a log-log plot of displacement vs time. The displacements are determined by integrating the velocity data at 0.1 msec intervals.

In previous reports in this series the data presented has been primarily the peak values of pressure and load with some pressure-time and load-time data given for approximately the first 25 msec of the load pulse. This was done because the early time data was urgently needed for input to the calculations and computer analysis being used to design the test program and to make predictions of natural period, displacement and failure threshold. For other purposes, such as studying the behavior of the wall after it fails, i.e., cracks, longer time information is required. Thus, all data presented in this report are for the full duration of the pulse, i.e., clear into the negative phase. Emphasis has also been placed on the pressure-time and displacement-time data with very little effort being devoted to the load cell data. Analysis of this data is considerably more complex and of lower priority as it will be of value when studying full building frame response; hence, it will be presented in a later report.

Section 3
SOLID WALL TESTS

A solid wall test is one in which an 8-1/2 by 12-ft wall, either a nonfailing wall or a structural wall panel, is placed in the shock tunnel completely blocking the tunnel. During this reporting period, loading study tests and five structural wall panel tests were conducted with solid wall panels. The wall panels were supported as simple beams (i.e., supported top and bottom with sides free to move) both with and without vertical preload. (Vertical preload simulates the load due to the weight of the structure above the panel of interest, as in the cases of bearing and curtain walls in multi-storied buildings.) A sketch of a simple beam support condition for a brick wall without preload is shown in Fig. 3-1. Sketches of the preloaded wall supports are given later in the section.

LOADING STUDY TESTS

Loading study tests are used to determine the peak overpressure, duration, and pulse shape of the blast wave generated in the shock tunnel as a function of the quantity and arrangement of the Primacord used, and to obtain the time history of the load imposed on wall panels by the blast wave. This data is necessary to design the wall panel tests, to obtain data for failure prediction calculations, and to aid in interpretation of the wall panel test results.

Ideally, load-time history information should be obtained from gages placed directly on the brick (or other material) of wall panels being tested. However, since these panels are usually tested to failure, to obtain such information would be difficult and expensive. Instead, load-time information is obtained using instrumented nonfailing walls – massive walls constructed of steel and laminated plywood and having modular panels containing instrumentation. These modular panels can be arranged to allow measurements to be made at a number of locations on the wall.

Fig. 3-1. Cutaway View of Shock Tunnel Showing Test Panel and Simple Beam Support Condition Hardware

The instrumentation locations for a loading study test with a solid wall is shown in Fig. 3-2. There were four gages mounted on the 8-1/2 × 12-ft modular nonfailing wall, B-12, B-13, B-14, and B-15. In addition, there were three gages on the tunnel wall: gage 7, 92-3/4 in. ahead of the nonfailing wall on the west side of the tunnel; gage 9, 52-1/4 in. ahead of the wall also on the west side of the tunnel; and gage 11, 110-3/8 in. ahead of the nonfailing wall on the east side of the tunnel.* Typical gage traces from a one strand Primacord test (peak load on the wall of approximately 1.5 psi), and a three strand test (peak load on the wall of approximately 7.0 psi), are shown in Appendix A. Also included in Appendix A are the digitized data for each of the solid wall loading study tests.

Summary plots of the loading study test data are shown in Figs. 3-3 through 3-7. These plots are the averaged data from all solid wall tests using the specified quantities of explosives. This varied from one to four tests for each plot and the tests which were used to make up a particular plot are listed in the caption for each figure. For example, Fig. 3-4 presents the data for all two strand, solid wall loading study tests; in particular, tests 01-13-71-02, 01-11-71-03, and 01-11-71-04.** The data presented in Fig. 3-4 is the average pressure on the wall as measured by the three gages: B-13 B-14, and B-15. The digitized data used to generate these plots is presented in Appendix A. Similar data for one, three, four and five strand tests are presented in Figs. 3-3, 3-5, 3-6, and 3-7.

---

* At least two of these tunnel wall gages are in operation in each of the failing wall tests to correlate between the loading study tests and the failing wall tests.

** These test numbers are read as follows: 01- the month, January; -13- the day of the month; -71- the year; -03 the third test conducted that day. This test designation is used throughout the program for both loading study and failing wall tests.

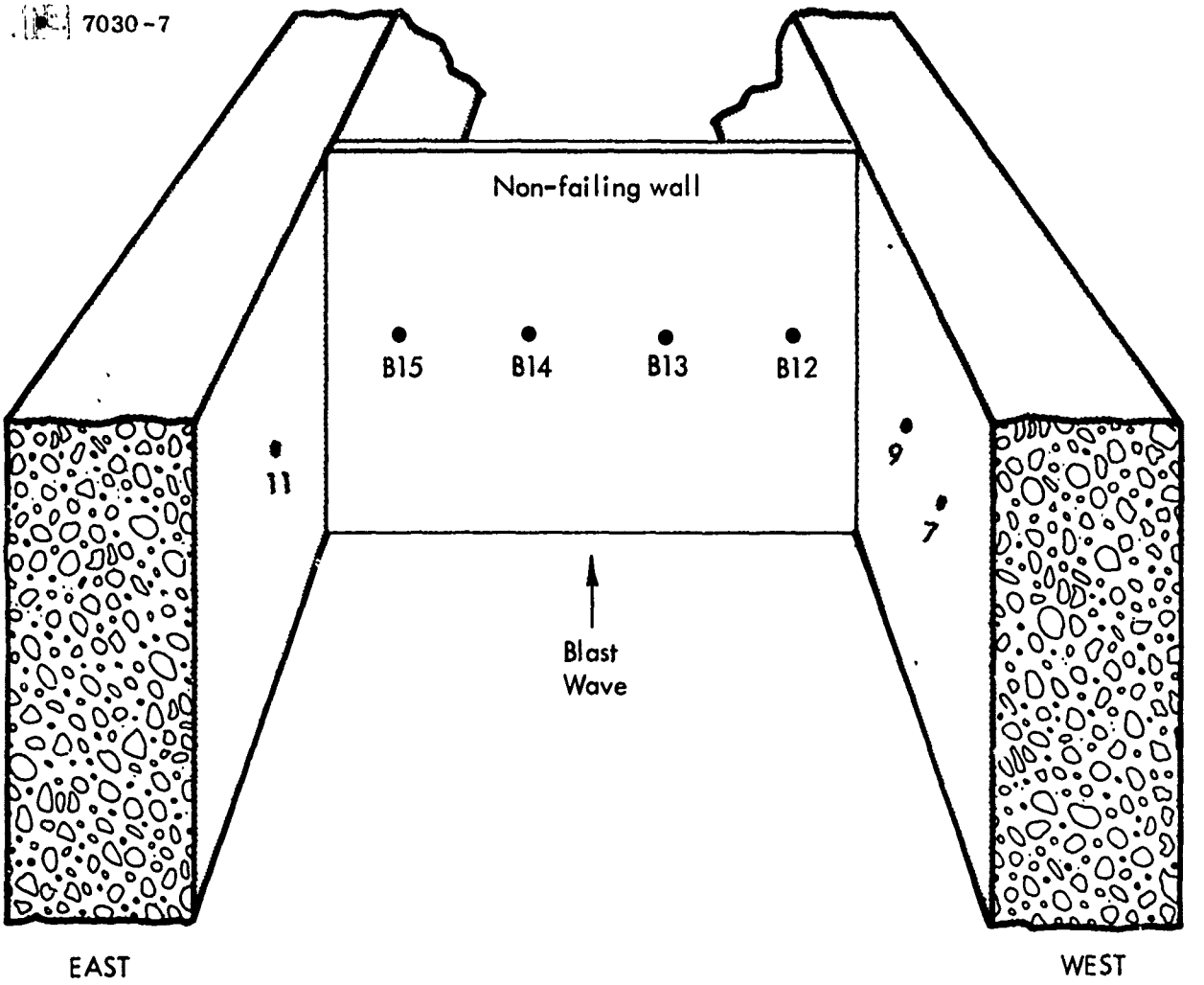

NONFAILING WALL GAGES

GAGE NO.	DISTANCE FROM FLOOR	DISTANCE FROM WEST WALL OF TUNNEL
B-12	51"	14-1/4"
B-13	51"	47 "
B-14	51"	75-1/4"
B-15	51"	132-1/2"

TUNNEL WALL GAGES

GAGE NO.	DISTANCE FROM FLOOR	DISTANCE FROM NON-FAILING WALL
Westwall-7	45"	92-3/4"
Westwall-9	45"	52-1/4"
Eastwall-11	49"	110-3/8"

Fig. 3-2. Instrumentation Location for Solid Wall Loading Test Series

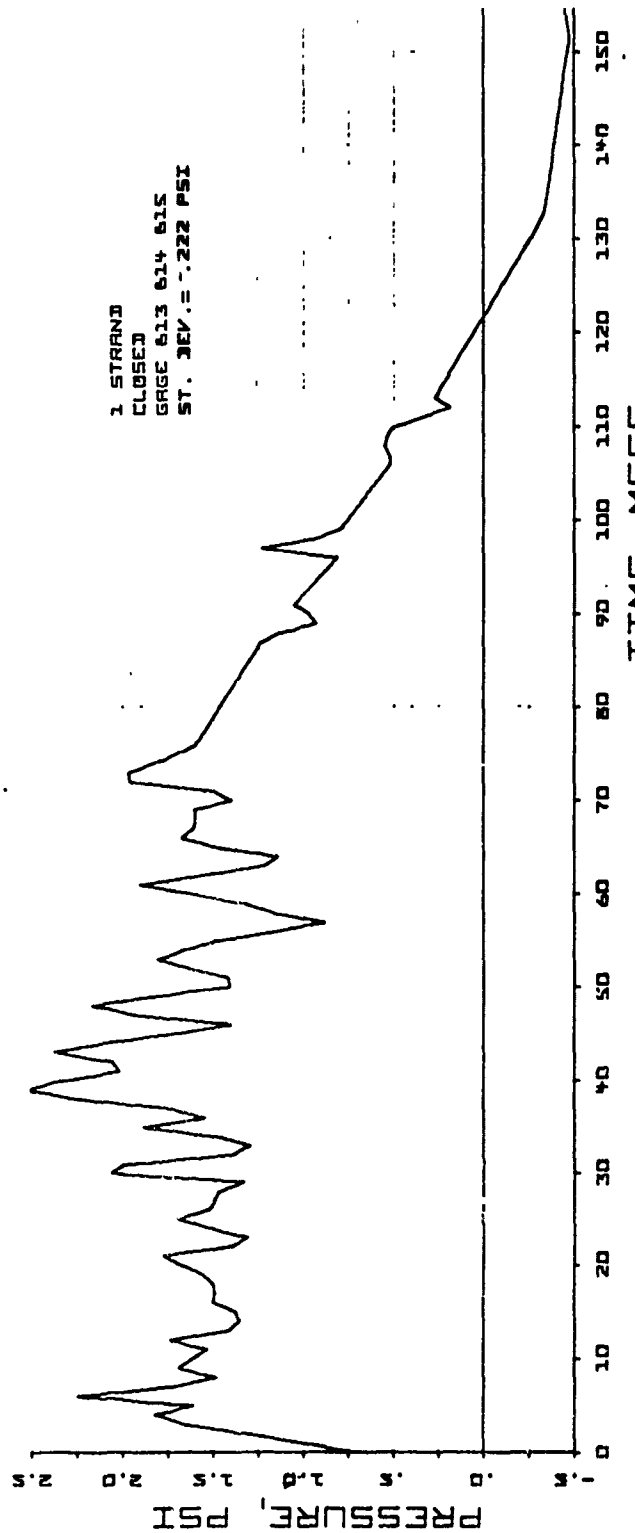

Fig. 3-3. Average Peak Overpressure vs Time for One Strand Solid Wall Loading Study Test 01-13-71-03; Gages B-13, B-14 and B-15

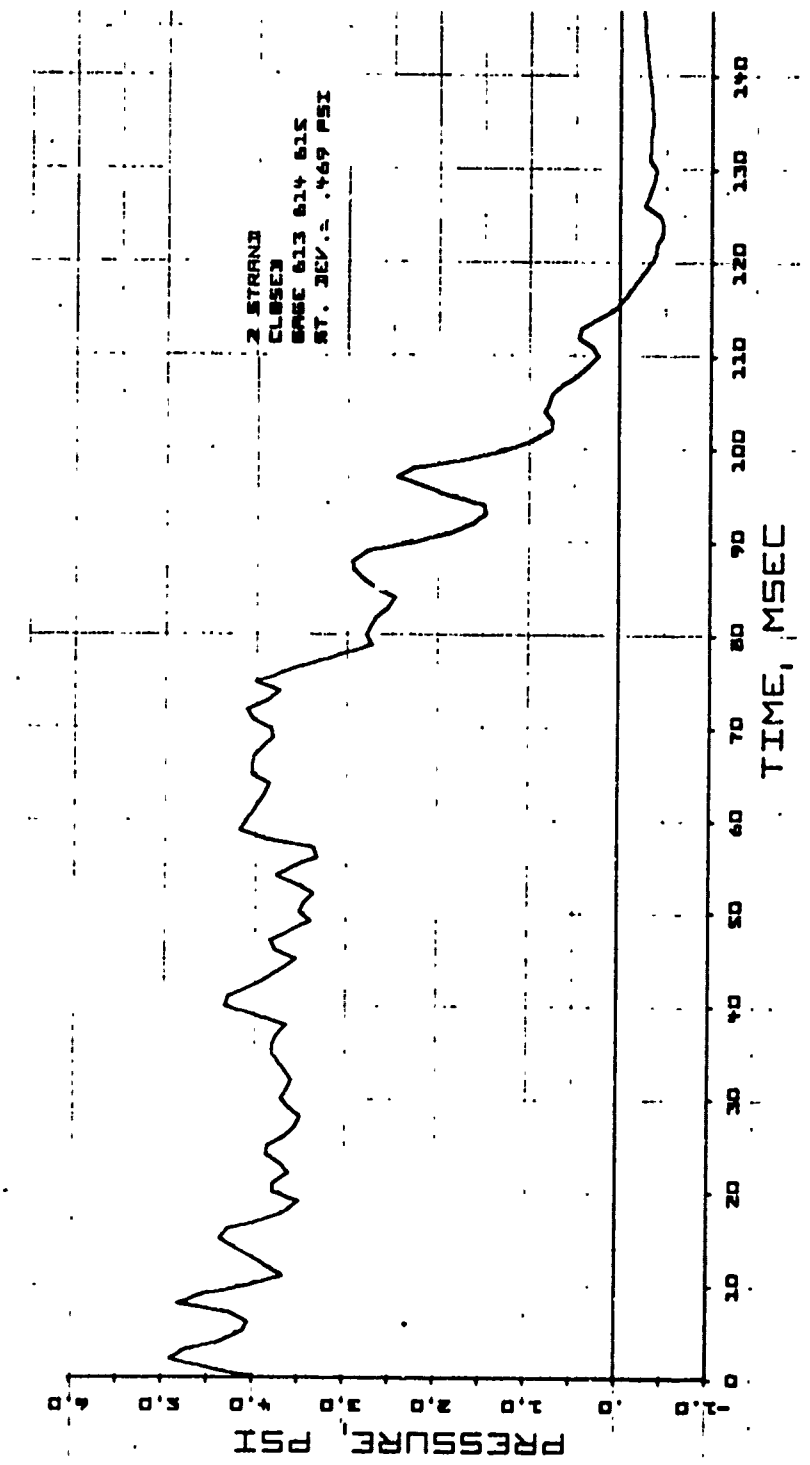

Fig. 3-4. Average Peak Overpressure vs Time for Two Strand Solid Wall Loading Study Tests 01-13-71-02, 01-11-71-03, and 01-11-71-04; Gages B-13, B-14 and B-15

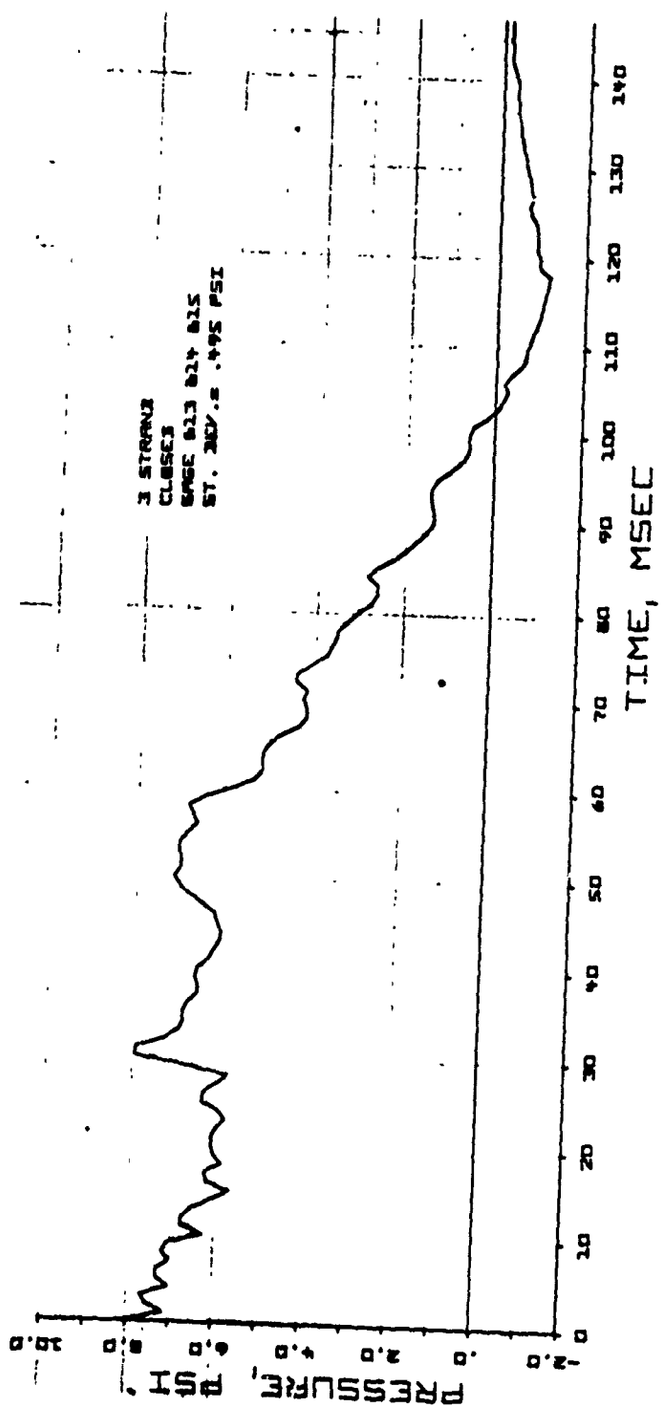

Fig. 3-5. Average Peak Overpressure vs Time for Three Strand Solid Wall Loading Study Tests 01-12-71-01, 01-12-71-02 and 01-13-71-01; Gages B-13 B-14 and B-15

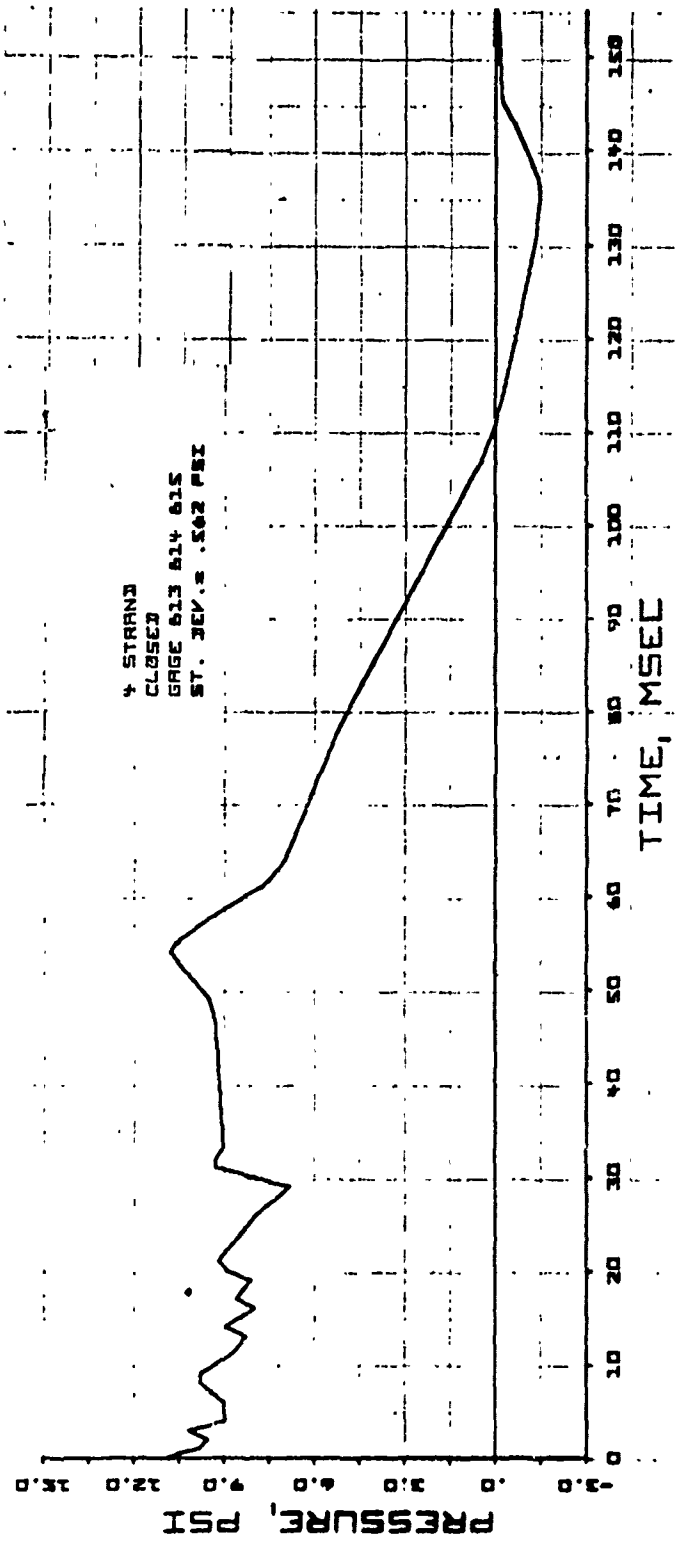

Fig. 3-6. Average Peak Overpressure vs Time tor Four Strand Solid Wall Loading Study Test 01-13-71-04; Gages B-13, B-14 and B-15

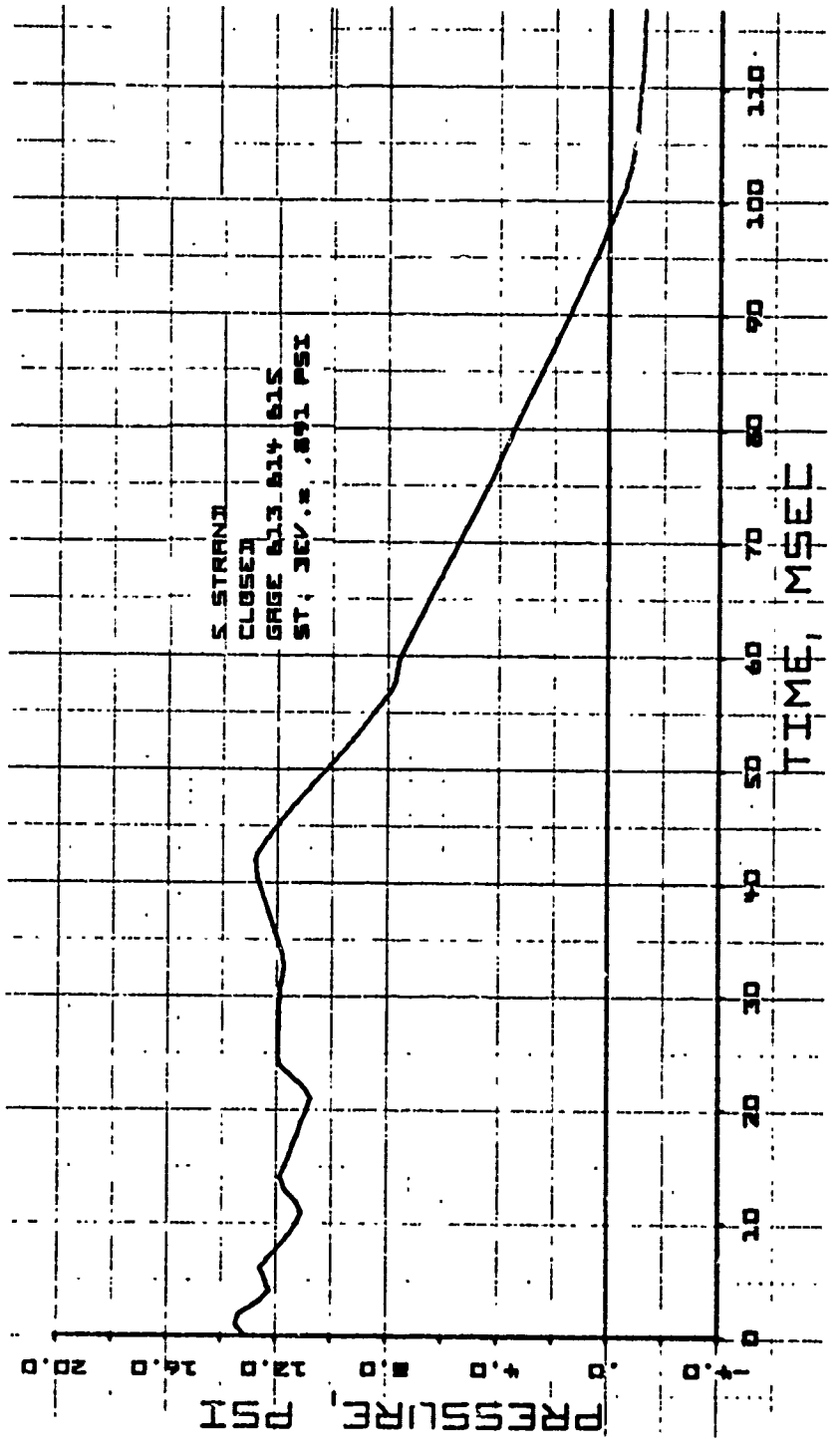

Fig. 3-7. Average Peak Overpressure vs Time for Five Strand Solid Wall Loading Study Tests 01-13-71-05, 01-13-71-06, and 01-13-71-07; Gages B-13, B-14 and B-15

WALL PANEL TESTS

During this reporting period, five solid exterior* structural wall panel tests were conducted: one 12-in. thick, nonreinforced brick wall supported as a simple beam; and four 8-in. thick nonreinforced brick walls supported as simple beams but with various levels of preload. All walls completely filled the 8-1/2 X 12 ft cross section of the tunnel.

Wall Panel Tests without Preload

Prior to discussing the results of these tests, we will briefly review the static test program and the analytical work performed with this test condition to help design the tests, to aid in the analysis of results, and to better understand the failure process in order to develop means for predicting the response of other wall panels in this same class.

To predict the failure characteristics of a particular wall panel, it is necessary to have a measure of its material properties. Therefore, during the construction of a wall panel, a group of static test specimens are fabricated. These usually consist of:

1. Brick and mortar beams for flexural strength tests.
2. Mortar cylinders for compressive and splitting strength tests.
3. Masonry assemblies for composite compressive and shear bond strength tests.
4. Brick and mortar couplets for tensile bond strength tests.
5. Single bricks for modulus of rupture and compressive strength tests.

These specimens are tested using standard ASTM procedures. These procedures and the static test data are discussed briefly in Section 7 and are presented in detail in a previous report (Ref. 5).

* Additional solid interior wall panel tests were conducted; these are discussed in Section 6.

Based on these static tests, the average material properties for the brick walls used in this program were as follows:

STATIC MATERIAL PROPERTIES	
E_{avg}	$= 1.3 \times 10^6$ psi
σ_r (expected)	= 185 psi
σ_r (maximum) 99%	= 260 psi
σ_r (minimum) 5%	= 105 psi

Based on these material properties, the preliminary predictions for the peak sustained reflected pressure (p_r) which would cause a 12-in. brick simple beam wall panel to fail are:

RESPONSE PREDICTIONS	
p_r (maximum)	= 3.15 psi
p_r (expected)	= 2.25 psi
p_r (minimum)	= 1.28 psi

Earlier in the program two 12-in. brick wall panels (wall 50 and wall 51) were tested at 4.0 psi and 4.3 psi, respectively, well above these predicted values. As expected, both wall panels failed catastrophically, indicating that the flexural strength (Modulus of Rupture) of these walls was well below 330 psi and 355 psi. In 1969, theoretical work was done on low-level fatigue, and in Ref. 6 a generalized failure theory was developed combining a statistical failure theory presented in Ref. 7 and the low-level fatigue ideas. From this failure theory, a somewhat different strength distribution is predicted for an 8 X 12 ft brick wall 12-in. thick (see Fig. 3-8). These values are as follows:

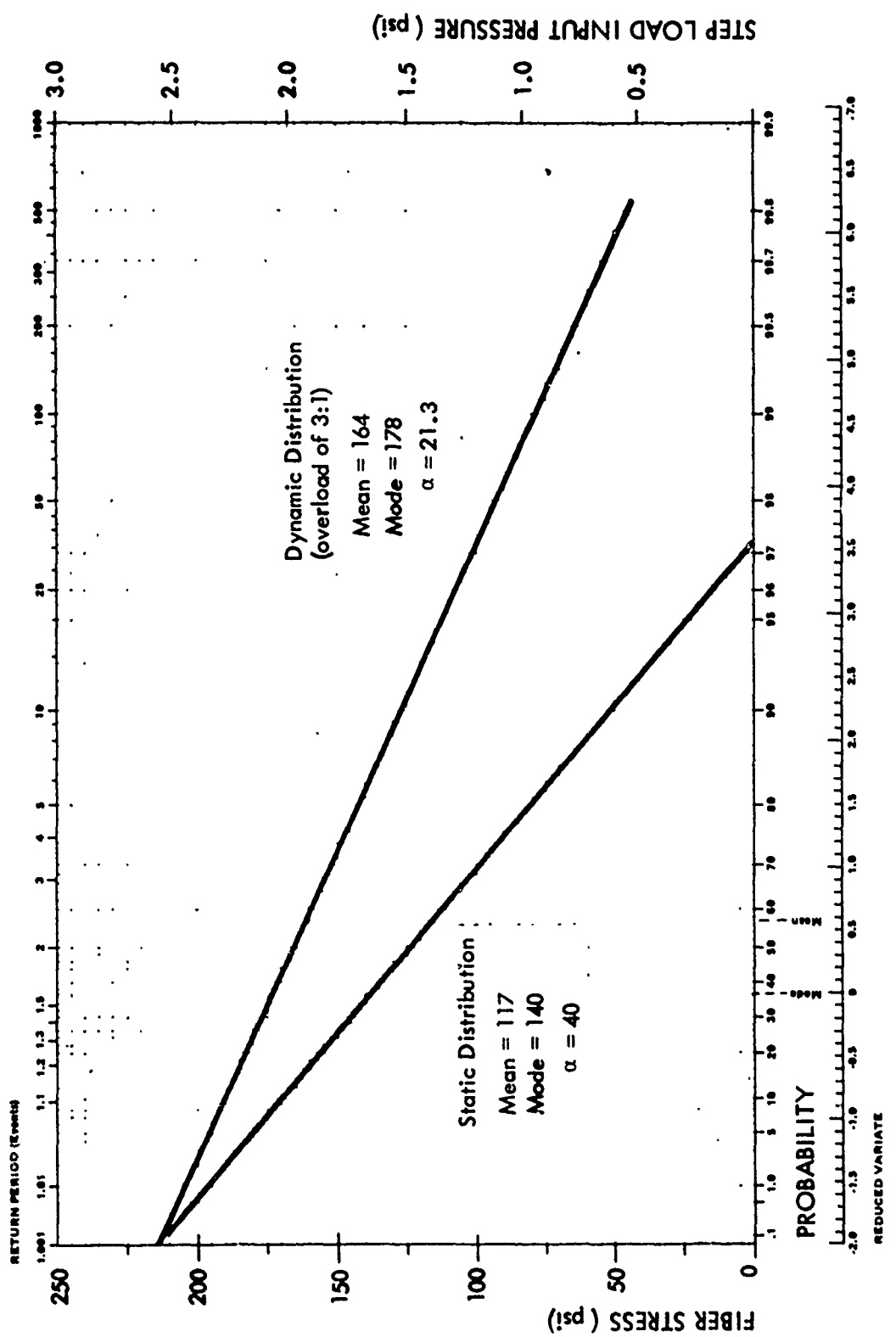

Fig. 3-8. Predicted Strength Distribution for 8 × 12 ft × 12 in. Brick Wall Based on the Failure Theory and Static Test

RESPONSE PREDICTIONS

MODULUS OF RUPTURE	FAILURE PRESSURE
σ_r (maximum) 99% = 200	p_r (maximum) = 2.41
σ_r (expected) = 117	p_r (expected) = 1.42
σ_r (minimum) 5% = 25	p_r (minimum) = .30

In addition to these calculations based on static test data, a major portion of the analytical program has been devoted to the use of computer analysis to expand the prediction capability. The computer code presently used on this program is the Structural Analysis and Matrix Interpretation System (SAMIS), developed by The Western Development Laboratories (WDL), of the Philco-Ford Corporation under contract to the Jet Propulsion Laboratory. This is a powerful and complex code using finite element techniques and is capable of handling either triangular elements (e.g., plates and shells) or line elements (e.g., trusses and frames). The computer prediction work on solid walls was presented in detail in a previous report (Ref. 6) and will not be repeated here. However, two curves from that work will be repeated to aid in the discussion of test results. These are Fig. 3-9, a plot of the calculated stress on a typical element on the center line of solid brick wall subjected to a 1 psi step load and Fig. 3-10, a plot of the calculated load that would be read by a load cell located on the support frame of the wall. Recently completed computer work on more complex wall forms, (i.e., those with openings) will be presented in later sections of this report.

The 12 in. brick wall tested during this reporting period (wall 52) provided the first opportunity to test some of the ideas presented in the failure theory found in Ref. 5. Hence, it was decided to subject the wall to one strand shock waves (peak reflected pressures of about 1.6 psi) and to: (1) check the lower bound strength; and (2) look for signs of cracking or partial failure. These one strand tests were repeated three times (test numbers 03-03-71-01 through 03-03-71-03) with no sign of cumulative damage (low-level fatigue) or any degradation in performance; hence, $\sigma_r \geq 133$ psi. The measured natural frequency of this wall was 38 msec.

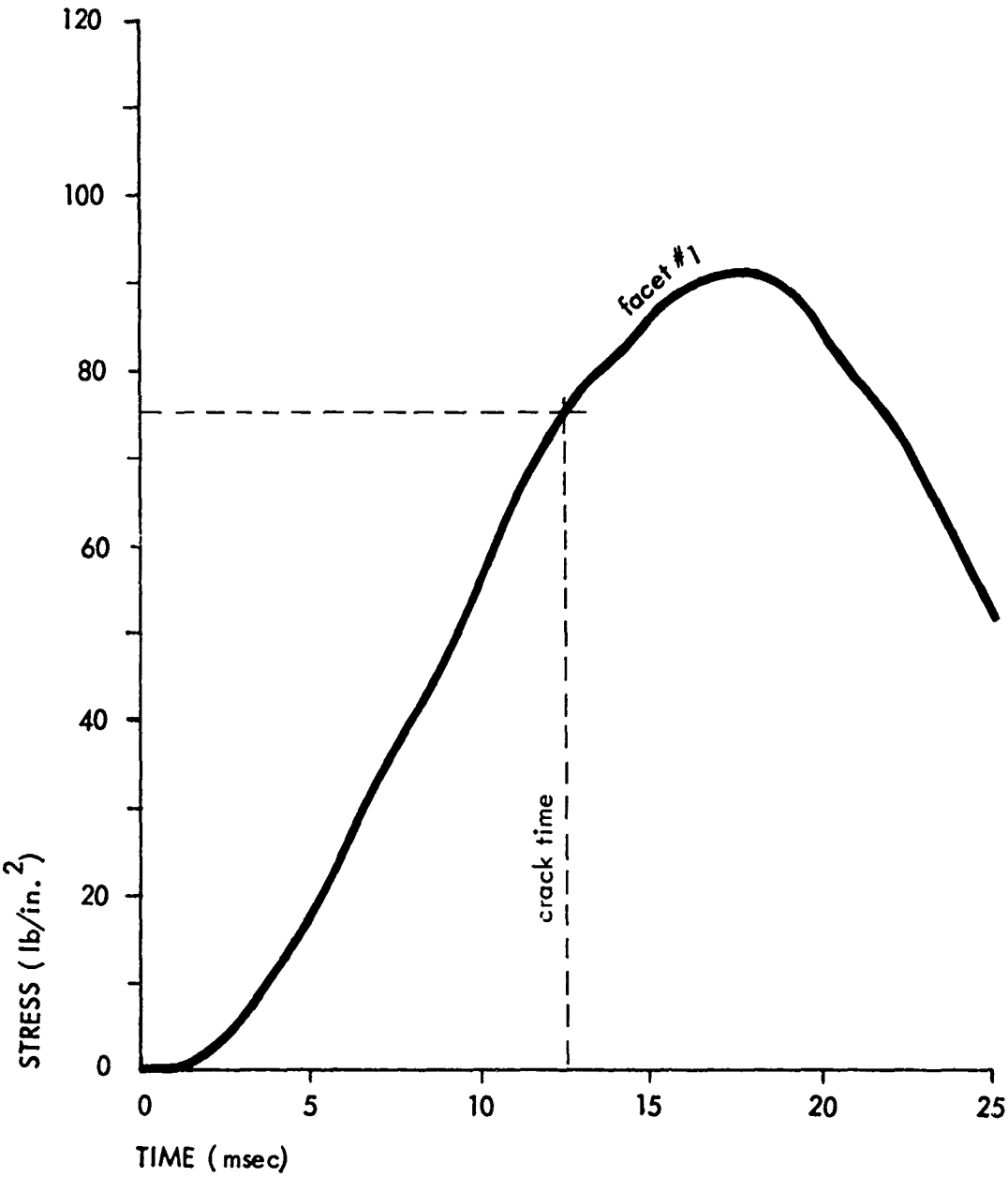

Fig. 3-9. Typical Stress/Time Relation for Facet on Structure Centerline of a 12-in. Brick with a 1 psi Step Load

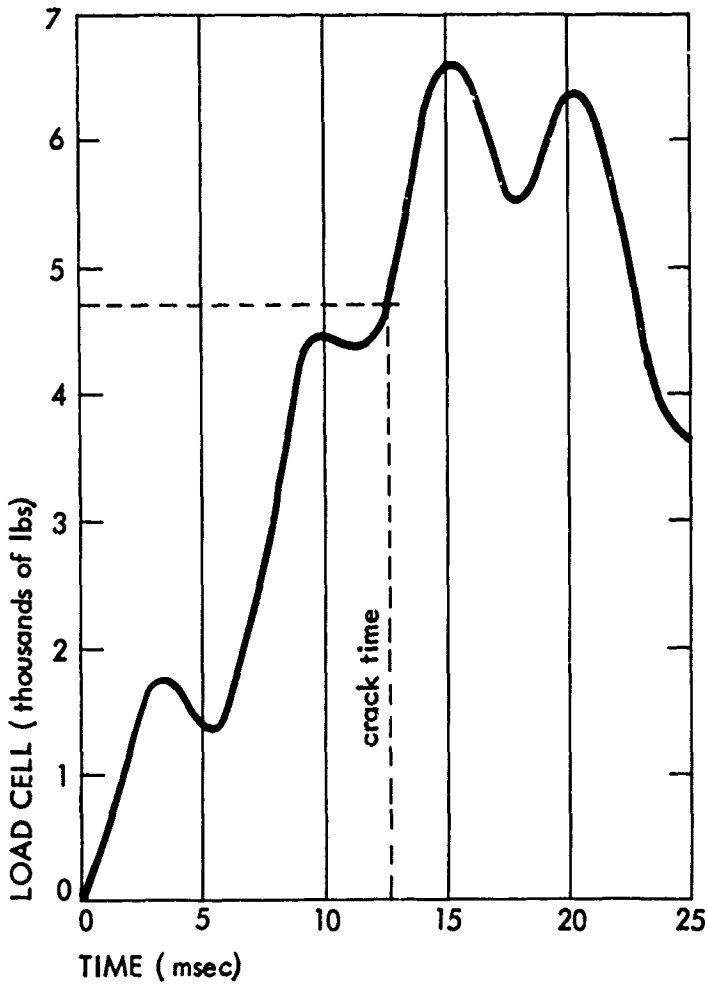

Fig. 3-10. Computed Load Trace, Nonfailing Wall, 1 psi Step Load Input

The results of these three tests are interesting and predictable since the static strength probability curve (Fig. 3-8) indicated that there was approximately 50 percent probability of a wall being at least this strong.

In the fourth test (test no. 03-03-71-04) the wall was subjected to a measured peak reflected overpressure of 4.2 psi. The wall failed with first cracks appearing at 12.5 and 13.2 msec. These cracks were horizontal and located at the center of the wall. The bottom half of the wall rotated until striking the floor; the top half rotated approximately 90 degrees and landed on top of the bottom half. The maximum total load as measured by the load cells was 74,000 lb.

A plot of the displacement of the center of this wall as a function of time is presented in Fig. 3-11. Pre- and post-test photographs of the failed wall are presented in Fig. 3-12.

The crack time of this wall, 12 to 13 msec, implies an apparent fiber stress of $\sigma_r = 332$, based on the dynamic stress prediction from SAMIS (see Fig. 3-9). If the failure theory concepts are correct and the strength distributions are accurate, the 4.2 psi reflected pressure is almost three times as great as the expected strength; hence, one would use the "Dynamic Strength Distribution" shown in Fig. 3-8. This distribution also shows that a modulus of rupture of $\sigma_r = 332$ is very rare, less than 1 percent probability. As more data are gathered, the theory and distributions will undoubtedly be modified but the current knowledge permits one to say $133 \leq \sigma_r \leq 332$ for wall 52 with complete certainty.

Wall Panel Tests with Preload

During this test program, four tests of brick wall panels with preload were conducted. To preload means to simulate "real world" load conditions induced by bearing-wall construction or high curtain-wall construction. Before presenting the test results of these walls, a brief discussion of the rationale used to design these tests will be presented (this information was presented in considerably more detail in Ref. 5). This will be followed by a description

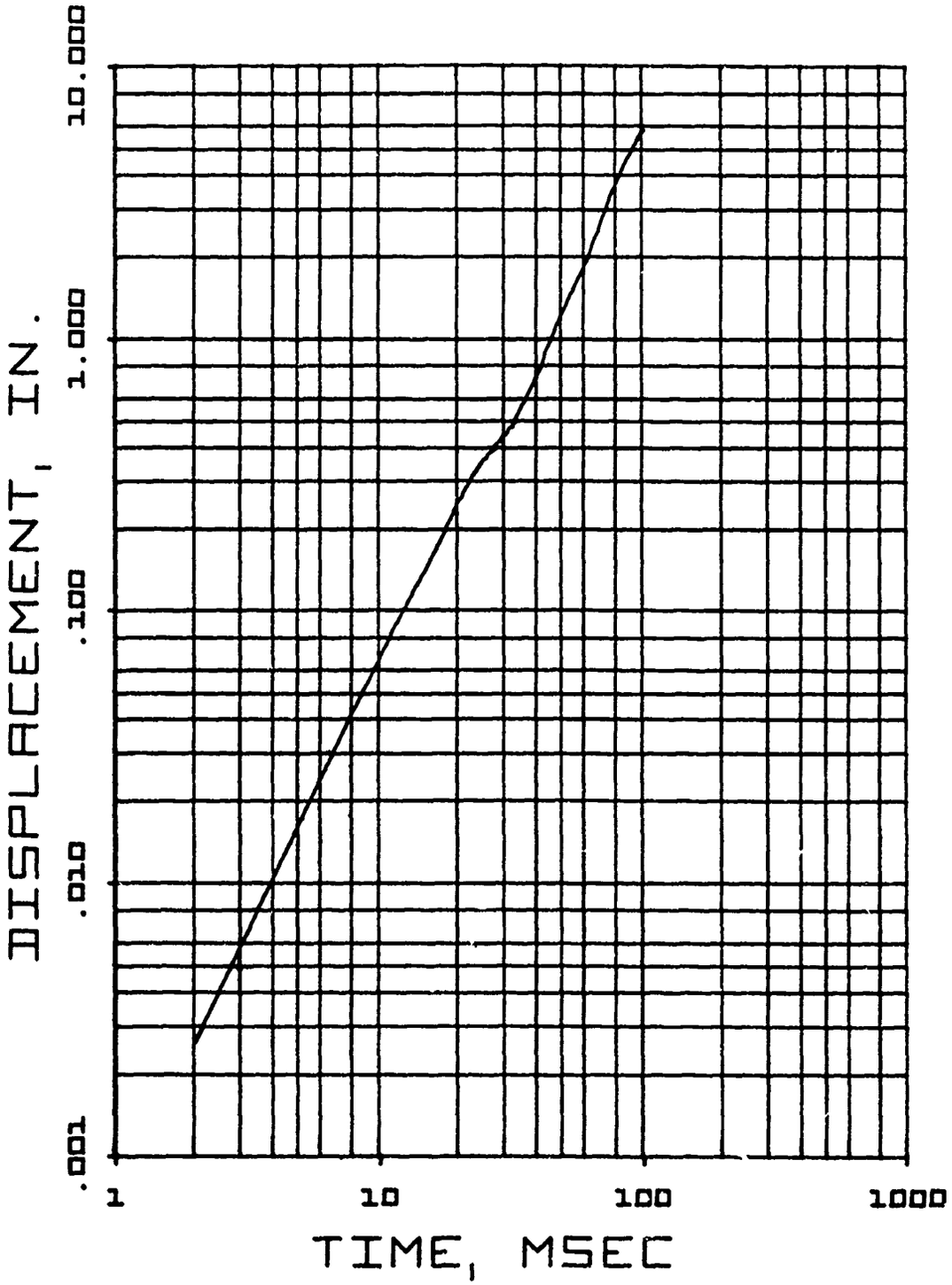

Fig. 3-11. Displacement as a Function of Time for 12 in. Nonreinforced Brick Wall No. 52 (Test No. 03-03-71-04)

Fig. 3-12. Pre- and Post-Test Photographs of 12 in. Nonreinforced Brick Wall No. 52 (Test No. 03-30-71-01), Peak Reflected Overpressure 4.2 psi

of the test design and test hardware, and a discussion of the analytical predictions which were made prior to these tests.

Theoretical Considerations

First consider the model presented in Fig. 3-13a and 3-13b and in particular, the "Elastic Bending Phase" in Fig. 3-13a. (In the first part of this discussion only the static case will be considered, i.e., dy/dt = 0.)

This model gives a rise to a "resistance function" of the form shown below.

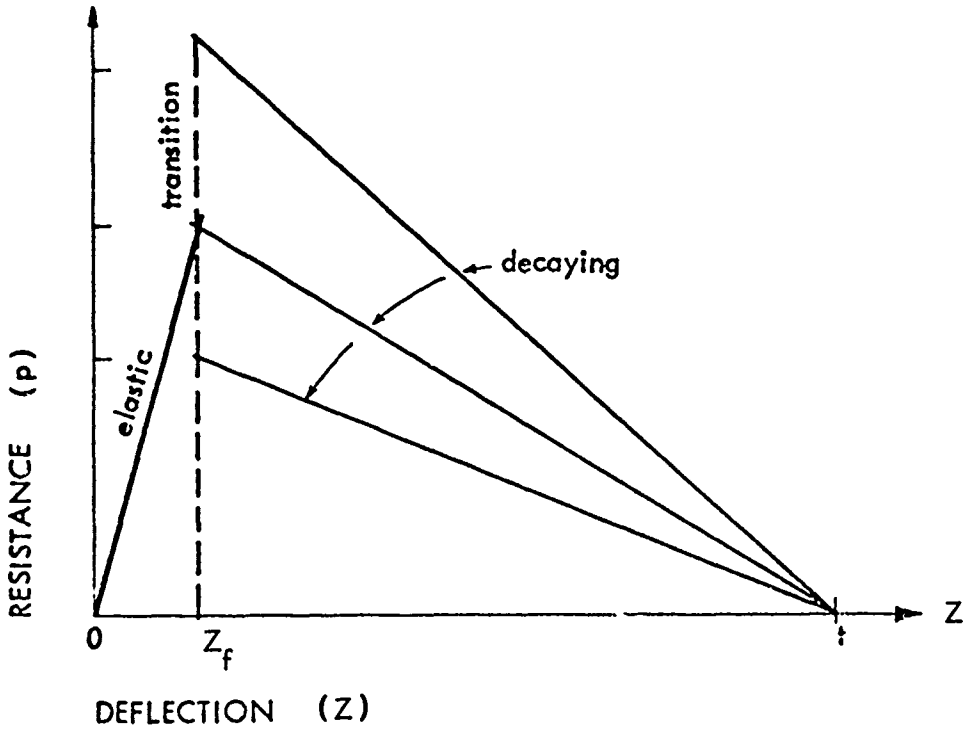

This suggests that a wall could apparently have increased resistance to post-fracture if it has a low modulus of rupture σ_r and a high preload P_v. That this can be true is shown in the following table.

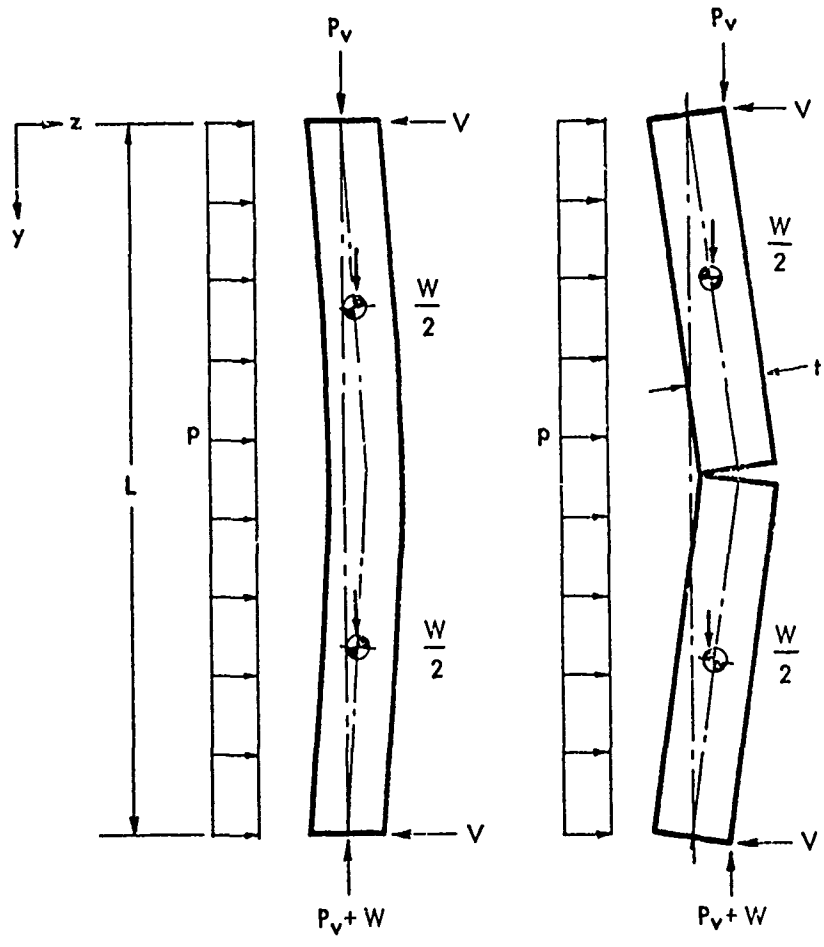

(a) Elastic Bending Phase (b) Secondary Phase

Let

L = 96 in.

t = 8 in.

W = 56 lb/in. of width, i.e., consider a 1-in.-wide beam

M = bending moment

p = pressure

σ_r = rupture modulus in psi

I = $t^3/12$ in. ^{4}/in.

A = area (in. ^{2}/in. of width)

p_v = preload in lb/in.

Fig. 3-13. Failure Model

σ_r	P_v	p (Static) PRE-FRACTURE	p (Static) POST-FRACTURE
50	0	0.49	0.20
50	2W*	0.63	0.98
150	0	1.42	0.20
150	2W	1.55	0.98
300	0	2.80	0.20
300	2W	2.83	0.98

It can be seen that ir certain cases a wall can indeed become stronger after fracture. For example, take a wall with σ_r = 50 psi and P_v = 2W (a three-story curtain wall). The resistance before fracture is p = 0.63 psi and p = 0.98 after fracture, or a 55 percent increase. This would give the "resistance function" shown as the solid curve in Fig. 3-14. Note that the assumptions leading to this type of resistance function are:

- The material must be brittle with a low modulus of rupture, σ_r.
- The preload force P_v must move from the center of the wall prior to fracture to the proper (strength-enhancing) face during the post-fracture period.
- The wall at the center must be capable of supporting (by friction only) a shear force H = tW/2L on a fractured line.
- The material must support vertical loads at the top, bottom, and center as the line contacts.

Fig. 3-14 also shows resistance curves for σ_r = 300 psi.

* In Ref. 5 effort was expended studying various load-bearing-wall configurations and curtain-wall configurations to establish reasonable bounds on preload based on construction and design practice. From this study it appeared that a three-story curtain wall provides about the same preload a one-story bearing wall might support. Hence, a preload of 2W seems a reasonable upper bound for an 8 in. brick wall.

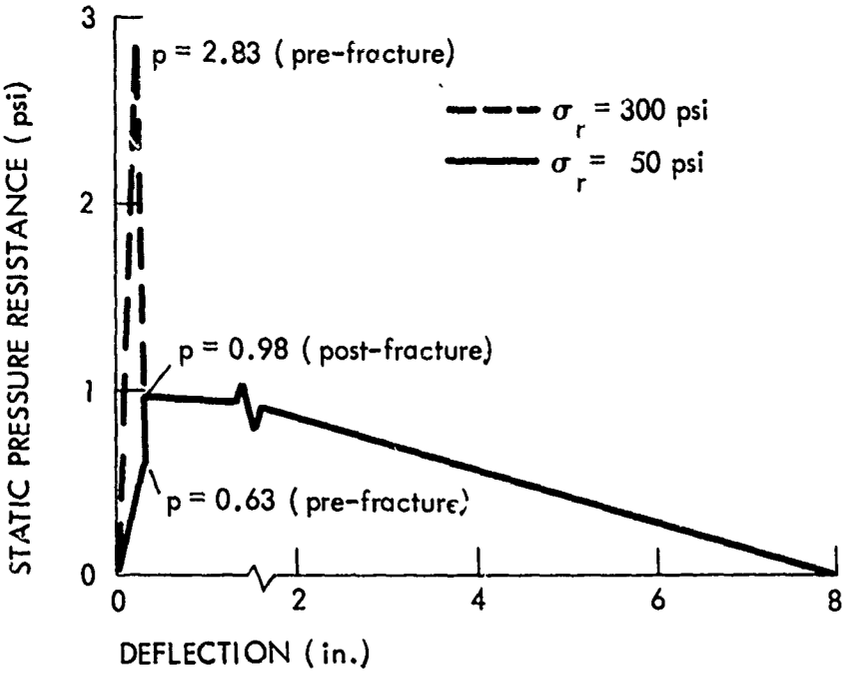

Fig. 3-14a. Resisting Function for an 8-in. Brick Wall with Preload of 2W Shifting to Tension Face, σ_r = 50 and 300 psi

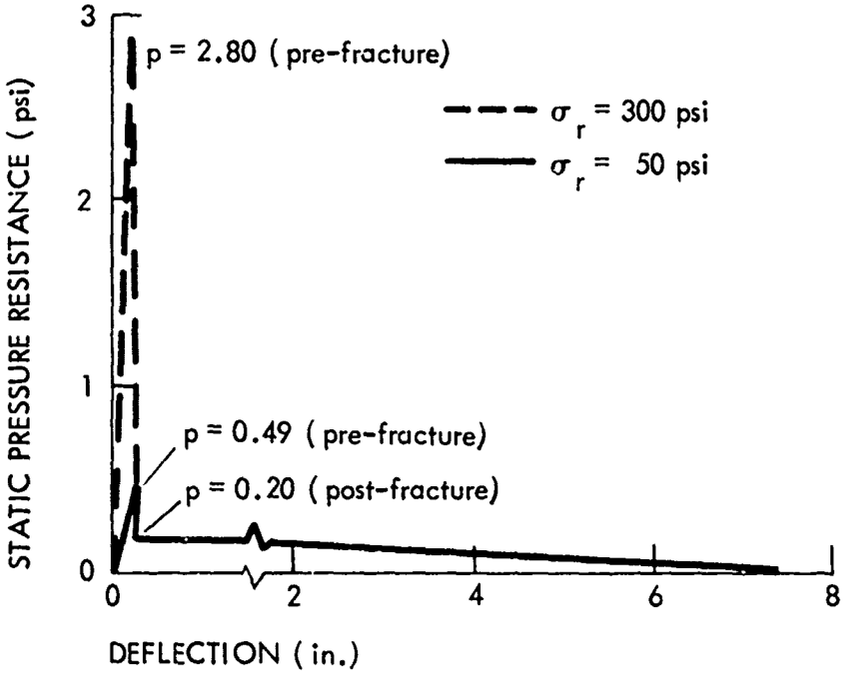

Fig. 3-14b. Resisting Function for an 8-in. Brick Wall without Preload but with Weight of Wall Shifting to Tension Face, σ_r = 50 and 300 psi

Experiment Design

The design objectives were to develop a preload mechanism that was low cost, easy to handle and provided the "proper" preload during both the elastic and inelastic phase of loading. That is, based on the proposed theoretical model, one would like the preload resistance to rotation to increase after fracture, simulating the shift of the preload force P_v from the centerline to the tension face. See Fig. 3-13.

One could induce easily a reasonable simulation of the static resistance curve, but dynamic considerations, which are of major importance, led to the pivotal system shown in Fig. 3-15.

If a two-phase freebody of the wall for this sytem is drawn, (see Fig. 3-16), it can be seen that: (1) the vertical loads do not shift to the tension face as in Fig. 3-13, and (2) the resistance of phase two only lasts 4 in. of travel. That is, if the wall has center pivots, the geometric resistance only exists for 4 in. = (t/2) of travel instead of the 8 in. if the pivot point shifted to the downstream face, or if the pivots were placed initially at the downstream face.

The model provides the factors for a table and plot comparable to that shown in Fig. 3-14. This is shown below and in Fig. 3-17 (for σ_r = 50 and 300).

σ_r	P_v	p (Static) PRE-FRACTURE	p (Static) POST-FRACTURE
50	0	0.49	0.10
50	2W	0.63	0.49
150	0	1.42	0.10
150	2W	1.55	0.49
300	0	2.80	0.10
300	2W	2.83	0.49

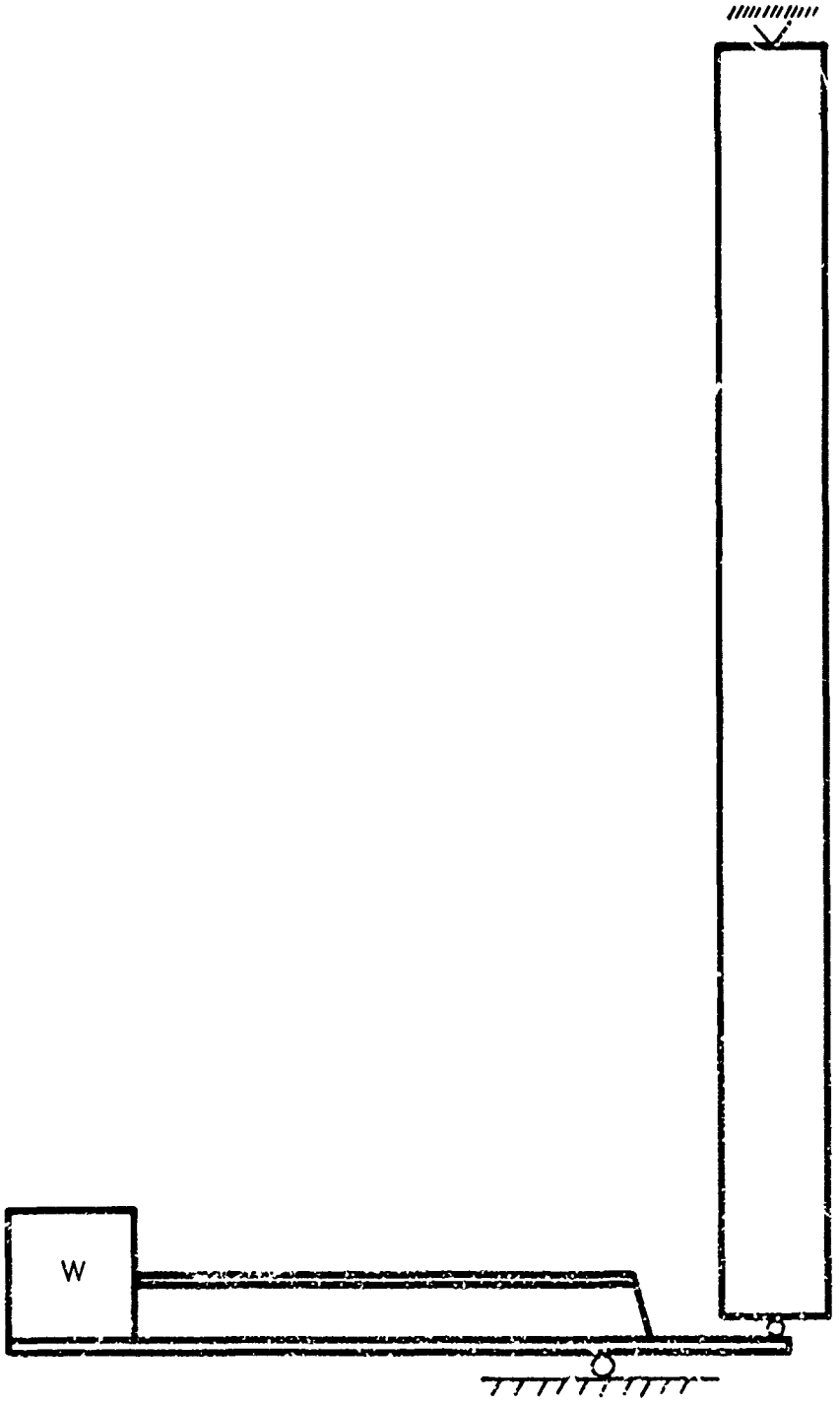

Fig. 3-15. Preload System Configuration

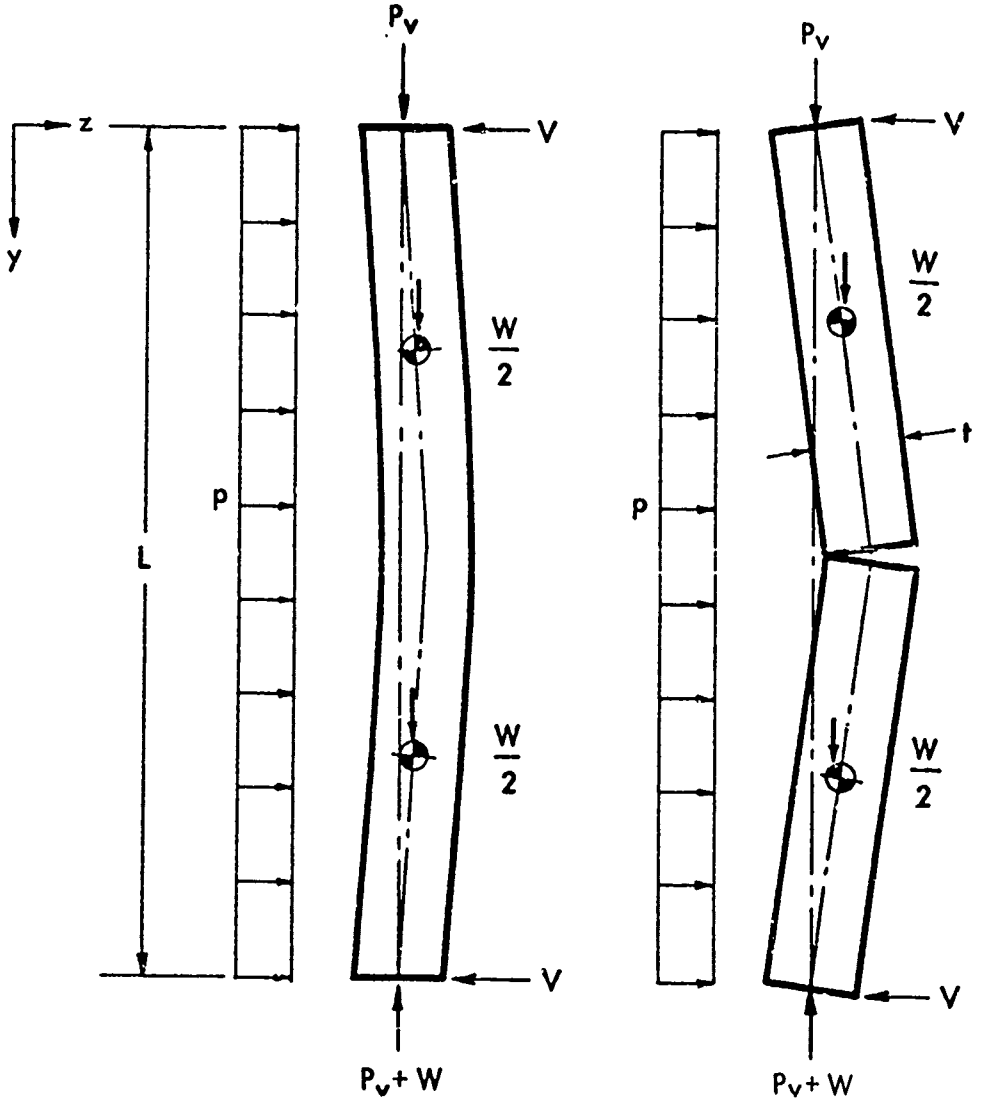

(a) Elastic Bending Phase

(b) Secondary Phase

Fig. 3-16. Failure Model

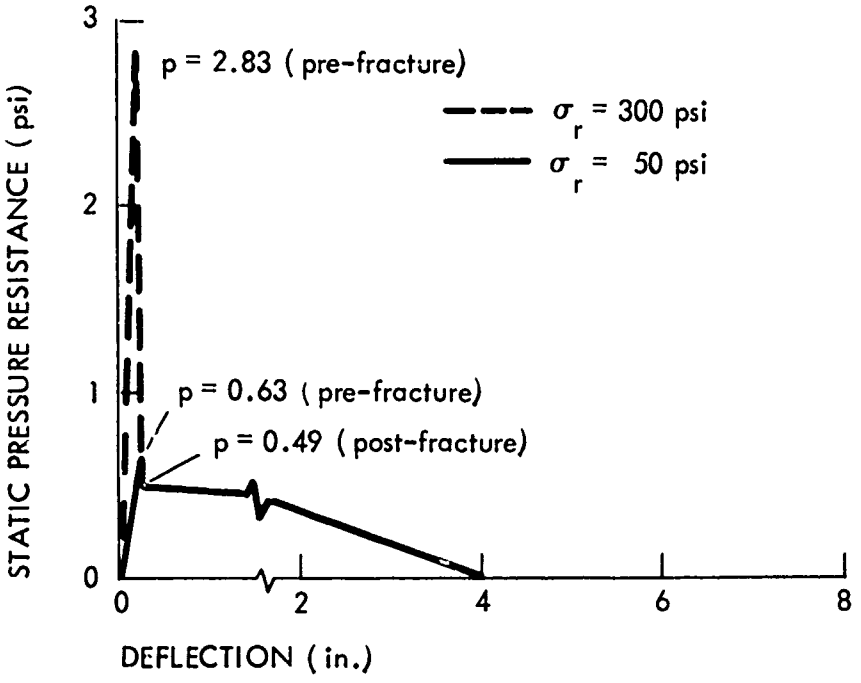

Fig. 3-17a. Resistance Function for an 8-in. Brick Wall with a Preload of 2W Beginning at the Central Pivot, σ_r = 50 and 300 psi

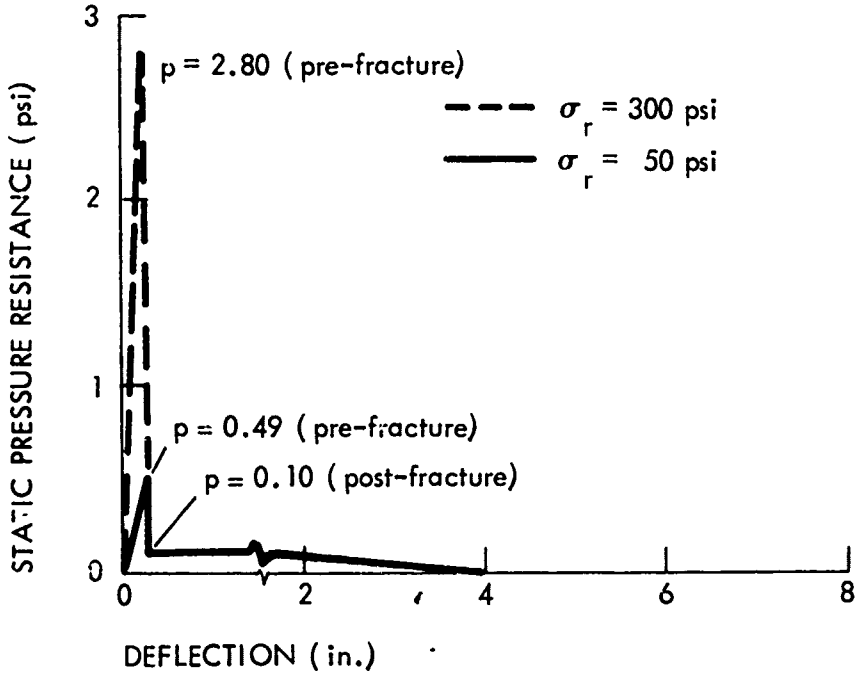

Fig. 3-17b. Resistance Function for an 8-in. Brick Wall without Preload, but with Weight of Wall Staying Over the Central Pivot, σ_r = 50 and 300 psi

Study the table, and the graph shown in Fig. 3-17. It can be seen that the post-fracture resistance is one-half that of the earlier "shifting-P_v" model. In addition, the resistance decreases to zero in one-half the center line travel. Some of these difficulties could be eliminated by placing the pivotal point at the tension face of the wall which would provide a resistance curve somewhat like that with the shifting vertical load shown in Fig. 3-14. The actual curve is shown in Fig. 3-18. The difference is that the elastic resistance is a bit higher, and the post-fracture strength is identical to the proposed model. Before adopting an experimental configuration, consider the dynamic problem somewhat further.

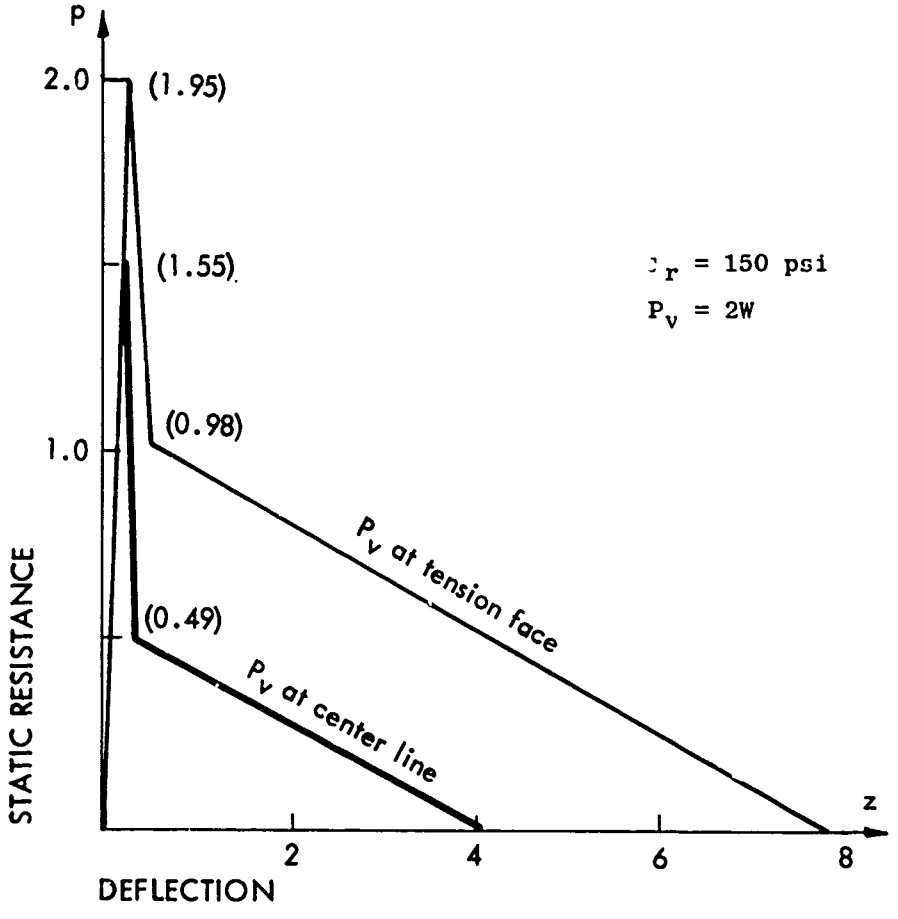

Fig. 3-18. Static Equivalent Resistance Function for 8-in. Brick Wall

For example, consider an academic problem of the cam and follower type as shown in the following sketch. Assume a massless spring with spring constant k, and $X = 0$, $X_1 = 0$ prior to the follower hitting the ramp.

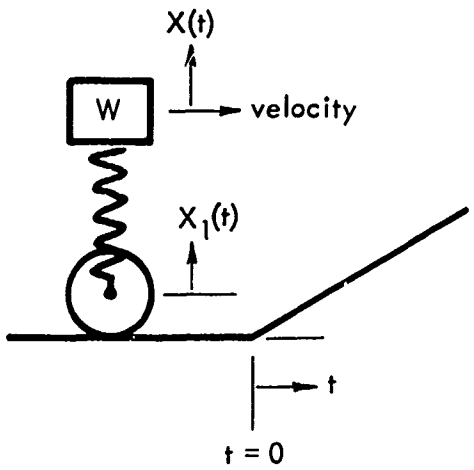

Let

$$r_1 = X - X_1$$

and

$$X_1 = bt$$

where b has the units of velocity. Then one may write

$$\frac{W\ddot{X}}{g} + k(X - X_1) = 0 \text{ for } t \geq 0$$

which has a solution

$$X = bt - \frac{b}{\omega} \sin \omega t$$

or

$$\eta = - \frac{b}{\omega} \sin \omega t$$

which can be illustrated in the sketch below.

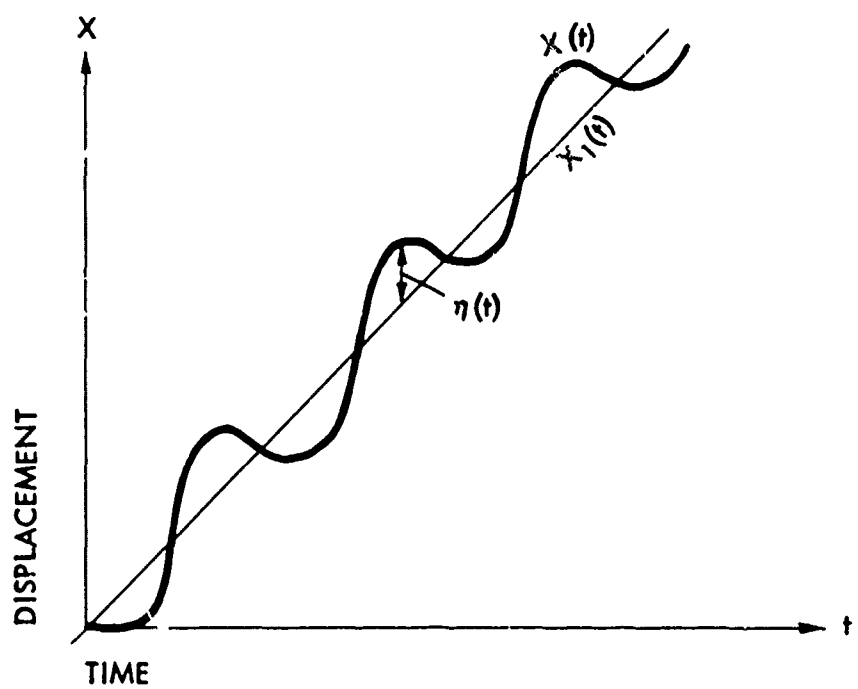

The next problem to be treated is shown as a lever arrangement where the lever is also a spring. Let one end start to move with a displacement given by δt, and let the lever arm lengths be ℓ and $\alpha\ell$ (see sketch).

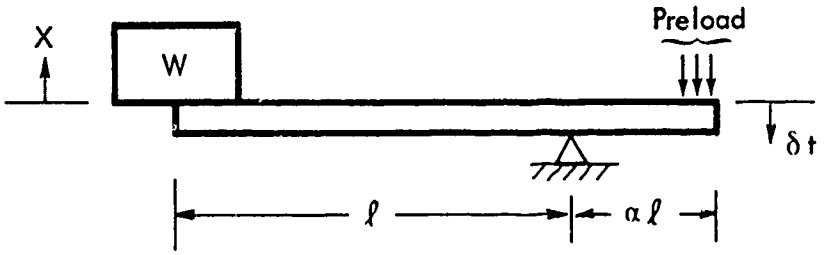

Then

$$X_1 = \frac{\delta}{\alpha} t$$

From the previous solution we see that the motion of W can be described by

$$X = \frac{\delta}{\alpha} t - \frac{\delta}{\alpha\omega} \sin \omega t$$

from which the oscillation of the lever (spring) about the line $X = \delta/\alpha\ t$ is

$$\eta = - \frac{\delta}{\alpha\omega} \sin \omega t$$

and the motion of mass would have the same form as shown in the preceding sketch.

The natural frequency can be written

$$\omega^2 = \frac{g}{X_{st}}$$

where

$$X_{st} = -\frac{W\ell^3}{3EI}(1 + \alpha)$$

or

$$\omega^2 = \frac{g}{W} \cdot \frac{3EI}{\ell^3(1 + \alpha)}$$

Therefore

$$[\eta]_{max} = \frac{\delta}{\alpha\omega} = \frac{\delta}{\alpha}\sqrt{\frac{W\ell^3(1 + \alpha)}{g3EI}}$$

Assume that it is desirable for the wall to move 4 in. in 100 ms. If $\alpha = 1/4$ then $\delta = 10$ in./sec would accomplish this. Let W = 1500 lb. Then, for example, one has

X_{static}	$[\eta]_{max}$	D.L.F. $= \left[\frac{\eta + X_{st}}{X_{st}}\right]$
1.00	2.0	3.0
0.10	0.63	7.3
0.01	0.20	21.0
0.001	0.063	64.0
0.0001	0.02	201.0

It is obvious that the stiffer the beam, the greater the D.L.F. and the stronger the support hardware must be. Now consider a few specific cases to establish the system response.

CASE	I	[η]	D.L.F.	τ
1	1.33 $in.^4$	3.04 in.	4.04	0.37 sec
2	100	0.235	18.6	0.037
3	1,000	0.0742	56.6	0.003

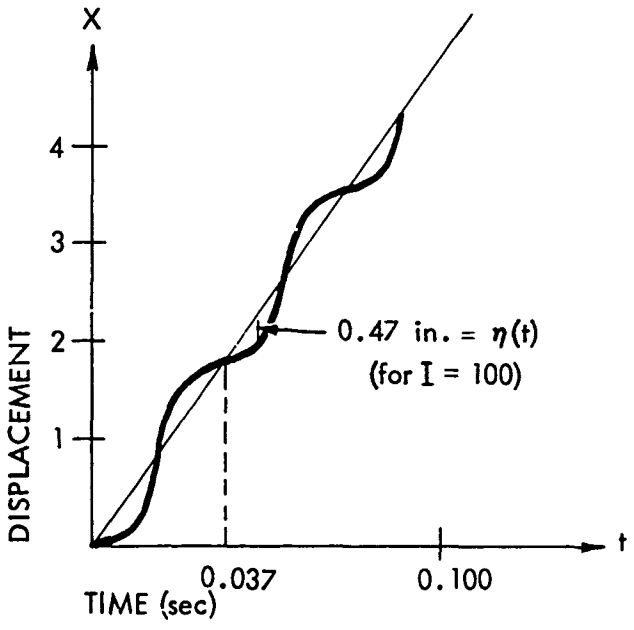

Observe that for case 2, the mass vibrates several times during the 100 msec of interest. The preload would be of the same nature, since it is directly proportional to the vibratory portion of the motion. Hence, the preload would go from + 18.6 P_v (static) to - 18.6 P_v (static), a very undesirable situation. In addition, for the preload structure to survive this, it would have to be very strong, i.e., with a design stress allowable of 1,000 psi, and thus would be very heavy and difficult to install. Since the design goal is a constant or a well-behaved preload, this vibrating form of motion cannot be used.

Next, consider the case of a yielding spring. Assume an ideally plastic material for this trial analysis, realizing that some actual difference in performance will result, but the concept will hold.

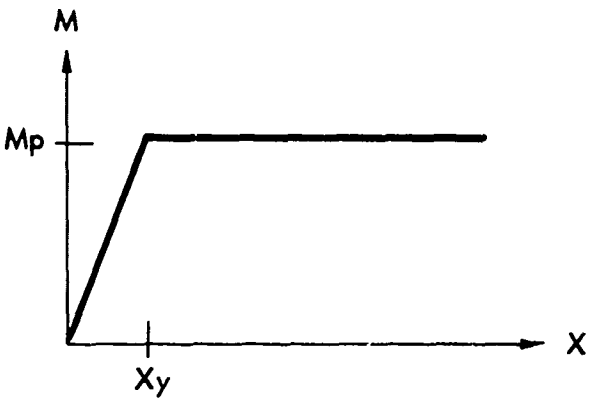

That is, M_p (full plastic moment) equals M_y (yield moment). If there were an elastic phase

$$X = \frac{\delta}{\alpha} t - \frac{\delta}{\alpha\omega} \sin \omega t$$

and

$$\dot{X} = \frac{\delta}{\alpha} - \frac{\delta}{\alpha} \cos \omega t$$

Assume that the spring yields immediately, i.e., $X = X_y$ at $t = 0$. The non-elastic phase of motion is described by the following differential equation.

$$M\ddot{X} + kX_y = 0 \text{ for } \tau \geq 0$$

or, with $\omega^2 = k/M$

$$\ddot{X} = -\omega^2 X_y$$

$$\dot{x} = - \omega^2 X_y \tau + C_1$$

$$X = - \omega^2 X_y \frac{\tau^2}{2} + C_1 \tau + C_2$$

Since it is assumed that $X_y = X_{st}$, that is, the spring is on the threshold of yield due to the static load in $t_y = t = 0$,

$$X = - \frac{g}{2} \tau^2$$

Since

$$\eta = X - X_1$$

and

$$X_1 = \frac{\delta}{\alpha} \tau,$$

$$\eta = - \frac{\delta}{\alpha} \tau - \frac{g}{2} \tau^2$$

The foregoing function is illustrated below and shows an increasing net displacement with time.

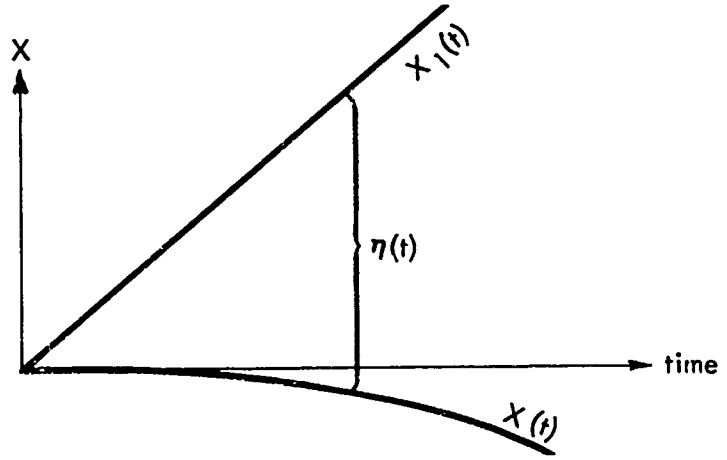

This function would provide a desirable preload force, i.e., P_v is constant. That is, if one had an ideally plastic spring and could provide a preload just below yield of the spring, the resistance function shown in Fig. 3-18 could be dynamically provided, i.e., the static equivalent resistance function could be maintained under dynamic test conditions.

Note in Fig. 3-18, if the wall pivots about the center line, the elastic portion of the system is modeled accurately, but the post-fracture resistance portion is reduced. Alternately, if preload is provided at the tension face, the post-fracture behavior is correctly modeled, and the pre-fracture behavior is enhanced.

Next one must consider a "real world" spring. In order to have an applicable spring constant or load deflection curve, the actual yielding portion (bars) of the preload structure (see Fig. 3-20) were statically tested as shown below. The results are plotted in Fig. 3-19.

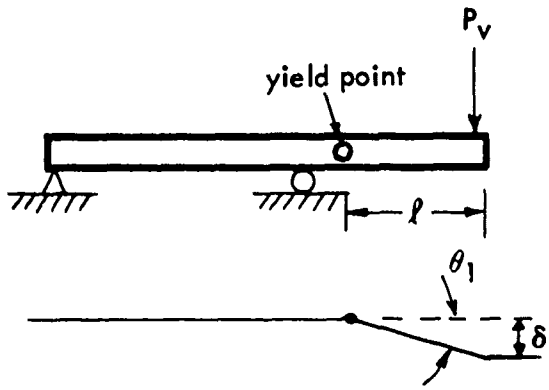

From Fig. 3-19, the resistance function shown in Fig. 3-21 evolved. That is, if the preload pivot is placed at the tension face of the wall, both pre-fracture and post-fracture strengths are enhanced by the test set up. Alternately, if we elect to pivot the wall about the center line, the pre-fracture strength is correctly modeled as in the ideally plastic material, and the post-fracture strength is closer to the proposed shifting P_v resistance line than the ideal spring provides.

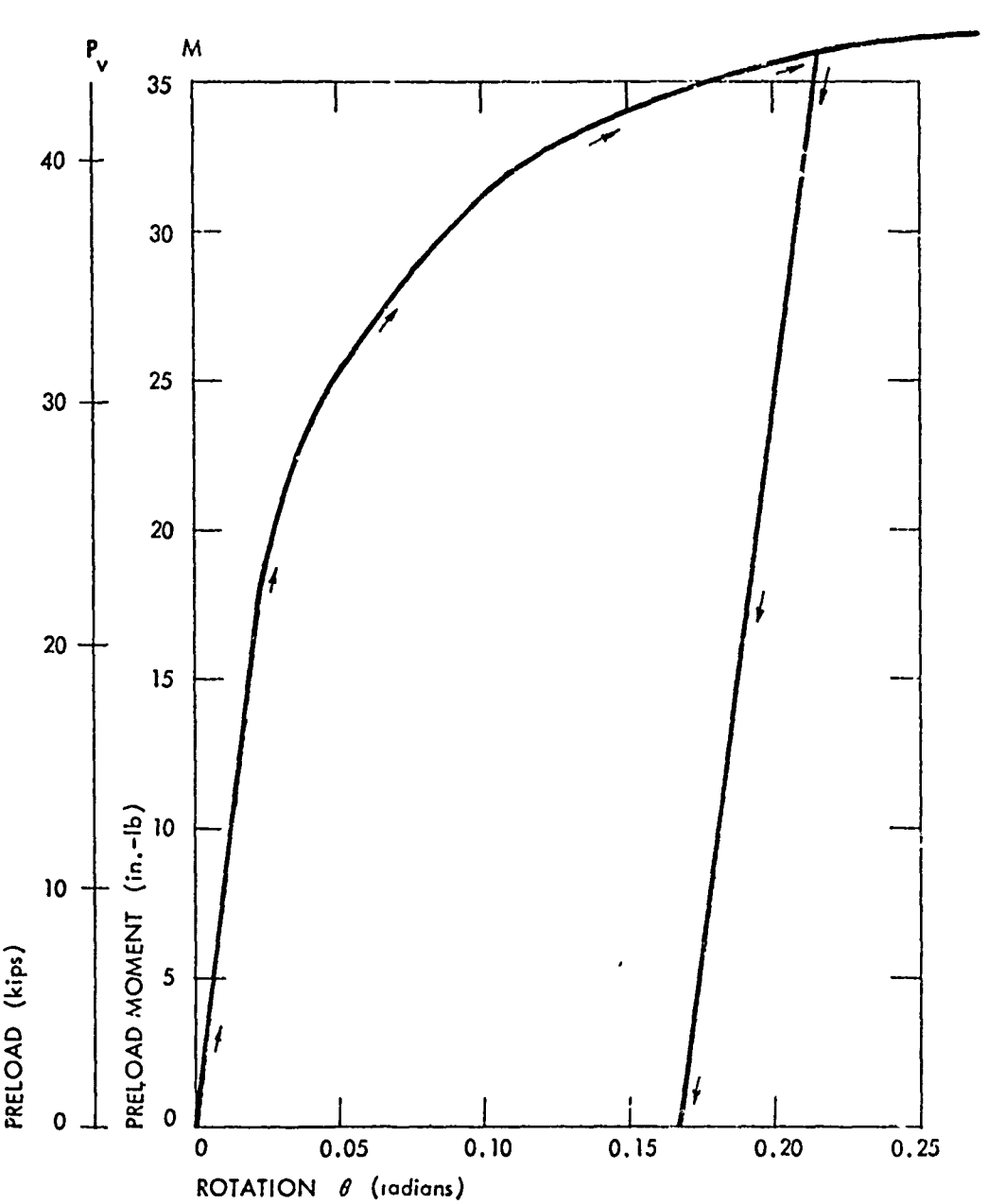

Fig. 3-19. Preload vs Deflective Curve for Preload Mechanism

The wall is unstable when

$$\Phi \cong \frac{4}{48} \text{ radians}$$

$$\delta = 8\Phi = 2/3 \text{ in.}$$

where δ is the vertical motion of the pivot point at the base of the wall.

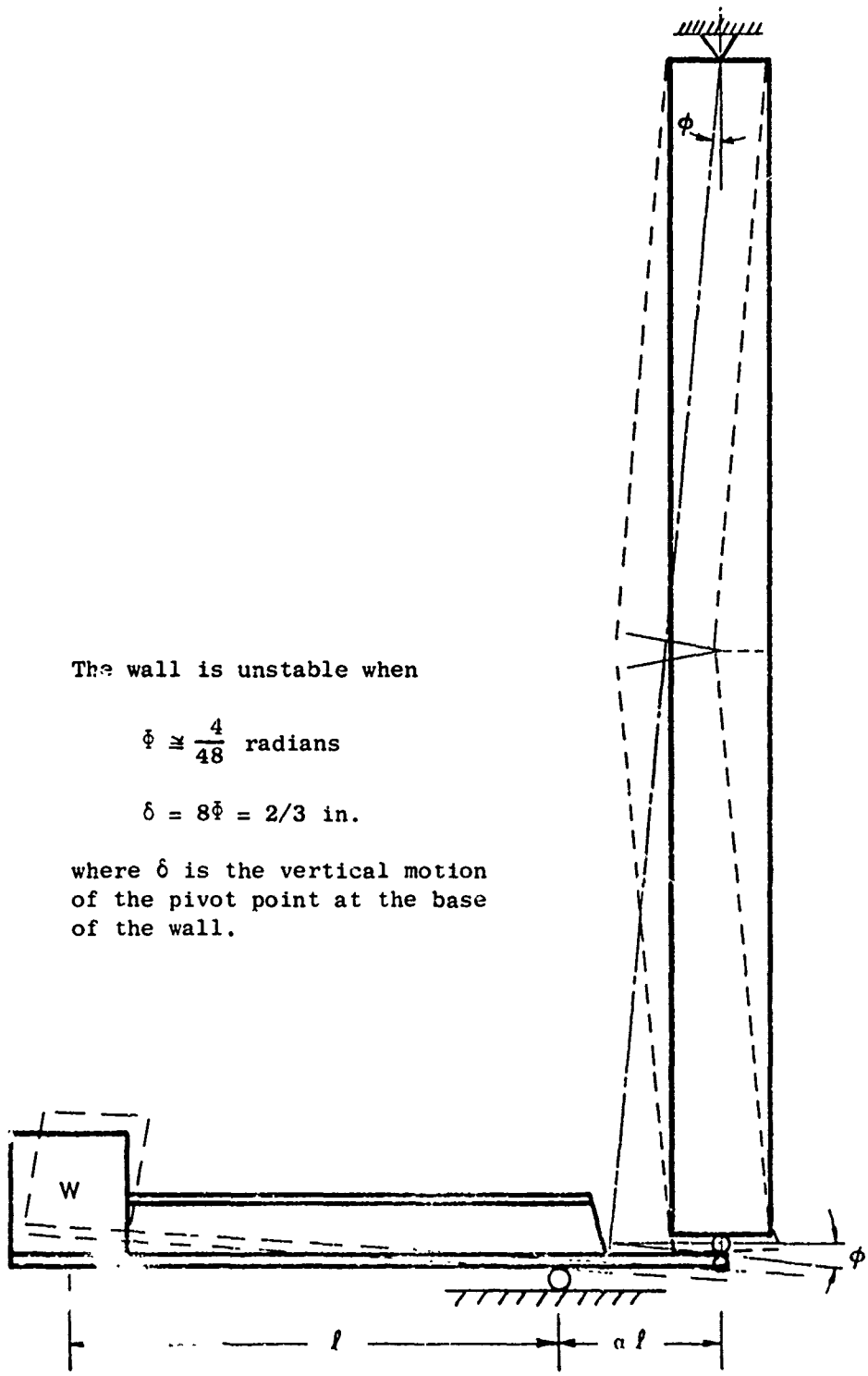

Fig. 3-20. Preload System Configuration

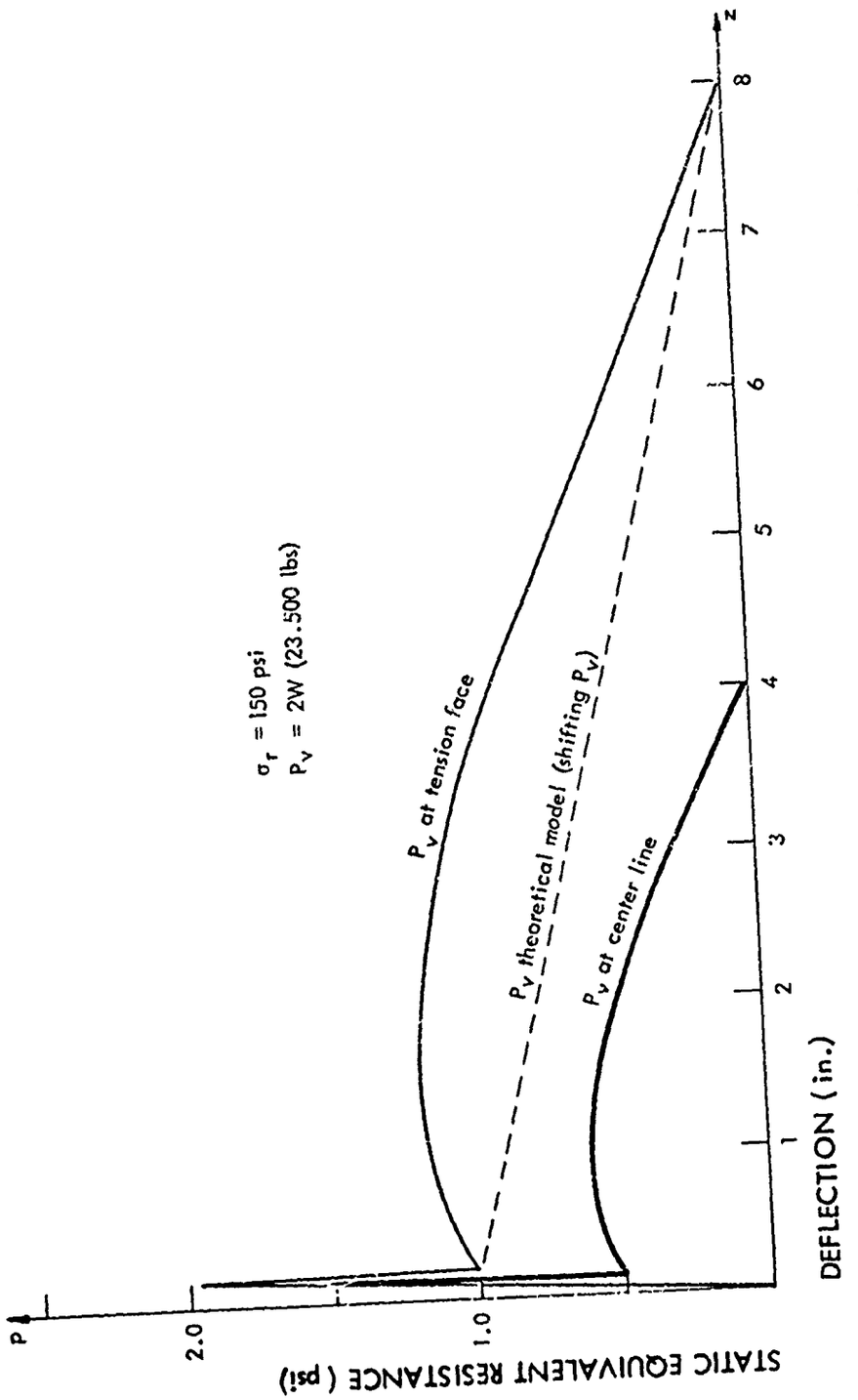

Fig. 3-21. Static Equivalent Resistance Functions for 8-in. Brick Wall

In order for a wall to collapse, there must be fracturing; therefore, this is a necessary condition for collapse. In addition, there must be enough energy in the loading to overcome the post-fracture resistance; therefore, this is a sufficient condition for collapse.

The decision was made to hold the pivot point at the center of the wall for the following reasons:

1. One of the desired goals is to establish lower bounds on failure; hence, it is undesirable to enhance the pre-fracture strength.

2. The URS test walls seem more probable to have strengths greater than 150 psi; hence, the pre-fracture resistance is enough higher than the post-fracture resistance to make the pre-fracture times more interesting.

3. This being the first preload test series, there is ample opportunity to alter the scheme after evaluating some of the test data.

Preload Wall Panel Test Results

A total of four 8-in. nonreinforced brick preloaded wall panels were tested during this reporting period. The wall numbers and preload values are summarized below.

WALL NO.	PRELOAD (lb)
64	16,500
65	16,500
66	23,500
67	23,500

Test Results, Wall No. 64 - Two one strand Primacord tests were conducted on this wall panel. The measured peak reflected overpressure for both tests was approximately 1.5 psi. On the first test (No. 08-30-71-01) the wall cracked but did not collapse. The first crack gage indicated a crack at 62 msec,

which is the time of the second maximum positive deflection. The second crack gage broke at 87 msec, which is 7 msec after the second negative maximum deflection. The third crack gage broke at 100 msec, which is the time of the third positive maximum deflection. The crack, which showed very little spalling, was horizontal along one course of bricks and was located just above the midpoint of the wall. The maximum measured load obtained by summing all load cells was 18,600 lb at about 20 msec vs a predicted 21,600 lb reaction, i.e., DLF = 1.73. On the second test (No. 08-30-71-02), the wall collapsed and all debris landed within 10 ft. The maximum measured load for this second test was 2,900 lb measured at approximately 15 msec. Pre- and post-test photographs of this wall are shown in Fig. 3-22 and a plot of displacement as a function of time is presented in Fig. 3-23.

Test Results, Wall No. 65 - A single test (No. 09-07-71-01), using one strand of Primacord was conducted on the wall. The measured peak reflected overpressure was 1.6 psi and the wall collapsed with all debris landing within 10 ft. Crack gages indicated a crack at one of the off-center gages at 19 msec which closed again at 20 msec and then reopened at 24 msec. The other two gages indicated cracks at 25 msec. The maximum measured load was 11,700 lb at approximately 20 msec. A plot of displacement vs time for this test is presented in Fig. 3-24.

Test Results, Wall No. 66 - A single one strand test (No. 09-13-71-01) was conducted which gave a measured peak reflected overpressure of 1.6 psi. The wall cracked on this test and was not tested again. The crack gages indicated cracks at the two off-center gages at 18 and 24 msec. The middle crack gage indicated a crack at 66 msec. Slight spalling was noted on the downstream (tension) side of the wall. However, on the upstream (compression) side of the wall, an open crack was visible and considerable spalling was noted. The crack was not along one row of bricks but included 3 courses of bricks with diagonal cracks going through the bricks to reach the next course. The maximum measured load was 7,500 lb.

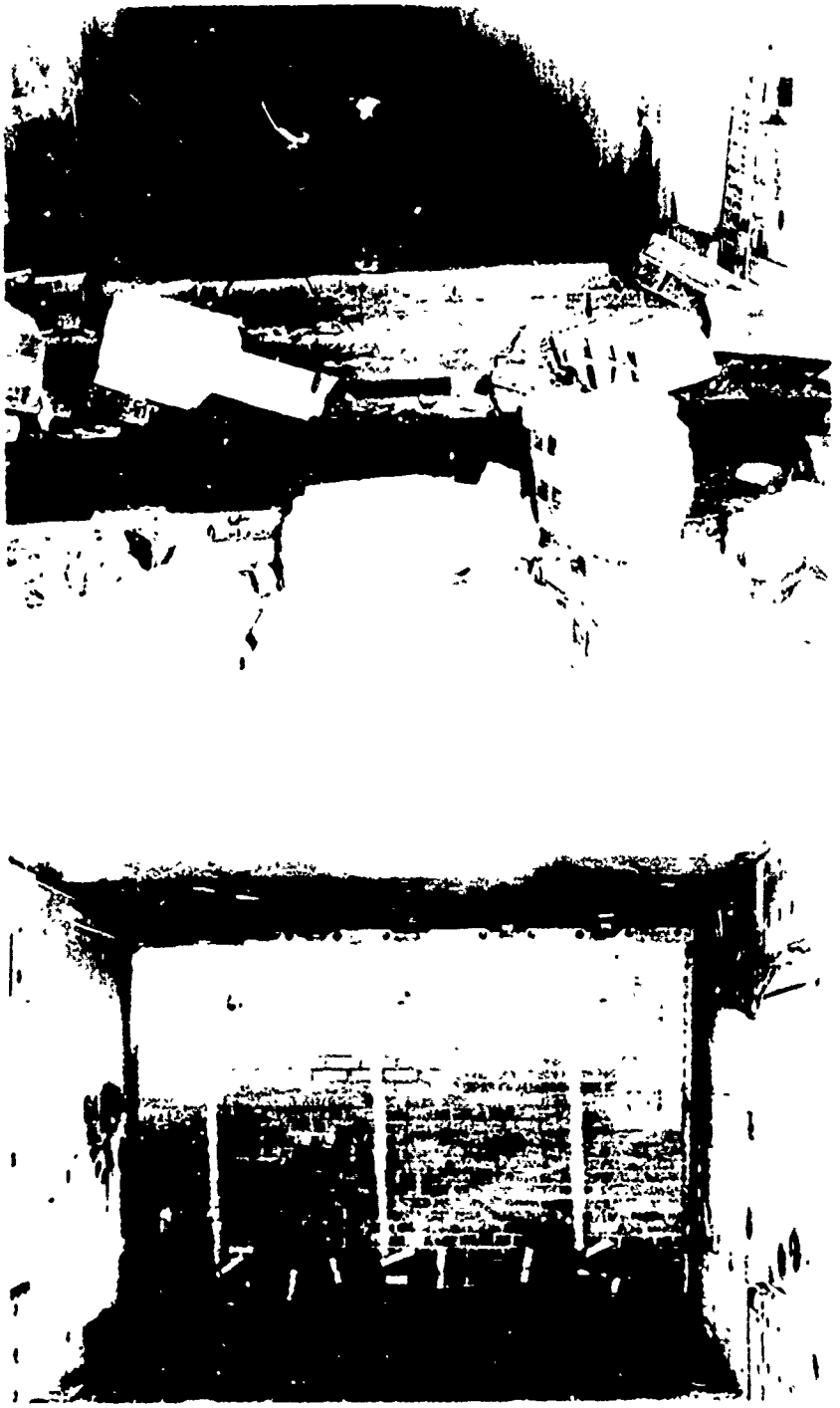

Fig. 3-22. Pre- and Post-Test Photographs of Wall No. 64, (No. 08-30-71-02), a 8 in. Nonreinforced Brick Wall with 16,500 lb Preload-Measured Peak Reflected Overpressure of 1.5 psi

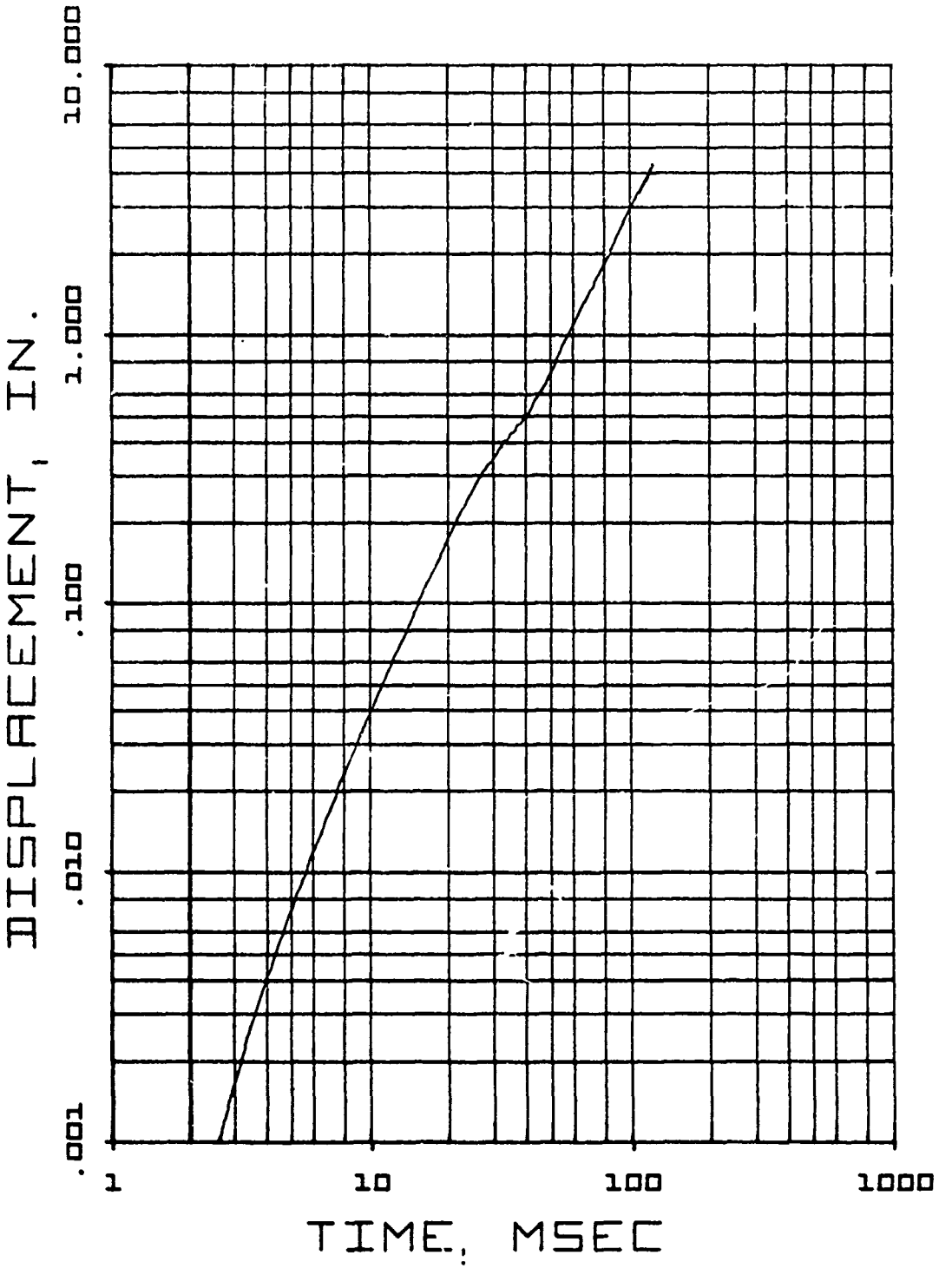

Fig. 3-23. Displacement as a Function of Time. Wall No. 64, Nonreinforced Preloaded Brick Wall (No. 08-30-71-02)

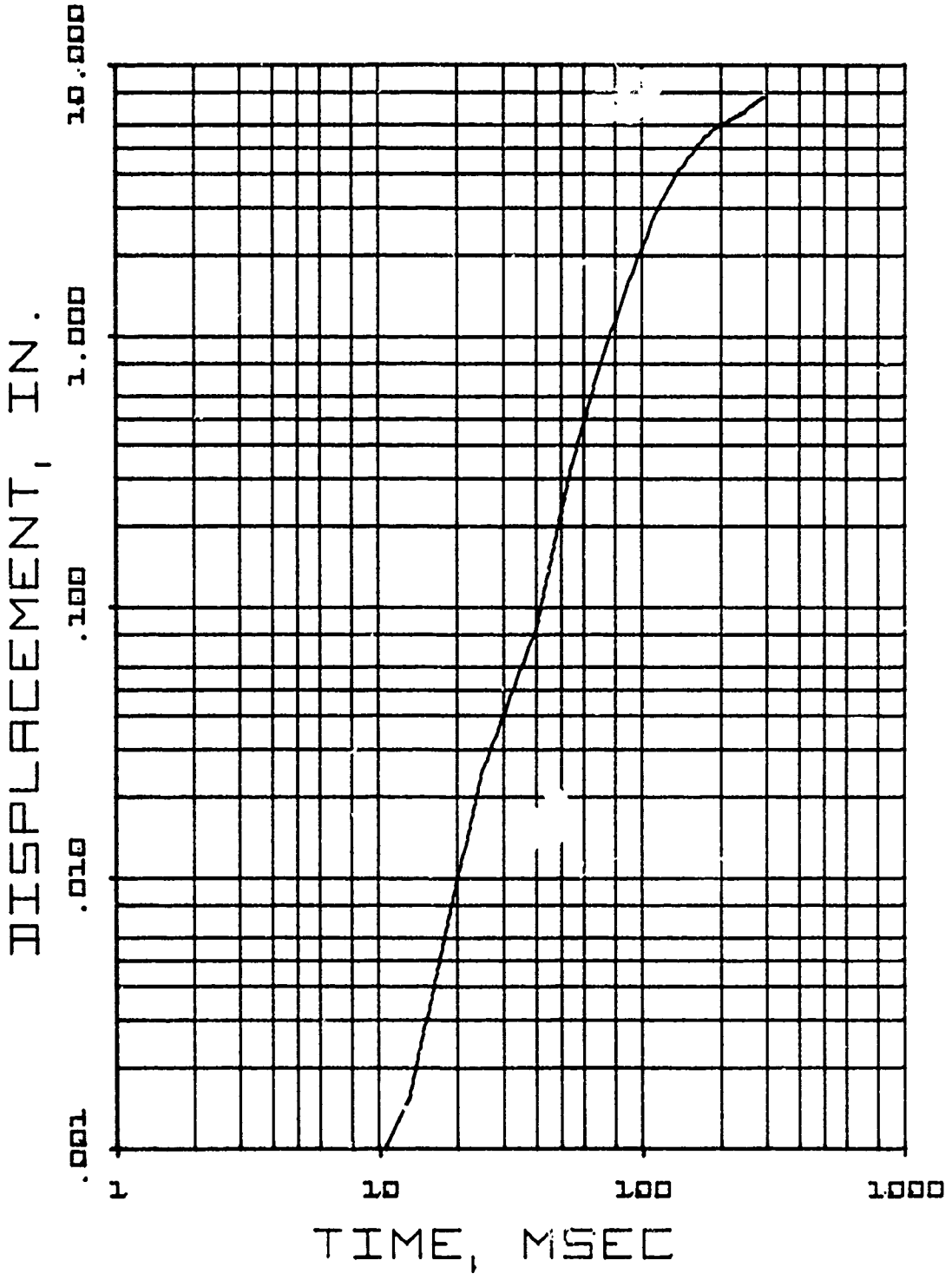

Fig. 3-24. Displacement as a Function of Time. Wall No. 65, Nonreinforced Preloaded Brick Wall (No. 09-07-71-01)

Test Results, Wall No. 67 - This wall was exposed to a measured peak reflected overpressure of 6.1 psi (Test No. 09-16-71-01). The wall collapsed and debris was scattered more than 40 ft with most of the debris between 10 and 30 ft. The three crack gages indicated cracks at 8 msec, 8 msec, and 9.5 msec. The maximum measured load was 34,000 lb at approximately 10 msec. A plot of displacement as a function of time is presented in Fig. 3-25.

These four preloaded walls behaved as predicted with an individual threshold of failure (that is, where cracks first appeared) of around 1.5 psi and an elastic strength increase from preload induced by a 3-story curtain wall or equivalent of the order of 10 percent which is far less than the scatter of material properties. This failure load infers an average modulus of rupture $\sigma_r \approx 180$ psi which is more like the static test data then failure theory predictions, see pg. 3-11.

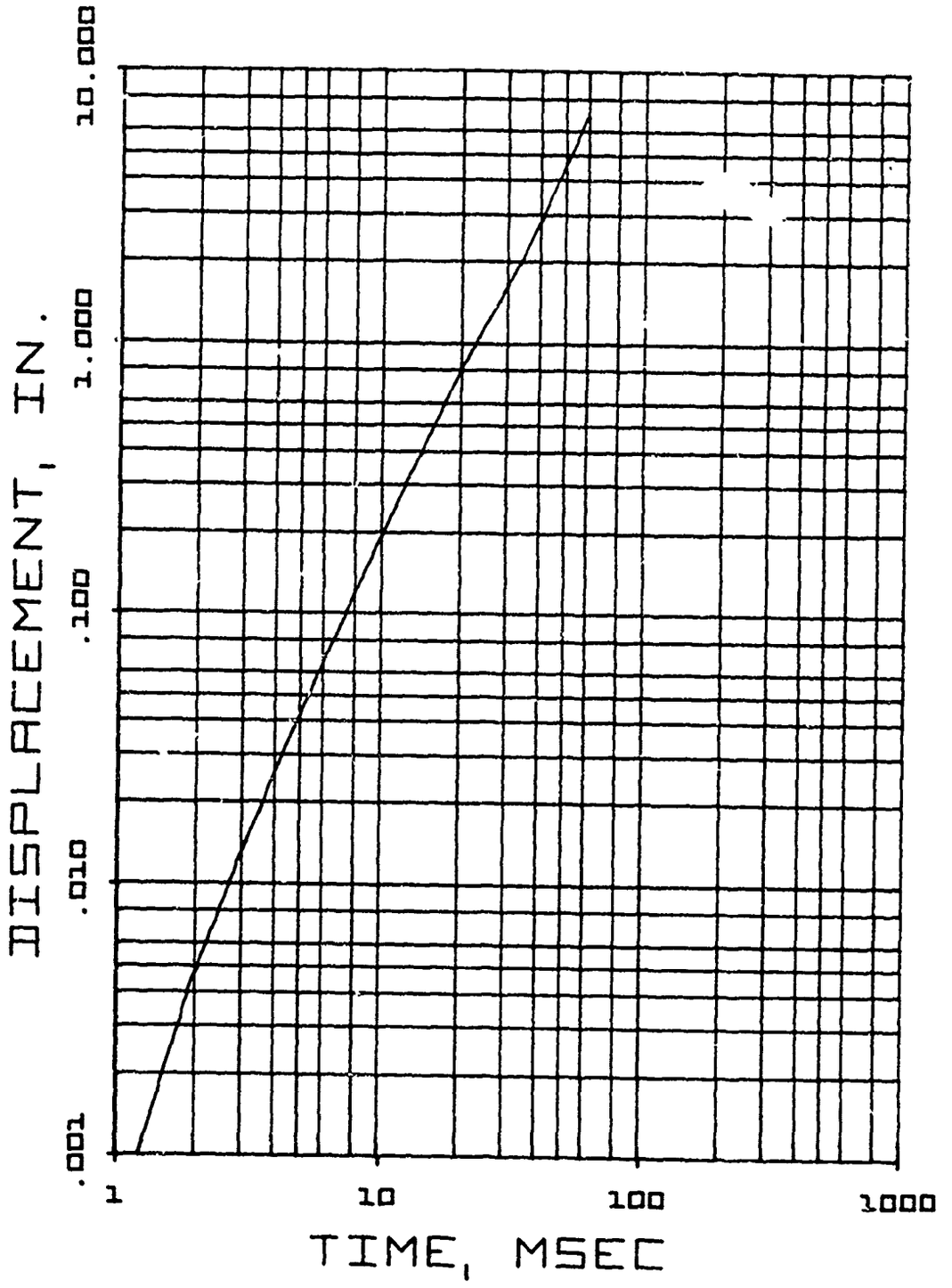

Fig. 3-25. Displacement as a Function of Time. Wall No. 67, Nonreinforced Preloaded Brick Wall (No. 09-16-61-01)

Section 4
WALLS WITH A DOORWAY

This section of the report presents the results from a loading test series of exterior walls with doorways, a discussion of some analytical work accomplished on this test geometry, and the results of two structural wall panel tests of 8 in. nonreinforced brick wall panels with doorways. All of these tests were conducted during this reporting period.

LOADING STUDY TESTS

The instrumentation locations for the loading tests are shown in Fig. 4-1. The loading information required for a wall with an opening is more complex than that required for the solid wall discussed in Section 3 because the blast wave can enter the opening which relieves the pressure on the front or blastward side of the wall and also loads the back side of the wall. Thus, one of the most interesting parameters is the net load or the difference between the load imposed on the front and back of the wall. As shown in Fig. 4-1, three pairs of gages are installed on the nonfailing wall with gages A, B and D installed on the front (toward the blast) and gages H, G and E installed at similar locations on the back of the wall. The net load at a point 12 in. from the doorway (i.e., the location of gage pair A-H) would then be the difference between the overpressures as a function of time measured at gage A and H. Also shown in Fig. 4-1 are the two shock tunnel monitor stations, gages 7 and 8 on the wall of the tunnel. Typical pressure gage traces and the digital data from this test series are presented in Appendix B. Summary plots for the gage pairs A-H, B-G, and D-E for one strand, three strand, and five strand tests are given in Figs. 4-2 through 4-10.

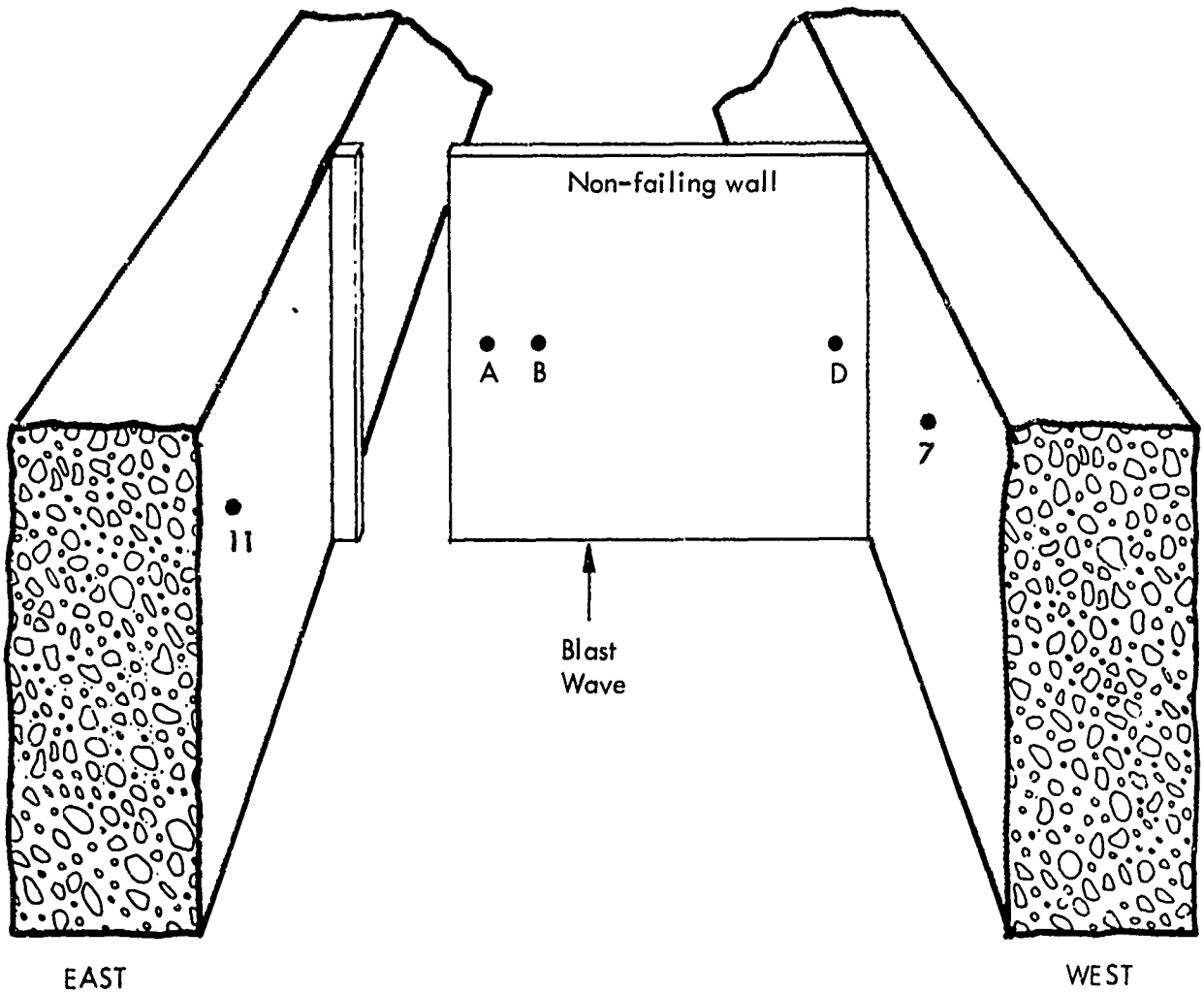

NONFAILING WALL GAGES

GAGE NO.	DISTANCE FROM FLOOR	DISTANCE FROM EDGE OF DOOR
A-H*	51"	12"
B-G*	51"	24"
D-E*	51"	108"

* Gages E, G and H are on back of the wall.

TUNNEL WALL GAGES

GAGE NO.	DISTANCE FROM FLOOR	DISTANCE FROM WALL
Westwall-7	45"	21"
Eastwall-11	49"	38"

Fig. 4-1. Instrumentation Location for Loading Study Tests with Doorway

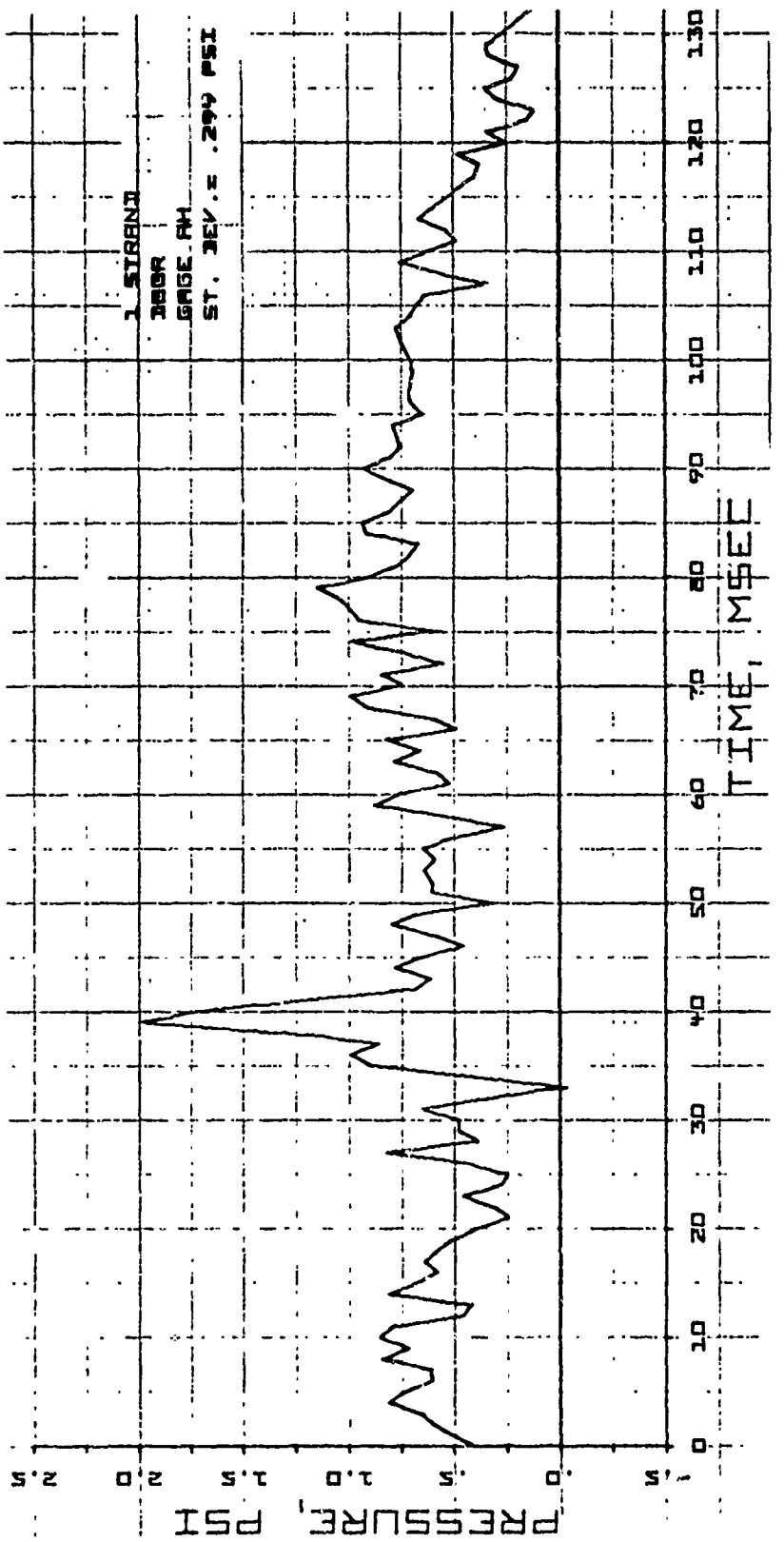

Fig. 4-2. Average Net Pressure as a Function of Time for One Strand Doorway Loading Study Tests 01-16-70-04, -05, and -06. Gage Pair A-H

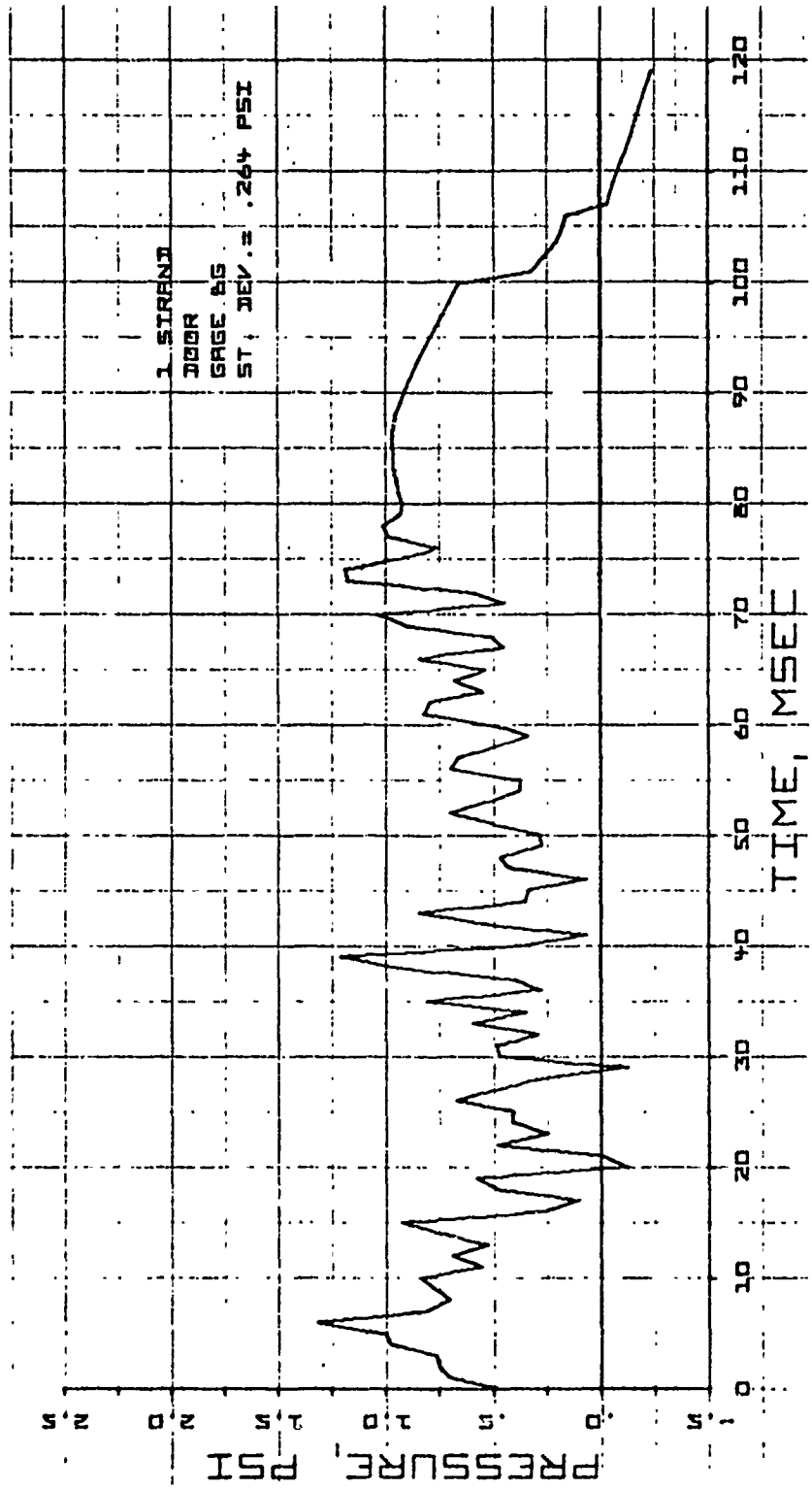

Fig. 4-3. Average Net Pressure as a Function of Time for One Strand Doorway Loading Study Tests 01-16-70-04, -05, and -06. Gage Pair B-G

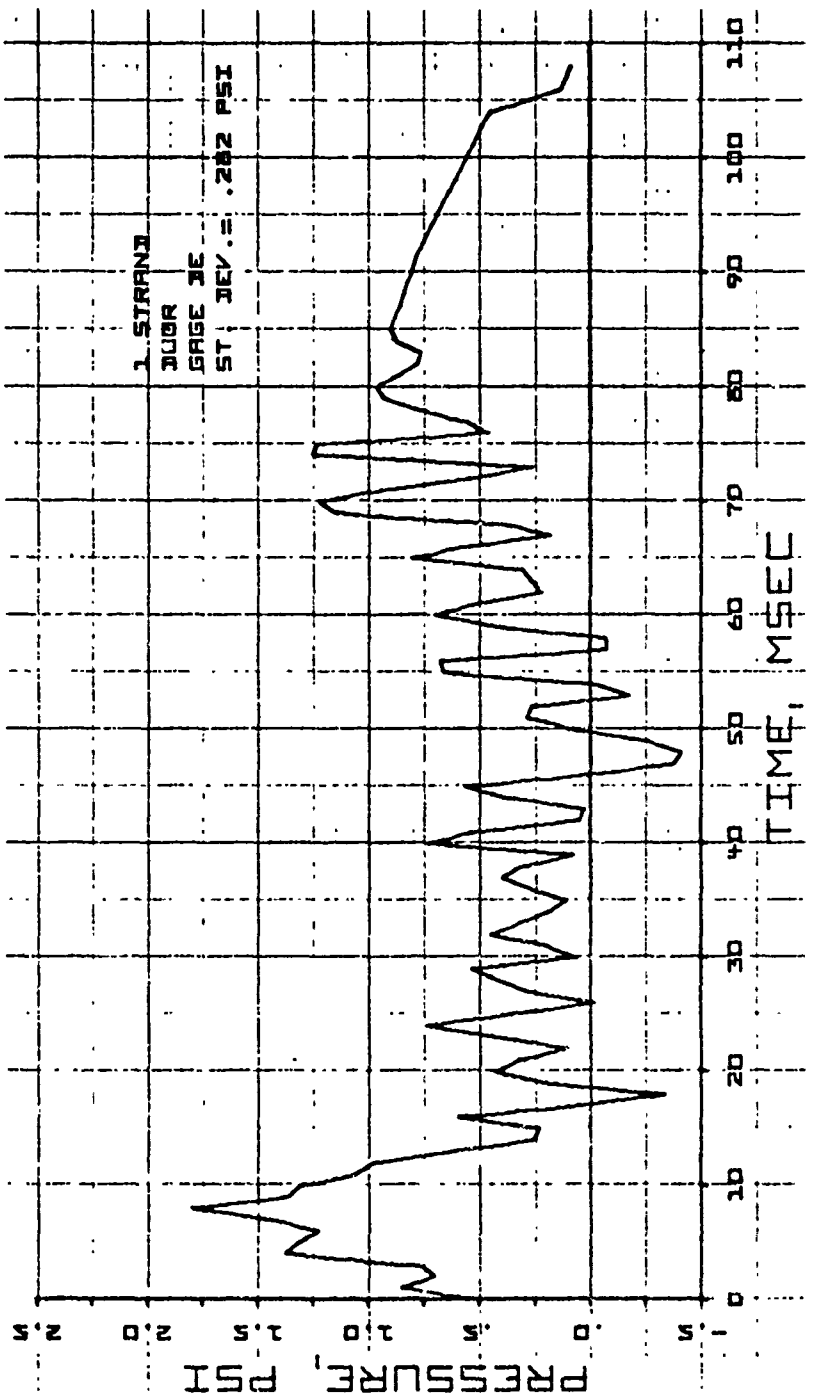

Fig. 4-4. Average Net Pressure as a Function of Time for One Strand Doorway Loading Study Tests 01-06-70-04, -05, and -06. ge Pair D-E

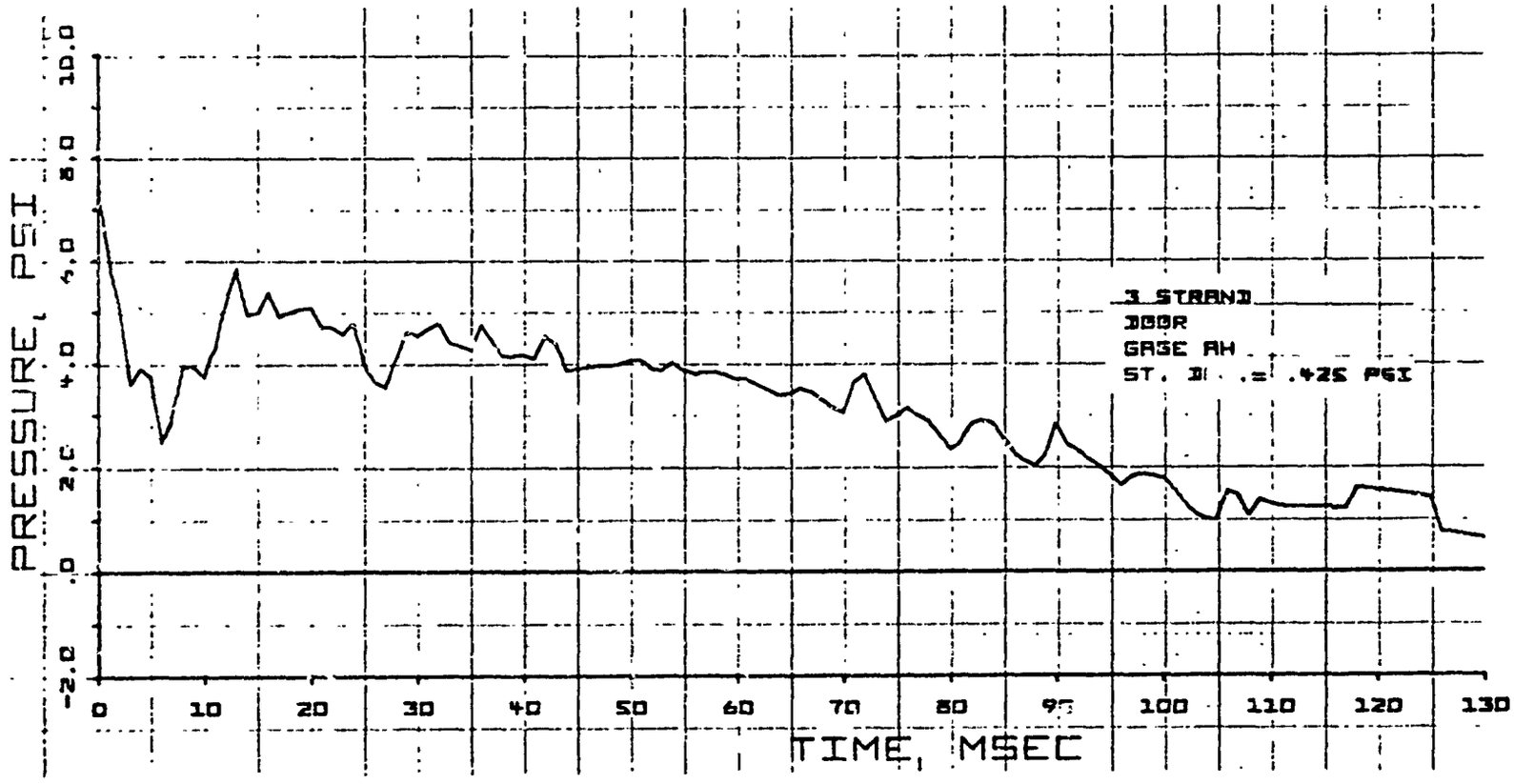

Fig. 4-5. Average Net Pressure as a Function of Time for Three Strand Doorway Loading Study Tests 01-16-70-03, 01-19-70-01 and -02. Gage Pair A-H

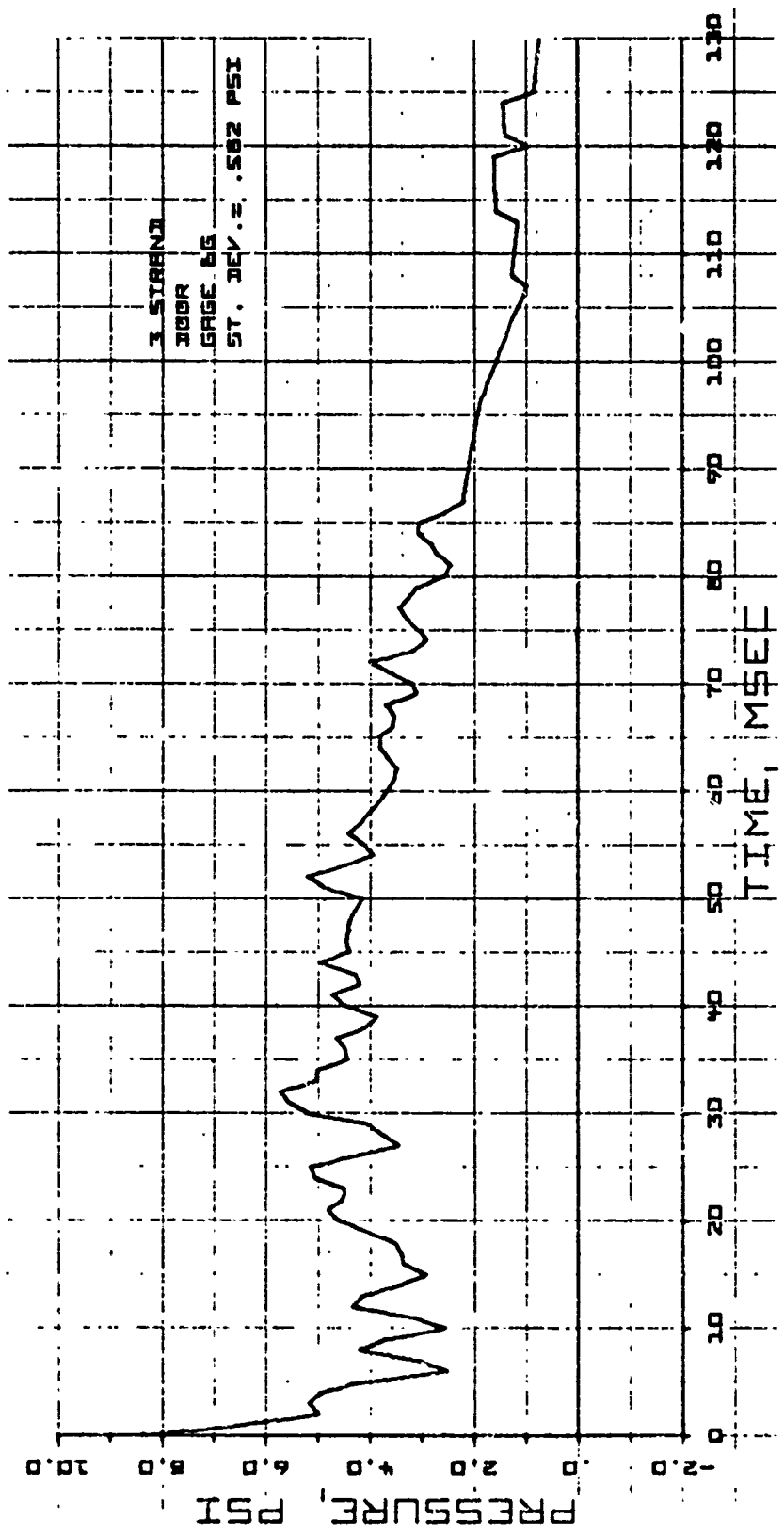

Fig. 4-6. Average Net Pressure as a Function of Time for Three Strand Doorway Loading Study Tests 01-16-70-03, 01-19-70-01 and -02. Gage Pair B-G

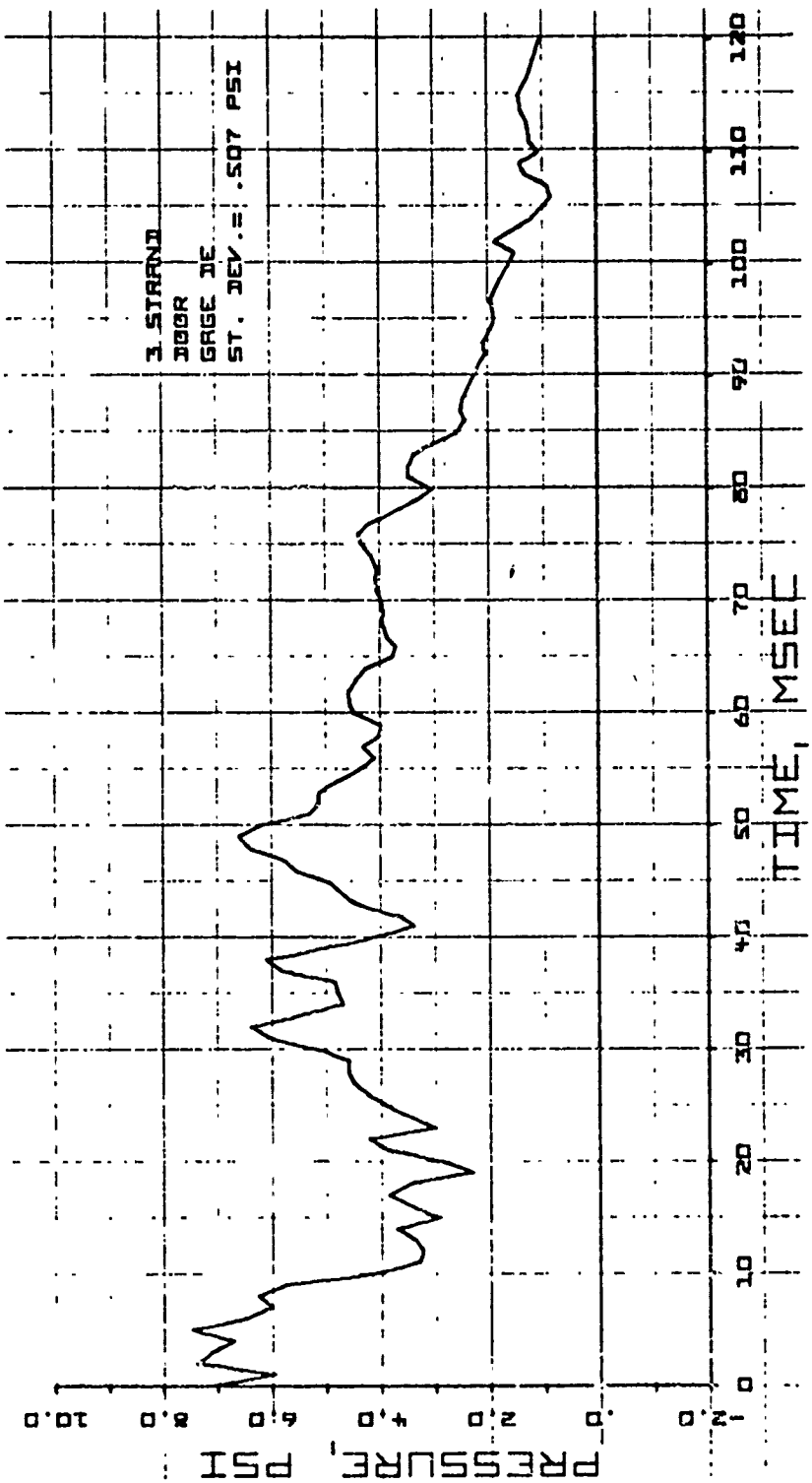

Fig. 4-7. Average Net Pressure as a Function of Time for Three Strand Doorway Loading Study Tests 01-16-70-03, 01-19-70-01 and -02. Gage Pair D-E

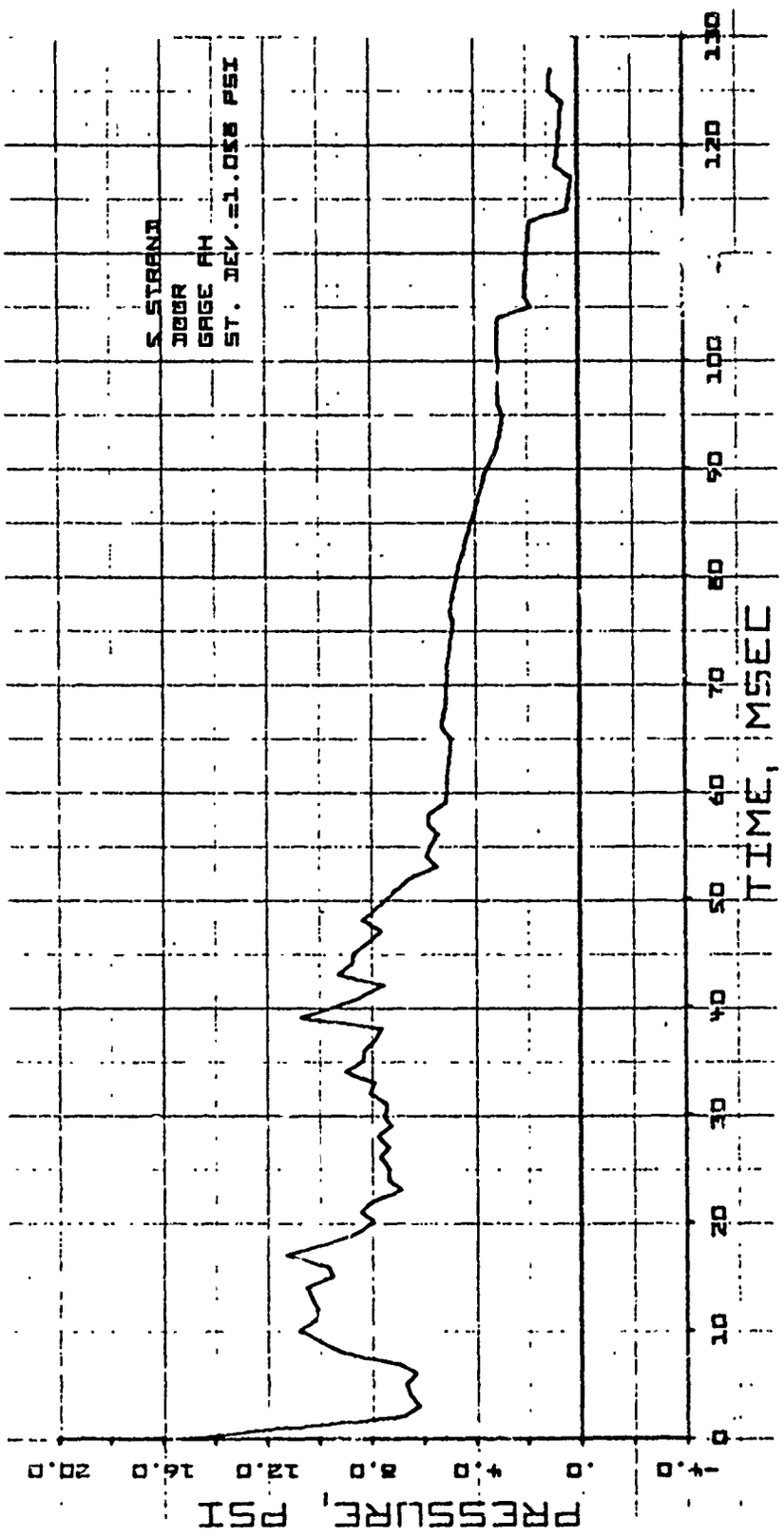

Fig. 4-8. Average Net Pressure as a Function of Time for Five Strand Doorway Loading Study Tests 01-19-70-03, -04, and 01-20-70-01. Gage Pair A-H

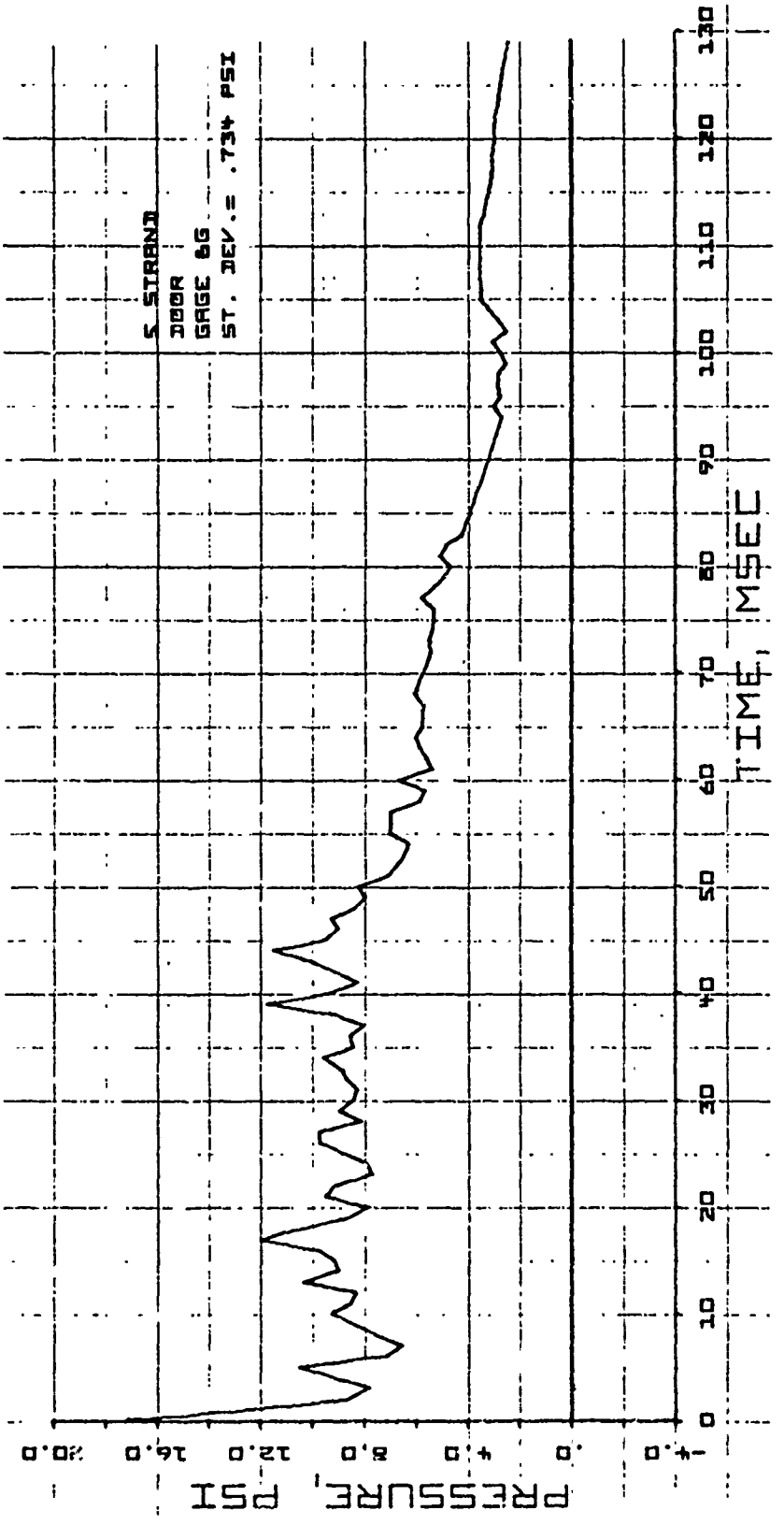

Fig. 4-9. Average Net Pressure as a Function of Time for Five Strand Doorway Loading Study Tests 01-19-70-03, -04, and 01-20-70-01. Gage Pair B-G

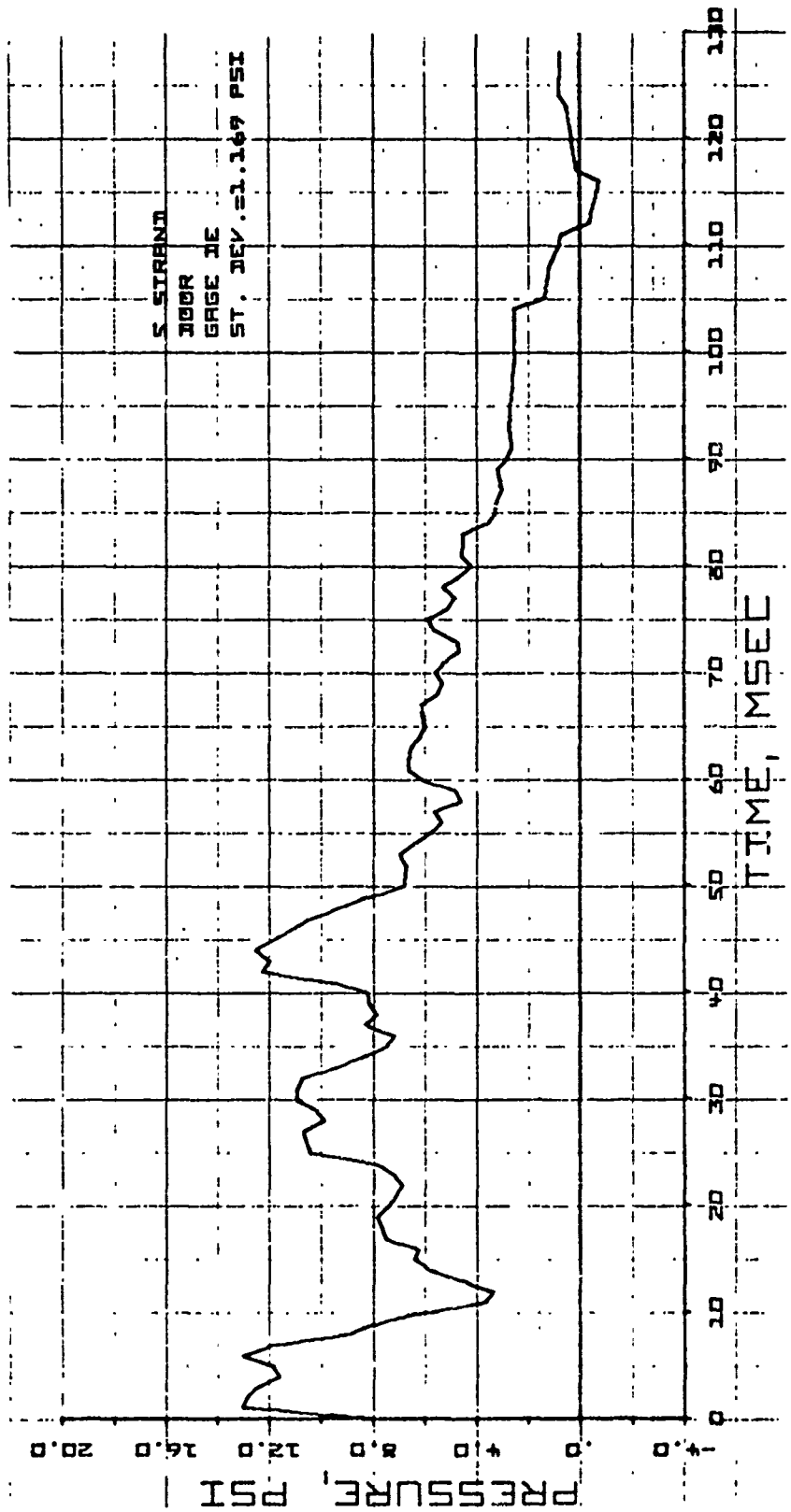

Fig. 4-10. Average Net Pressure as a Function of Time for Five Strand Doorway Loading Study Tests 01-19-70-03, -04, and 01-20-70-01. Gage Pair D-E

THEORETICAL CONSTRAINTS – Walls with a Doorway

To make calculations and predictions of this test geometry, the value of the more advanced and complete analysis procedures made available with the SAMIS computer code becomes obvious. When an opening (such as a door) is made in a wall panel, not only does the structure and its response change, but the loading function changes even more dramatically. With changes such as this, manual analysis becomes almost impossible.

The structural modeling for a brick wall with a doorway using the SAMIS computer code is shown in Fig. 4-11. The wall is the basic 8- by 12-ft by 8-in. brick wall with a 3-ft doorway cut from the right-hand side. The facets shown in the shaded area are removed from the computation.

A good deal of effort was expended trying to determine an acceptably accurate loading for the computer code. The dynamic response prediction is a step-by-step numerical integration of structural behavior; hence, loading must be supplied to each facet at each time increment used in the numerical integration.

In the case of the doorway, each facet is loaded differently at each time period, and input loads must be supplied at an interval between 1/10 and 1/20 of the highest period of the structure. For our system this meant one load every 0.1 msec or 200 input loads per mass for a 25 msec response prediction. However, the computer code has a built-in feature whereby it can generate linearly interpolated loads between points supplied.

Thus, to simplify the computation process by reducing the number of data points handled, straight-line approximations of the pressure-time plots obtained from the loading study are made. The rationale behind the use of this simplified data input is presented in detail in Ref. 5, and a typical example of SAMIS input data presented in this reference is given in Fig. 4-12. This input data was based on preliminary loading study data analysis available at that time. Comparisons of these straight-line approximations with the presently available data from Figs. 4-5 through 4-7 is shown in Fig. 4-13.

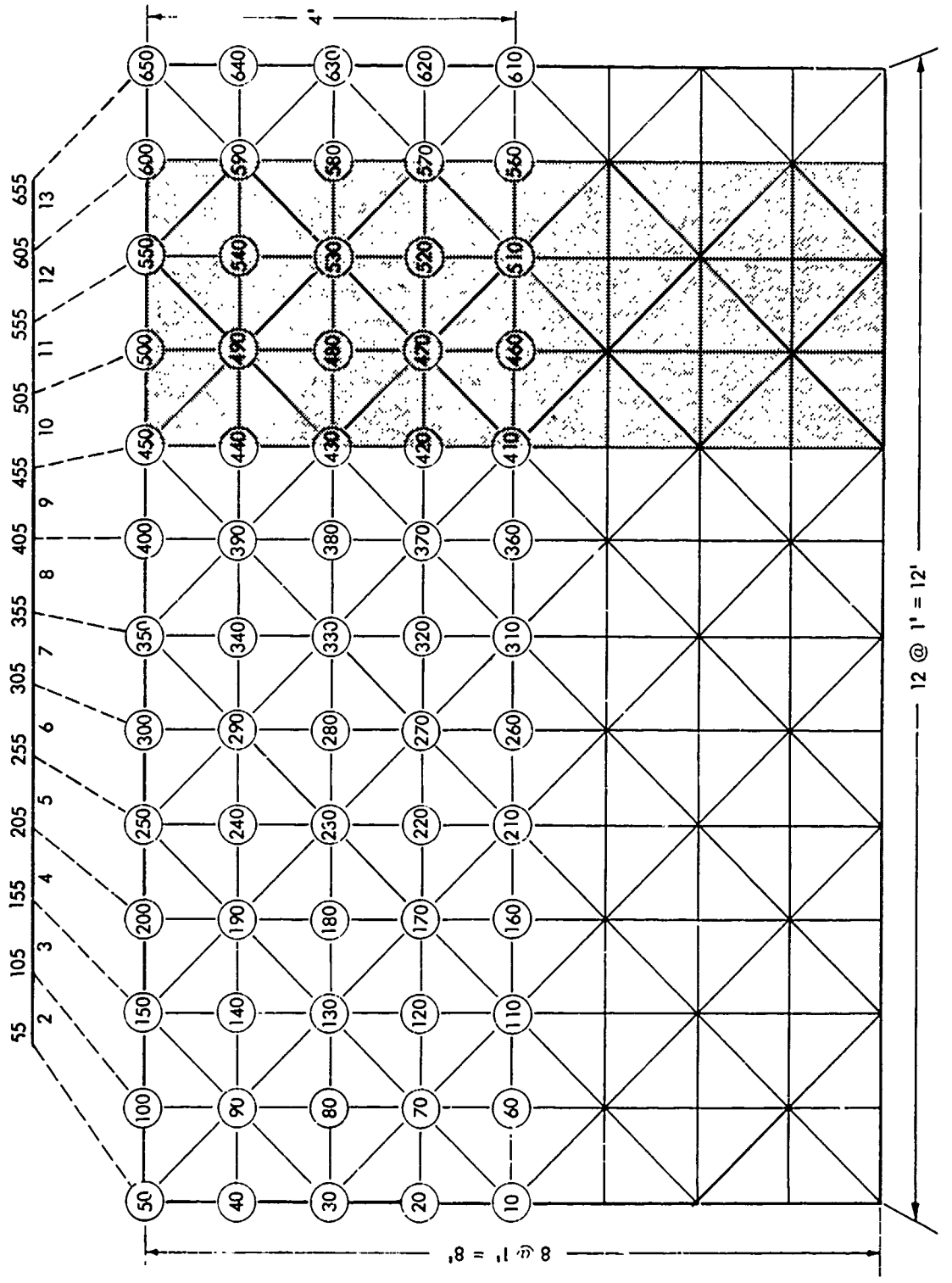

Fig. 4-11. Basic Grid and Line Elements

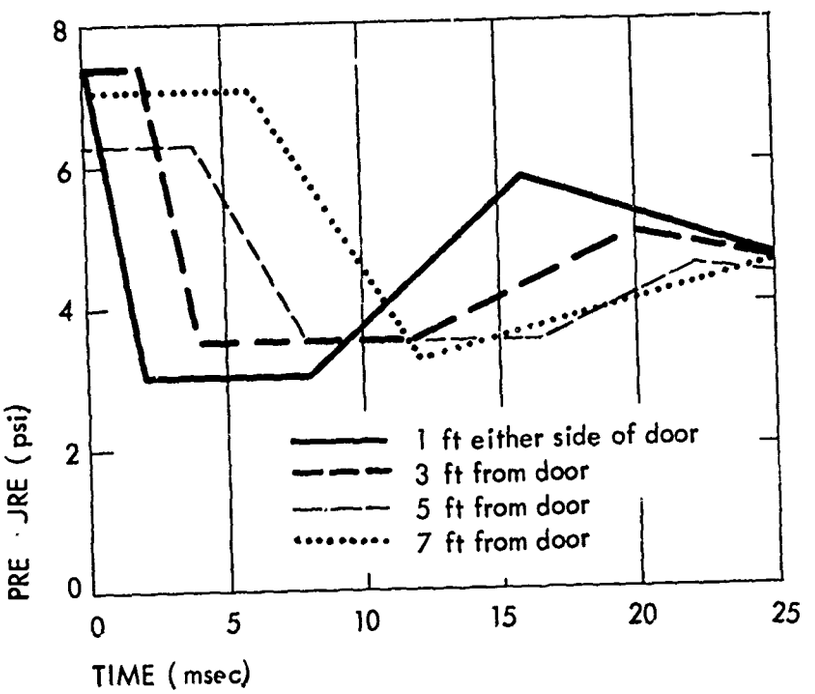

Fig. 4-12. SAMIS Input Loads for Three Strands of Primacord

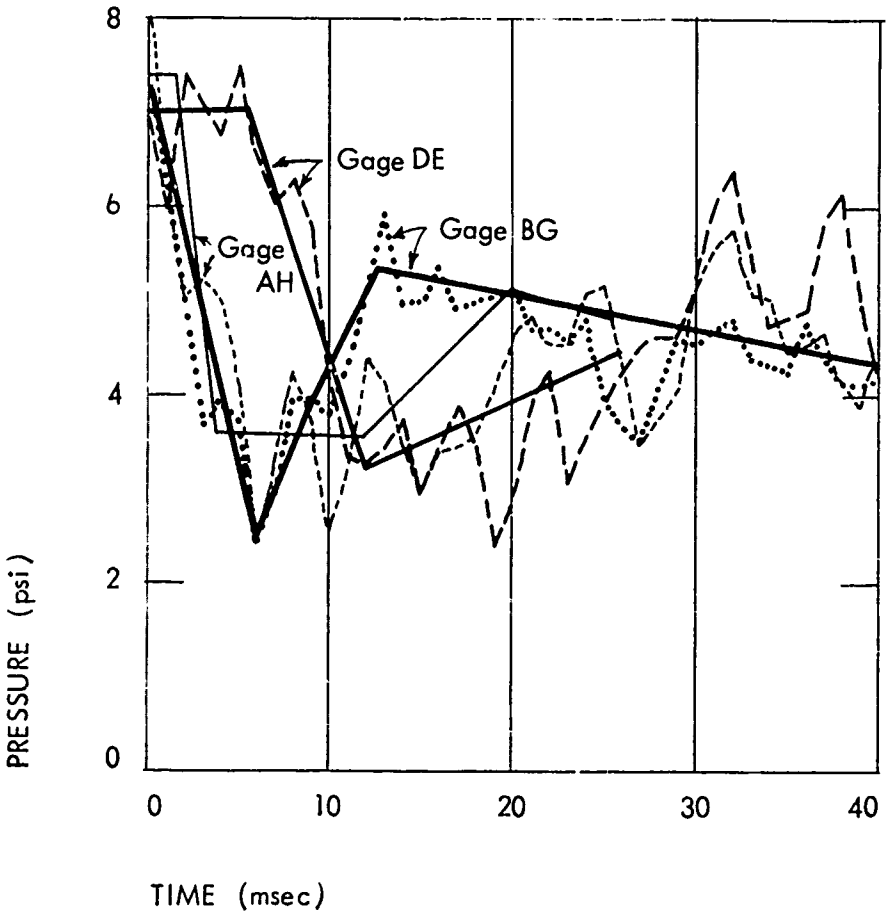

Fig. 4-13. Comparison of SAMIS Input Data in Fig. 4-13 With Loading Study Data From Figs. 4-5, 4-6 and 4-7

It is possible that some minor adjustments could be made to better approximate the measured loading study data; however, the overall correlation is quite good, and it is anticipated that these minor changes will not significantly affect the previous computer prediction of this test geometry. Some of these predictions are shown in Figs. 4-14 through 4-19, which illustrate the deflection contours (normalized to one psi)* for an 8-in. brick wall with a doorway for each millisecond, for times 12 msec through 17 msec.

In Fig. 4-14, the deflection nearest the tunnel wall is greater than that near the door (25 percent greater). This is intuitively pleasing because the higher loads remain longer near the wall; the rarefaction wave relieves the load near the door first. Moving forward in time (see Figs. 4-15 through 4-19), a uniformly deflected wall is approached at about 14 msec, which might be called the fundamental half period, i.e., T = 28 msec. As time progresses, we observe that at t = 17 msec, a peak displacement is achieved adjacent to the doorway. This interesting phenomenon is further illustrated in Fig. 4-20 on a time vs displacement plot for Nodes 10 (at wall), 210 (center of panel), and 410 (next to the doorway). From this figure it is apparent that failure is expected to begin adjacent to the wall more often than adjacent to the doorway.

Some preliminary calculations have been done to predict the fracture stress of 8-in. nonreinforced brick walls with doorways. This required reference to the basic static test data summarized in Section 7. By using the failure theory and the basic brick data, the fracture stress plot (shown in Fig. 4-21) and the flexure stress plot (shown in Fig. 4-22) were obtained. This data would predict a mean fracture stress of 130 psi, a probable fracture time (crack) at between 11 and 12 msec, a most probable stress of 162 psi, and no failure at a 1 psi reflected overpressure. Figure 4-23 is a computer prediction for the load cells, which also aids in the test prediction correlations.

* To derive deflections for loadings other than one psi, multiply the deflections on Fig. 4-14 through 4-19 by the actual loading.

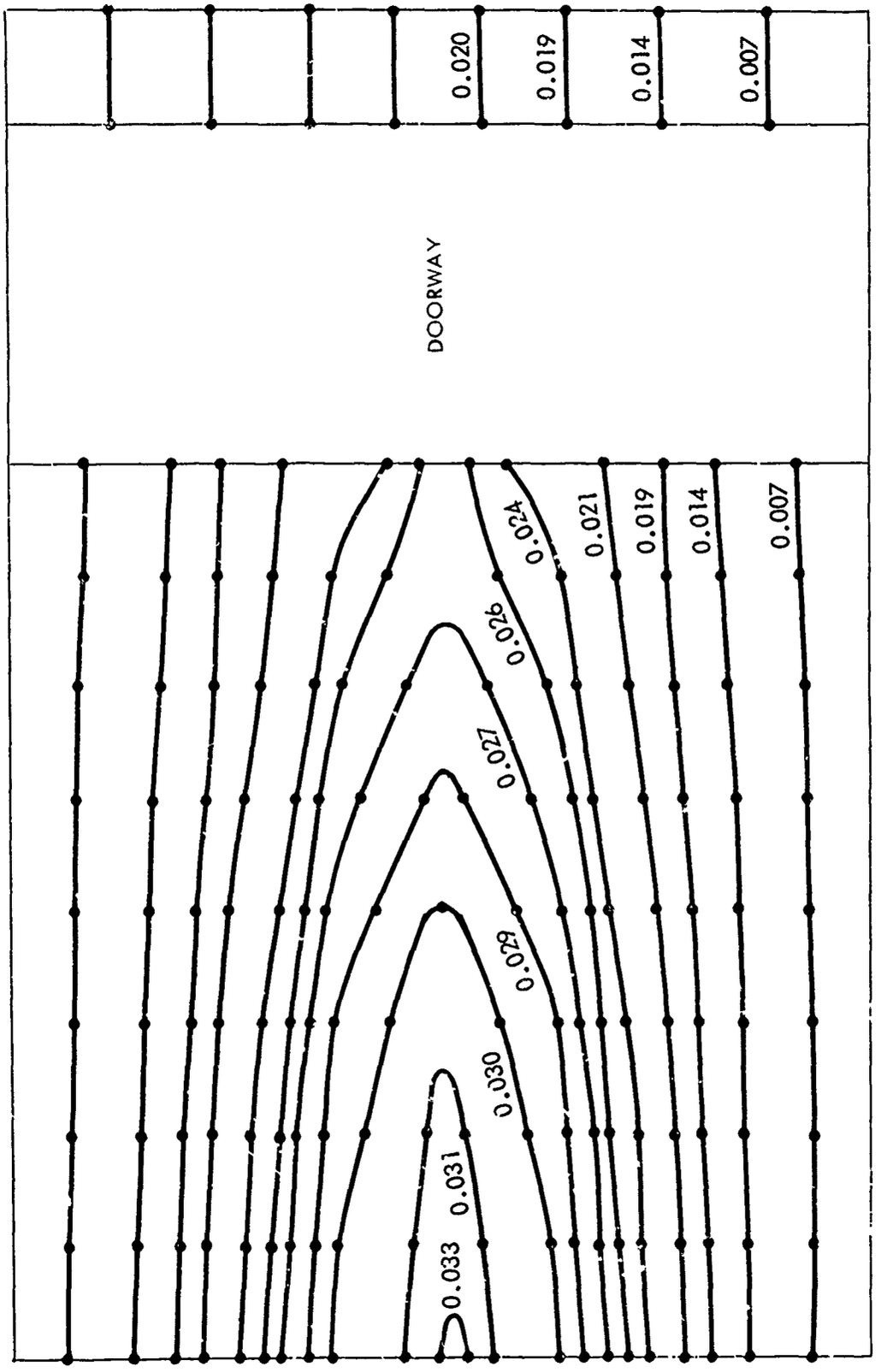

Fig. 4-14. Wall with Doorway Deflection Contour (in.) at 12 msec, Normalized to 1 psi Loading

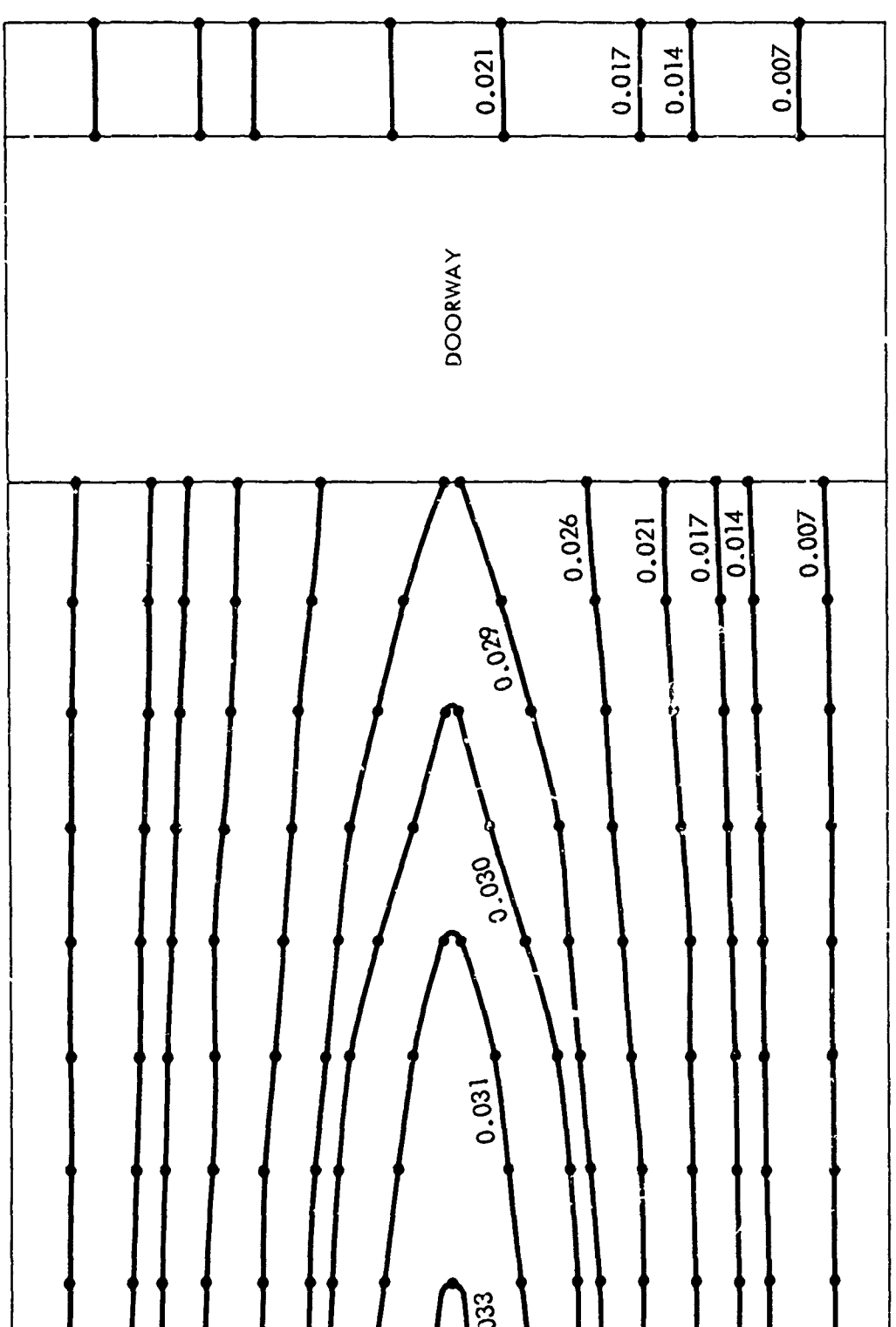

Fig. 4-15. Wall with Doorway Deflection Contour (in.) at 13 msec, Normalized to 1 psi Loading

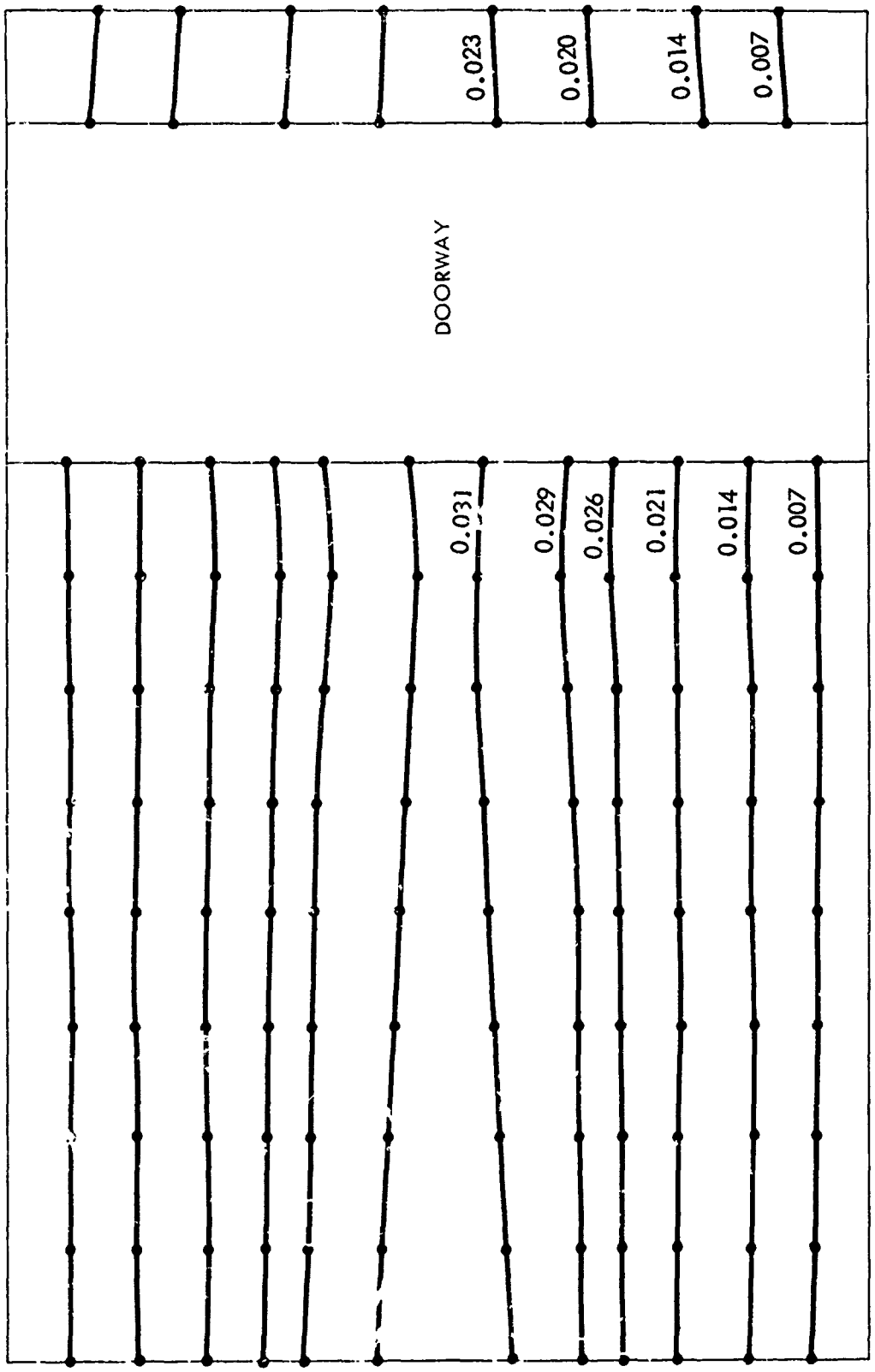

Fig. 4-16. Wall with Doorway Deflection Contour (in.) at 14 msec, Normalized to 1 psi Loading

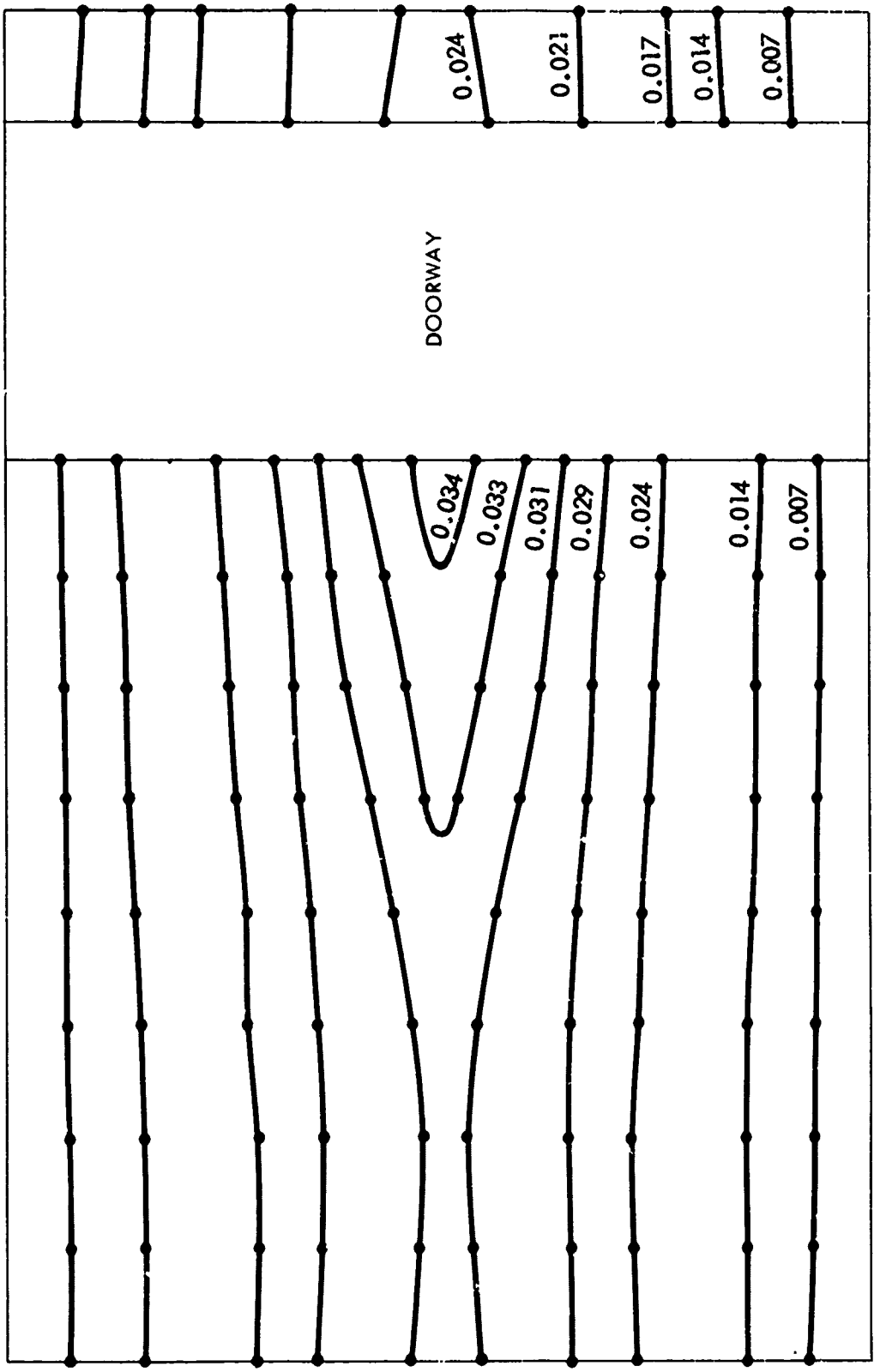

Fig. 4-17. Wall with Doorway Deflection Contour (in.) at 15 msec, Normalized to 1 psi Loading

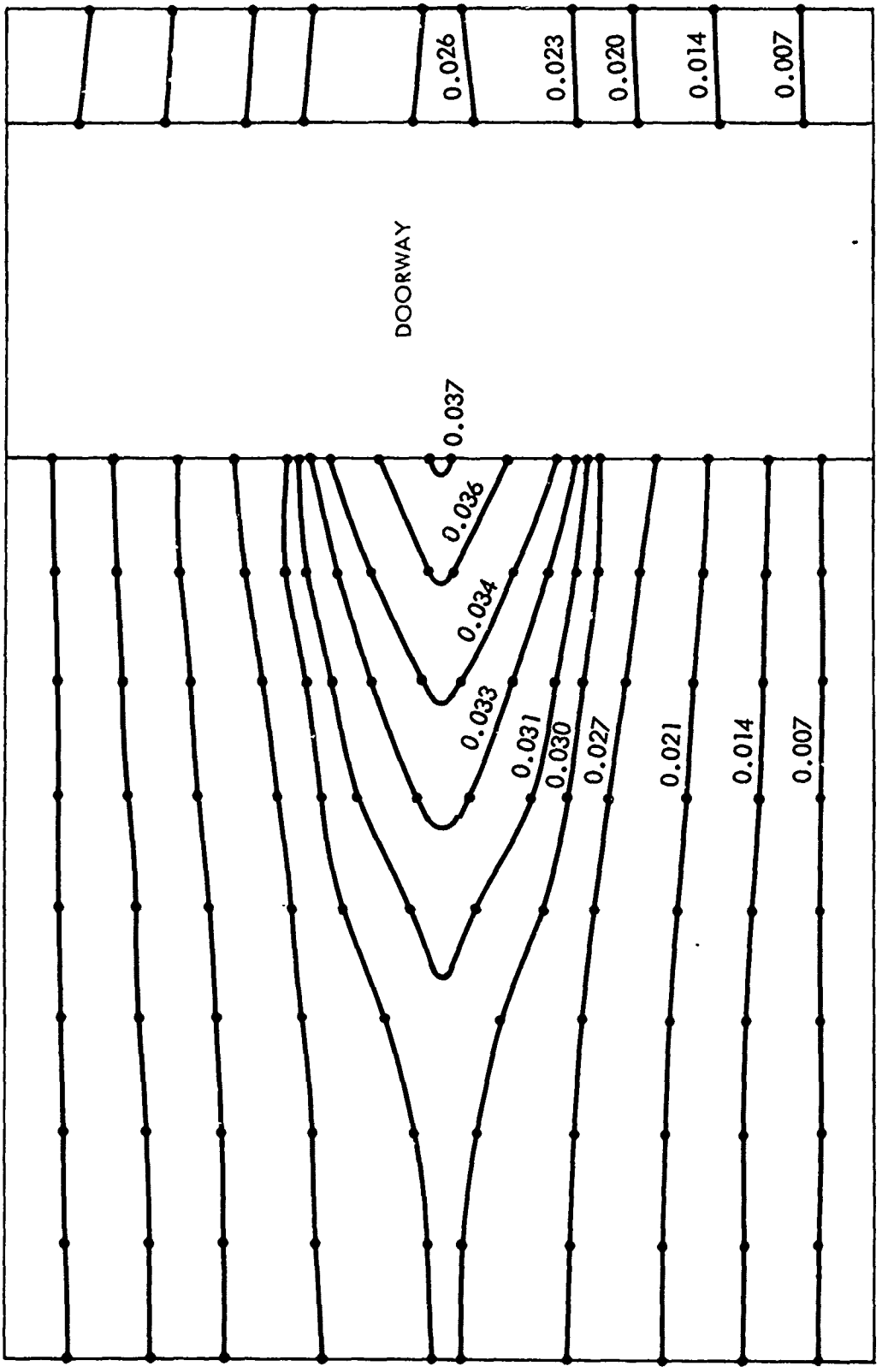

Fig. 4-18. Wall with Doorway Deflection Contour (in.) at 16 msec, Normalized to 1 psi Loading

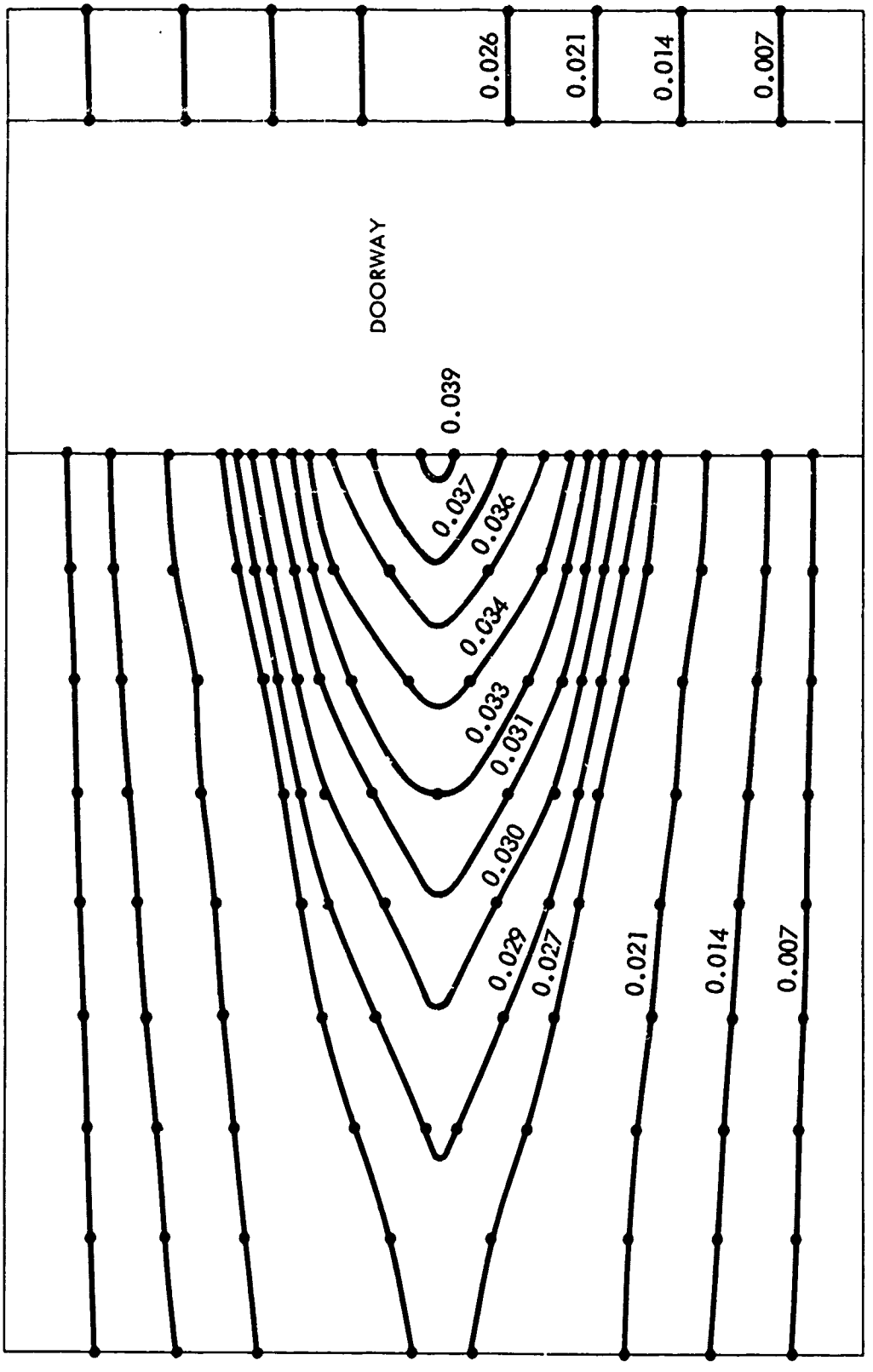

Fig. 4-19. Wall with Doorway Deflection Contour (in.) at 17 msec, Normalized to 1 psi Loading

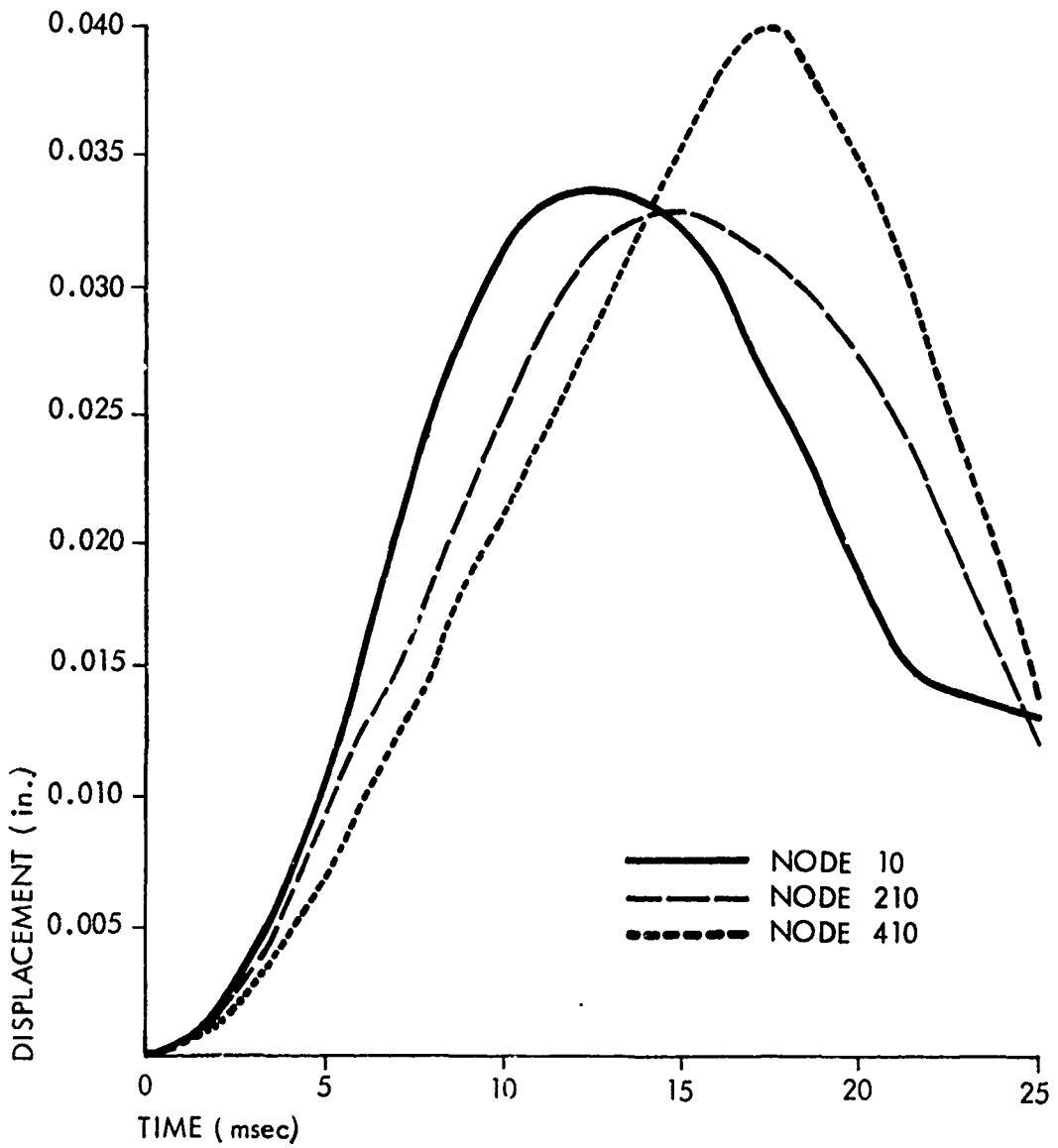

Fig. 4-20. Displacement vs Time Plot for Wall with Doorway, Normalized to 1 psi Loading

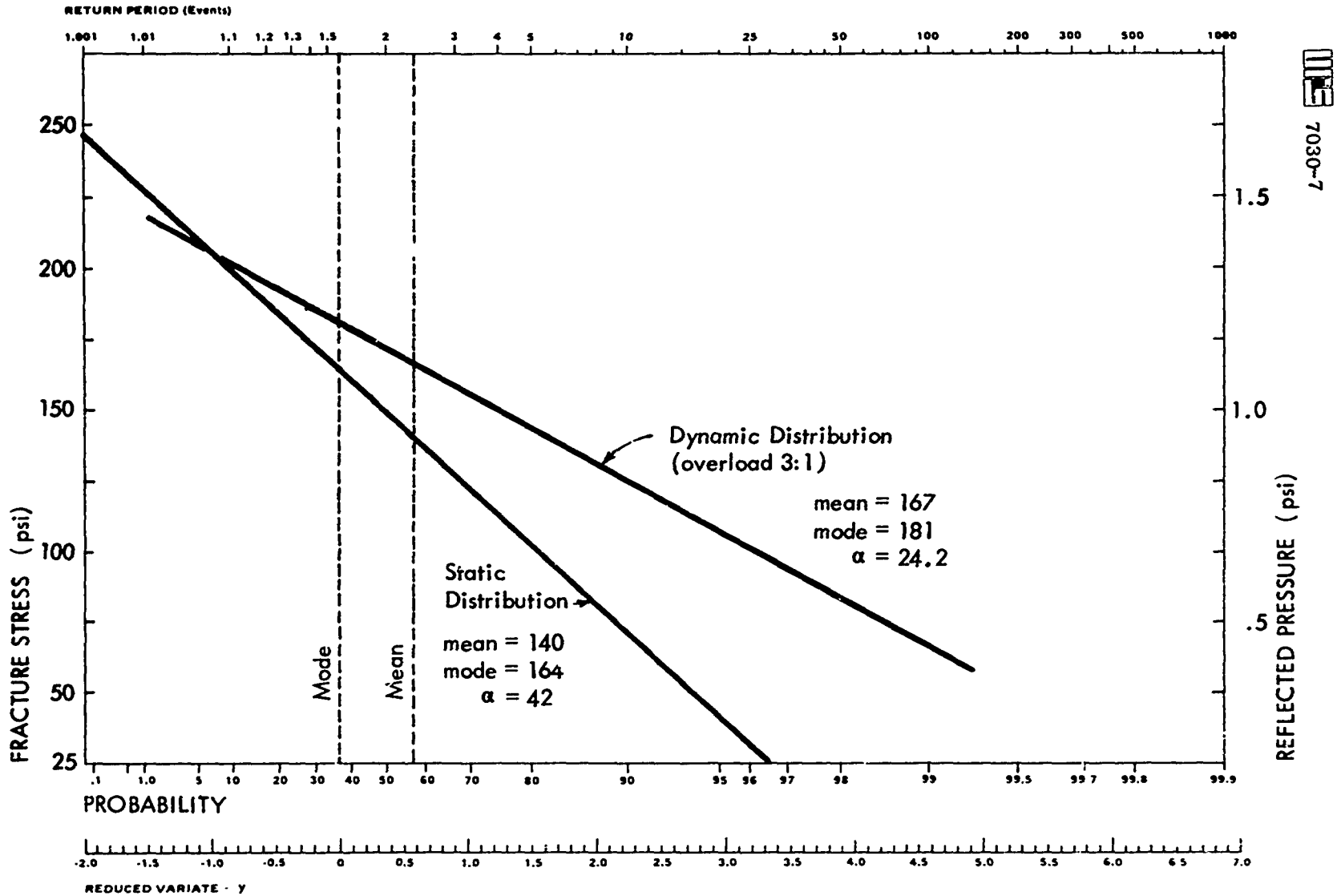

Fig. 4-21. Extreme Probability Plot of Fracture for 8- × 12-ft × 8-in. Walls with Various Support Conditions and a 3- × 8-ft Doorway (based on static test data and "failure theory")

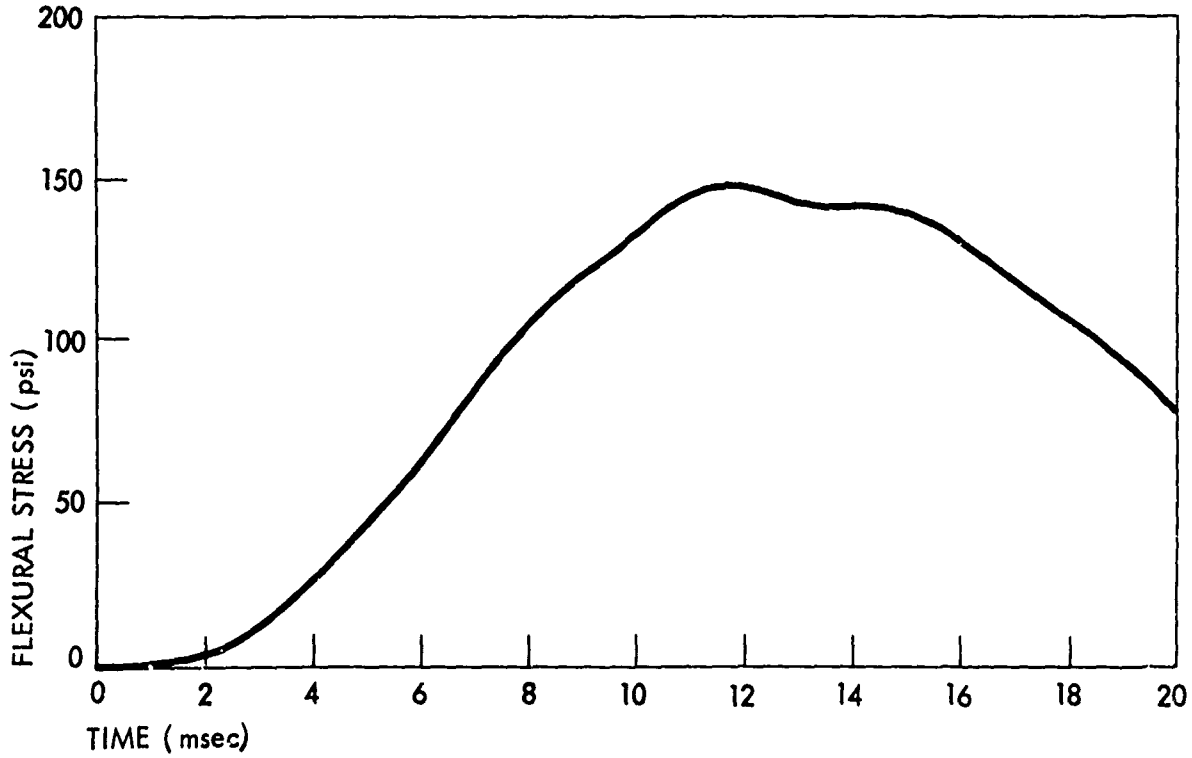

Fig. 4-22. Doorway Wall Panel Stress Area of Node 10, Normalized to 1 psi Loading

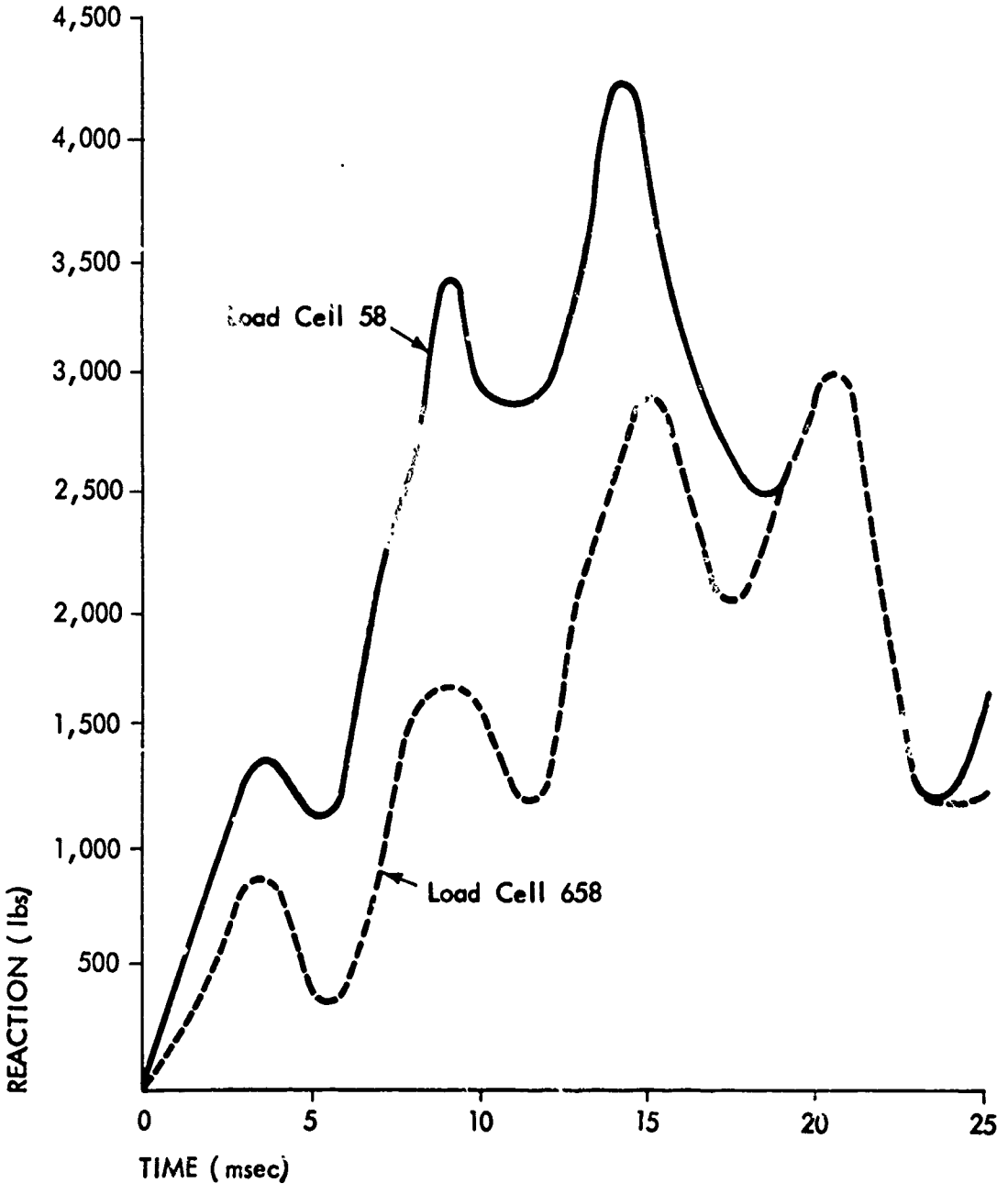

Fig. 4-23. Load vs Time for Load Cells 58 and 658, Normalized to 1 psi Loading

STRUCTURAL WALL PANEL TESTS - Walls with a Doorway

During this reporting period two 8-in. nonreinforced brick structural wall panels with a doorway were tested. These were Wall No. 45 (Test Nos. 02-24-71-01 and -02) and Wall No. 48 (Test Nos. 02-26-71-01 through -05). The doorways in these walls were 33-1/2 in. wide, were on the east side of the walls, and ran from floor to ceiling. The solid portion of the walls was 99 in. high and 102-3/4 in. wide, making the open area of the doorway approximately 17.5 percent of the total area. A photograph of one of these walls in place in the Shock Tunnel is shown in Fig. 4-24.

Wall No. 45 - 8-in. Nonreinforced Brick Wall with Doorway

This wall was tested twice. In the first test (No. 02-24-71-01) a small charge of approximately 12 ft of Primacord was used to "plink" the wall and obtain the natural period of the wall as installed in the Shock Tunnel. The measured natural period for this wall was 33 msec.

The second test (No. 02-24-71-02) used two 60-ft strands of Primacord which yielded 3.6 psi peak reflected overpressure on the wall. The wall failed with a crack gage indicating a break at 11 msec. (Due to a problem in the recording, all crack gages recorded at the same time, so that the particular gage which broke first is unknown.) As noted from the motion picture films, this crack was horizontal and at the center of the wall.

The two halves of the wall rotated out of the support frame with the lower half rotating until it struck the floor. The upper half rotated 90 degrees and landed directly on top of the lower half. The maximum total load, as measured by the load cells located at the four corners of the wall panel, was 32,000 lb. A post-test photograph of the wall is presented in Fig. 4-25a. A plot of displacement as a function of time for this test is presented in Fig. 4-26.

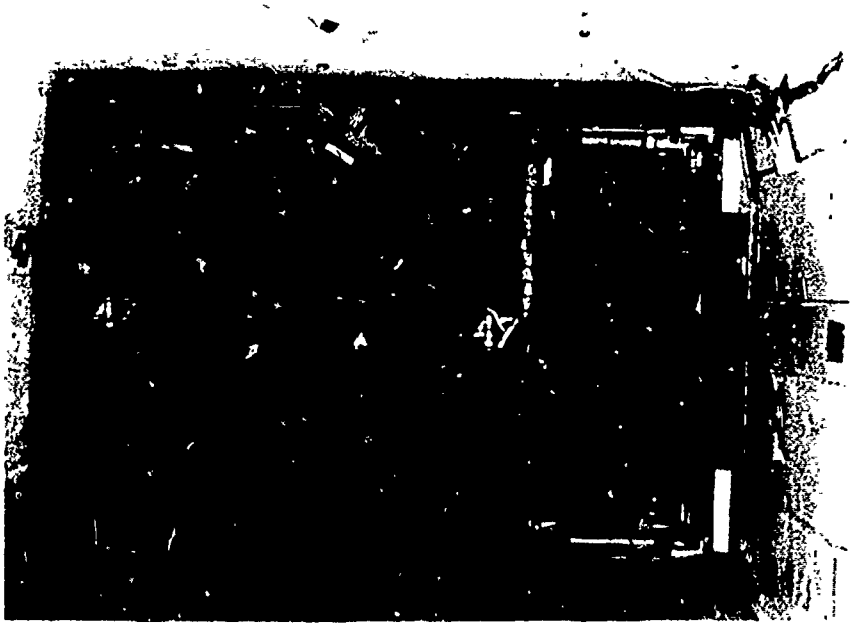

Fig. 4-24. Pre-Test Photograph of an 8 in. Nonreinforced Brick Wall with Doorway Placed in the Tunnel

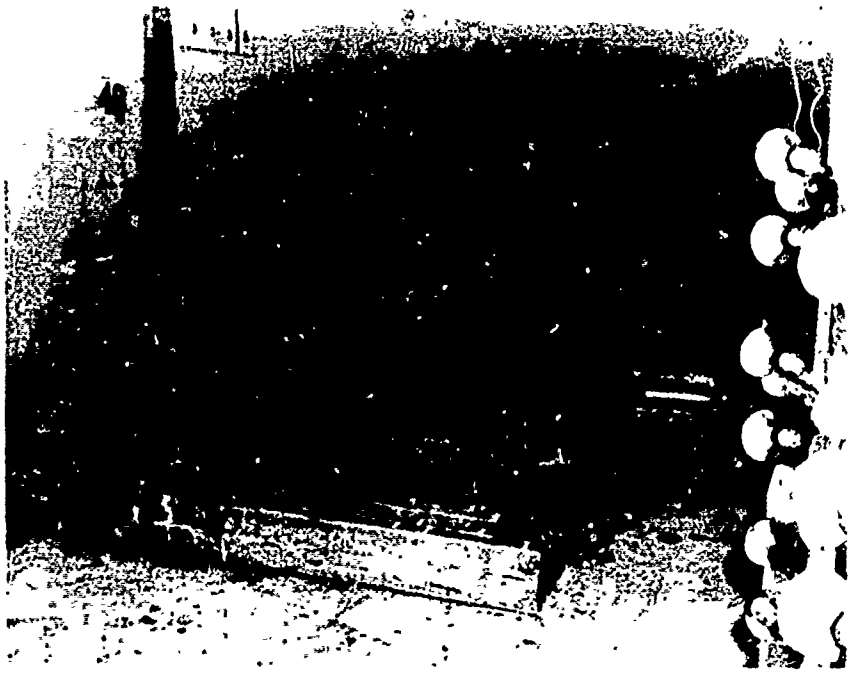

a. Wall No. 48
Test No. 02-
26-71-05

b. Wall No. 45
Test No. 02-
24-71-02

Fig. 4-25. Post-Test Photographs of Walls No. 45 and 48, 8 in. Nonreinforced Brick with Doorway

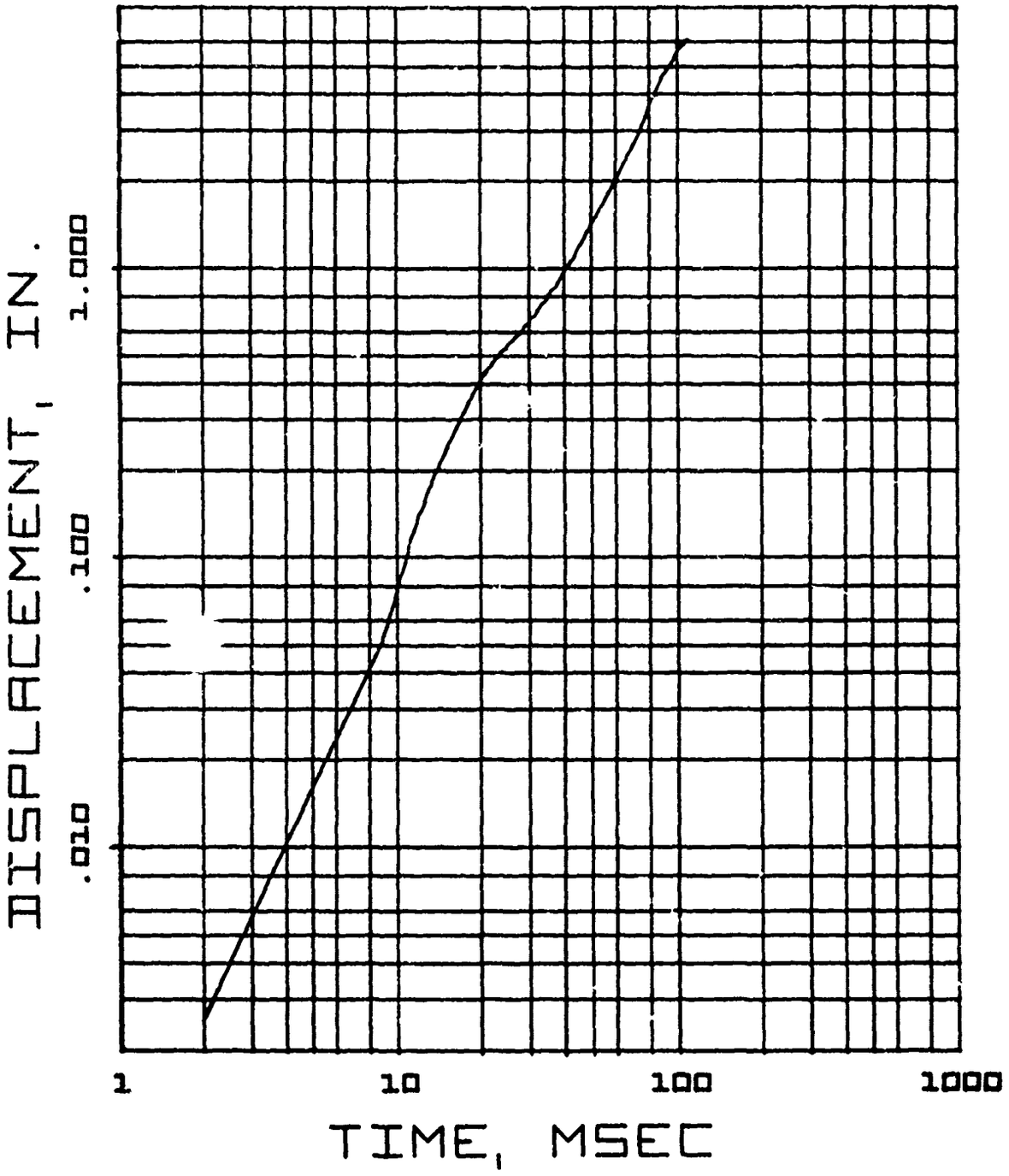

Fig. 4-26. Displacement as a Function of Time for Wall No. 45, 8 in. Nonreinforced Brick with Doorway

Wall No. 48 - 8-in. Nonreinforced Brick Wall with Doorway

Five tests were conducted on this wall panel. The first test (No. 02-26-71-01) used a short length of Primacord (approximately 10 ft) and was conducted to obtain the natural period of the wall. This was again found to be 33 msec.

The next three tests (02-26-71-02, -03 and -04), using one strand of Primacord, subjected the wall panel to a peak reflected overpressure of 1.7 psi with a 100 msec positive phase duration. The purpose of these tests was to gain information on multiple loadings and fatigue. No visible damage was caused by these tests.

The fifth test (No. 02-26-71-05) used two 60-ft lengths of Primacord and subjected the wall panel to a peak reflected overpressure of 3.5 psi. Three crack gages were placed on this wall. The first, located farthest from the door, broke first at 16 msec. The second gage, at the middle of the wall, followed at 24 msec, and the one next to the door failed at 28 msec. This pattern was expected, based on the deflection predictions shown in Figs. 4-14 through 4-19. The wall panel failed with a failure process very similar to Wall No. 45, and the total load, as measured by the load cells for this test, was 26,000 lb. A post-test photograph of this wall is shown in Fig. 4-25b, and a plot of displacement as a function of time is presented in Fig. 4-27.

SUMMARY

As with the solid walls, the experiments have been well-behaved and within predicted ranges.

For example, one would expect a reasonable probability of failure at one strand or 1.5 psi if σ_r is small enough. From our SAMIS prediction, at p_r = 1.5 we have a flexural stress of $\sigma_r \simeq 225$ psi (see Fig. 4-22). The failure theory curve (Fig. 4-21) indicates that there would be a 99 percent chance of failure. Wall No. 45 failed with p_r = 3.5 psi ($\sigma_r \simeq 525$ psi as in Fig. 4-22), whereas Wall No. 48 survived three one-strand shots with a peak of 1.7 psi and failed with p_r = 3.5 psi; hence, $225 < \sigma_r \leq 525$.

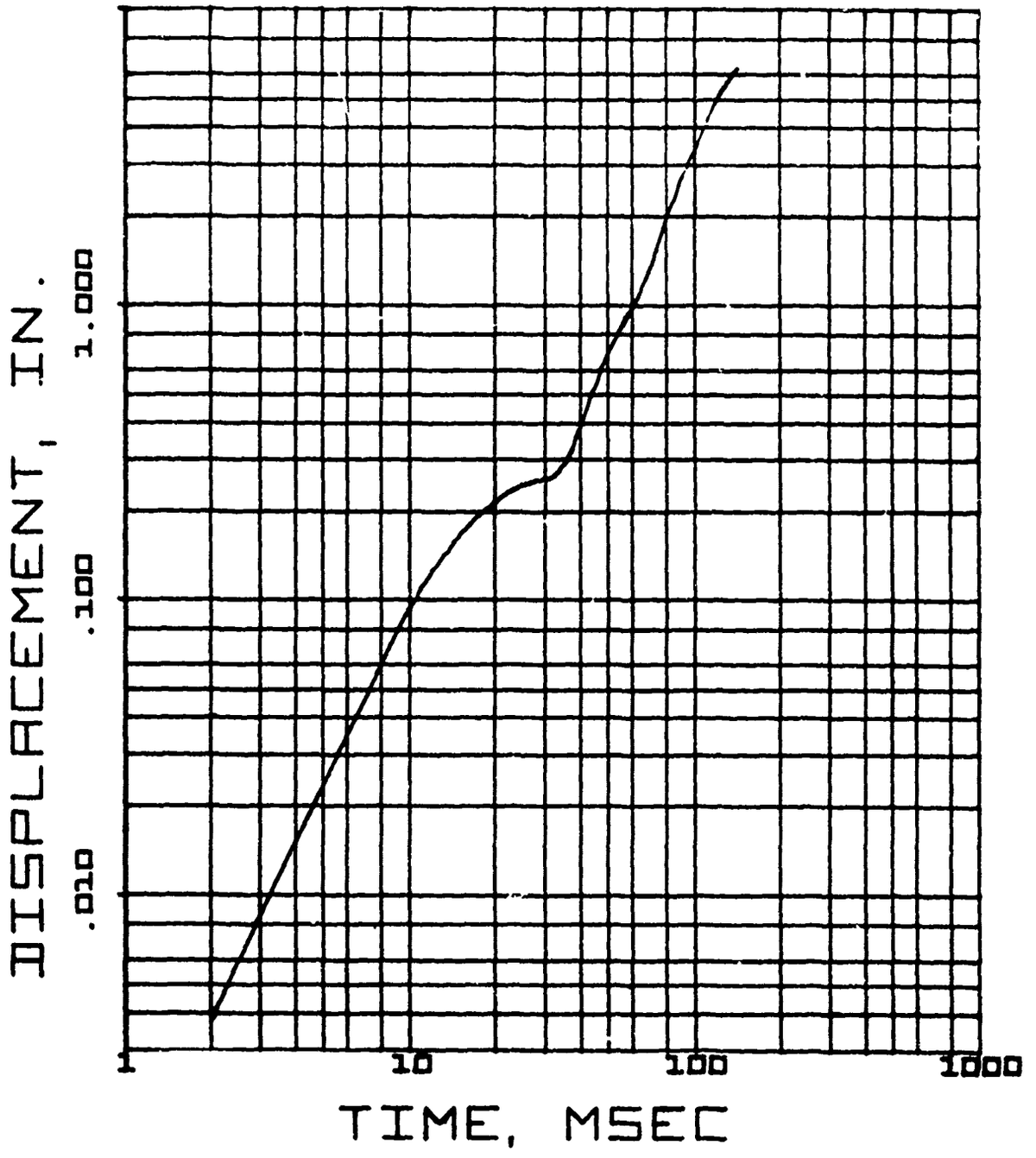

Fig. 4-27. Displacement as a Function of Time for Wall No. 48, 8-in. Nonreinforced brick with Doorway

If a wall survived 1.7 psi, one would expect that at failure one would get a reaction equal to or greater than the predicted load cell readings from SAMIS.

Reaction Predicted = 24,200 lb (nonfailing wall)

Wall 45 (at failure) = 26,000 lb

Wall 48 (at failure) = 32,000 lb

Section 5
WALLS WITH A WINDOW

This section includes the results from a loading study test series of exterior walls with windows; a discussion of the preliminary analytical work completed on this test geometry; and the results of two tests of 8-in. nonreinforced brick wall panels with windows, and two tests of 8-in. nonreinforced concrete block wall panels with windows, all four of which were conducted during this reporting period.

LOADING STUDY TESTS

During this loading study program two window sizes were investigated, 62 × 64 in. (a 27 percent opening) and 38 × 62 in. (a 16 percent opening). The instrumentation locations for tests with each of these window sizes is shown in Figs. 5-1 and 5-2. It will be noted in these figures that pairs of gages are installed on the wall to obtain net load at each point on the wall, as was discussed in Section 4 for the doorway geometry. Typical gage traces and the digitized data for this test series are presented in Appendix C. Summary plots for the three gage pairs A-E, C-G, and D-H, for one, three, and five strand tests with each of the window sizes are presented in Figs. 5-3 through 5-19.

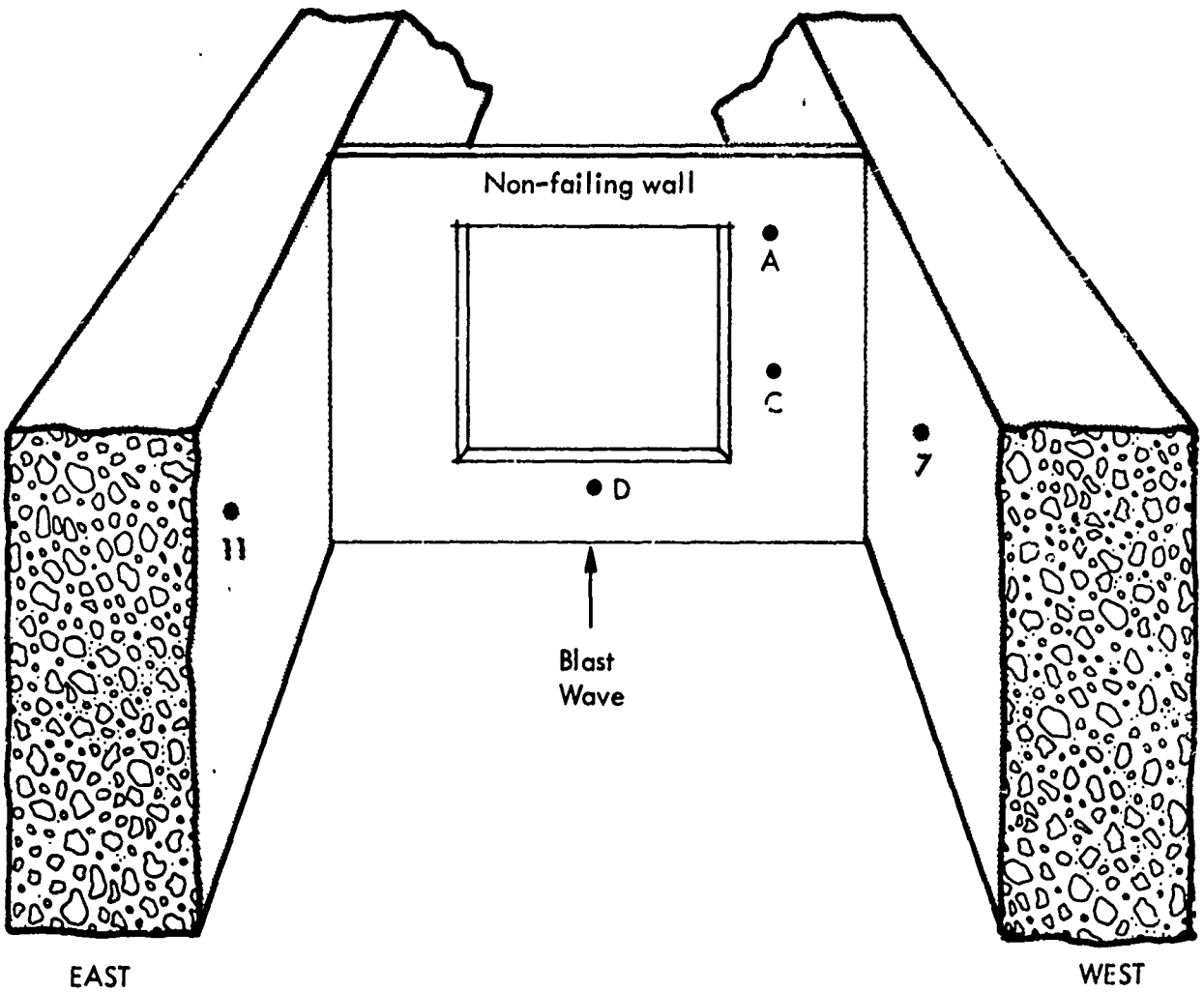

NONFAILING WALL GAGES

GAGE NO.	DISTANCE FROM FLOOR	DISTANCE FROM WINDOW
A-E*	89-1/2"	12"
C-G*	51"	12"
D-H*	14"	7"

* Gages E, G and H are on back of the wall.

TUNNEL WALL GAGES

GAGE NO.	DISTANCE FROM FLOOR	DISTANCE FROM WALL
Westwall-7	45"	21"
Eastwall-11	49"	38"

Fig. 5-1. Instrumentation Location for Loading Study Tests with 62 x 64 in. Window

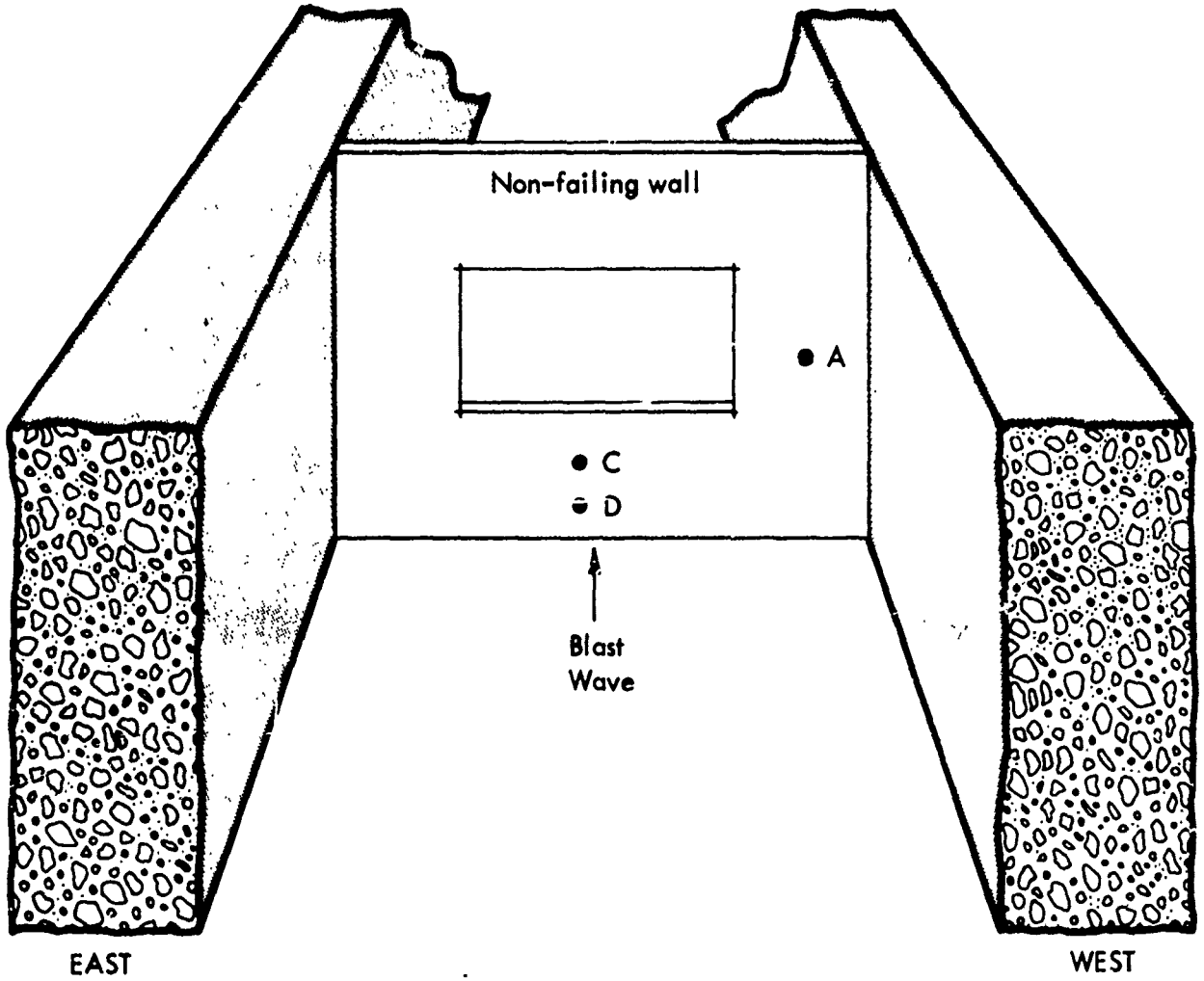

NONFAILING WALL GAGES

GAGE NO.	DISTANCE FROM FLOOR	DISTANCE FROM WINDOW
A-E*	51"	24"
C-G*	27-1/2"	6-1/2"
D-H*	14-1/2"	19-1/2"

* Gages E, G and H are on back of the wall.

TUNNEL WALL GAGES

GAGE NO.	DISTANCE FROM FLOOR	DISTANCE FROM WALL
Westwall-7	45"	21"
Eastwall-11	49"	38"

Fig. 5-2. Instrumentation Location for Loading Study Tests with 38 x 62 in. Window

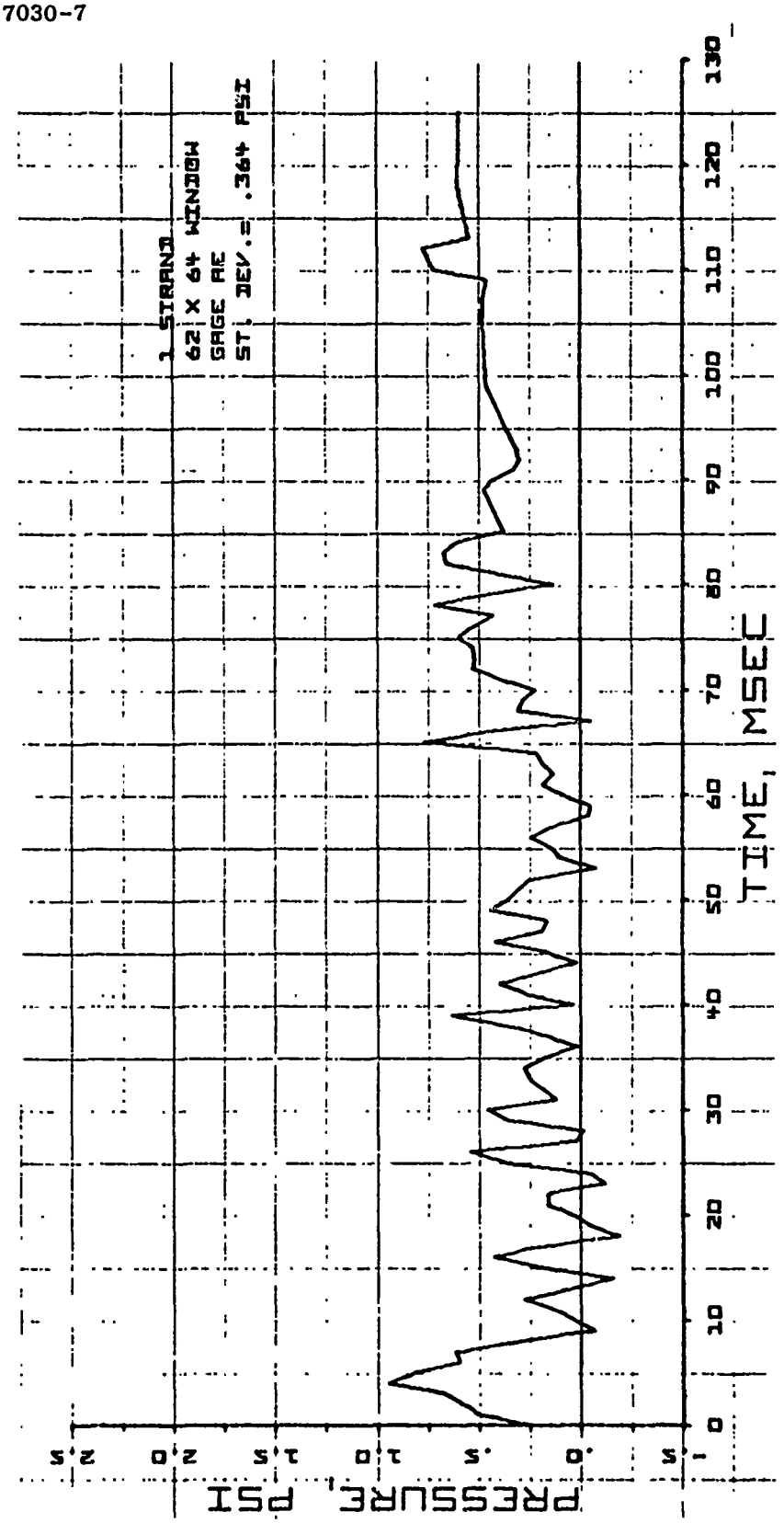

Fig. 5-3. Average Net Pressure as a Function of Time for One Strand 62 x 64 in. Window Loading Study Tests 01-23-70-01, -02, and -03. Gage Pair A-E

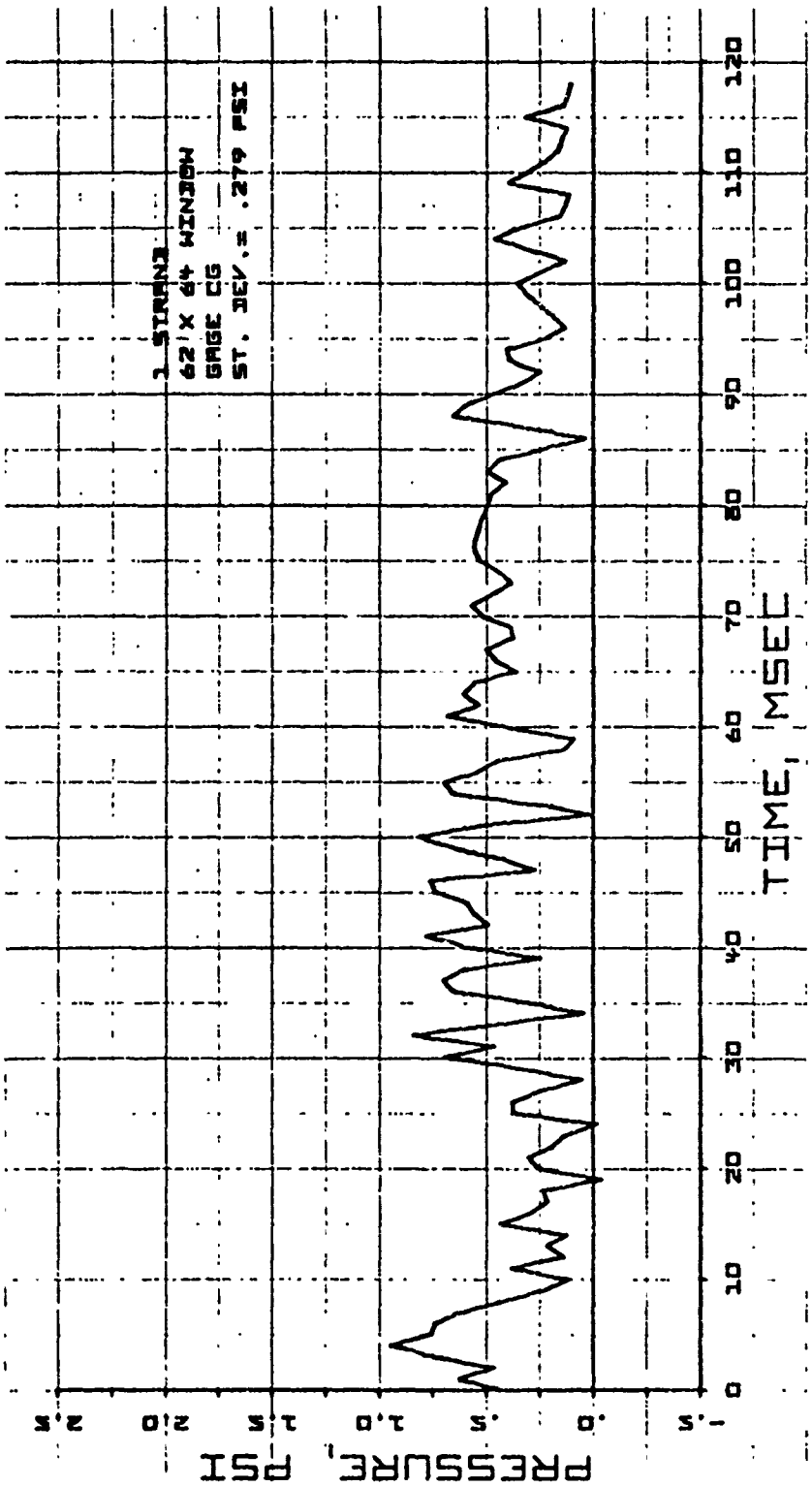

Fig. 5-4. Average Net Pressure as a Function of Time for One Strand 62 X 64 in. Window Loading Study Tests 01-23-70-01, -02 and -03. Gage Pair C-G

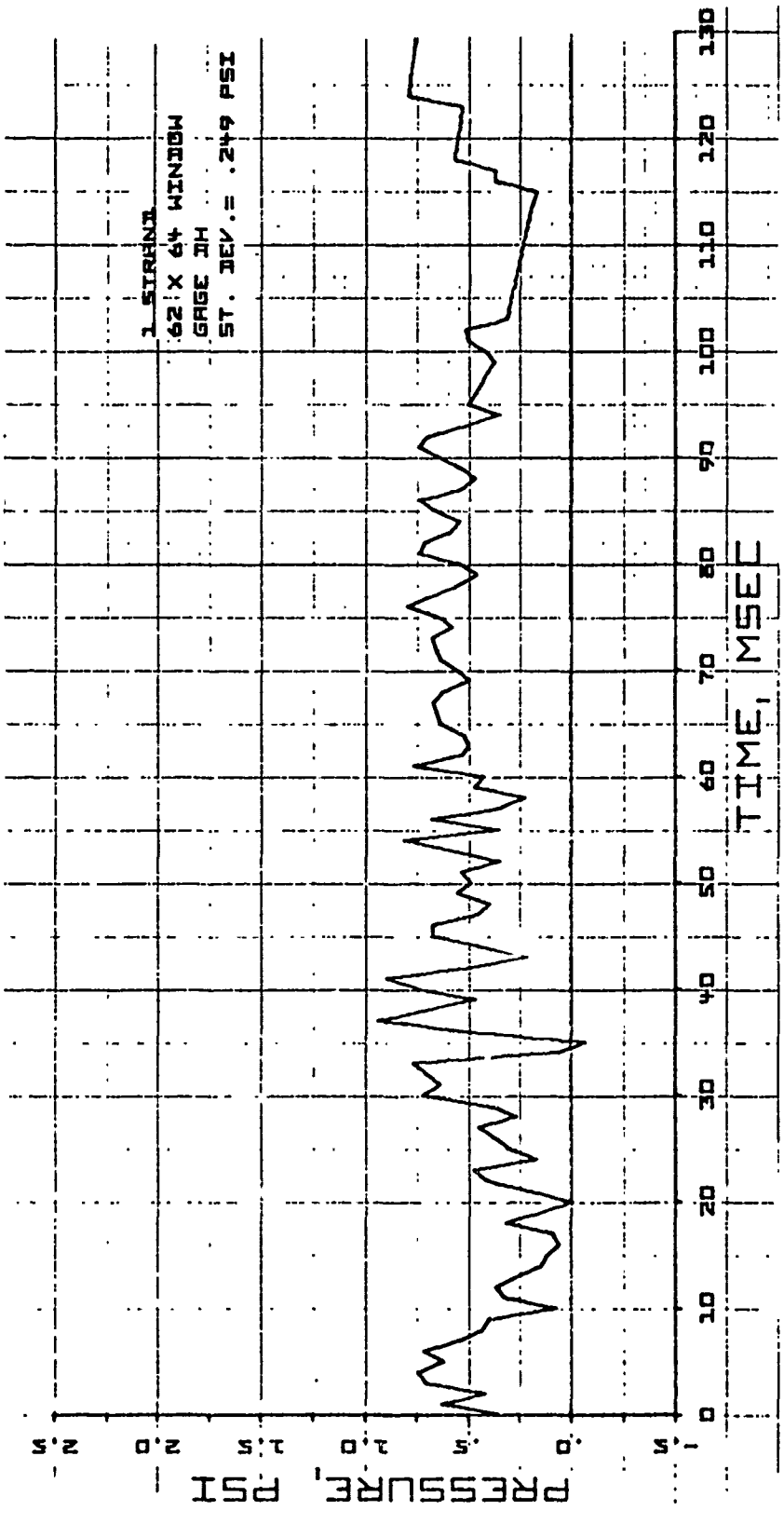

Fig. 5-5. Average Net Pressure as a Function of Time for One Strand 62 X 64 in. Window Loading Study Tests 01-23-70-01, -02 and -03. Gage Pair D-H

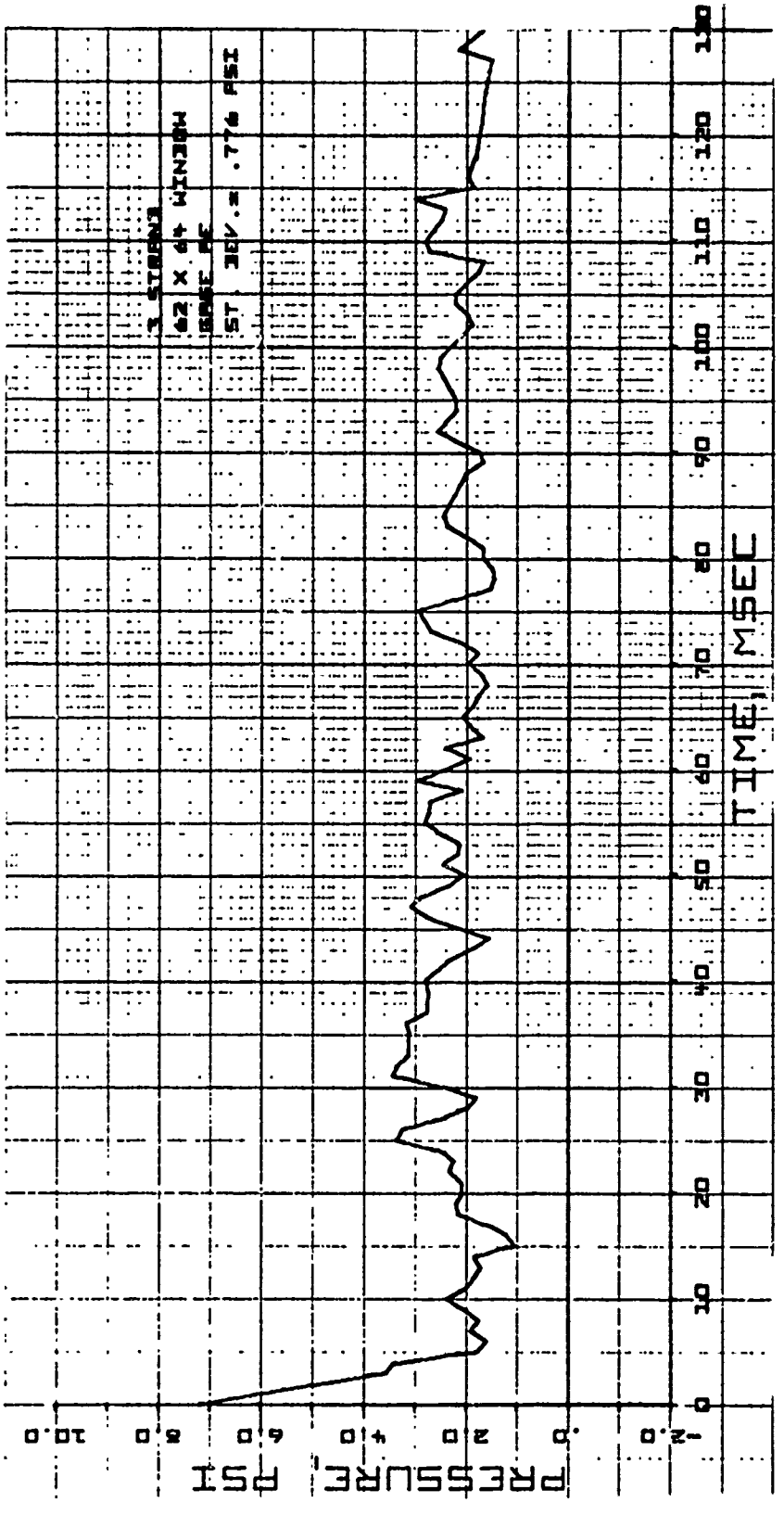

Fig. 5-6. Average Net Pressure as a Function of Time for Three Strand 62 X 64 in. Window Loading Study Tests 01-26-70-01, 02-09-70-01 and -02. Gage Pair A-E

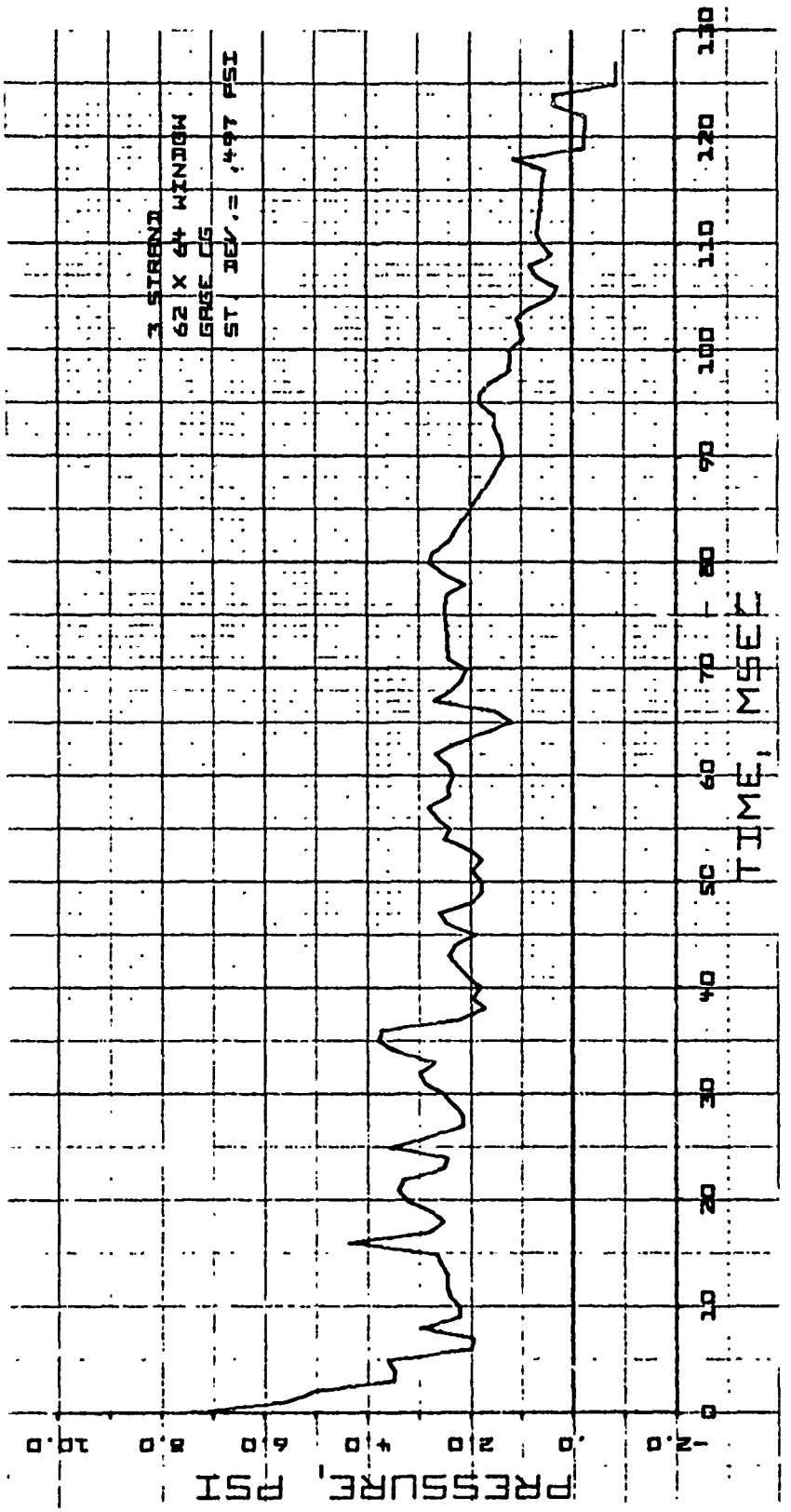

Fig. 5-7. Average Net Pressure as a Function of Time for Three Strand 62 X 64 in. Window Loading Study Tests 01-26-70-01, 02-09-70-01 and -02. Gage Pair C-G

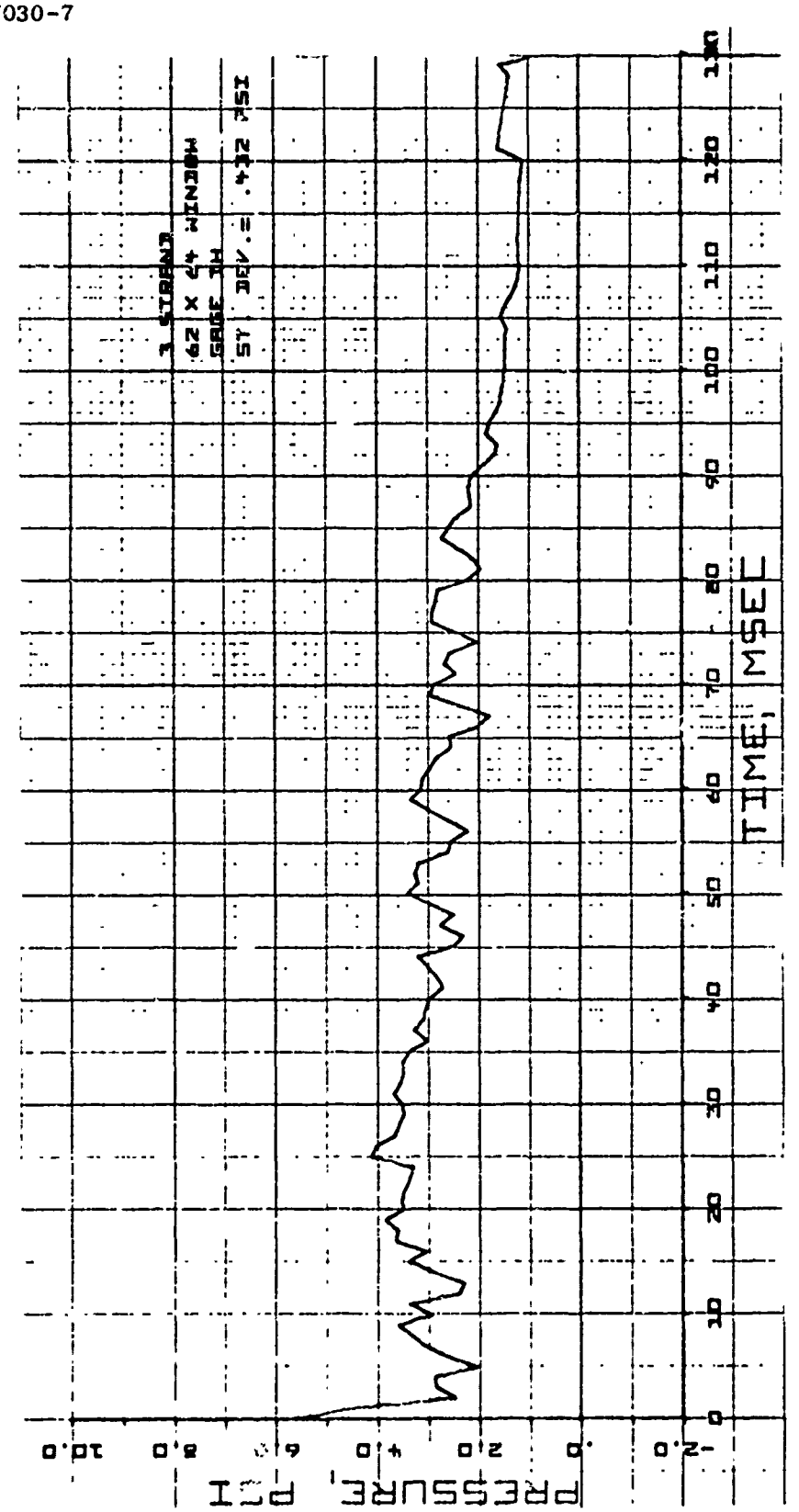

Fig. 5-8. Average Net Pressure as a Function of Time for Three Strand 62 X 64 in. Window Loading Study Tests 02-26-70-01, 02-09-70-01 and -02. Gage Pair D-H

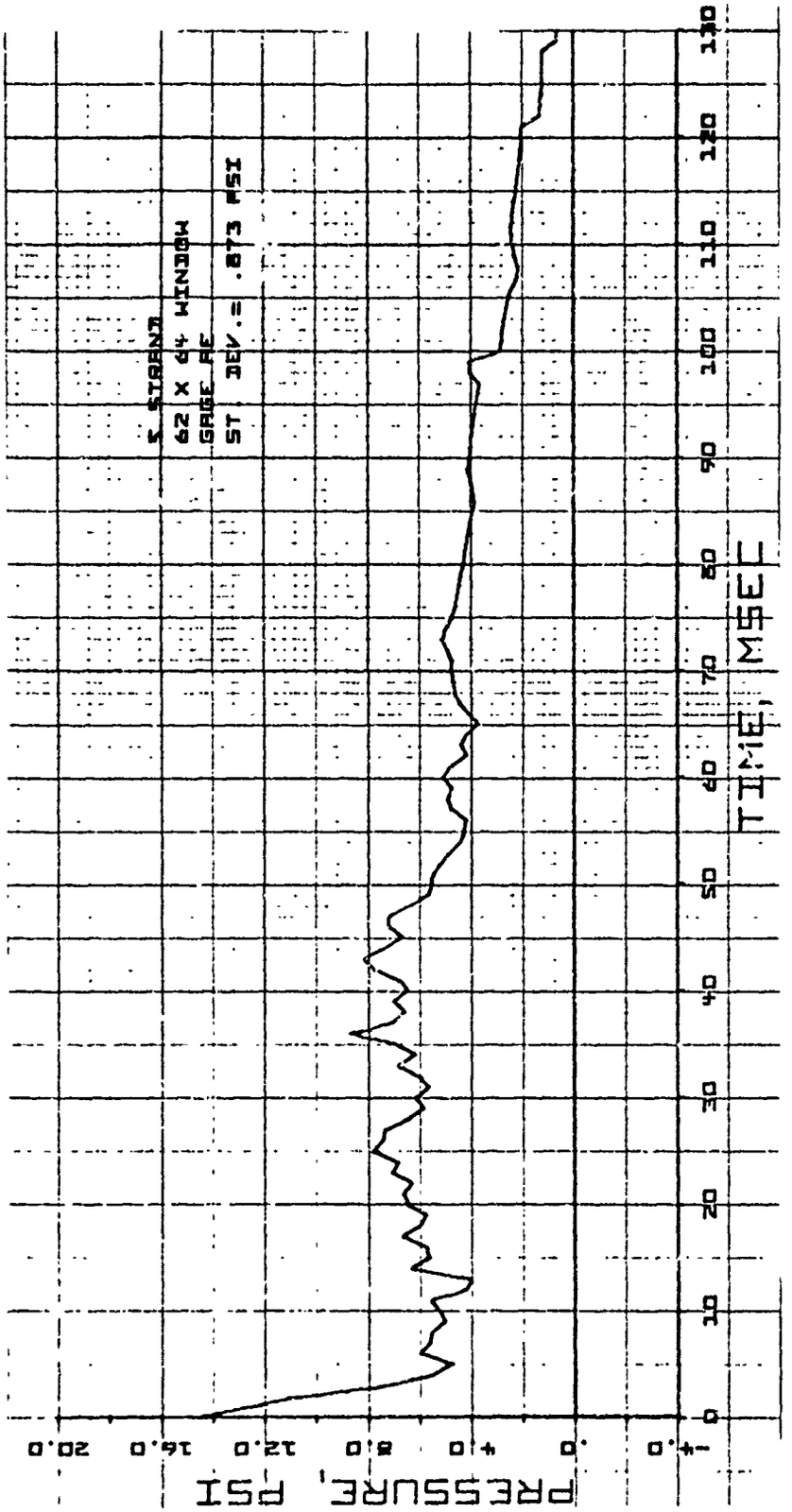

Fig. 5-9. Average Net Pressure as a Function of Time for Five Strand 62 X 64 in. Window Loading Study Test 02-10-70-01, -02, -03 and 02-11-70-01. Gage Pair A-E

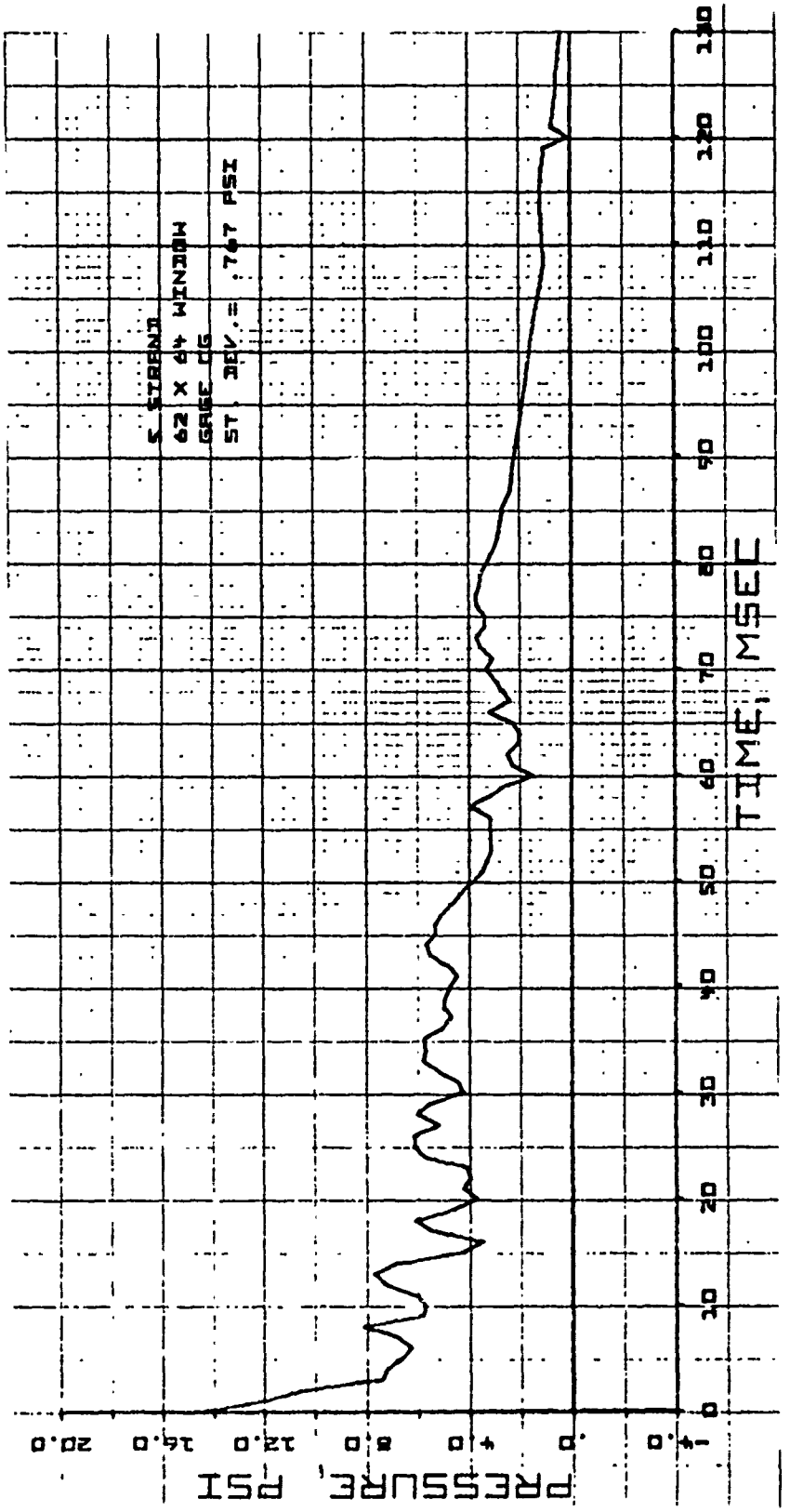

Fig. 5-10. Average Net Pressure as a Function of Time for Five Strand 62 X 64 in. Window Loading Study Test 02-10-70-01, -02, -03 and 02-11-70-01. Gage Pair C-G

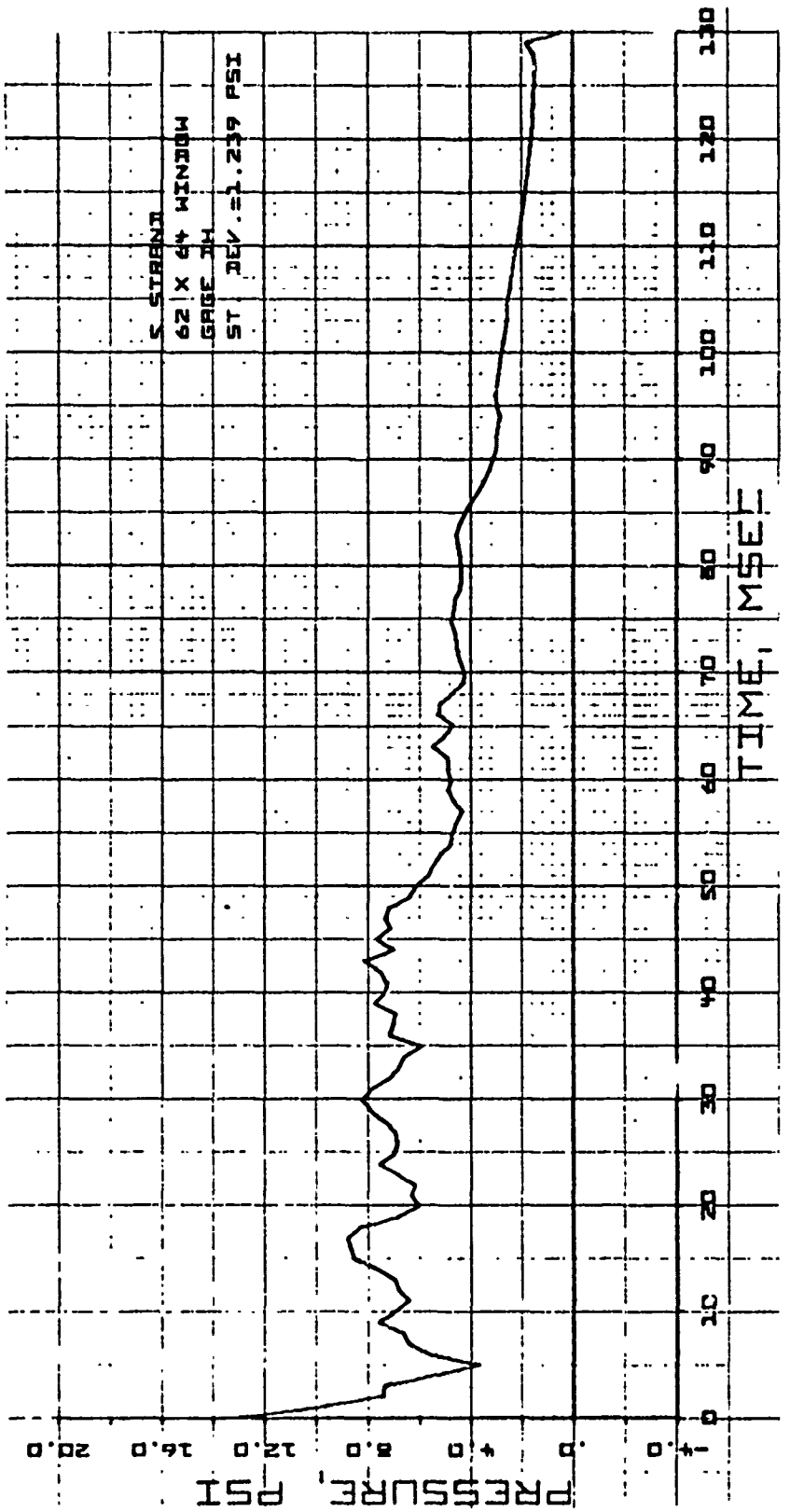

Fig. 5-11. Average Net Pressure as a Function of Time for Five Strand 62 x 64 in. Window Loading Study Tests 02-10-70-01, -02, -03 and 02-11-70-01. Gage Pair D-H

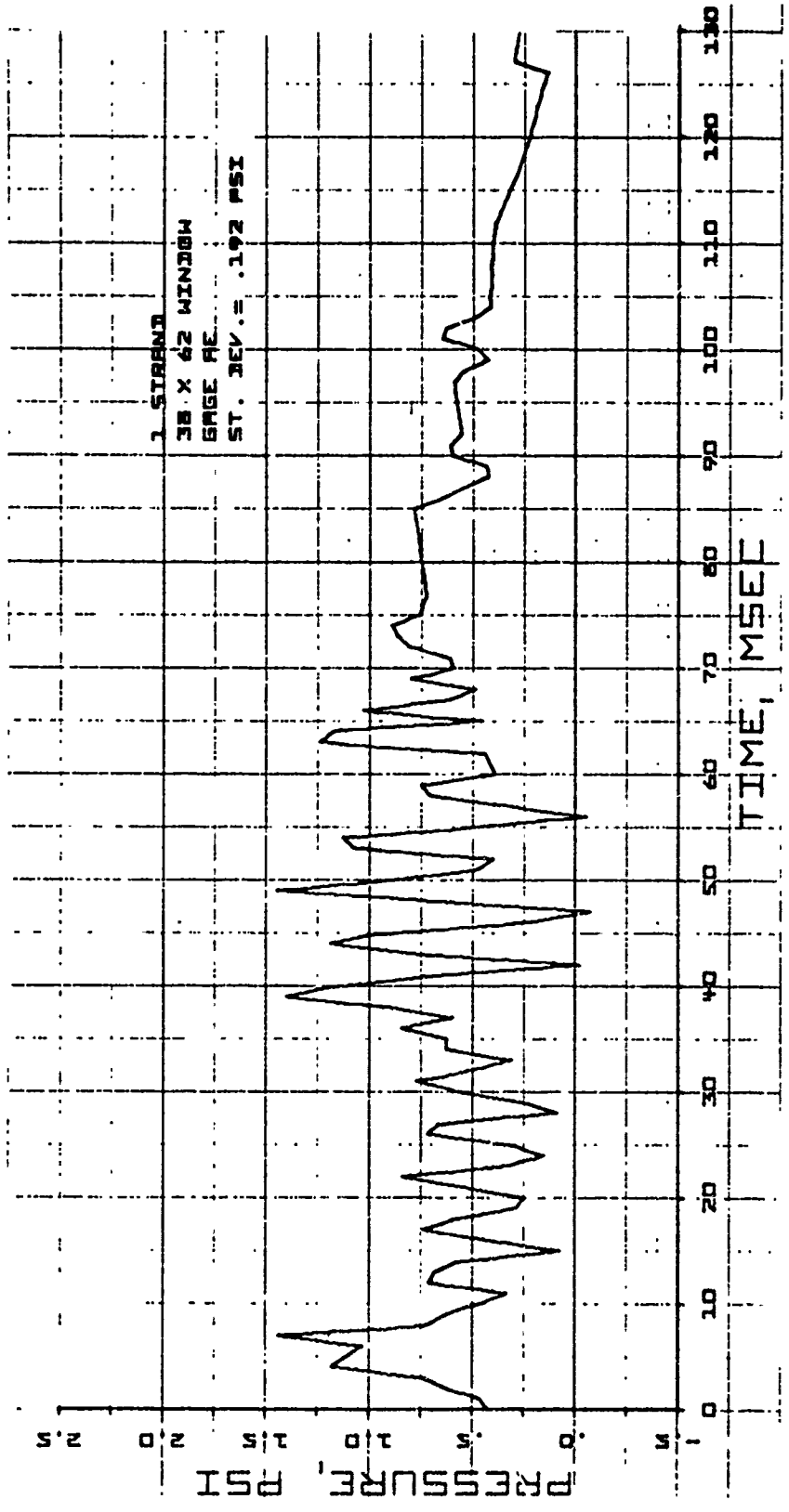

Fig. 5-12. Average Net Pressure as a Function of Time for One Strand 38 X 62 in. Window Loading Study Tests 02-25-70-02, -03 and -04. Gage Pair A-E

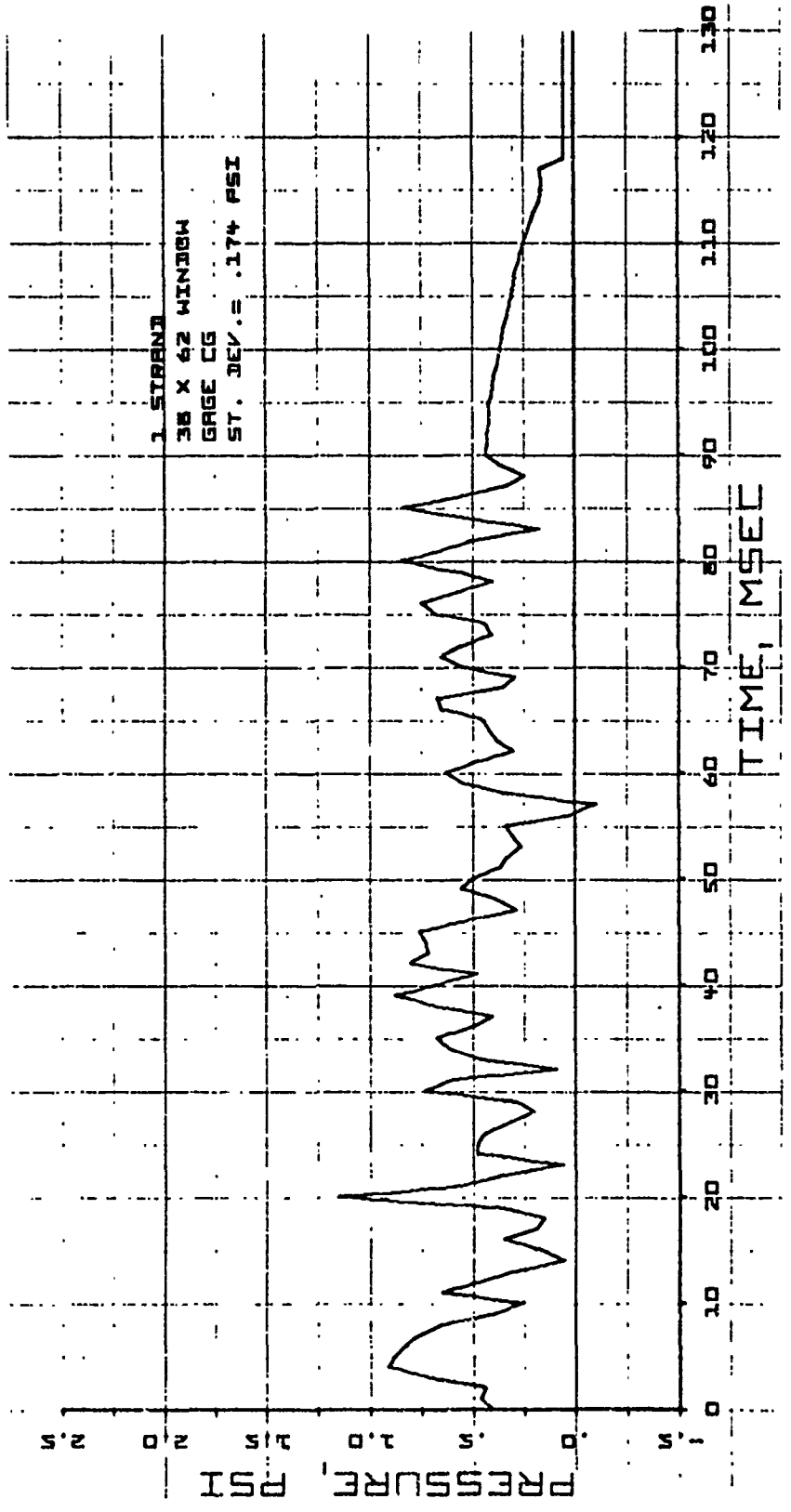

Fig. 5-13. Average Net Pressure as a Function of Time for One Strand 38 × 62 in. Window Loading Study Test 02-25-70-02, -03 and -04. Gage Pair C-G

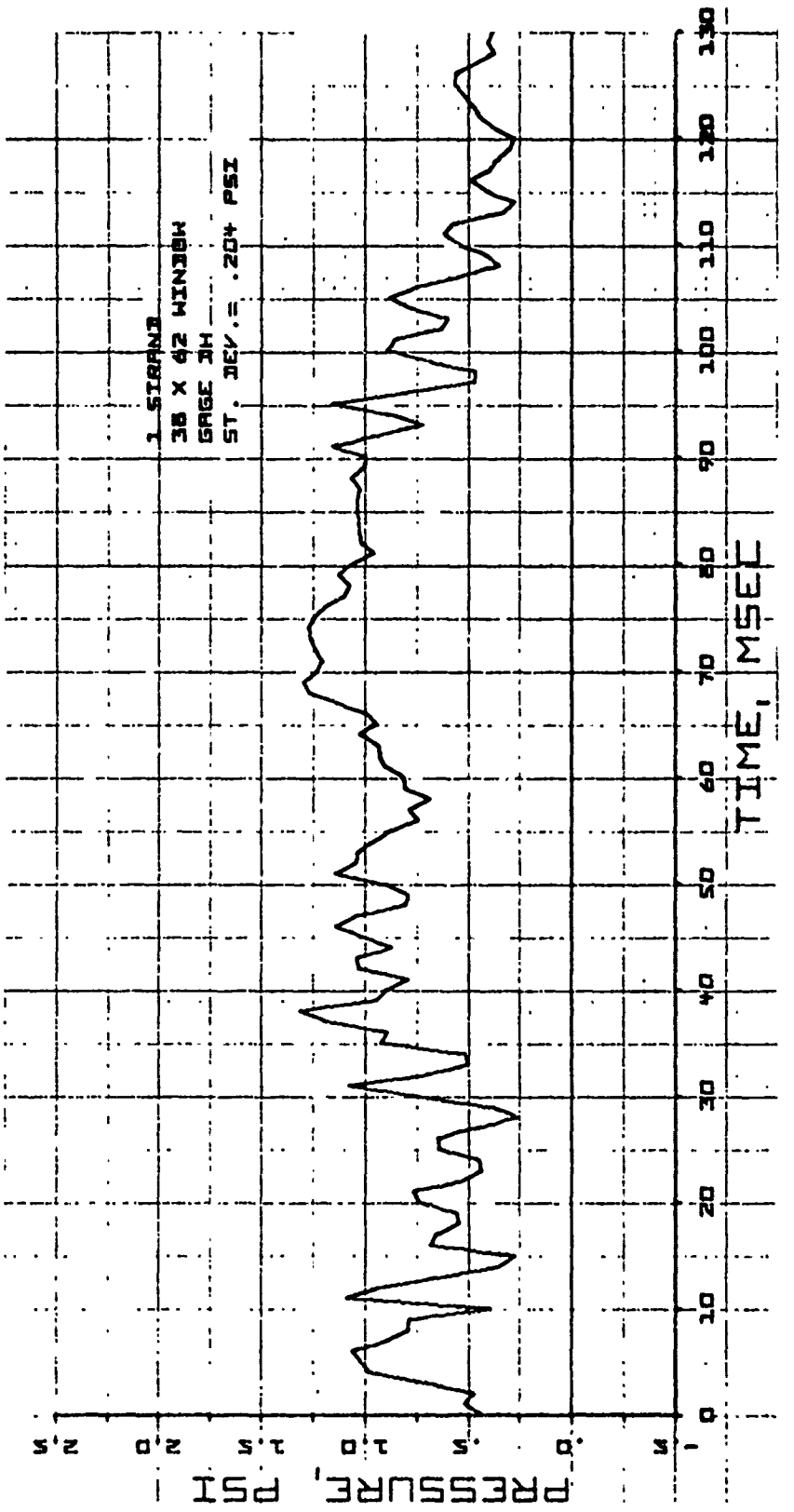

Fig. 5-14. Average Net Pressure as a Function of Time for One Strand 38 X 62 in. Window Loading Study Tests 02-25-70-02, -03 and -04. Gage Pair D-H

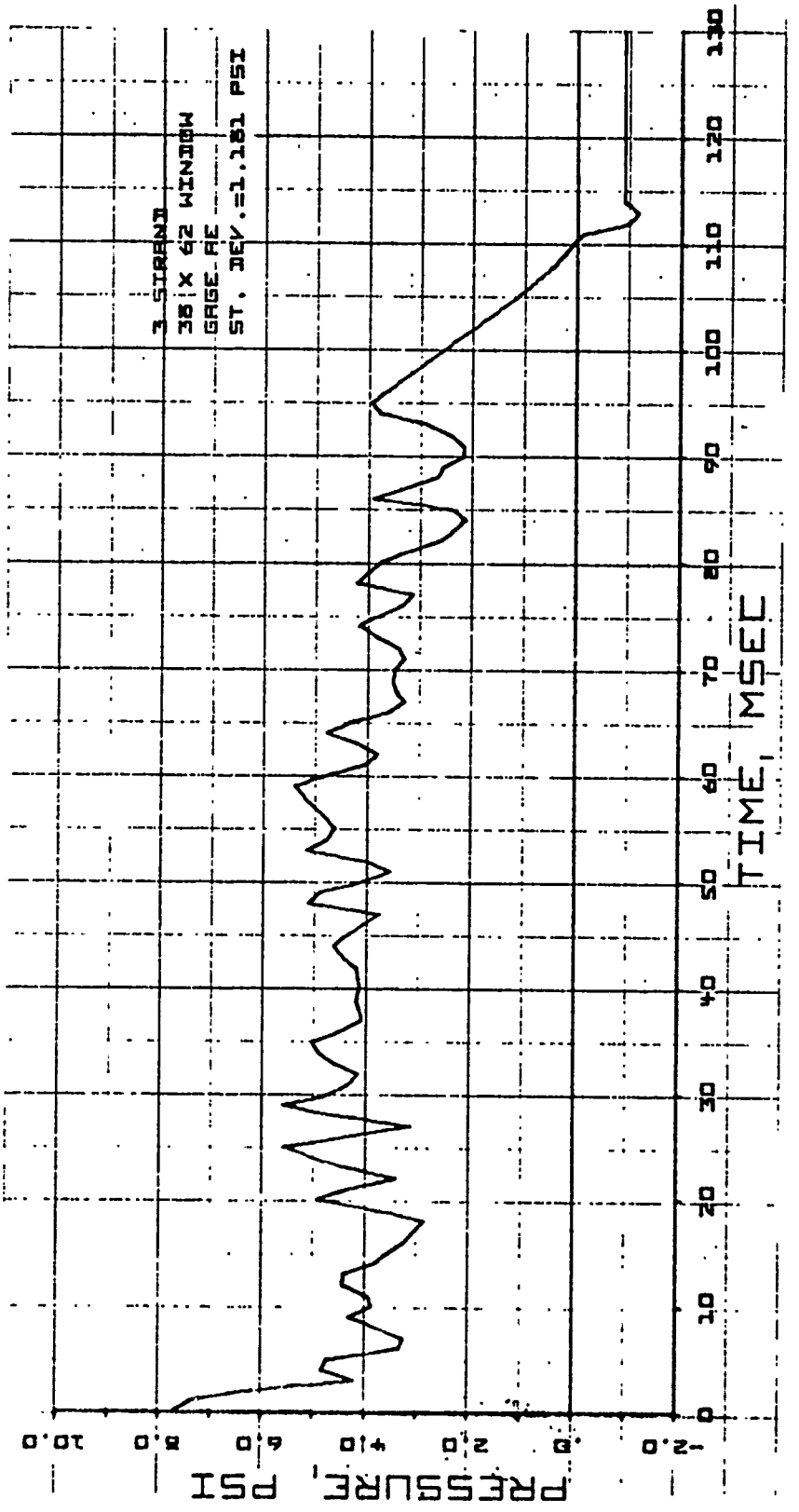

Fig. 5-15. Average Net Pressure as a Function of Time for Three Strand 38 × 62 in. Window Loading Study Test 02-25-70-05, -06 and -07. Gage Pair A-E

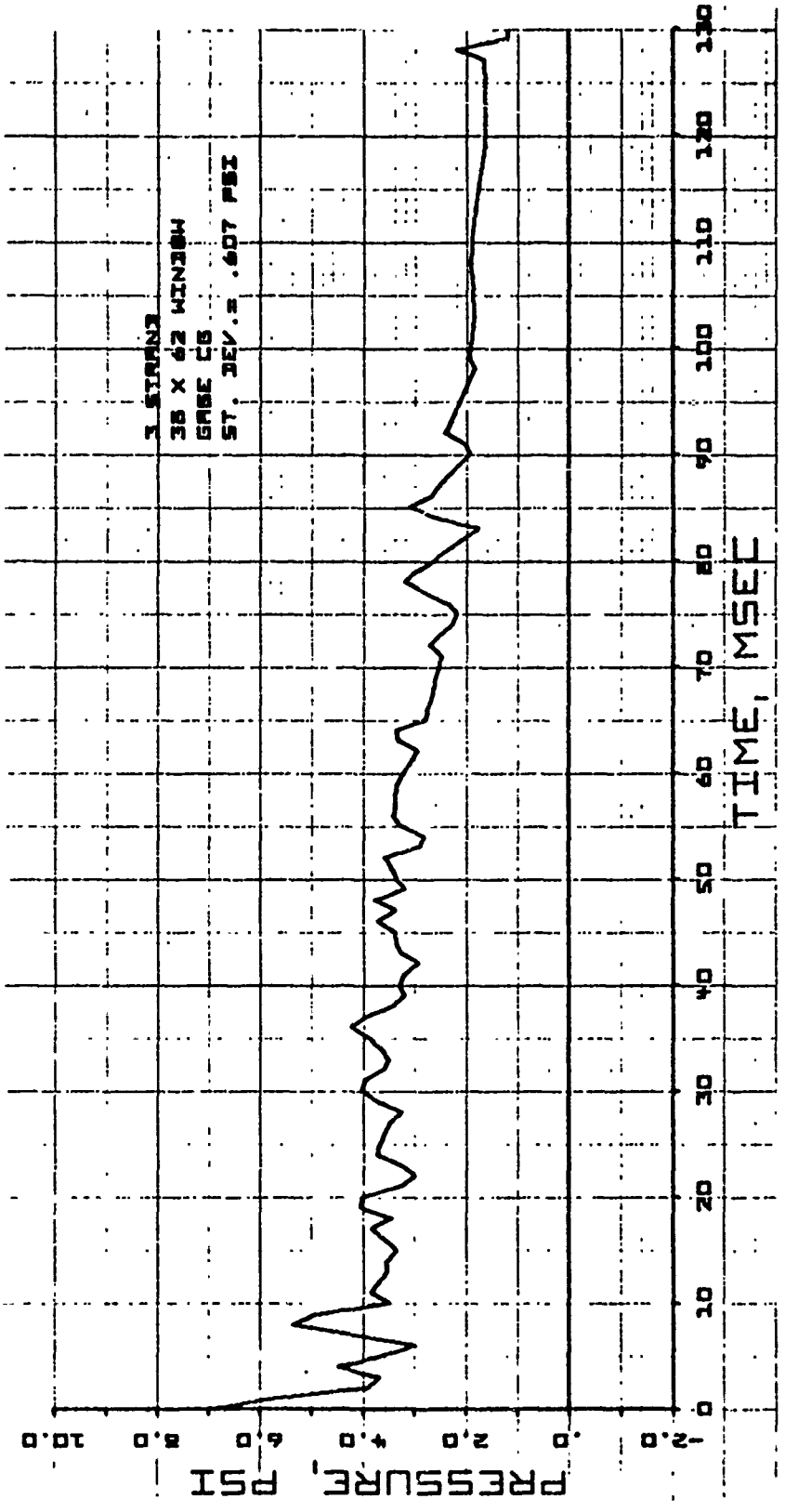

Fig. 5-16. Average Net Pressure as a Function of Time for Three Strand 38 X 62 in. Window Loading Study Test 02-25-7, -05, -06 and -07. Gage Pair C-G

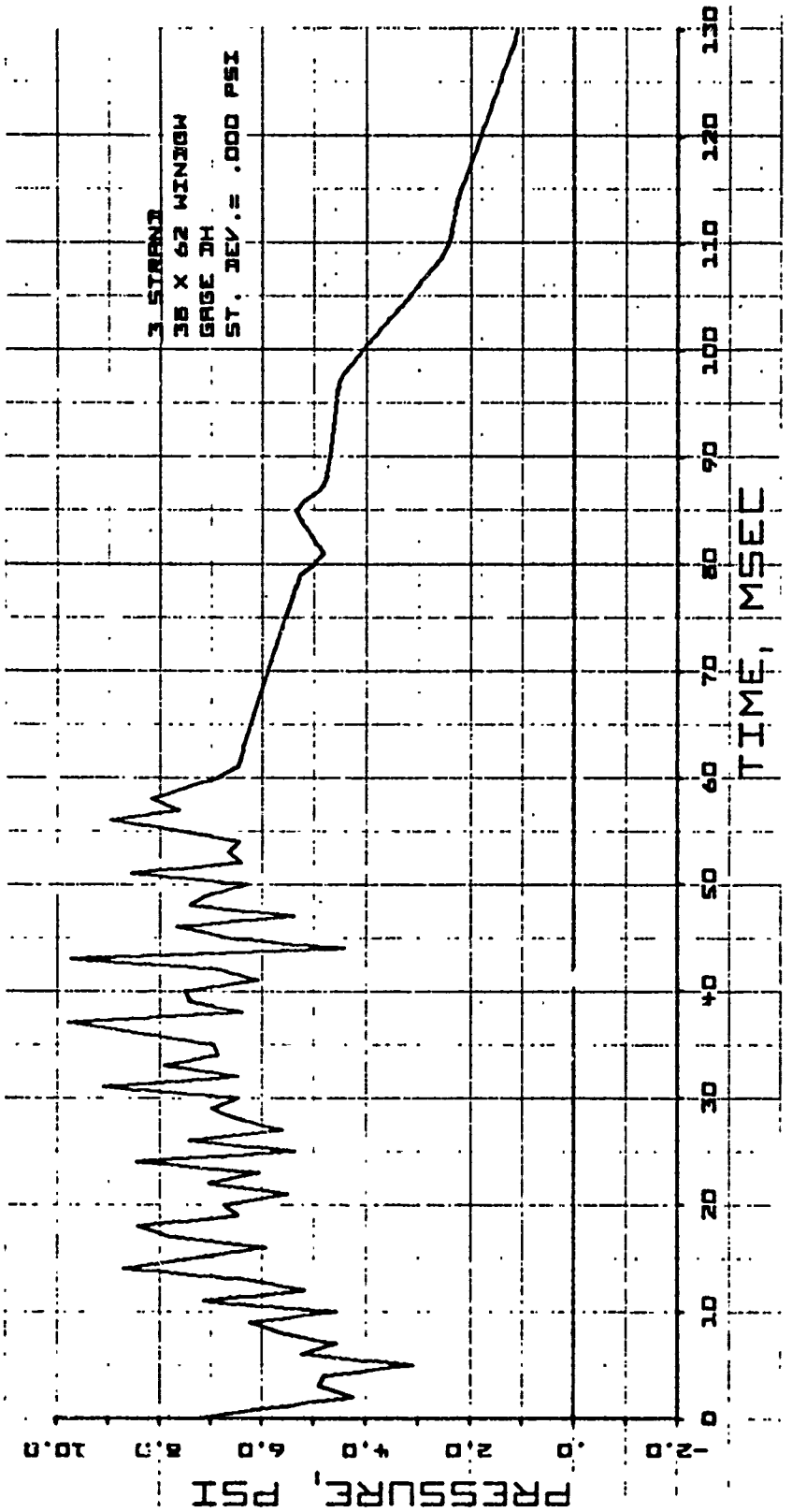

Fig. 5-17. Average Net Pressure as a Function of Time for Three Strand 38 X 62 in. Window Loading Study Test 02-25-70-05, -06 and -07. Gage Pair D-H

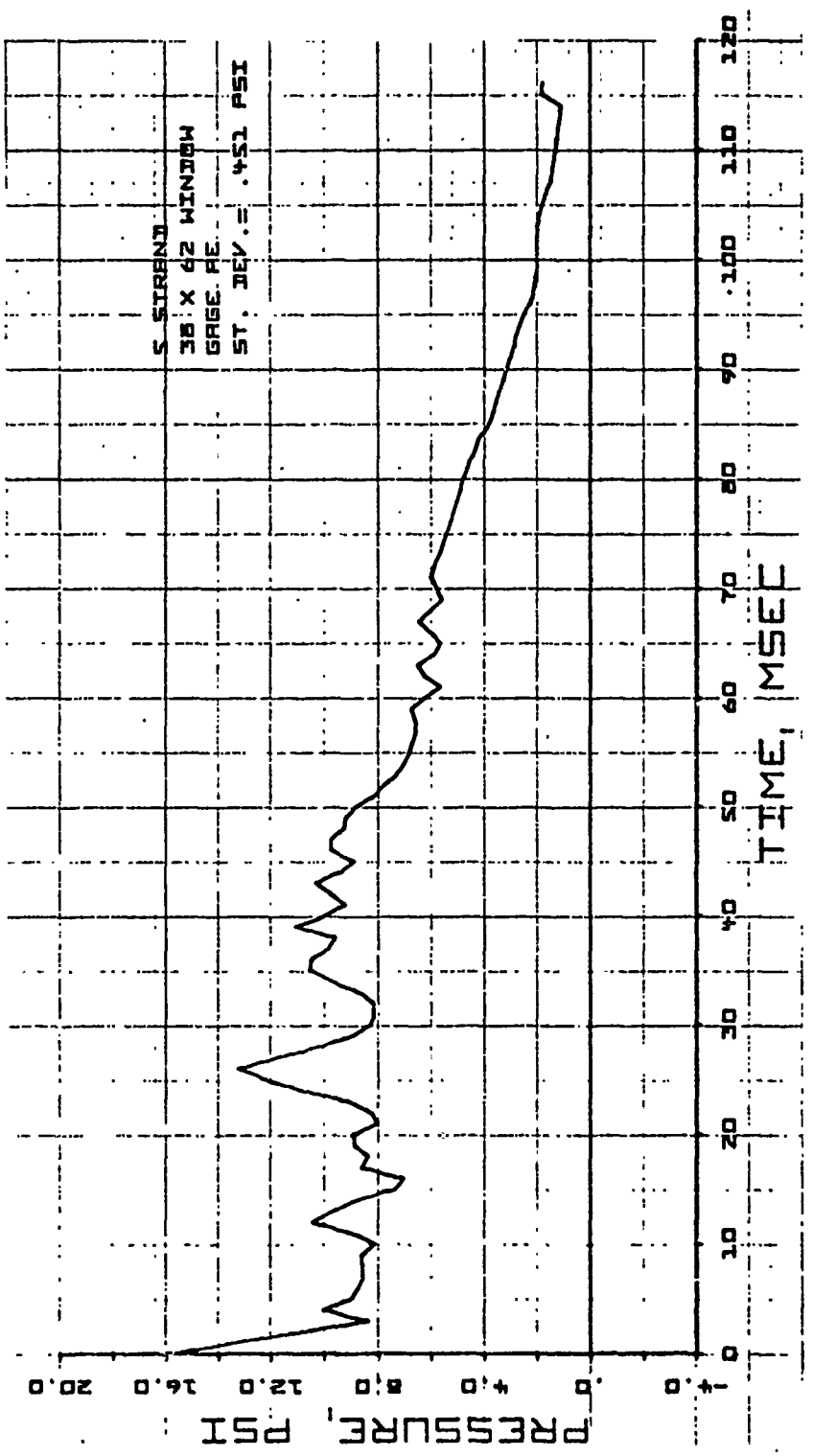

Fig. 5-18. Average Net Pressure as a Function of Time for Five Strand 38 X 62 in. Window Loading Study Test 02-26-70-01, -02 and -03. Gage Pair A-E

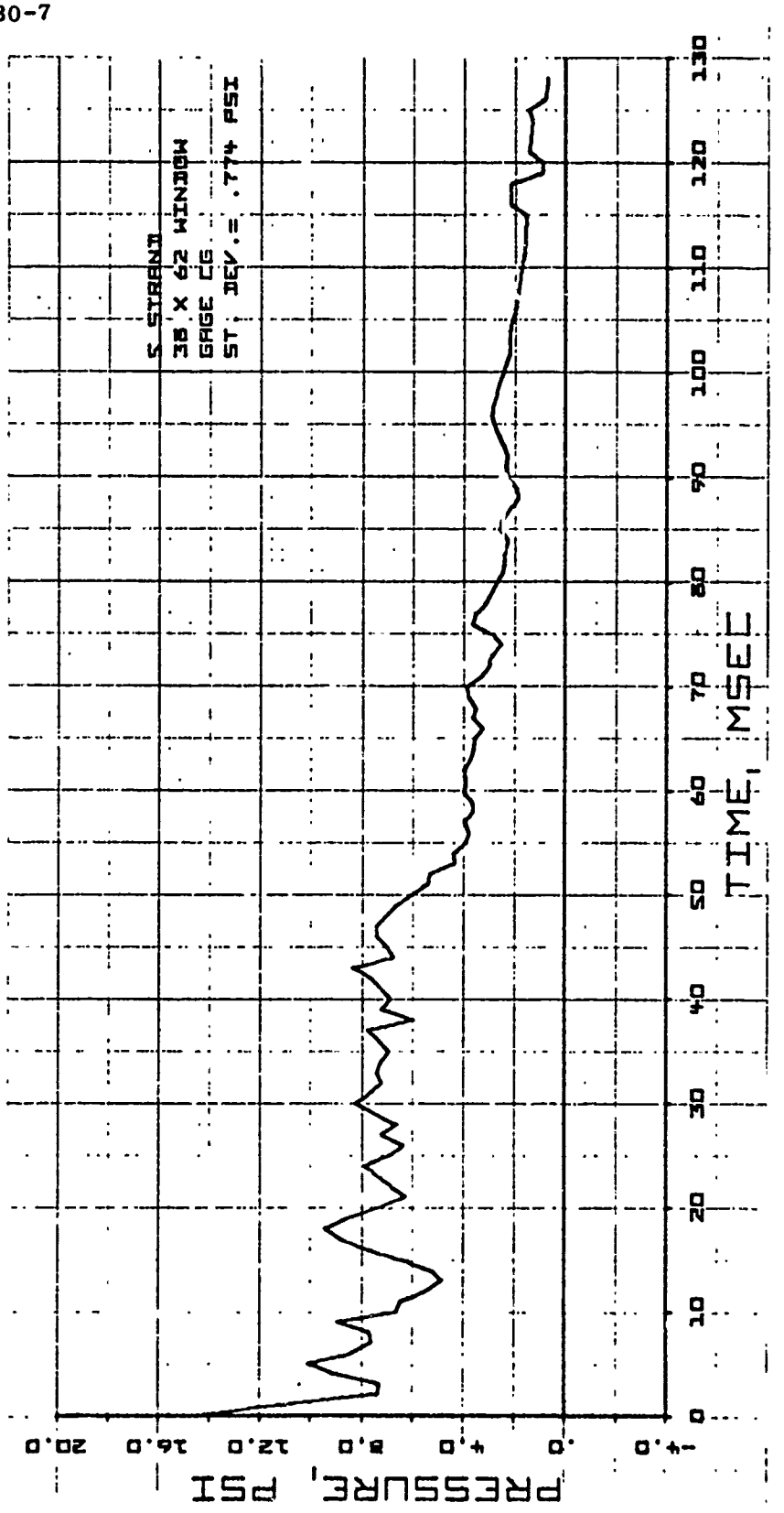

Fig. 5-19. Average Net Pressure as a Function of Time for Five Strand 38 X 62 in. Window Loading Study Test 02-26-70-01, -02 and -03. Gage Pair C-G

THEORETICAL CONSIDERATIONS - Walls with Windows

The format of the analytical effort was basically the same as described in Section 4 for doorways. That is:

1. Selection of a structural model for SAMIS.
2. An approximation of load form from loading tests.
3. Plotting of selected output.
4. Interpretation for testing and prediction.
5. Correlation with test data.

STRUCTURAL MODEL

Figure 5-20 illustrates the facet pattern and Fig. 5-21 the nodal pattern used in the SAMIS analysis. Note that only one-quarter of the wall is used, as the wall is symmetric about both the x and y axis, whereas the doorway is only symmetric about the x axis. The facet size is reduced in the area of the corner of the window to increase the accuracy of stress predictions in the area of stress concentrations.

LOADING

The loading at each point used for input is shown below for three strands.

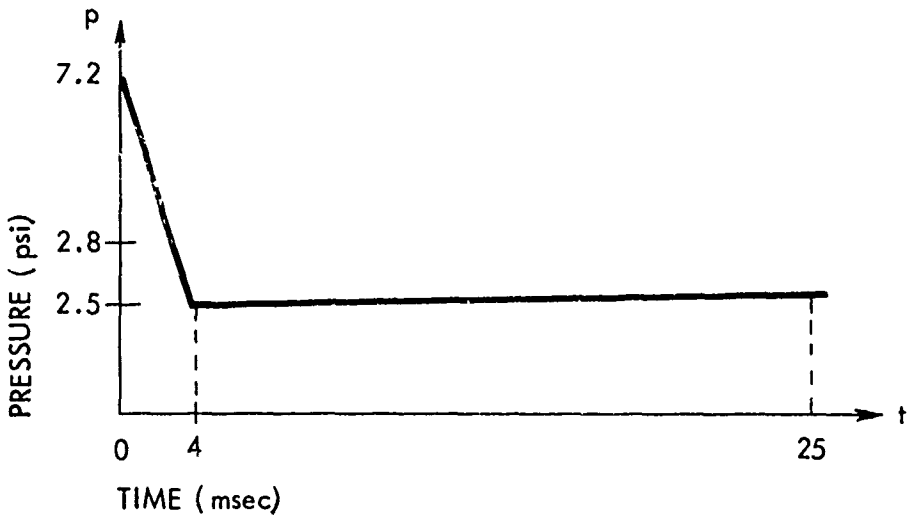

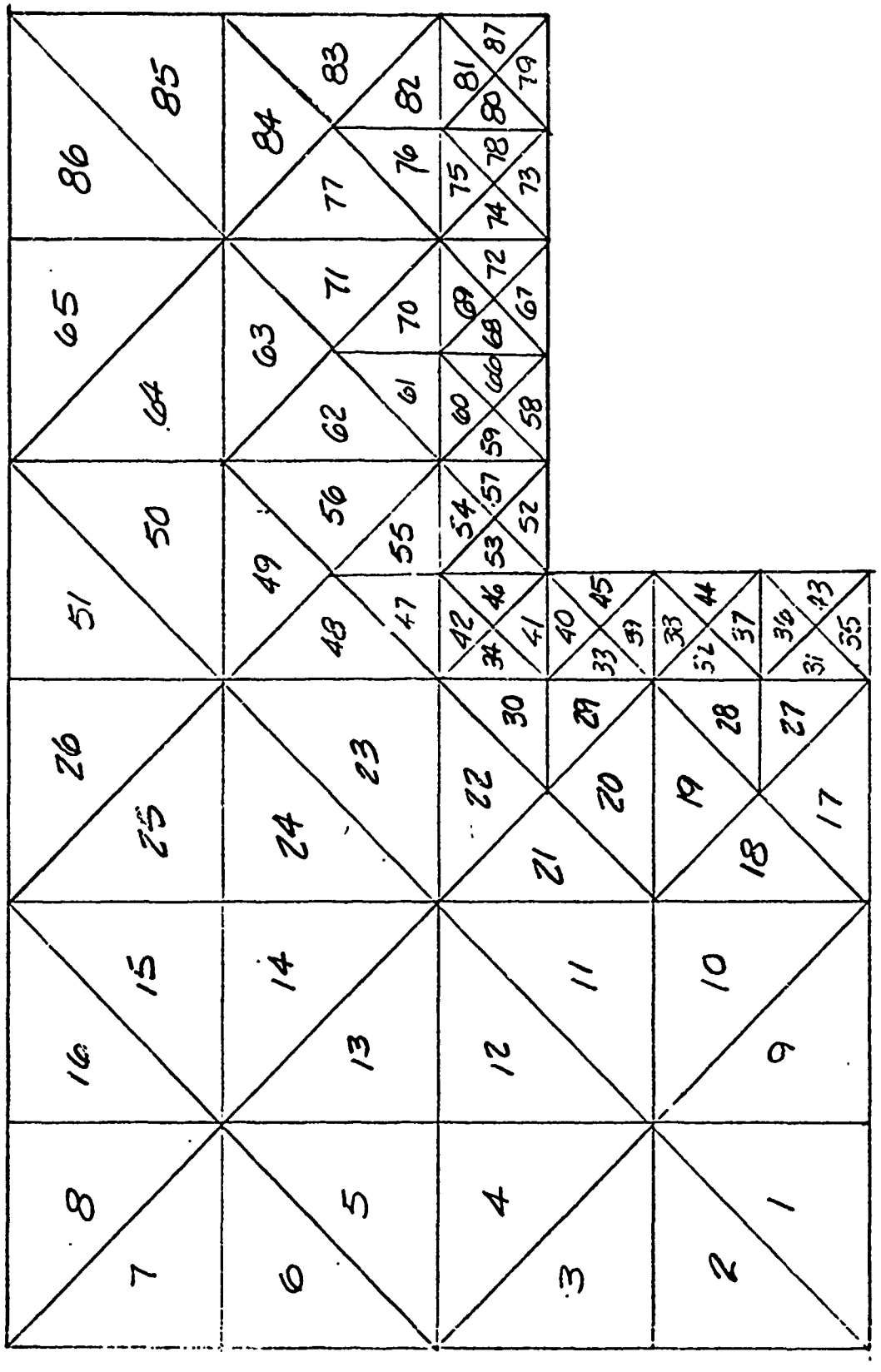

Fig. 5-20. Facet Pattern

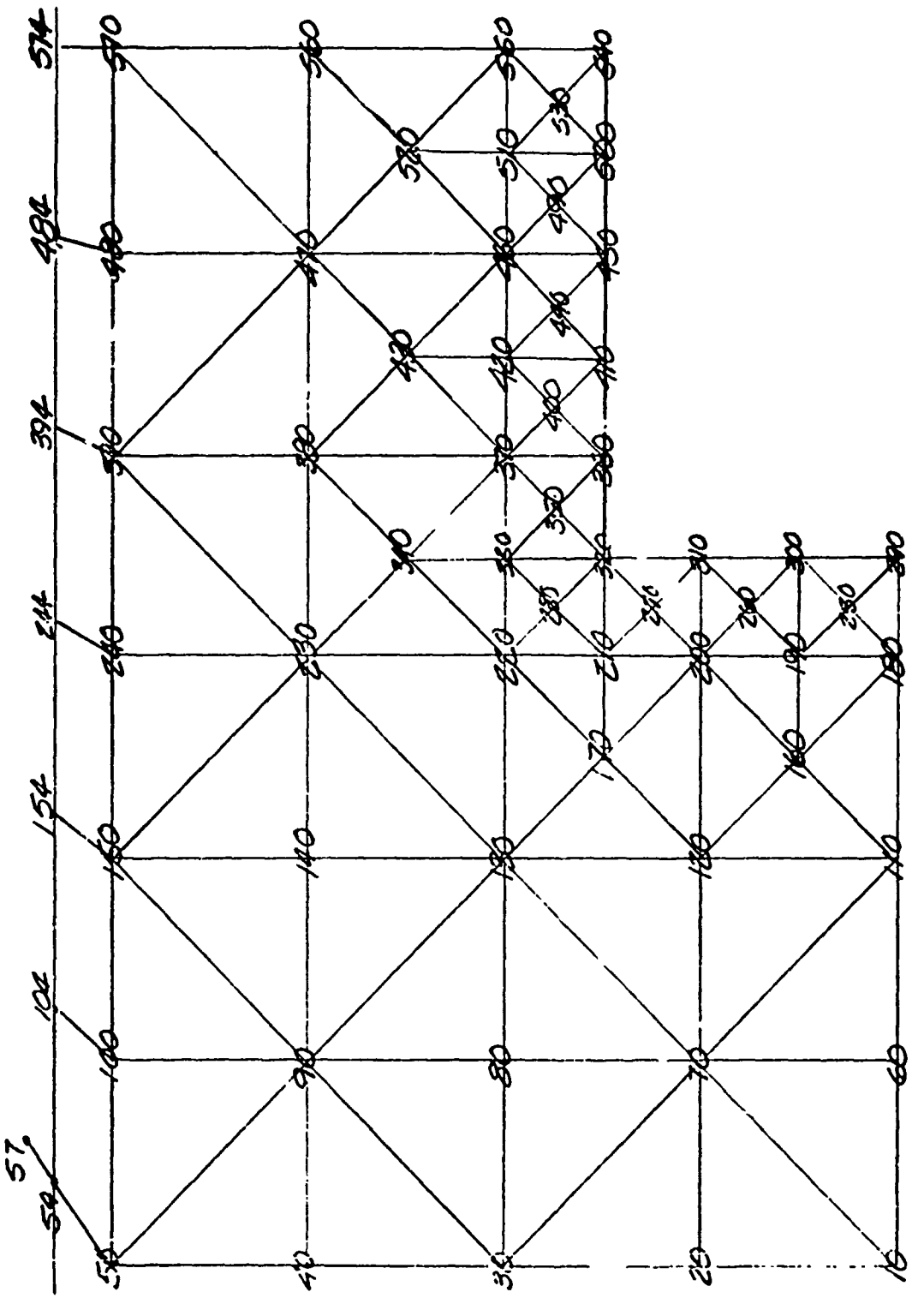

Fig. 5-21. Node Locations

This loading was used for all facets on the wall because loadings at different gage locations did not deviate significantly one from another as was the case for the doorway.

COMPUTER PREDICTIONS

Figures 5-22 through 5-29 are a few selected figures plotted from the SAMIS output for an 8-in. brick wall with windows for a peak reflected pressure (p_r) of 1 psi. The figures are somewhat self-explanatory with Figs. 5-22 through 5-24 illustrating deflection contours with time; Fig. 5-25 is a plot of velocity and deflection vs time for Node 60. Figure 5-26 is a plot of the predicted load cell trace, and Figs. 5-27 and 5-28 plot stress vs time for elements 22 and 34 in the corner region of the window. The angle θ plotted on Figs. 5-27 and 5-28 are the angles of the tensile-stress trajectory measured clockwise from a vertical, i.e., they are normal for the projected crack (see Fig. 5-29).

From the stress predictions, we see that a one-strand shot (p_r = 1 psi for modeling purposes) produces corner stresses on the order of 110 psi. Hence, there was a reasonable probability of flexural failure with one-strand shots.

TEST RESULTS - Walls with Windows

During this reporting period, two 8-in. nonreinforced brick walls with windows and two 8-in. nonreinforced concrete block walls with windows were tested. All walls were supported as simple beams.

The brick walls (Wall Nos. 56 and 57) were nominally 12 ft wide and 8-1/2 ft high, including the steel support frame. Each wall included a 62 in. x 38-1/2 in. open window. A pre-test photograph of one of the walls and a dimensional sketch are presented in Fig. 5-30.

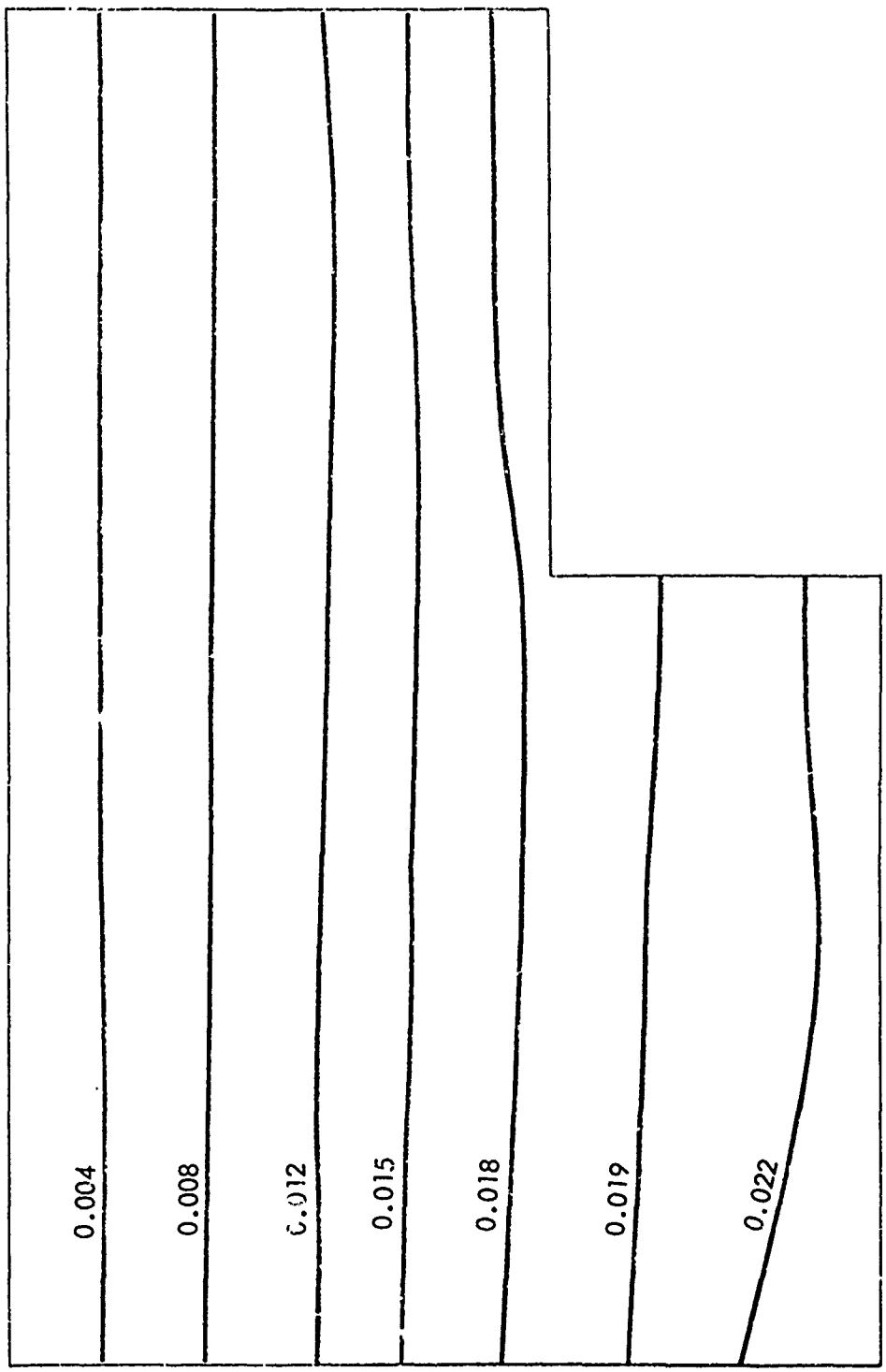

Fig. 5-22. Deflection Contours (in.), t = 0.013 sec, Normalized to 1 psi Loading

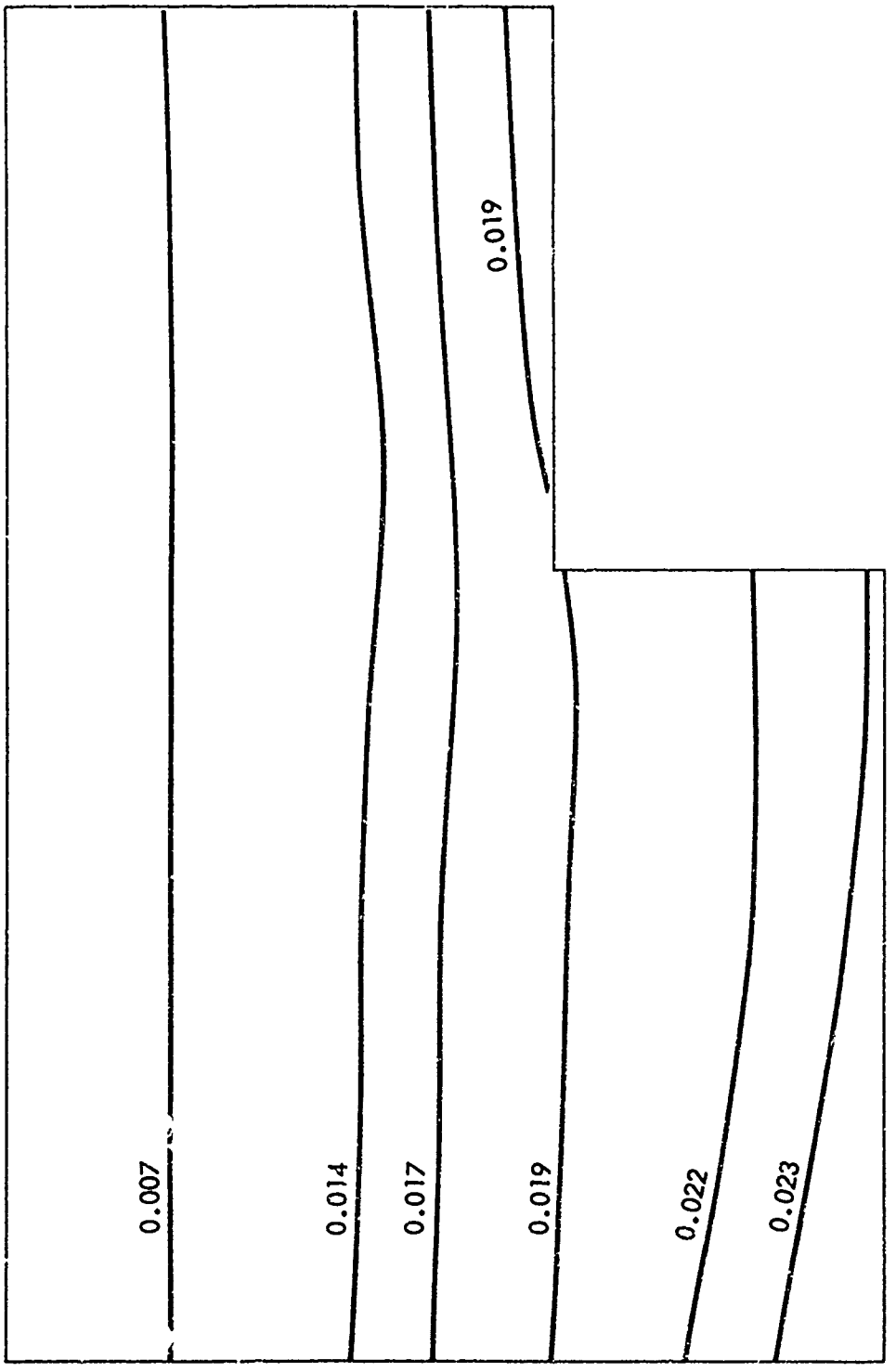

Fig. 5-23. Deflection Contours (in.), t = 0.014 sec, Normalized to 1 psi Loading

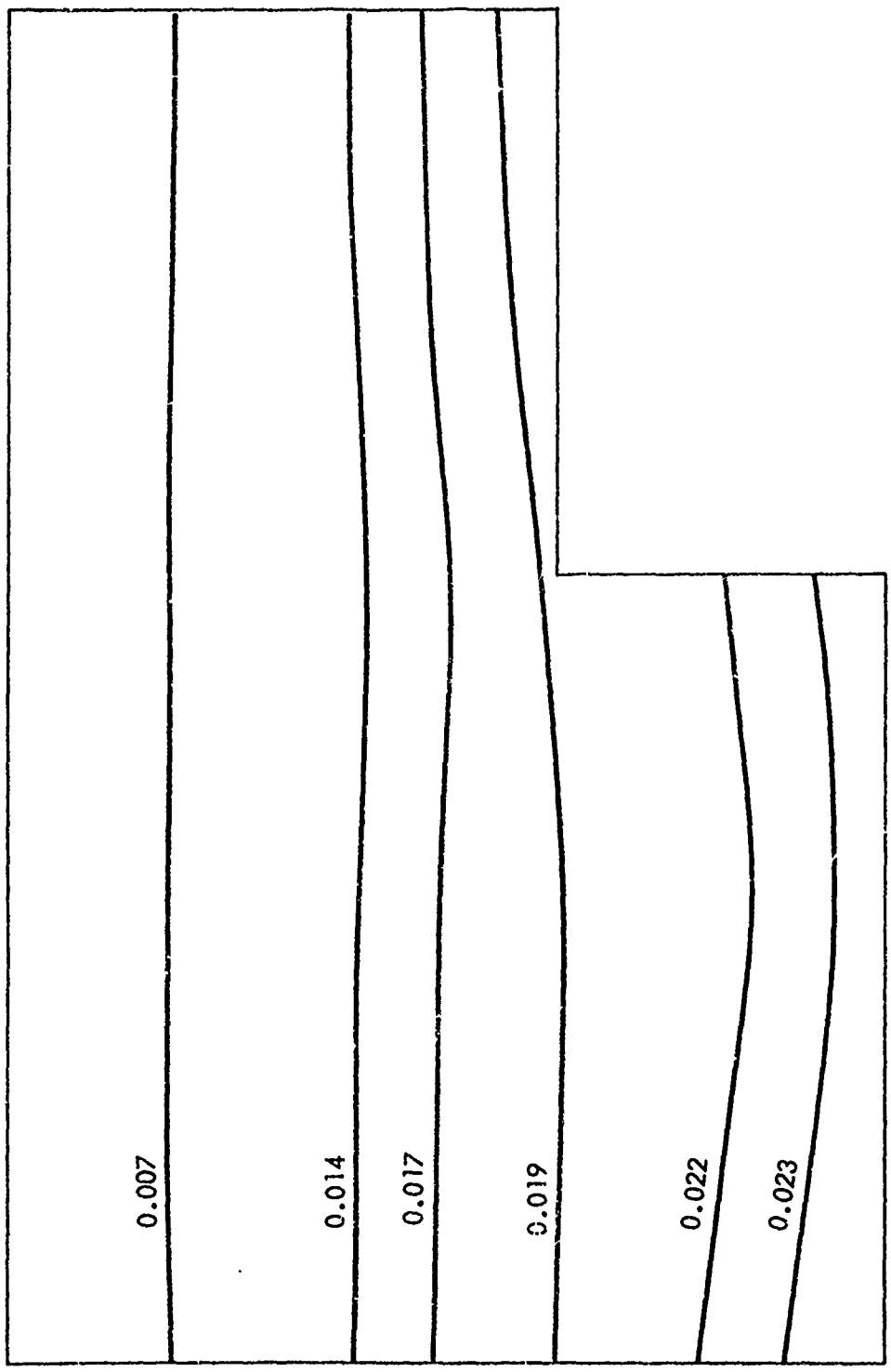

Fig. 5-24. Deflection Contours (in.), t = 0.015 sec, Normalized to 1 psi Loading

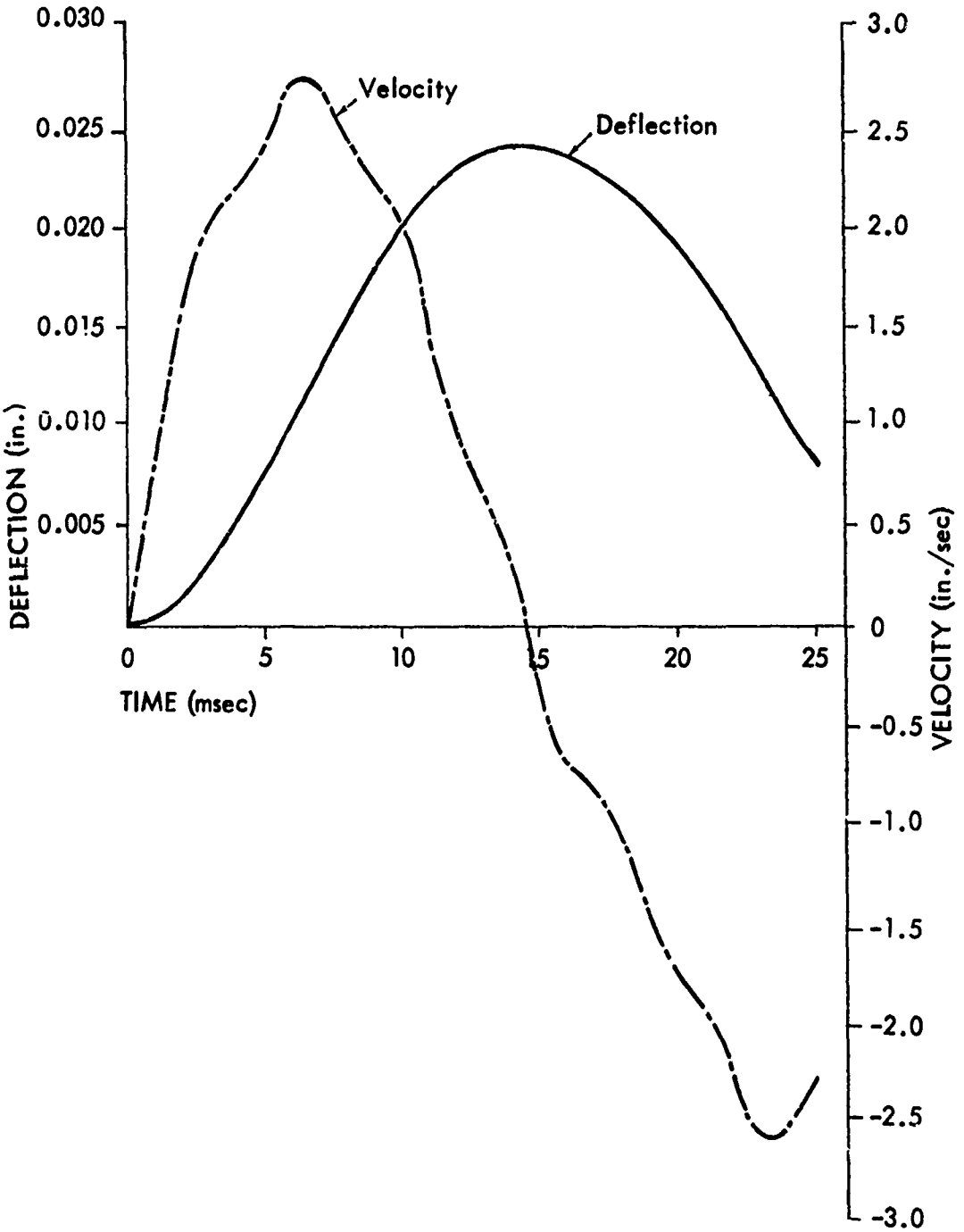

Fig. 5-25. Velocity and Deflection vs Time for Node 60, Normalized to 1 psi Loading

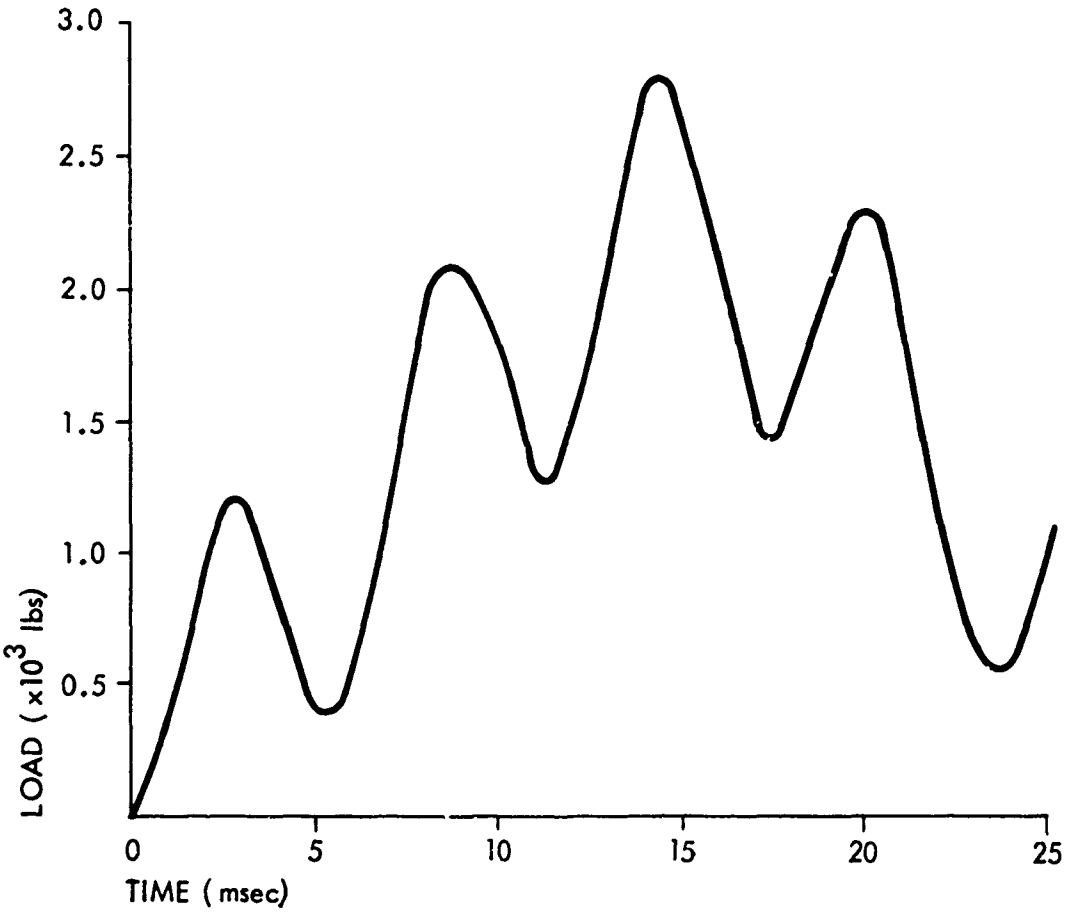

Fig. 5-26. Load Cell vs Time, Normalized to 1 psi Loading

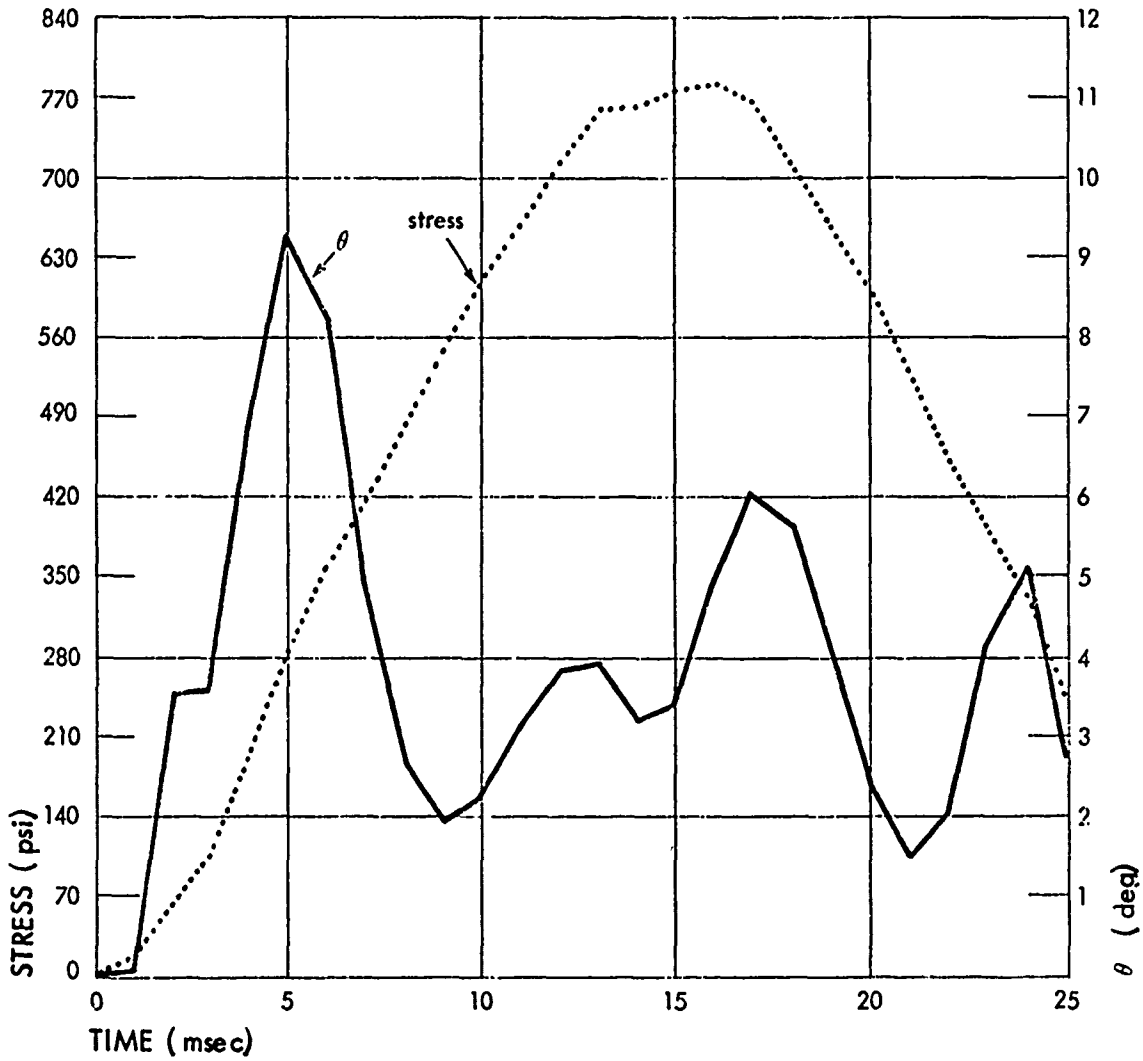

Fig. 5-27. Plot of Stress vs Time and θ vs Time for Element No. 22 (not normalized; p_r = 7.2 psi)

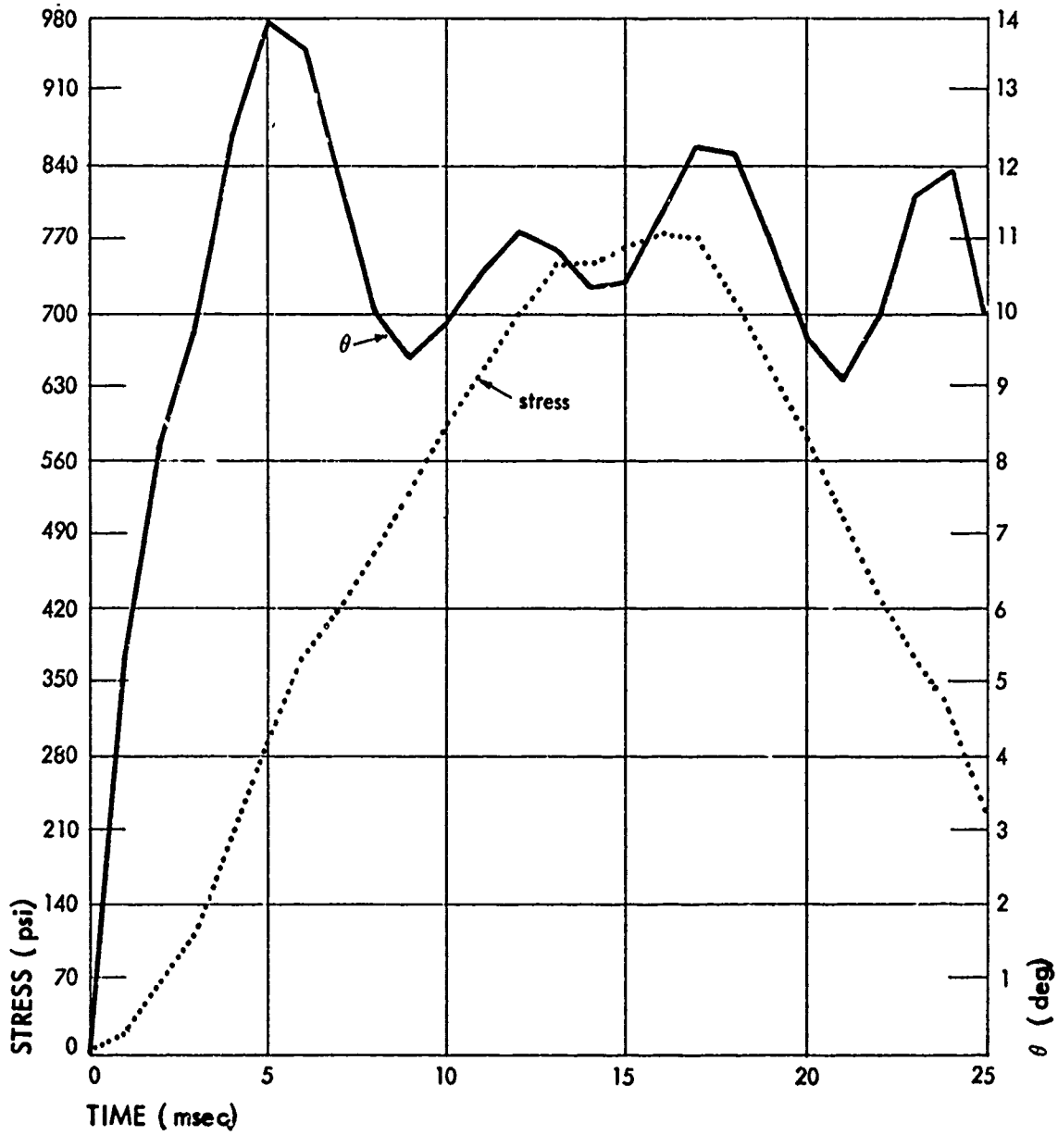

Fig. 5-28. Plot of Stress vs Time and θ vs Time for Element No. 34 (not normalized; p_r = 7.2 psi)

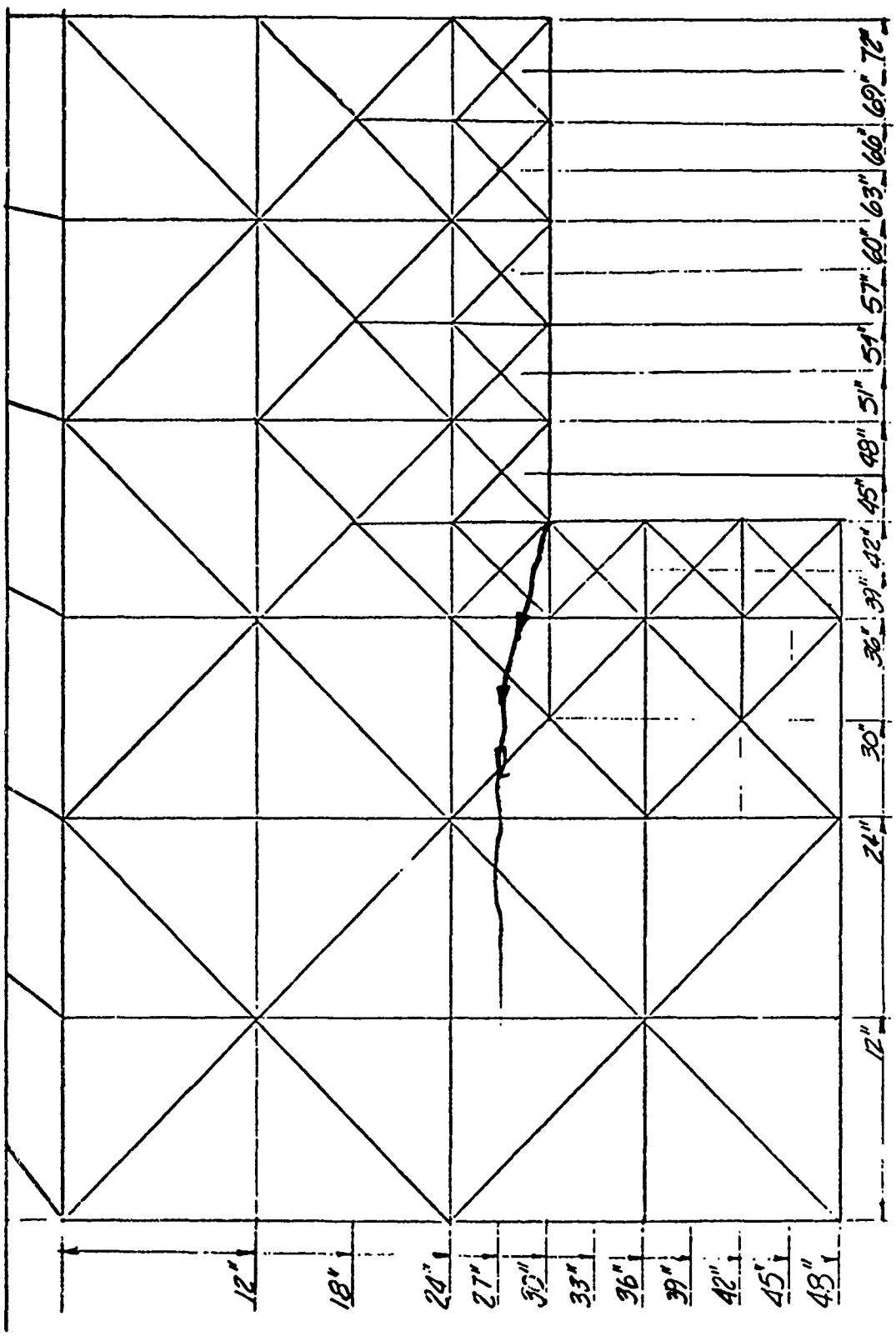

Fig. 5-29. Coordinates and Predicted Crack Trajectory

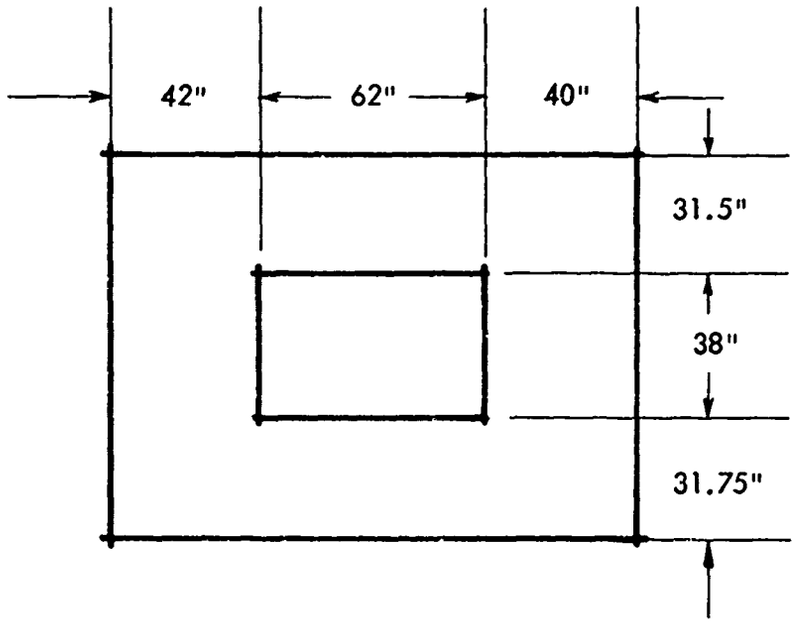

Fig. 5-30. 8-in. Nonreinforced Brick Wall Panel with a Window

Wall No. 56 - 8 in. Nonreinforced Brick Wall with Window

This wall was tested once (Test No. 02-18-71-01) using two strands of Primacord. The measured maximum reflected overpressure was 3.6 psi. The wall failed with first cracks appearing horizontally at the top and bottom of the window. The wall collapsed with the bottom section rotating until impact with the floor and the top section rotating 90 degrees and landing on top of the bottom section. One window side panel separated, and the other remained attached to the top section until impact with the floor. The maximum total load as measured by the load cells was 28,000 lb. A plot of displacement as a function of time for this test is presented in Fig. 5-31 and a post-test photograph in Fig. 5-32.

Wall No. 57 - 8 in. Nonreinforced Brick with Window

Four tests were conducted on this wall panel. The first three (03-05-71-01, -02 and -03) used one strand of Primacord and subjected the panel to a measured peak reflected overpressure of 1.3 psi and a net load of approximately 0.5 psi (see Figs. 5-4 and 5-5).

During the first test, cracks appeared at 19 and 79 msec. These cracks increased in size with the two subsequent loadings, and after the third test, compression cracks about 1 in. deep were noted on the upstream side.

The fourth test (03-05-71-01) used two strands of Primacord and subjected the wall to a measured peak reflected overpressure of 3.8 psi. The wall failed with the bottom section rotating until striking the floor and the top section rotating 90 degrees and landing on the bottom section. One side panel separated, and the other remained attached to the top section. The maximum total load measured by the load cells was 13,500 lb. A post-test photograph of this wall is presented in Fig. 5-33 and a plot of displacements as a function of time in Fig. 5-34.

The two concrete block walls (Test Nos. 60 and 61) were nominally 12 ft wide and 8-1/2 ft high including the steel support frame; each contained a

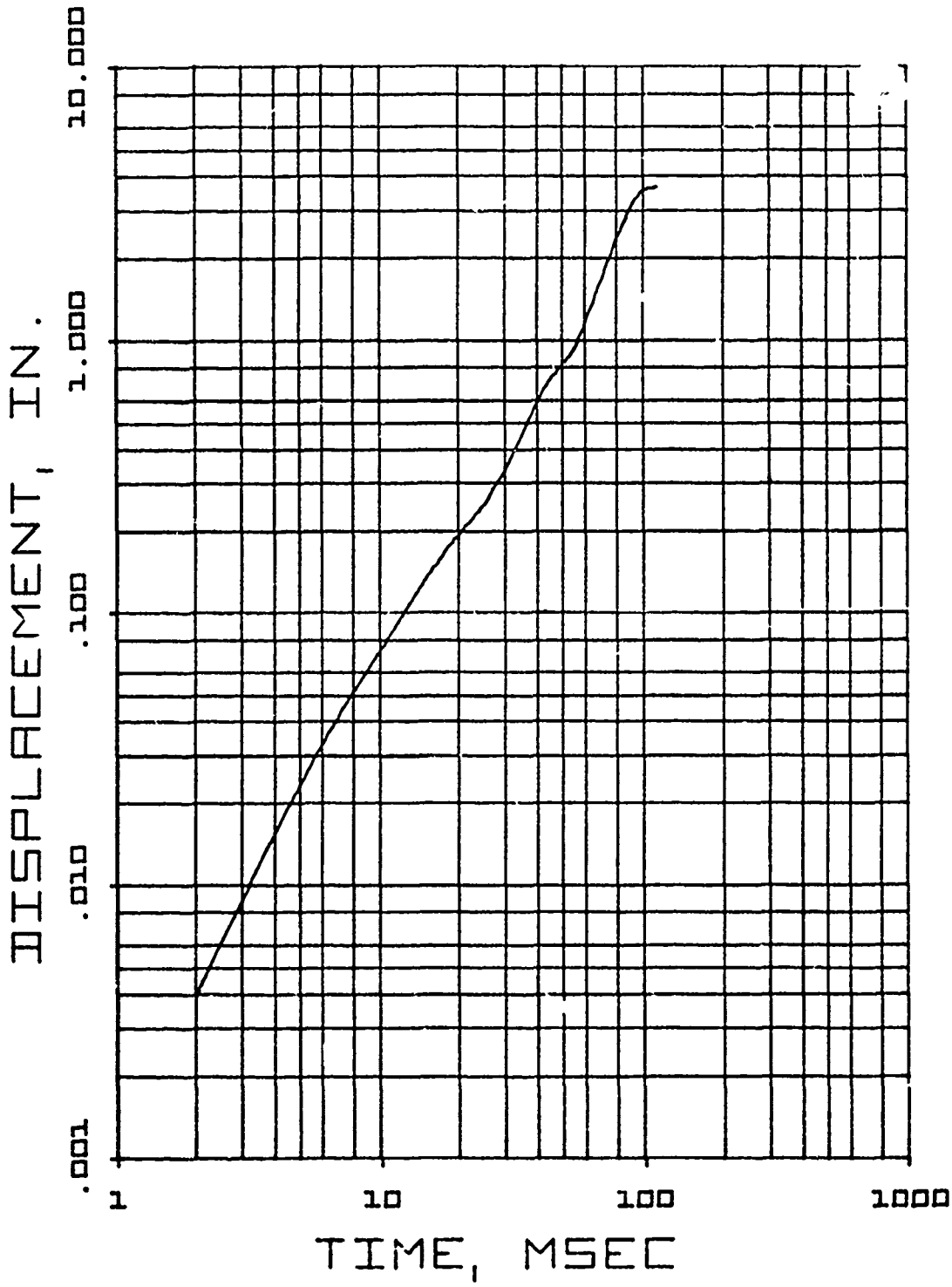

Fig. 5-31. Displacement as a Function of Time for Wall No. 56, 8 in. Nonreinforced Brick with Window (Test No. 02-18-71-02)

Fig. 5-32. Post-Test Photograph of Wall No. 56, Brick with Window

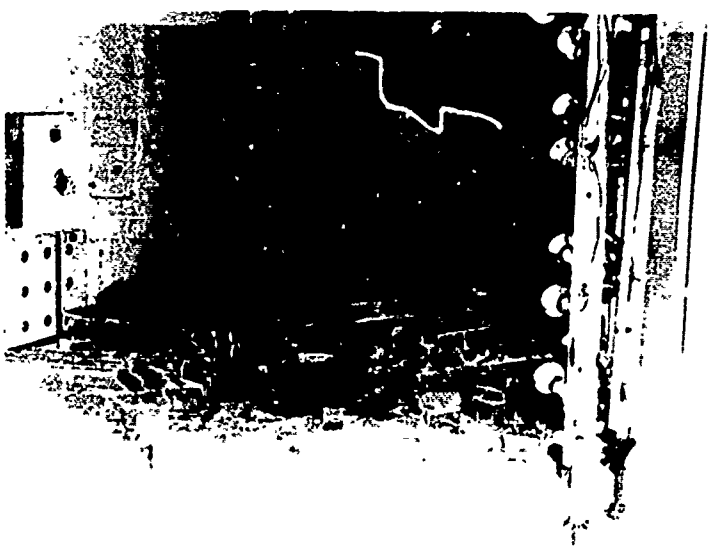

Fig. 5-33. Post-Test Photograph of Wall No. 57, Brick with Window

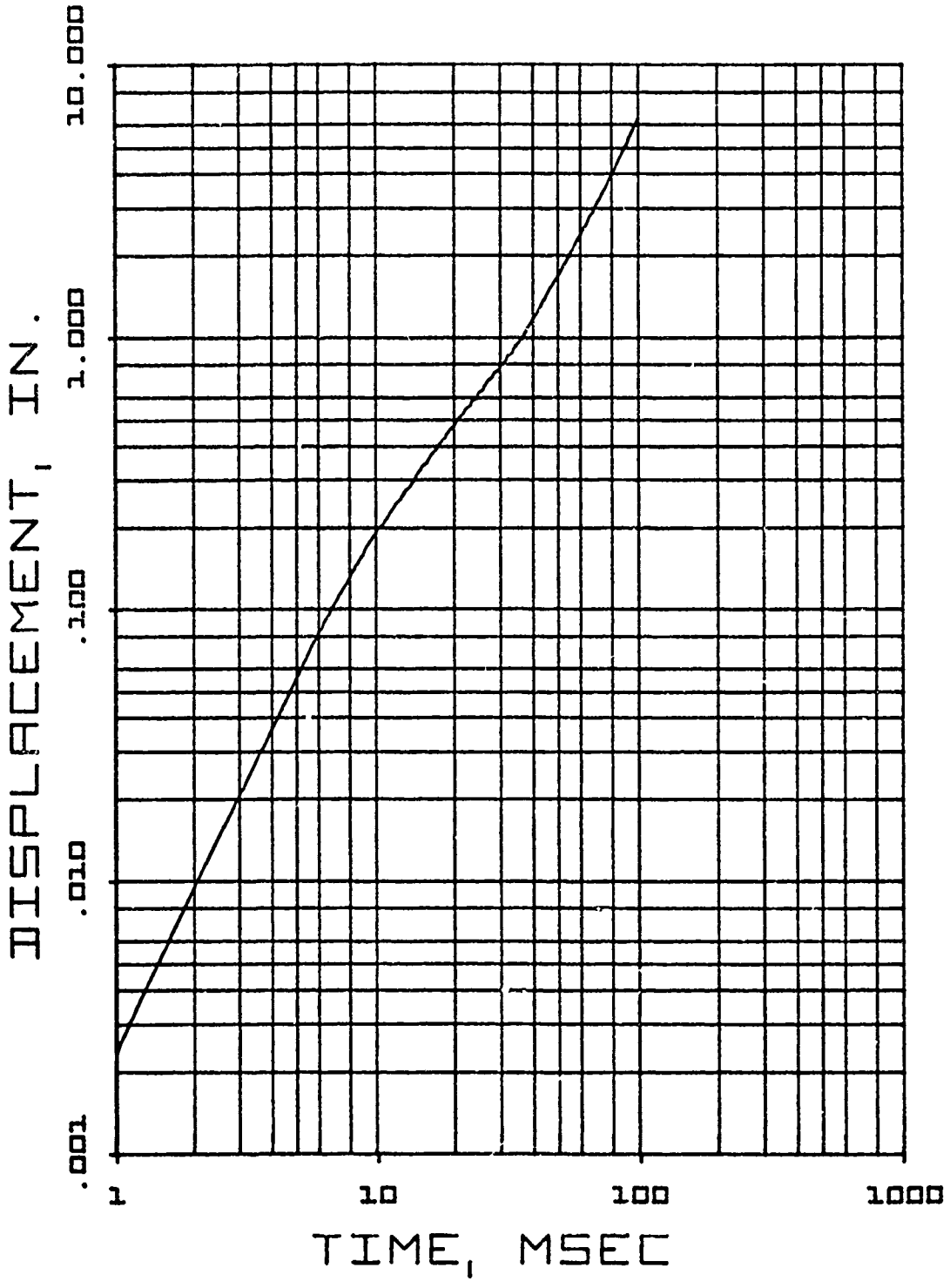

Fig. 5-34. Displacement as a Function of Time for Wall No. 57, 8 in. Nonreinforced Brick with Window (Test No. 03-05-71-04)

39 in. high X 62 in. wide window. The wall was nonreinforced and constructed of standard 15-1/2 X 7-1/2 X 7-1/2 in. concrete blocks. A pre-test photograph of Wall No. 60 and a dimensional sketch of the wall are shown in Fig. 5-35.

Wall No. 60 - 8 in. Nonreinforced Concrete Block with Window

The first test (04-26-71-01) conducted on this wall used a short (approximately 10 ft) length of Primacord to obtain a measure of the natural period. This was measured as 29 msec. The wall cracked at 79 msec and numerous cracks were visible in the wall after the test.

In the second test (04-26-71-02), which used one 60 ft strand of Primacord, the wall failed with the majority of debris landing within 15 ft and small pieces as far as 30 ft. The measured peak reflected overpressure was approximately 1.5 psi, and the total measured load obtained from the load cells was 8,100 lb at approximately 24 msec. A plot of displacement as a function of time for this wall is presented in Fig. 5-36 and post-test photographs in Fig. 5-37.

Wall No. 61 - 8 in. Nonreinforced Concrete Block with Window

This wall was tested three times. The first test (05-17-71-01) used a 10 ft length of Primacord to obtain the natural period which was found to be 30 msec. The wall cracked in three places on either side of the window during this shot with cracks occurring at 5 and 10.5 msec.

The second test (05-17-71-02) used one strand of Primacord 60 ft long which gave a measured overpressure of 1.5 psi. The wall did not collapse and the previous visible cracks were enlarged.

The third test (05-17-71-03) also used one strand of Primacord 60 ft long which gave a peak measured overpressure of 1.5 psi. The wall failed with the majority of the debris landing within 15 ft of the original mounting location. The total measured load obtained from the load cells was 6,000 lb. A plot of displacement as a function of time is presented in Fig. 5-38 and post-test photographs in Fig. 5-39.

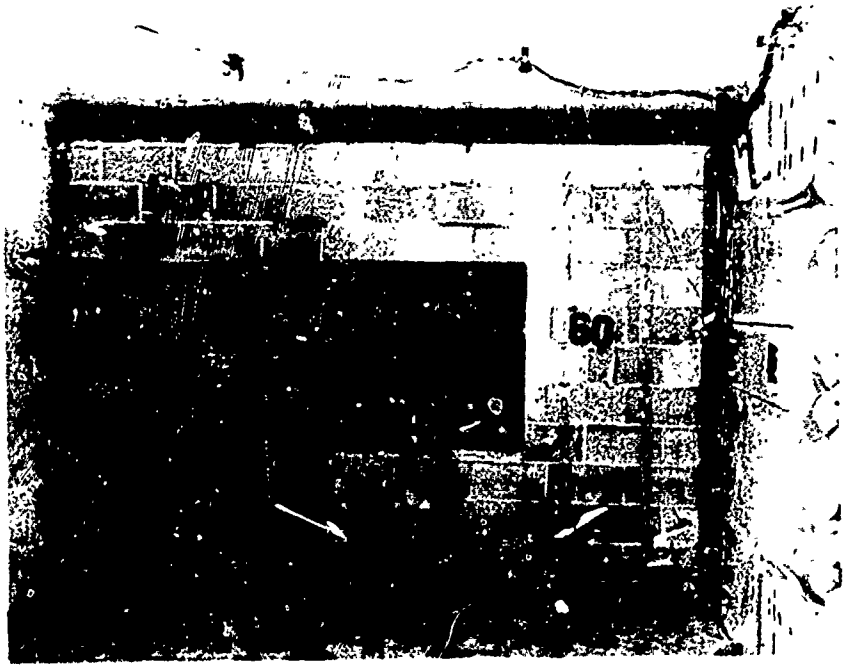

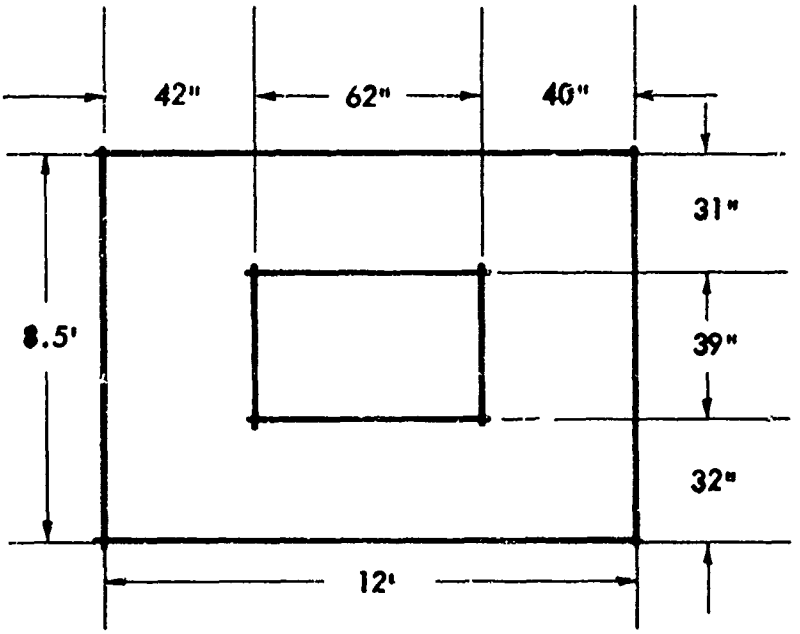

Fig. 5-35. Concrete Block Wall with a Window

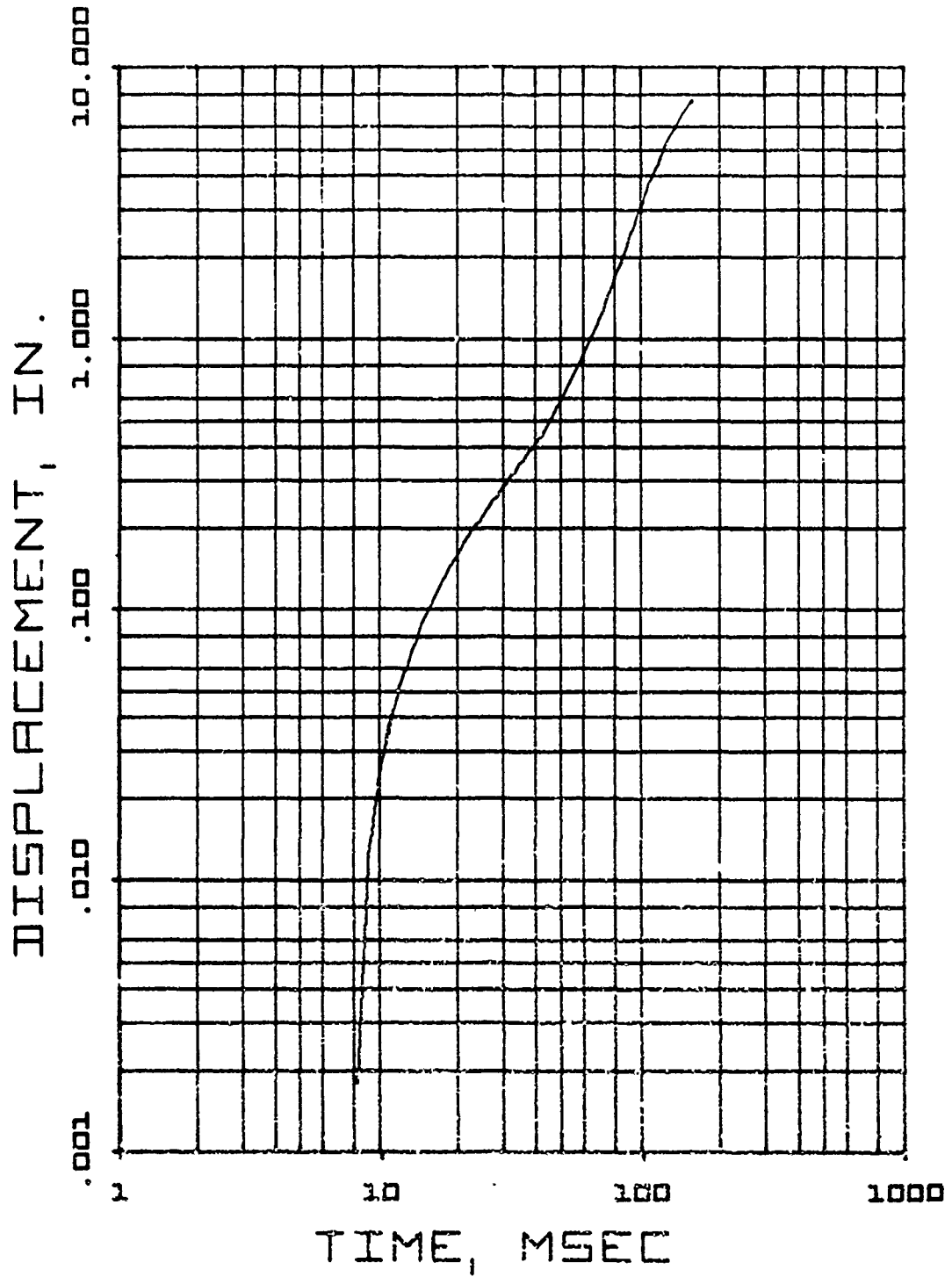

Fig. 5-36. Displacement as a Function of Time for Wall No. 60, 8 in. Nonreinforced Concrete Block with Window (Test No. 04-26-71-02)

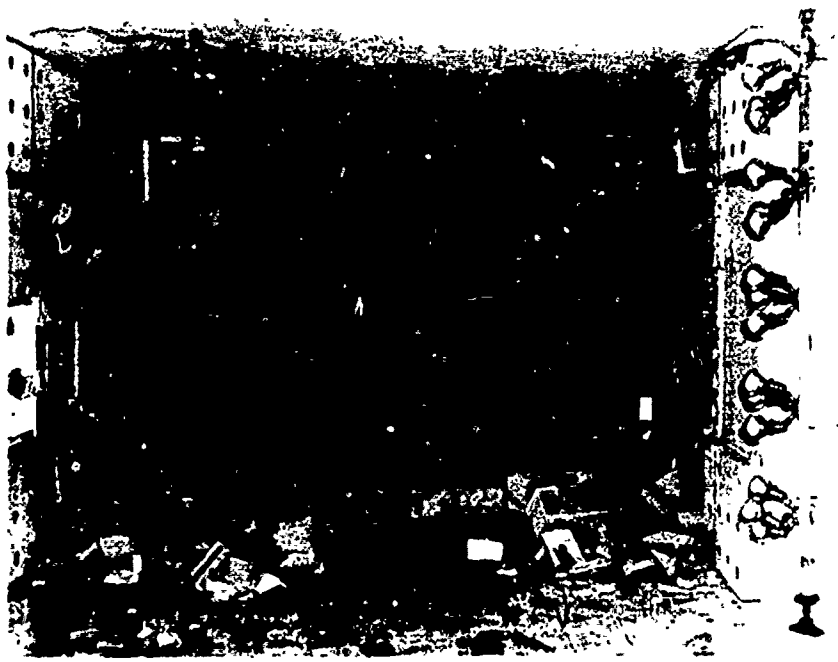

Fig. 5-37. Post-Test Photograph, Wall No. 60, 8 in. Nonreinforced Concrete Block with Window (Test No. 04-26-71-02)

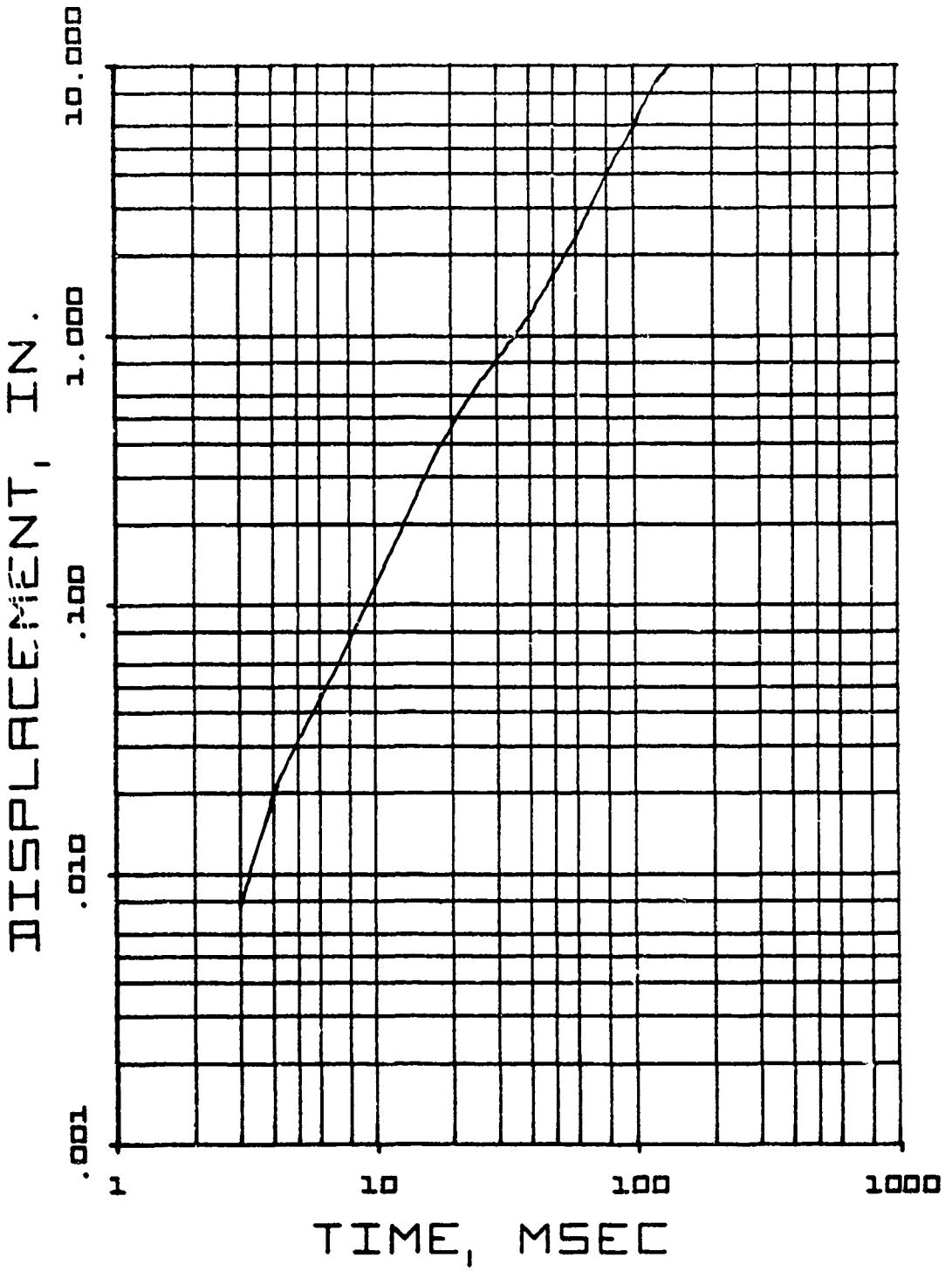

Fig. 5-38. Displacement as a Function of Time for Wall No. 61, Nonreinforced Concrete Block with Window (Test No. 05-17-71-03)

Fig. 5-39. Post-Test Photographs, Wall No. 6J, 8 in. Nonreinforced Concrete Block with Window (Test No. 05-17-71-03)

DISCUSSION OF TEST DATA VS PREDICTION

Test Wall No. 56, with an overpressure of 3.6 psi, failed as predicted with cracks propagating from the corners of the windows. The predicted stress level for 3.6 psi is σ_r = 400 psi, which is well above the maximum strength of the brick wall. The load cell prediction is 38,300 lb. On this test the crack gages failed to function; hence, time of failure was not determined. However, the load cells recorded and read 28,000 lb, from which one might estimate the failure time from 10 to 13 msec (see Fig. 5-31) and a failure stress of $\sigma_r \approx$ 320 psi.

Wall No. 57 was first subjected to a 1.3 psi pressure which cracked three of the four corners. SAMIS predictions are σ = 145 psi, load cell reading 14,100 lb. The actual reading was 13,500 lb.

Walls 60 and 61 were concrete block walls which, as predicted, were much weaker than the brick walls.

In general, the window walls behaved as predicted and provided further verification for the prediction technique.

The concrete block walls with windows both failed at very low pressure as expected. From the static test data σ_r (average) = 27 psi and Fig. 5-29 (element stress), one would predict wall failure at p_r = 0.25 psi on the average and with (max) = 55 psi $p_r \approx 0.5$ psi.

Section 6
ROOM WITH A WINDOW

One of the more interesting test geometries is the case where the exterior wall of a building which contains windows is sufficiently strong so that only the window glass fails, and the blast wave enters this window impinging on the interior wall at the back of the room. To investigate this case, a room was constructed in the Shock Tunnel with the exterior wall (toward the blast wave) a nonfailing wall with a window. The interior wall was a solid nonfailing wall for the loading test series and either a concrete block or hollow clay tile wall for the wall panel tests.

LOADING STUDY TESTS

The window used in the front nonfailing wall for these tests was 62 in. wide and 54 in. high, with a 6-in. wide vertical supporting beam located at the center of the window. The effective open area for this window was approximately 20 percent of the total wall area. The room was approximately 15 ft long and had a smooth wooden floor installed over the trusses. A sketch showing the test geometry and the gage array is shown in Fig. 6-1. Summary plots of the data from the three gages located on the back wall (gages W, X and Y) are presented in Figs. 6-2 through 6-5.

ANALYTICAL WORK

The only computation and analytical work performed on this test geometry to date has been the wall strength predictions based on the static test results.

With the rupture modulus "σ_r" averaging 18 psi for clay tile and 27 psi for concrete blocks, one expects failure at rather low pressures. From the loading test data, one can assume that the pressure is relatively uniform across the wall. For walls with a natural period on the order of 35 msec, the pressure is equivalent to a step load of 1.4 psi for one strand of Primacord. The

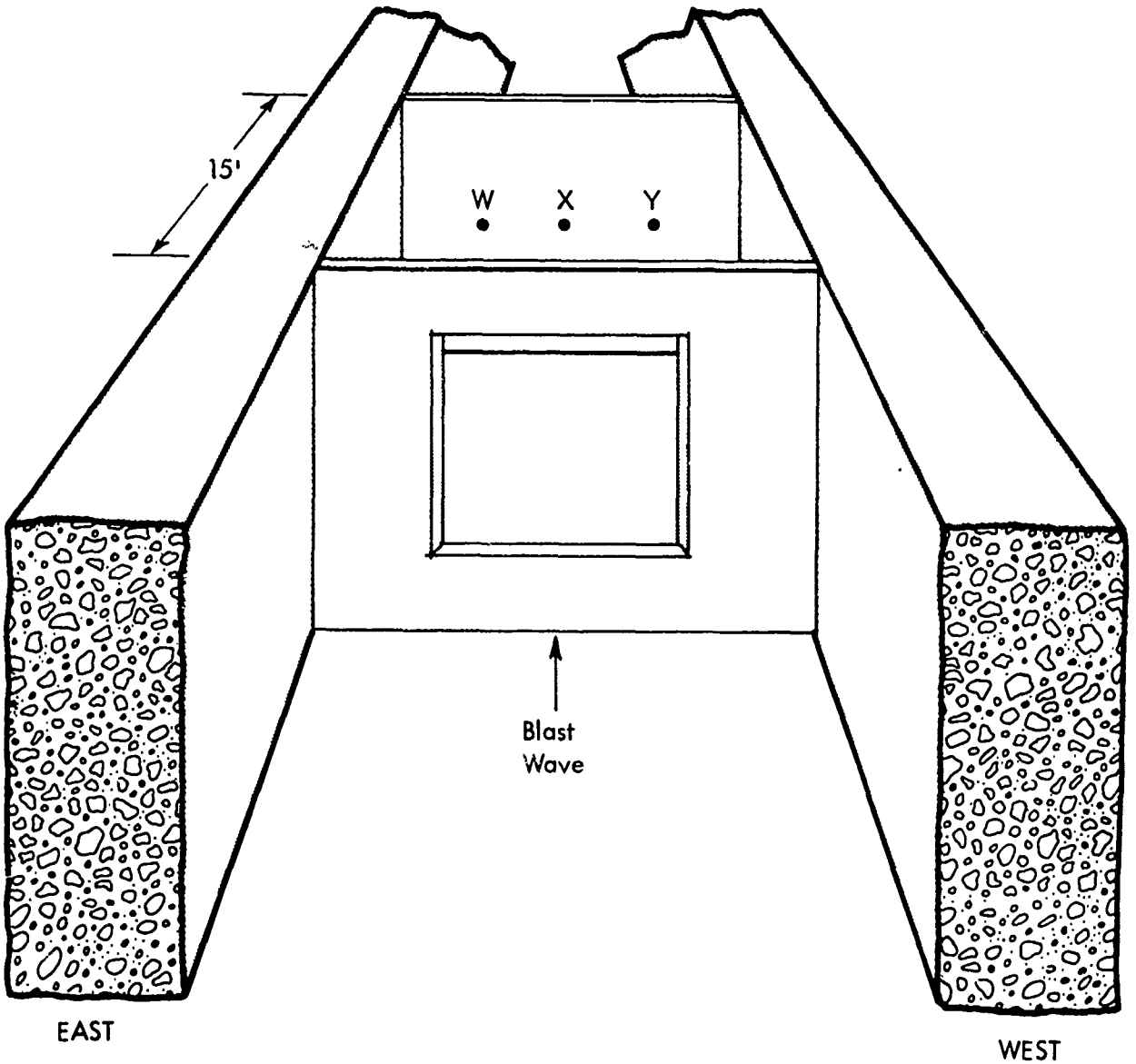

Fig. 6-1. Test Setup for Window Wall Loading Test Series

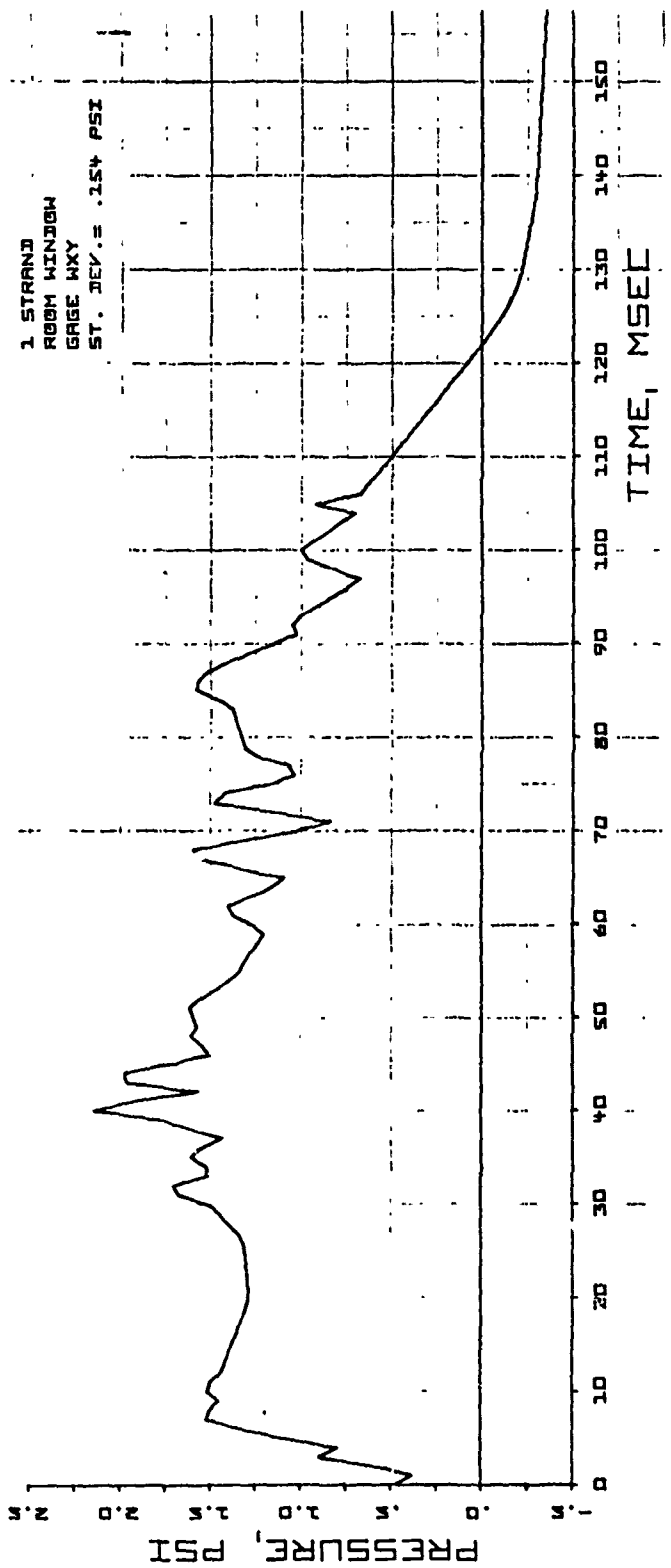

Fig. 6-2. Average Net Pressure as a Function of Time for One Strand, Room with 62 X 64 in. Window Loading Study Tests. Gages W, X, and Y

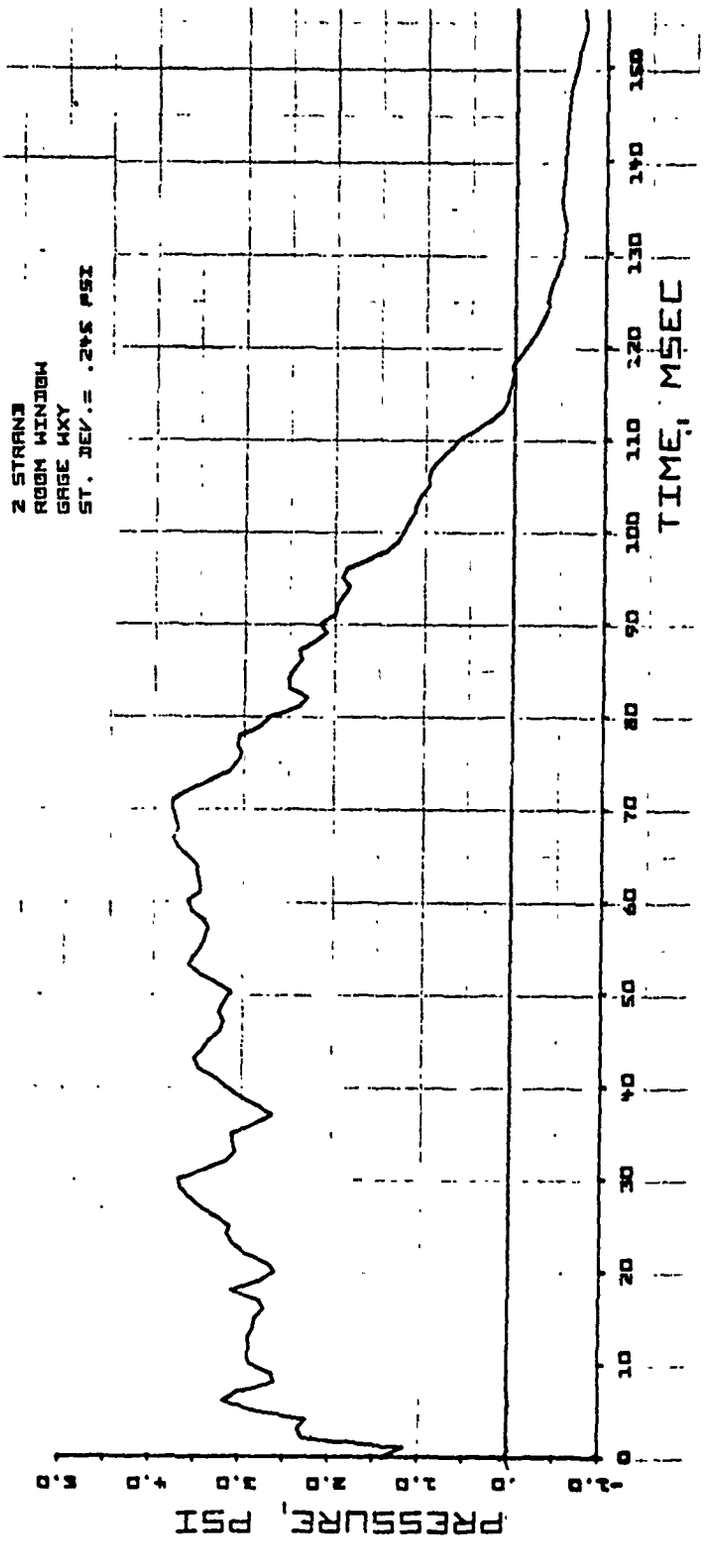

Fig. 6-3. Average Net Pressure as a Function of Time for Two Strand, Room with 62 X 64 in. Window Loading Study Tests. Gages W, X, and Y

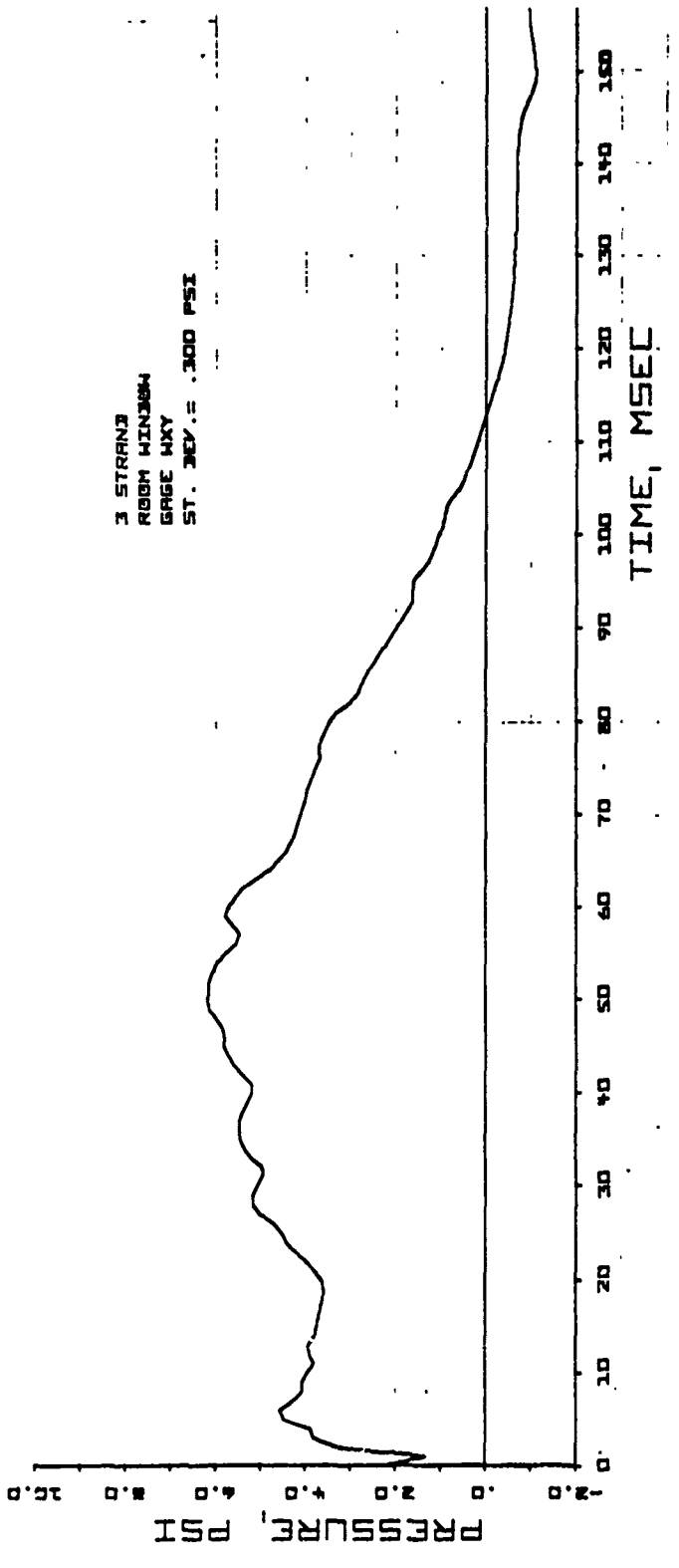

Fig. 6-4. Average Net Pressure as a Function of Time for Three Strand, Room with 62 × 64 in. Window Loading Study Tests. Gages W, X, and Y

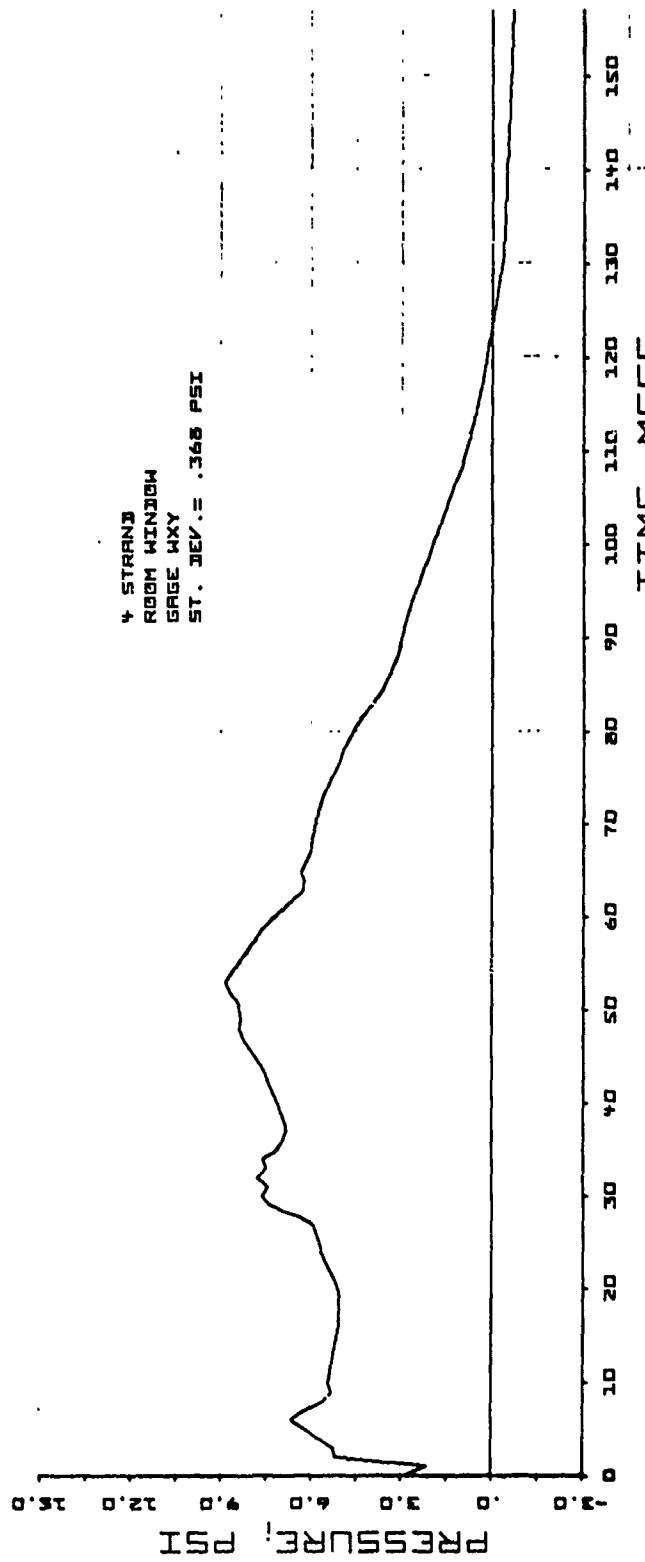

Fig. 6-5. Average Net Pressure as a Function of Time for Four Strand, Room with 62 X 64 in. Window Loading Study Tests. Gages W, X, and Y

stress level induced by this much load is 345 psi for concrete block and 540 psi for clay tile, which is far more than the indicated resistance; hence, failure is expected.

WALL PANEL TESTS

Two 8 in. thick nonreinforced concrete block interior walls (Nos. 58 and 59) and two approximately 6 in. thick nonreinforced hollow clay tile interior walls (Nos. 62 and 63) were tested in this room geometry. The walls were nominally 12 ft wide and 8-1/2 ft high, including the steel mounting frame, and were located 15 ft behind the nonfailing wall with a window occupying approximately 20 percent of the wall area. This was the same wall used in the loading study. The walls were supported as a simple beam.

The concrete block walls were constructed of standard 15-1/2 X 7-1/2 X 7-1/2 in. blocks with 1/2 in. mortar joints. The tile walls were constructed of standard 12 X 6 X 6 in. hollow clay tile with one glazed face. The back face was covered with an approximate 1 in. layer of mortar.

Wall No. 58 - 8 in. Nonreinforced Concrete Block Interior Wall

The first test (05-21-71-01) with a 10 ft length of Primacord cracked the wall; the crack gages indicated this occurred at 9 and 15 msec. Post-test inspection of the wall indicated a horizontal crack all the way across the wall. No usable natural period information was obtained.

The second test (05-21-71-02) with one 60 ft length of Primacord collapsed the wall with most of the debris landing within 15 ft; pieces were found as far as 30 ft from the original position. The estimated average peak reflected overpressure on the wall, based on the loading study, was 1.5 psi and the maximum load obtained from the load cells was 11,600 lb at about 22 msec. A plot of displacement as a function of time is presented in Fig. 6-6 and pre- and post-test photographs in Fig. 6-7.

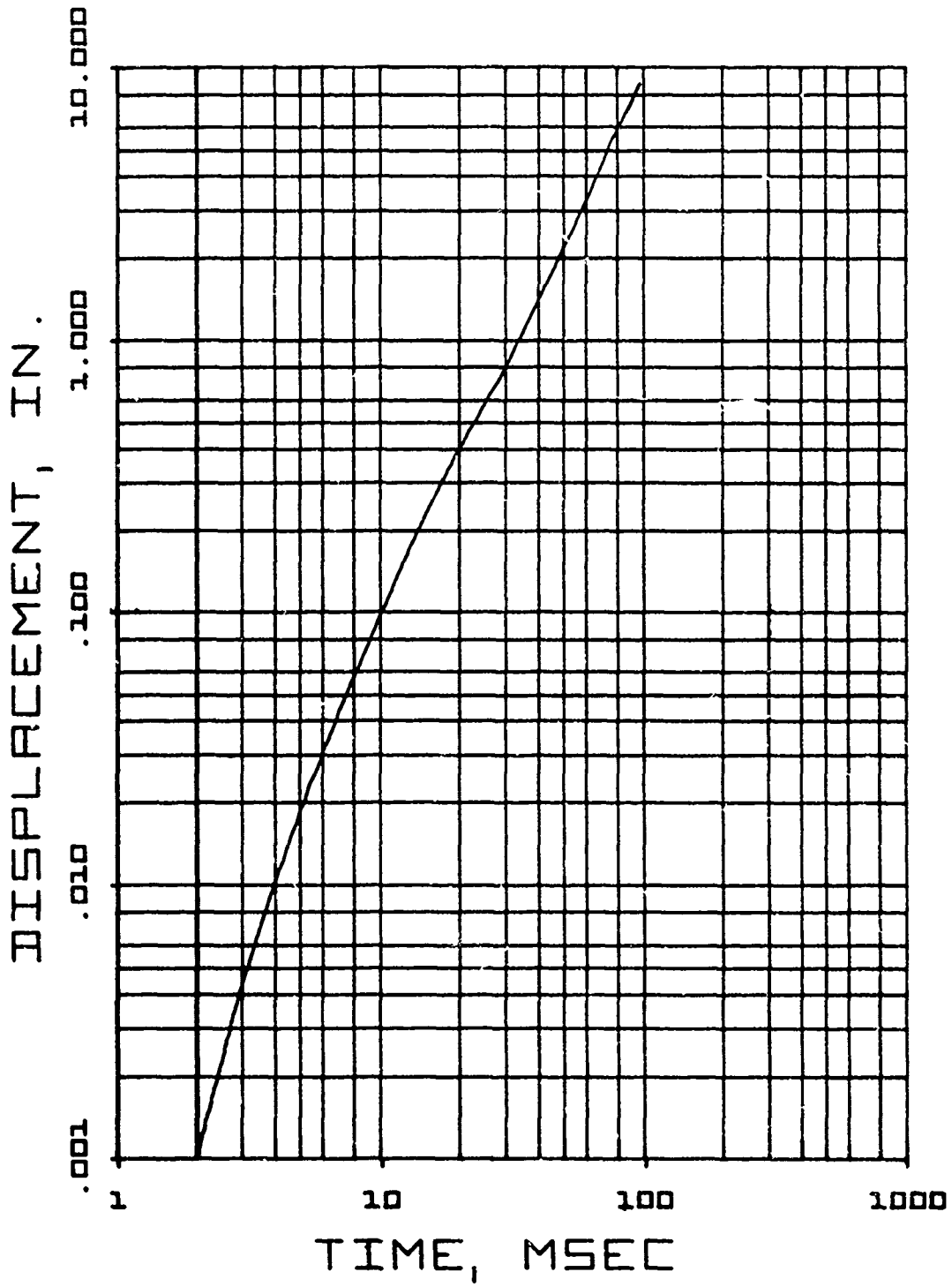

Fig. 6-6. Displacement as a Function of Time for Wall No. 58, Nonreinforced Concrete Block Interior Wall (Test No. 05-21-71-02)

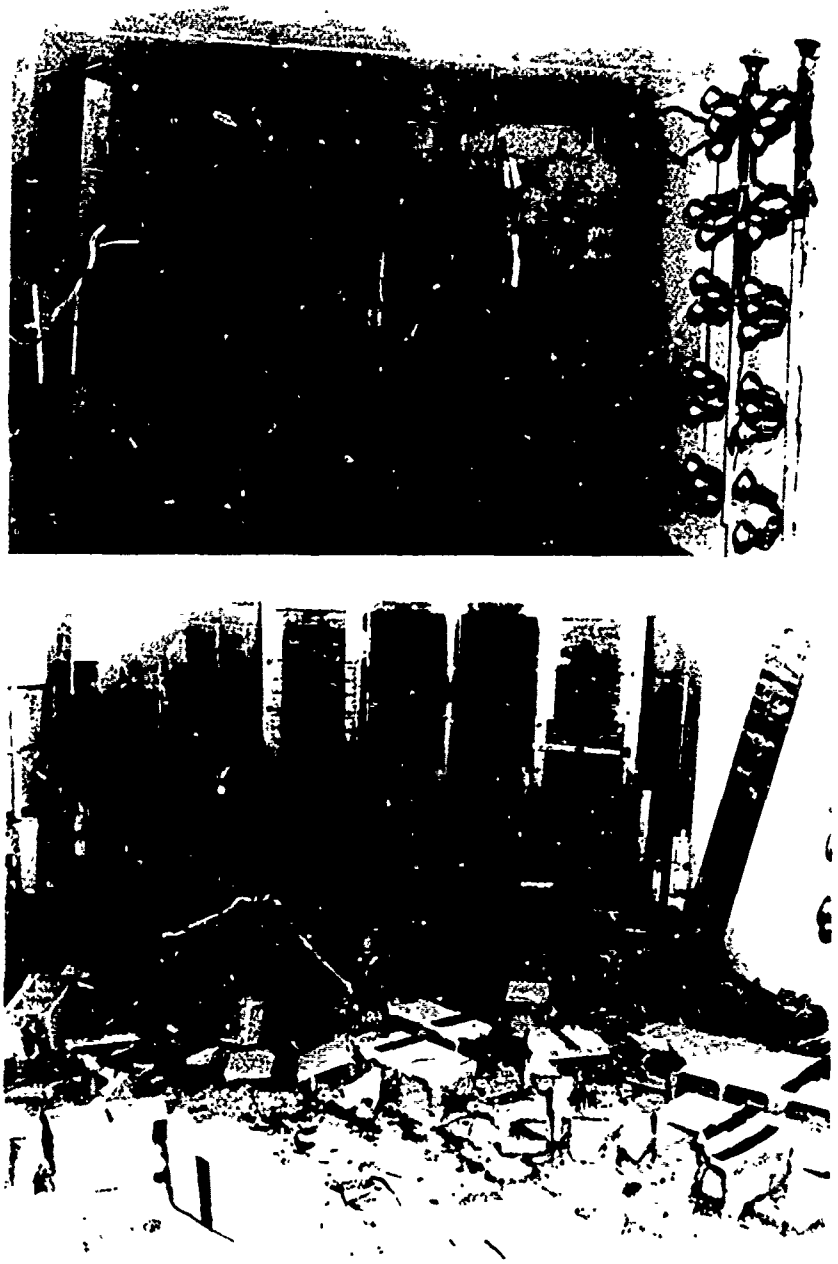

Fig. 6-7. Pre[illegible]st-Test Photographs of Wall No. 58, 8 in. Nonreinforced Conc[illegible]lock Interior Wall (Test No. 05-21-71-02)

Wall No. 59 - 8 in. Nonreinforced Concrete Block Interior Wall

Since the first wall (No. 58) in this series cracked with a 10 ft length of Primacord, the first test (No. 05-26-71-01) on this wall (No. 59) was conducted with a 2 ft length. The shorter length caused no visible damage to the wall, and was so low it was difficult to obtain an accurate measure of the natural period. From the data available the natural period is estimated to be between 30 and 35 msec.

The second test (05-26-71-02), with one 60 ft length of Primacord, collapsed the wall with a greater spread of debris than from Wall No. 58. (See Fig. 6-8 for post-test photographs of this wall.) The estimated average peak reflected overpressure was 1.4 psi, and the maximum load obtained from the load cells was 10,500 lb. The three crack gages indicated crack times of 15.3, 19.3, and 20.4 msec.

A plot of displacement as a function of time is presented in Fig. 6-9.

Wall No. 62 - Nonreinforced Hollow Clay Tile Interior Wall

This wall was also tested with a 2 ft length of Primacord on the first test (05-23-71-01). No damage was noted and the estimated natural period was 37 msec.

In the second test (05-23-71-02), using one 60 ft length of Primacord, the wall collapsed scattering debris as far as 30 ft. The three crack gages indicated failure at 21, 26, and 26 msec. The estimated average peak reflected overpressure on the wall was 1.5 psi and the measured load from the load cells was 9,800 lb at approximately 20 msec. A plot of displacement as a function of time is presented in Fig. 6-10; post-test debris is shown in Fig. 6-11.

Wall No. 63 - Nonreinforced Hollow Clay Tile Interior Wall

The first test (05-28-71-01), using a 2 ft length of Primacord, did no visible damage to the wall. The response of the instrumentation was so small that it was impossible to obtain a measure of the natural period.

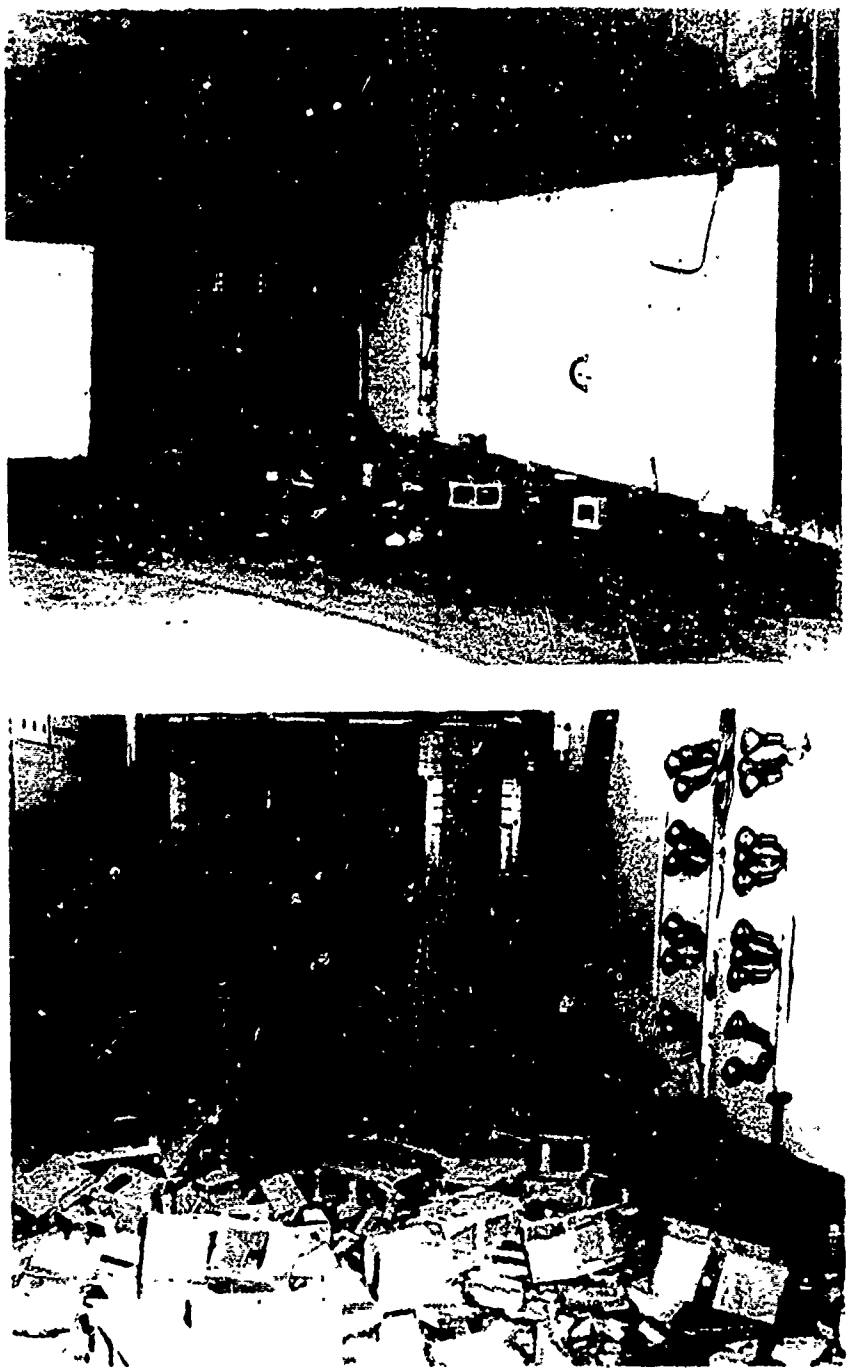

Fig. 6-8. Post-Test Photographs, Wall No. 59, Nonreinforced Concrete Block Interior Wall (Test No. 05-26-71-02)

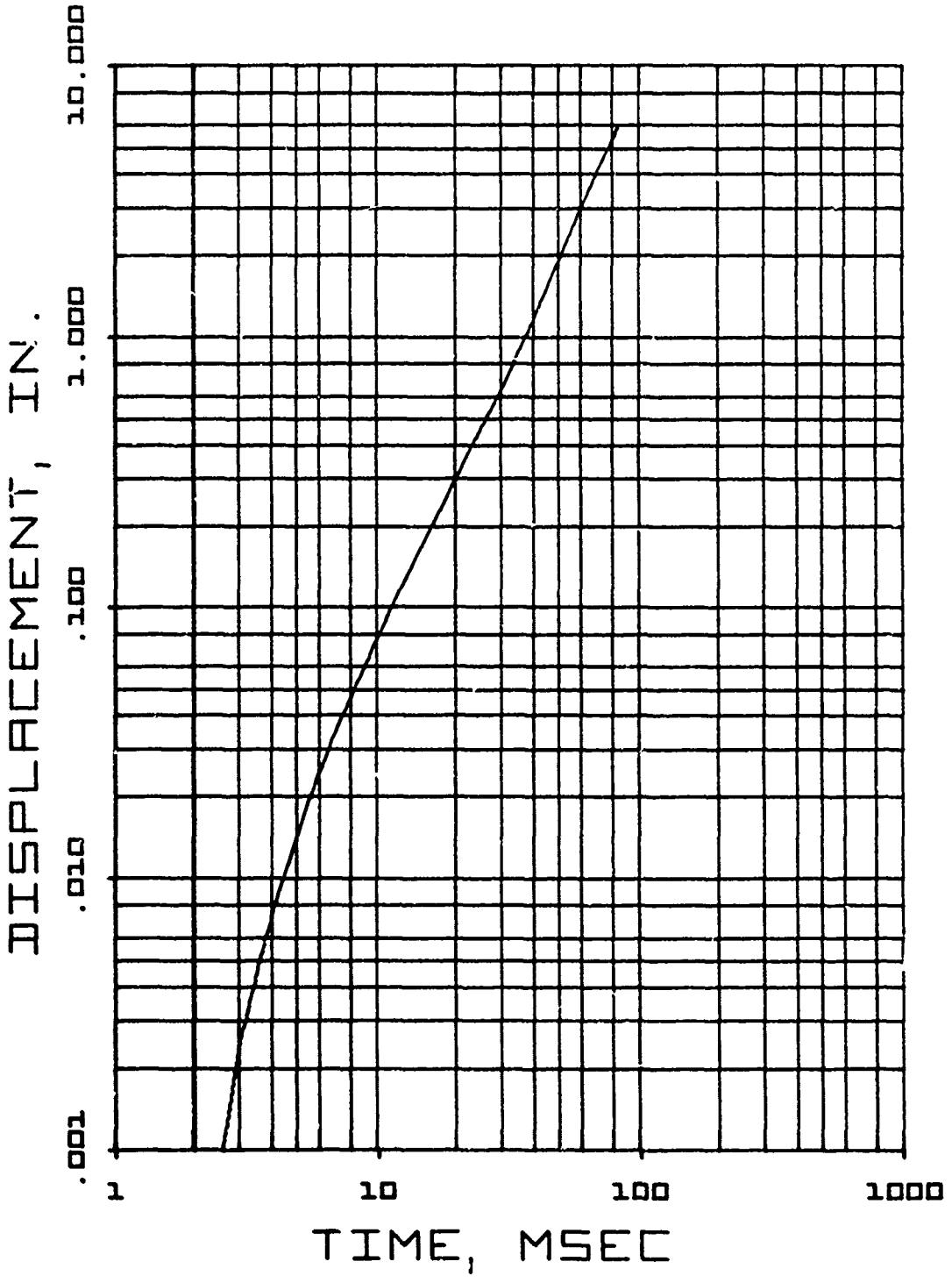

Fig. 6-9. Displacement as a Function of Time for Wall No. 59, Nonreinforced Concrete Block Interior Wall (Test No. 05-26-71-02)

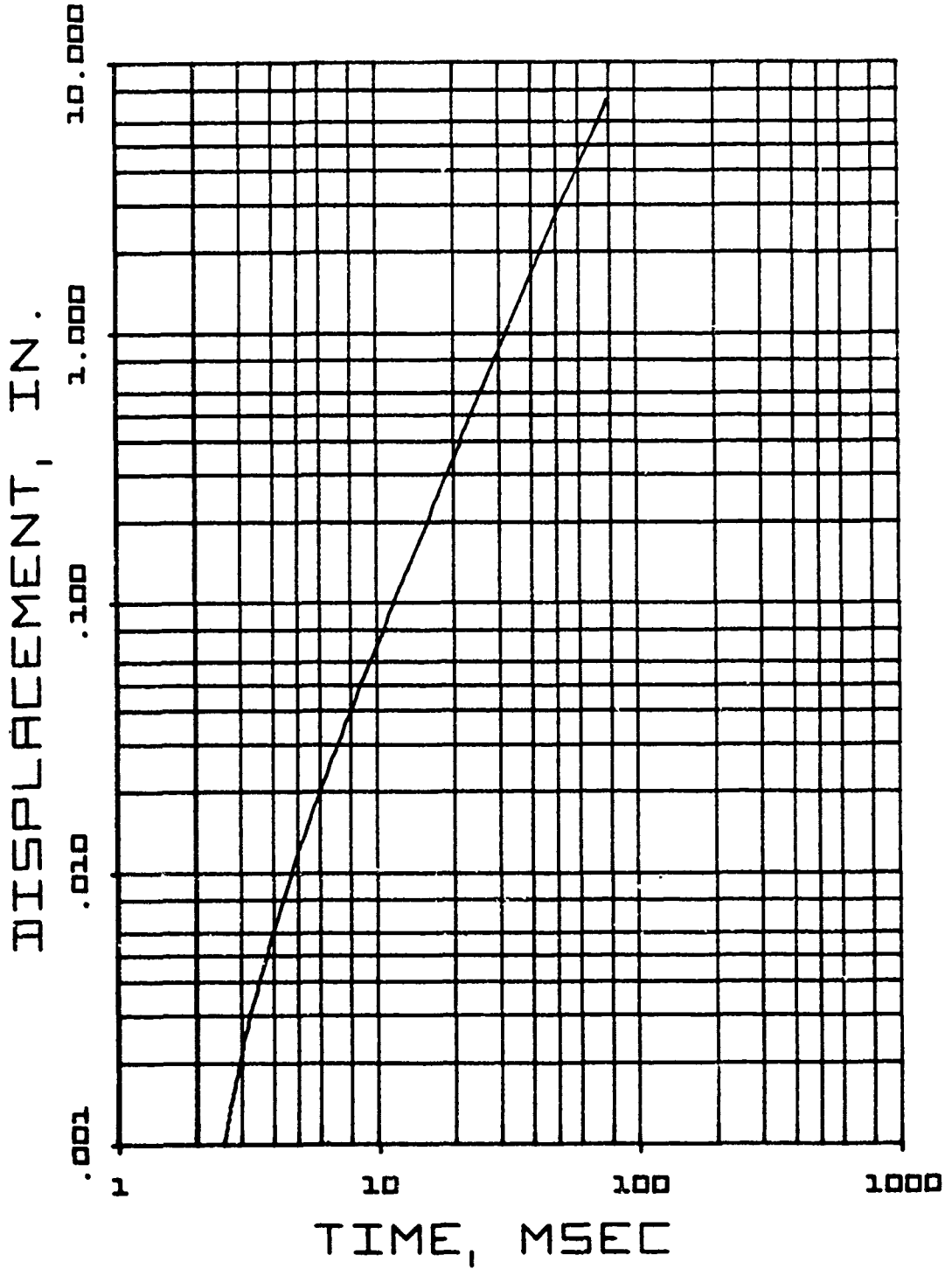

Fig. 6-10. Displacement as a Function of Time for Wall No. 62, Nonreinforced Concrete Block Interior Wall (Test No. 05-23-71-02)

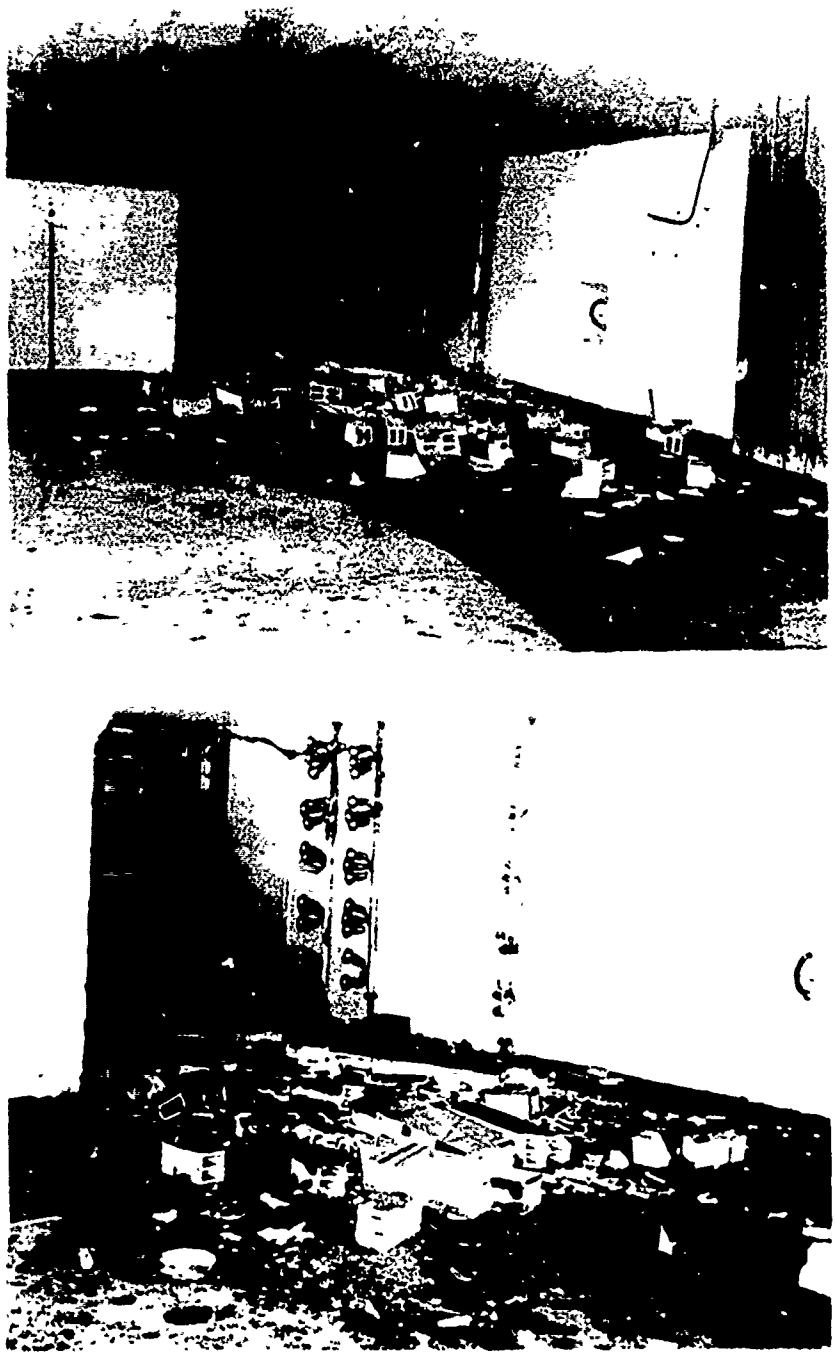

Fig. 6-11. Post-Test Photographs, Wall No. 62, Nonreinforced Hollow Clay Tile Interior Wall (Test No. 05-23-71-02)

The next test (05-28-71-01), with one 60 ft strand of Primacord, collapsed the wall with a debris pattern similar to Wall No. 62 (see post-test photographs in Fig. 6-12). The estimated average peak reflected overpressure was 1.5 psi, and the total load obtained from the load gages was 12,200 lb. The three crack gages indicated failure times of 18, 22.5, and 23 msec. A plot of displacement as a function of time is presented in Fig. 6-13.

Fig. 6-12. Post-Test Photographs, Wall No. 63, Nonreinforced Hollow Clay Tile Interior Wall (Test No. 05-28-71-02)

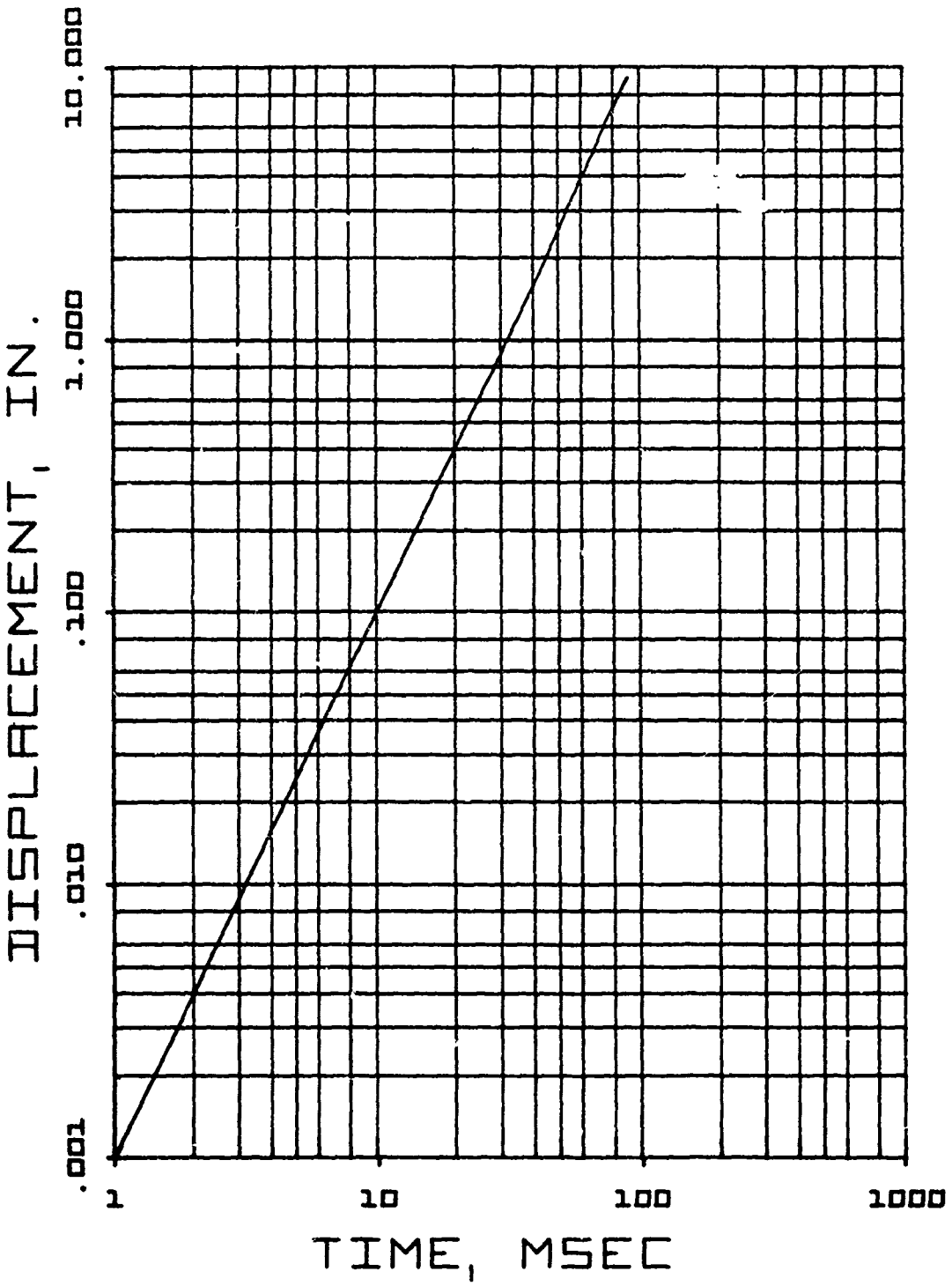

Fig. 6-13. Displacement as a Function of Time for Wall No. 63, Nonreinforced Hollow Clay Tile Interior Wall (Test No. 05-28-71-02)

Section 7
STATIC TEST PROGRAM

INTRODUCTION

In conjunction with the shock tunnel dynamic tests, a static test program is being conducted to determine the quality of construction of the test items fabricated, to obtain estimates of the strength of specimen walls prior to the dynamic tests, and in the future, to compare the properties of on-site constructed masonry with similar units constructed under laboratory conditions. Specific static test specimens were constructed for:

1. Physical properties of the mortar.
2. Bond strength of mortar to masonry units.
3. Flexural and compression strength of masonry assemblies.

TEST EQUIPMENT AND PREPARATION OF SPECIMENS FOR TESTING

A Soiltest CT756 hydraulic concrete tester, 200,000 lb capacity, meeting ASTM Specification C-39, was used for statically loading the test specimens. All beams were tested for flexural strength by the ASTM standard method for a simple beam with third-point loading — designation C78-64. A diagram of the beam in place for testing is shown in Fig. 7-1.

Deflection of the beam at mid-span was measured by an optical displacement follower, by a dial gage or by a LVDT displacement gage, to the point of failure. Measurement of the strain to failure was recorded by electrical strain gages at a top and bottom mid-span location on the beam.

The mortar cylinders for compression tests were capped with either sulphur or plaster of paris upon removal from the cardboard molds. An SR-4 strain gage, 1/2-in. long, was attached to the curved surface of some of the cylinders to record a load-vs-strain curve during testing.

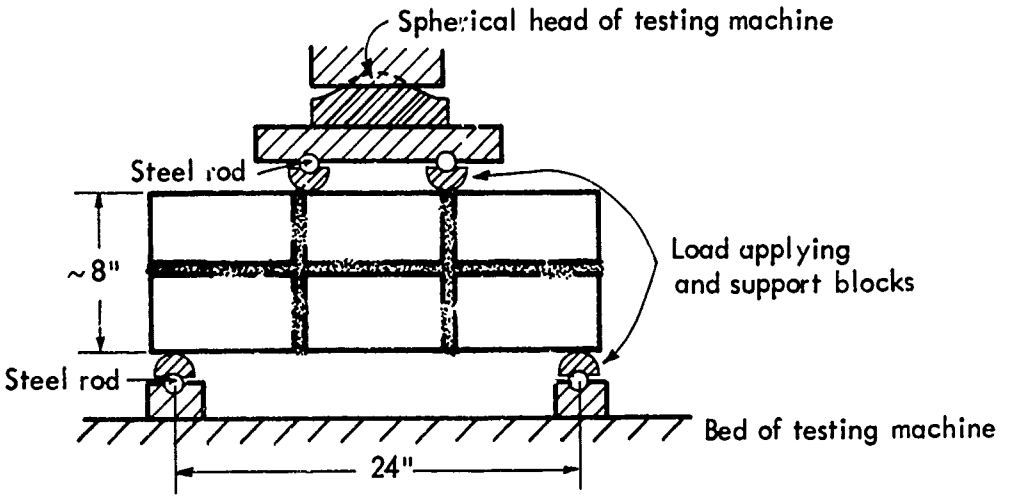

Fig. 7-1. Simple Beam with Third-Point Loading

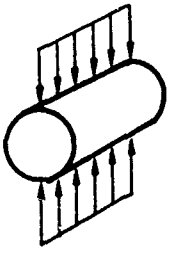

The determination of the splitting tensile strength was obtained from the remainder of the mortar cylinders as described in ASTM Designation C496-64T. The load was applied along the length of the cylinder as shown in the adjoining sketch.

The masonry assemblies were utilized for the determination of composite compressive strength and brick and mortar shear bond strength. The specimens were positioned for testing as shown:

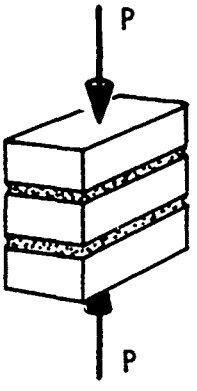

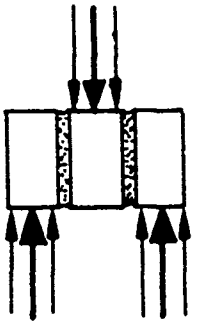

The load was distributed evenly through steel plates on top and bottom for compressive strength. For shear bond tests, the specimen was supported on soft wood blocks under the outer bricks, and the load was applied through a wood block resting on the center brick.

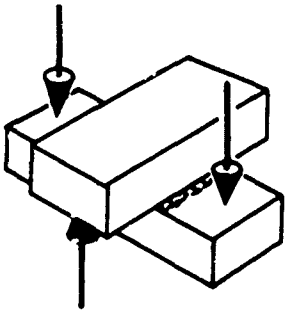

The tensile bond strength of mortar to brick was determined by crossed brick couplets according to ASTM Specification C321-64. The upper brick of the couplet was supported on two prongs fastened to the lower platen of the tester. The upper platen rested on the lower brick of the couplet via two prongs as indicated in the adjoining sketch.

WALL MATERIALS AND RESULTS

Materials, construction, testing and data analysis techniques associated with brick walls are described in Appendix A of Ref. 5. Figure 7-2 shows the construction of the brick beams. Test materials were purchased from a commercial supplier and were representative of those commonly used in local building construction. A Portland cement meeting the requirements of ASTM Specification for Portland Cement, Type I, (designation C150-66) was used in the preparation of the required mortar mixture along with a mason's sand from the San Francisco Bay Area. No analysis of the sand properties was performed.

The Type "S"* mortar mixture was proportioned by volume (measurement by on-site construction methods) according to the following: 1 part Portland cement, 1/4 to 1/2 part hydrated lime, and 4 parts damp loose sand. The amount of water applied to each batch of mortar was adjusted to produce a consistency that could be conveniently handled by a mason. To obtain measurements of compressive and of splitting strengths, three 2-in.-diameter by 4-in.-long cardboard cylindrical molds were filled for each new batch of mortar.

All the walls and static test specimens were built by experienced masons using standard construction techniques. The walls were built in a nonreinforced Flemmish bond pattern with "tie bricks" every sixth course.

A group of static test specimens corresponding to each wall consisted of:

1. Brick and mortar beams for flexural strength.
2. Mortar cylinders for compressive and splitting strength.
3. Masonry assemblies for composite compressive and shear bond strength.
4. Brick and mortar couplets for tensile bond strength.
5. Single bricks for modulus of rupture and compressive strength.

---

* Uniform Building Code, 1967, Article 2403.

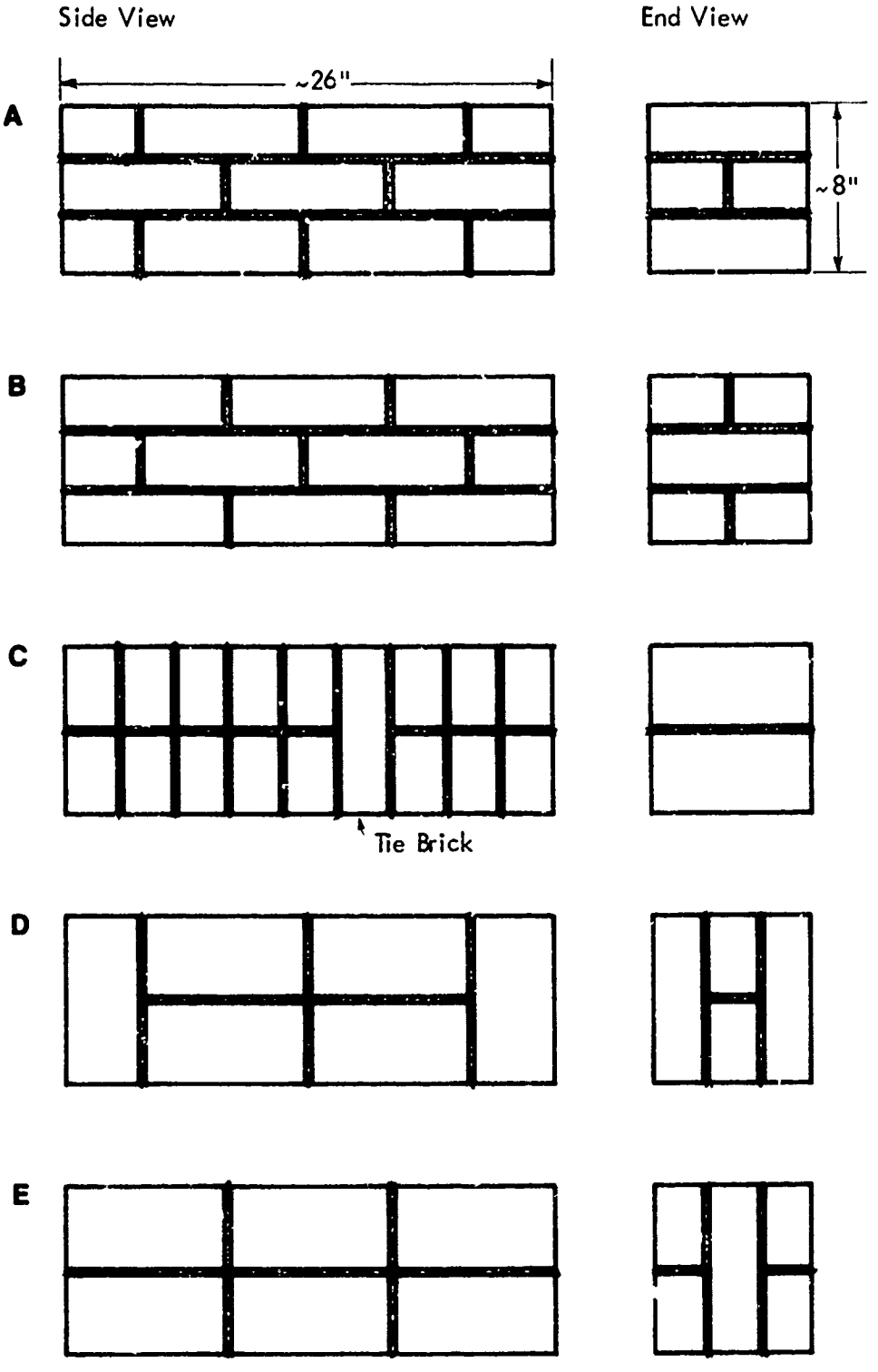

Fig. 7-2. Brick Beam Patterns

Several patterns of brick and mortar beams were constructed. The side and end views of each pattern are shown in Fig. 7-2 in the position for testing flexural strength. Patterns D and E are identical to brick patterns A and B, respectively, but are turned 90 degrees.

The mortar joint thickness of each beam was approximately 3/8 in. and the nominal dimensions of the beams were 26 in. long, 8-1/2 in. wide and 8-3/4 in. high. All beams were built in a horizontal position except pattern C which was built in a vertical position (on end). Beam C was patterned and built in the standing position to simulate a vertical element of the dynamic test walls. After construction, five tiers of bricks were stacked on top of the beams until ready for testing.

Two batches of beams were built in the laboratory to act as a control for the static test specimens constructed at the building site. The beams were constructed with the same materials as were the on-site construction beams but the measurement of mortar materials was performed more accurately.

The masonry assemblies consisted of three bricks stacked vertically with a mortar bed between bricks. The average dimensions of these samples were 8-1/2 in. long, 3-7/8 in. wide and 8-3/4 in. high.

The walls and corresponding static test samples were constructed and stored for curing in the underground tunnel complex, where the mean temperature for July is 53 to 60F and for January, 45 to 56F. The mean humidity ranges from 75 to 85 percent.

Brick Results

The results of static testing of samples of brick construction are summarized in Table 7-1. More detailed analysis of these results, and some additional data may be found in Appendix A of Ref. 7-1.

Table 7-1

SUMMARY OF STATIC TEST DATA

DESIGNATION				BEAM PROPERTIES			MORTAR PROPERTIES (average)		BOND PROPERTIES (average)		COMPOSITE COMPRESSION STRENGTH (psi)
BATCH NO.	DATE	IDENT. NO.	BRICK PATTERN	FLEXURAL STRENGTH (psi)	DEFLECTION AT FAILURE (in.)	STRAIN AT FAILURE (in./in. $\times 10^{-4}$)	COMPRESSIVE STRENGTH (psi)	TENSILE STRENGTH (psi)	TENSILE STRENGTH (psi)	SHEAR STRENGTH (psi)	
1	7/67	1	A	168			2442	-	11	71	3650
		2	A	171			2494	-	-	81	3360
		3	A	170			2572	-	-	-	-
2	8/67	4	A	42			2320	261	37	81	4870
		5	A	224			1770	209	-	100	4350
		6	A	68			1549	208	-	82	5620
		7	A	141			1670	125	-	-	-
3	12/67	20	A	121	0.052		2696	263	74	111	
		21	A	168	0.060		2654	520	79	107	
		22	A	169	0.050		2511	600	85	103	
4	1/68	23	A	215			2963	513	66	164	
		24	A	182	0.014		3047	493	58	131	
		25	A	268	0.028		2936	510	58	77	
		26	A	105	0.051		2490	588	50	118	
5	3/68	27	A	211	0.020		2899	513	81	66	
		28	A	171			2613	555	95	80	
		29	A	185			2545	552	83	70	
		30	A	199	0.031		2619	519	68	161	
6	4/68	31	A	187		3.6	3098	576	127	220	
		32	A	235	0.024	2.8	2606	532	130	357	
		33	A	167		3.0	1941	582	109	158	
		34	A	162			2570	550	126	103	
7	1/69	44-1	E	303		26.7	1479	450	37	104	2089
		44-2	C	damaged							
		45-1	E	243	0.033	12.1	1676	379	82	154	1462
		45-2	C	141	0.015	1.2					
		46-1	E	213	0.025	4.6	2069	254	87	53	1903
		46-2	C	damaged							
8	8/69	47-1	E	228	0.021	4.4	1326	438	150		2053
		47-2	C								
		48-1	B	266			1672	356	71		1877
		48-2	C	49							
		49-1	E		Not yet tested						
		49-2	C		Not yet tested						
9	4/69	50-1	E	248		7.9	2674	455*	52*	93*	2240*
		50-2	C	166		1.4					
		50-3	C	125	0.019	1.0					
		50-4	C	123	0.077	1.4					
		50-5	C	153		3.4					
		50-6	C	142		1.2					
		50-7	C	164		1.0					
		51-1	E	287	0.[illegible]	3.1	2188	452	78	125	2325
		51-2	C	158	0.034	1.0					
		52-1	B	200			1922	476	63		2330
		52-2	C								

* Average per batch number.

Table 7-1 (cont.)

10	3/70	56-1	C	121			2597	445	60		1529
		56-2	B	293							
		57-1	B	252			1292	332	55		2135
		57-2	C	73							
11	6/71	64					1566				
		65					2046				
		66					2109				
		67									
		68-1	1/2B	208	0.005						
		68-2	1/2B	253	0.0035						
		69	B	125	0.0037						
BY-1B	7/68	106	A	159	0.018	1.2	[illegible]	822*	76*	-	-
		101	B	211	0.010	1.8					
		102	B	233	0.010	1.0					
		103	B	256	0.011	1.0					
		104	B	229	0.022	1.0					
		105	B	156	0.012	0.2					
BY-1A		106	A	159	0.018		4166*	822*	76*	-	-
		107	A	170	0.013	2.4					
		108	A	189	0.017	4.6					
		109	A	192	0.011						
		110	A	225	0.009						
		111	A	163	0.016						
BY-1D		112	D	254	0.021	7.3	4463*	804*	73*	-	-
		113	D	189	0.03[illegible]	11.3					
		114	A	206	0.013						
		115	A	226	0.018	11.3					
		116	D	231	0.011						
		117	D	270	0.014						
EY-1E		118	E	326	0.010	6.0	4224*	696*	65*	-	-
		119	E	278	0.016	5.7					
		120	E	272	0.007						
		121	E	148	0.013						
		122	E	241	0.009						
		123	E	281	0.010	4.1					
EY-2C		124	C	141	0.025	11.9	-	-	77*	-	-
		125	C	158	0.016	7.3					
		126	C	166	0.007	0.7					
		127	C	145	0.020	1.1					

* Average per batch number.

Table 7-1 (cont.)

1-CT	3/71	1-CT	A-4[1]	7	0.0045	2535
		2-CT	A-3	49[2]	0.006	
		3-CT	B-4	7	0.001	
		4-CT	B-4	14	0.00145	2244
		5-CT	B-4	21	0.0015	
		6-CT	B-4	7	0.0045	
		7-CT	B-4	21	0.003	
1-CB	3/71	1-CB	A-3	7.1[3]	0.0015	2582
		2-CB	A-3[4]	5.3	0.001	1792
		3-CB	A-2[5]	55	0.0056	
		4-CB	A-2[6]	19	0.0016	1668
		5-CB	A-2[6]	27	0.0018	
		6-CB	A-2[6]	49	0.0032	

NOTES:

1. The letter corresponds to the direction of load application and the number is the number of tiles in the beam.
2. This is a test of the 3-tile beam remaining after breaking beam 1-CT.
3. Weight of loading mechanism supported by jack for all concrete block tests.
4. Same beam as no. 1-CB.
5. Same beam as no. 2-CB.
6. Broken 3-block beam.

Clay Tile

The structural tile walls and accompanying beams (identified in Table 7-1 by the letters "CT") were built by the masons who built the brick walls. Test beams and walls were constructed of 12 × 6 × 6 in. structural tile, nonreinforced, with 3/8-in. thick type "S" mortar joints. Mortar samples were collected in the same manner as for brick walls. Before testing, clay tile walls and test specimens were cured under the same conditions as brick walls, i.e., at approximately 50F and over 70 percent relative humidity.

The test equipment was the same as used for earlier brick specimen testing, although deflection was measured on a dial gage instead of the optical displacement follower formerly used. Figure 7-3 shows the loading patterns for clay tile beams. No strain gages were installed on any of the test specimens Mortar samples were tested in compression only.

Clay Tile Results

Six beams were tested for flexural strength. The first beam failed at an off center mortar joint, allowing testing of the remnant as a three-tile beam which proved much stronger than any of the four-tile beams. The remaining beams failed on center at forces low enough to render the data highly uncertain. There were no failures of the tiles themselves, as bonding between the mortar and the relatively smooth surfaces of the tiles proved to be very poor. Consequently, the data shown in Table 7-1, relative to clay tile walls, should be taken more as an indicator that these walls were very weak in flexure rather than as a mathematically precise indicator of their relative strength.

Concrete Block

Concrete block walls were built in two configurations:

1. With window openings, and
2. To be used behind a nonfailing wall with an opening

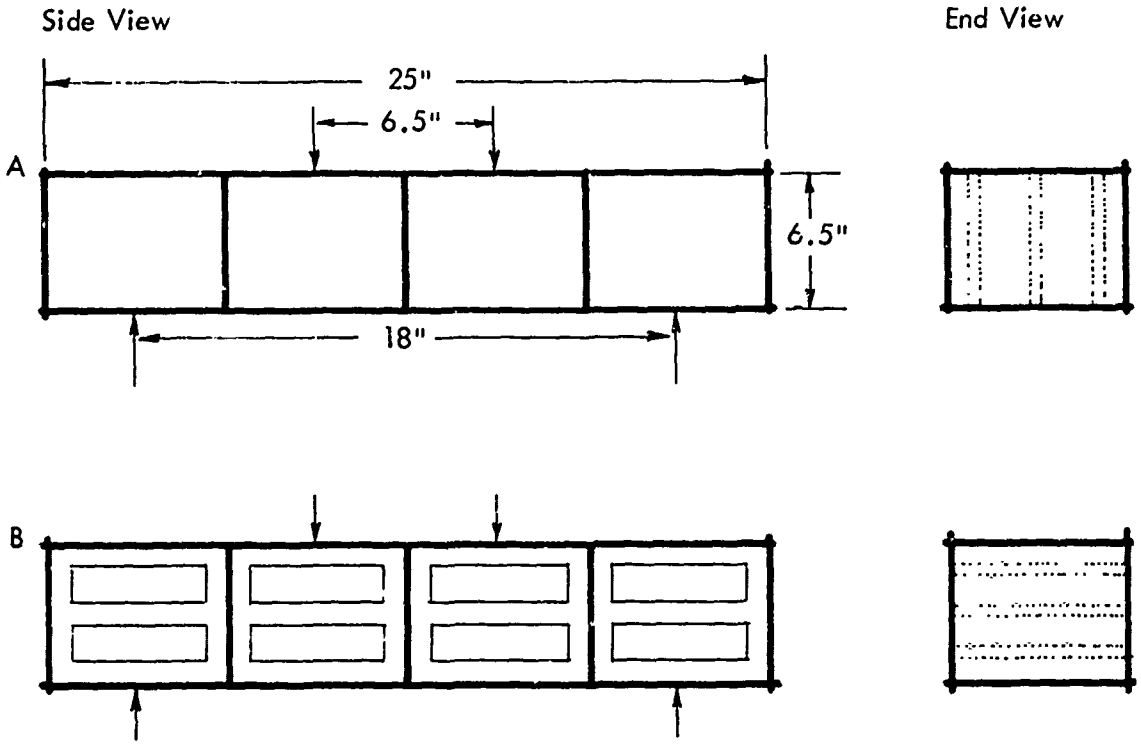

Fig. 7-3. Clay Tile Loading Pattern

to simulate interior walls. The dimensional limitations of the Soiltest CT756 hydraulic concrete tester precluded use of the full size concrete blocks in test beams, so half-size blocks, also used in wall construction, made up the test beams. These are identified in Table 7-1 by the letters "CB."

Concrete Block Results

As with the clay tile beams, mortar adhesion to the concrete blocks was very poor, and flexural strength was very low. In fact, blocks broke off two of the beams tested before testing began. Again, the values associated with flexural strength should be regarded as qualitative, rather than quantitative, indicators. Figure 7-4 shows the loading pattern for concrete block beams.

CRACK GAGE TESTS

During the static test program, additional research was conducted on various crack gages. Failure of the downstream side of the wall in tension results in cracking, which has been detected during the course of the tests reported here by means of the aluminum foil-epoxy gage system shown in Fig. 7-5. As shown, the opening of the crack gage reduces the input voltage to zero. The epoxy used (Adhesive Engineering Type 1180) is brittle; hence the crack propagates through the foil and epoxy without allowing the foil to stretch significantly. (If the foil did stretch significantly, the recorded time of crack occurrence would be delayed.)

If the epoxy failed to bond to the foil properly in the region of the crack, a delay could occur. In addition, the narrow strips of foil are difficult to handle and install, and once installed, impossible to repair. Consequently, some recent effort has been devoted to resolve any questions about the foil gages, and to develop, if possible, superior alternatives. The type of gages considered are shown in Table 7-2; the last three of these are known to be superior crack indicators.

The gages under tests were mounted on two types of test specimens: brick piers consisting of three-brick assemblies, used for shear bond tests in the static test program, and brick beams (see Fig. 7-6). These assemblies were

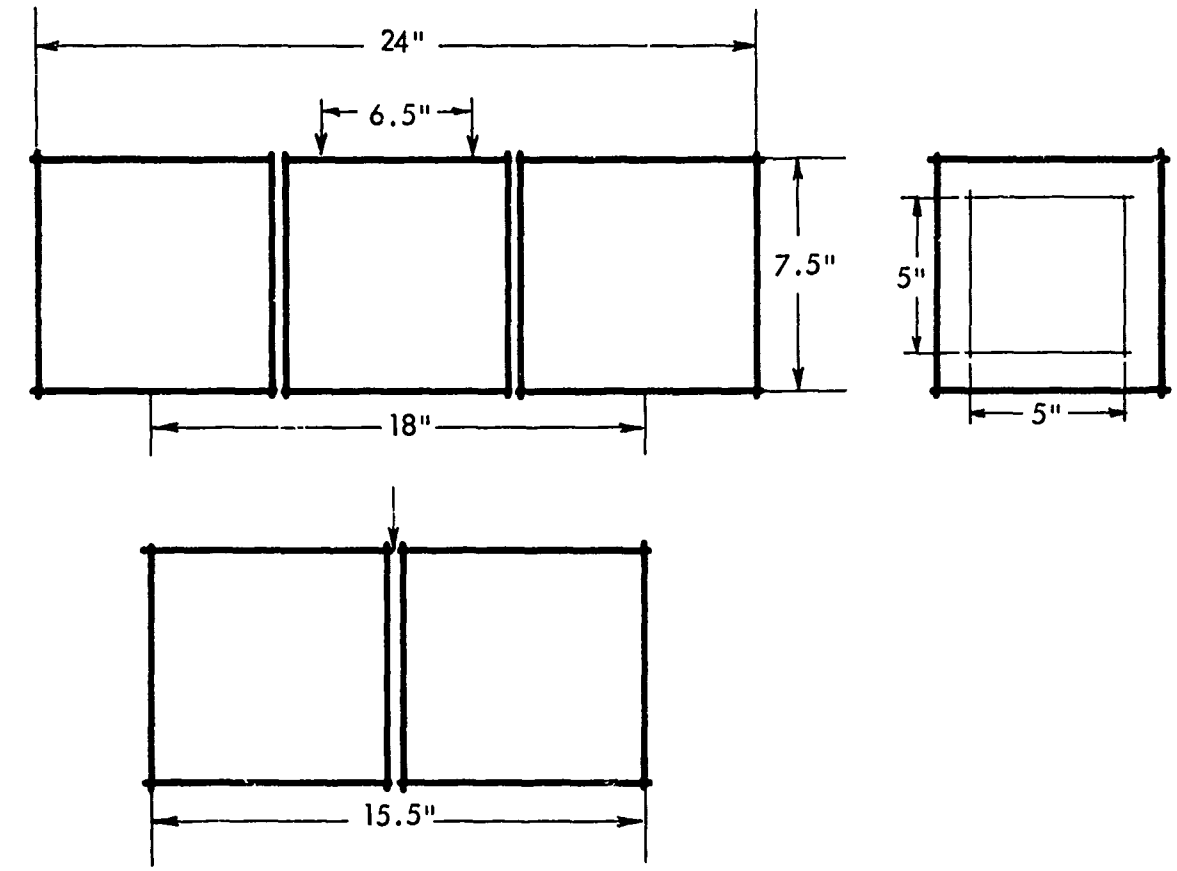

Fig. 7-4. Concrete Block Loading Pattern

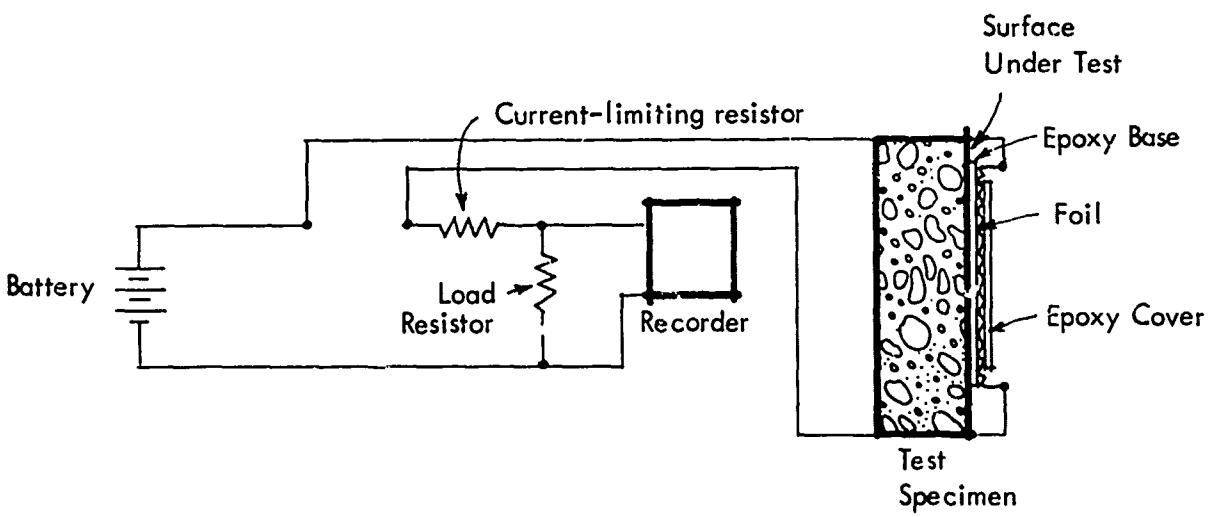

Fig. 7-5. Crack Gage System

Table 7-2

CRACK GAGE TYPE

GAGE TYPE	CONSTRUCTION
1	Aluminum foil on 0.1 in. epoxy, covered by 0.04 in. epoxy
2	Silver-conducting paint on epoxy
3	Silver-conducting point on Krylon®
4	Silver-conducting paint on Varathane®

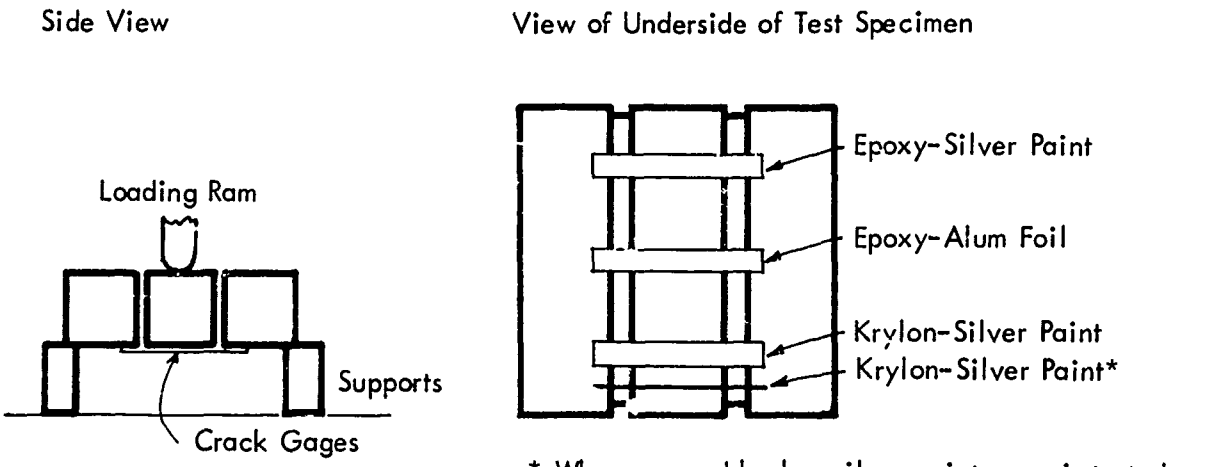

* Where second krylon-silver paint gage is tested, the outer gage is 1/8" wide, the inner, 1/2" wide.

Fig. 7-6. Crack Gage Test Conditions (brick "pier" shown)

loaded hydraulically to failure as described previously, and the hydraulic pressure was closely monitored. An abrupt reduction in the hydraulic load gives an indication of the time of failure of the test specimen; that is, the time the specimen first cracks. Therefore, this time T_p should closely correspond to the point at which the crack gages open.

The first three tests were in conjunction with the horizontal brick piers in bending with the pier and crack gages mounted as shown in Fig. 7-5. Results are shown in Table 7-3.

Table 7-3

RESULTS FROM BRICK PIER TESTS, TIMES FROM T_p (msec)

TEST NO.	GAGE TYPE		
	1	2	3
1	0*	0.85	0.35
2	-0.6	-150.5	-0.2
3	+0.6	-0.125, +0.22**	2.13

* No signal from the hydraulic system was recorded for this test, hence, no T_p time is available.

** This time is for the narrow gage. Two type 2 gages were made. The first time is for a gage about 1/4 in. wide; the second for a gage about 1/8 in wide.

Note that gage type 1, for this small number of tests, appears to exhibit very uniform results. Since these gages were mounted along the center line of the test specimen, it is difficult to tell if this apparent consistency is the result of gage consistency, or whether the specimen may be considered to have failed when the crack propagated across its center line. The type 3 gage which failed early in the second test was mounted across an area of poor brick-to-mortar bonding. This early gage failure, then, may be an indication of failure of a section with little or no structural significance. (There was no abrupt pressure change at this time.)

The next series of tests, conducted with beams, contained one data point in which such a pressure change was discernible prior to "ultimate" failure.

During this test, partial failure of the beam was audible some time before "ultimate" failure. Playback showed a pressure drop at T_p - 1037 msec, an initial indication from the gage (2) involved at T_p - 1037.2 msec (in the form of a short duration spike), and final opening of the gage at T_p - 1014 msec. After the initial pressure drop, the pressure gradually rose to its original maximum value, possibly exceeding it slightly, after which the complete failure of the beam occurred. Gage mounting was like that in the pier tests, except that both the span under test and the crack gages were much longer.

Table 7-4 shows the results of the beam tests. Here, the silver-painted gages, whether over epoxy or over Varathane appear to be slightly superior to the foil in small scale tests.

Table 7-4

RESULTS FROM BRICK BEAM TESTS, TIMES FROM T_p (msec)

TEST NO.	GAGE TYPE		
	1	2	3
1	-2.7	0.8	1.1
2	1.1	-1037.1 (-1014)*	-0.62
3	2.7	-0.4	1.1
4	3.0	1.5	5.4

* Final gage opening.

The drop in hydraulic pressure was too gradual to give precise indication (over the desired time-span) of test specimen failure; hence, there is uncertainty in time T_p which is large compared to the observed differences between gages. The small time differences observed between gages in a situation in which loading is applied very slowly are encouraging, as is the fact that the gages open at minus times nearly as often as they do at plus times.

It appears that any of the crack gage systems under consideration will serve the desired purpose; that is, they will give an indication of local structural failure at a time close to when that failure occurs. The errors in

timing that may result due to slight errors in gage bonding appear to be small in comparison to possible crack propagation times in slowly loaded specimens. Where clean breaks are observed in test gages, delay times are short. Care in gage installation appears to be a more rigid requirement than selection of a specific gage type from within those considered here.

Section 8

REFERENCES

1. Hill, E.L., et al., Structural Characteristics of NFSS Buildings, Vols. I-IV, Research Triangle Institute, Final Report OU-237, Durham, North Carolina, February 1967.

2. Kapil, Agit, Report on URS Tests, General American Research Division, further reference not available.

3. Goodale, T., The Ignition Hazard to Urban Interiors During Nuclear Attack Due to Burning Curtain Fragments Transported by Blast, URS 7030-5, Summary Report, URS Research Company, San Mateo, California, December 1971.

4. Goodale, T., An Attempt to Explore the Effect of High Blast Overpressure on the Persistence of Smouldering Combustion in Debris, URS 7030-6, Summary Report, URS Research Company, San Mateo, California, December 1971.

5. Wilton, C., et al., Loading and Structural Response of Wall Panels, URS 709-4, URS Research Company, San Mateo, California, November 1969.

6. Wilton, C., B. Gabrielsen and P. Morris, Structural Response and Loading of Wall Panels, URS 709-11, URS Research Company, San Mateo, California, July 1971.

7. Willoughby, A.B., et al., A Study of Loading, Structural Response, and Debris Characteristics of Wall Panels, URS 680-5, URS Research Company, July 1969.

8. Edmunds, James E., Experiments to Determine Debris Formation From Corrugated Steel and Brick Walls, URS 751-4, URS Research Company, January 1970.